

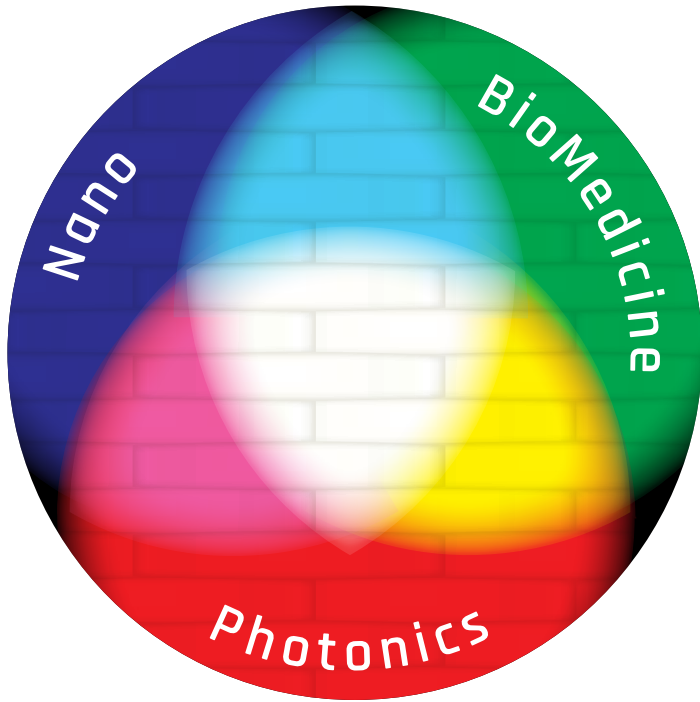


DJURO KORUGA

# **HYPERPOLARIZED**

# LIGHT

Fundamentals of NanoBiomedical Photonics



Djuro Koruga

# Hyperpolarized Light

Fundamentals of Nanobiomedical  
Photonics

ZEPTEK BOOK WORLD  
2018

*Library*  
SPECIAL EDITIONS

**Djuro Koruga**  
**HYPERPOLARIZED LIGHT**  
Fundamentals of Nanobiomedical Photonics

---

*Original title:*  
ĐURO KORUGA  
Hiperpolarizovana svetlost, osnove  
nanobiomedicinske fotonike

*Published by*  
ZEPTER BOOK WORLD D.O.O,  
Belgrade, Knez Mihailova 42  
email: office@bookworld.zepter.rs

*For the publisher*  
SLAVKA ILIĆ

*Library editor*  
LJUBOMIR LATINOVIĆ

*Translation*  
VESNA TOMOVIĆ

*Technical editor*  
VOJISLAV SIMIĆ

*Cover design*  
DRAGAN LONČAR

*Printed by*  
PLANETA PRINT, Belgrade

*Printed copies:* 1000

ISBN 978-86-7494-143-0

CIP - Каталогizacija u publikaciji - Narodna biblioteka Srbije, Beograd

61:[544.528.2:773

KORUGA, Đuro, 1947-

Hyperpolarized Light : fundamentals of nanobiomedical photonics / Djuro Koruga.  
- Beograd : Zepter Book World, 2018 (Beograd : Planeta print). - V, 312 str. : ilustr. ;  
24 cm. - (Library Special Edition / [Zepter BookWorld])

Prevod dela: Hiperpolarizovana svetlost. - Autorova slika. - Tiraž 1.000. - About the  
Author: str. 300. - Collaborating Authors in Chapter VII: str.301-303. - Glossary: str.  
304-308. - Bibliografija uz svako poglavlje. - Registar.

ISBN 978-86-7494-143-0

a) Фотоника

COBISS.SR-ID 262351628

# **Contents**

## **PREFACE 1**

## **INTRODUCTION 7**

- 1. *Light and the Phenomenon of Life* 9
  - 1.1. *Light and Ancient Civilizations* 9
  - 1.2. *Life and Deterministic Chaos* 9
  - 1.3. *Genetic Material and Light* 10
  - 1.4. *PHOTON: the Enigma of Contemporary Science* 11
  - 1.5. *ELECTRON: „It Would Also Be Nice To Know What an Electron Is“* 11
  - 1.6. *Light–Matter Interaction* 11
  - 1.7. *Biomolecules and Light* 12
  - 1.8. *Biological Tissues and Light* 12
  - 1.9. *Human Organism and Light* 13
  - 1.10. *The Light Model of Embryogenesis* 13
  - 1.11. *Tally: Challenge for the Light–Matter Interaction* 14
- References 15

## **LIGHT 17**

- 2.1. *Photon in 3D Space* 19
  - 2.1.1. *Light and Classical Mechanics* 22
  - 2.1.2. *Photon, Light and the Origin of Quantum Mechanics* 25
  - 2.1.3. *Universal Physical Constants:  $G$ ,  $c$  and  $h$*  28
- 2.2. *Systematization of Physics by Penrose* 33
- 2.3. *Light, 5D -Space and Fractal Mechanics* 34
- 2.4. *Five-Dimensional Light Nanotechnology* 43
- 2.5. *Five-Dimensionality of Light and Levitation* 46

2.6. „He does not gamble“	48
2.7. Photon and Light	52
References	54

## **MATTER 57**

3.1. Basic Knowledge about the Electron	59
3.2. Lagrangian and Hamiltonian	63
3.3. Tunneling Electrons	65
3.4. Electron Models in Physics	69
3.5. Classification of Intermolecular Forces	77
3.6. Do We Need a New Electron Model?	83
References	86

## **LIGHT-MATTER**

### **INTERACTION 89**

4.1. Poincaré Sphere (light)	91
4.2. Bloch Sphere (electron)	96
4.3. Larmor's Determination of the Magnetic Moment of the Electron	98
4.4. Light-Water Interaction	99
4.5. Interaction of Collagen and Microtubules with Linearly Polarized Light	101
4.6. Experiments: Interaction Between Light and the Amniotic Fluid	106
References	111

### **FIBONACCI PHENOMENA IN BIOLOGY 113**

5.1. Clathrin	115
5.2. Microtubules	117
5.3. Cilia and Flagella	119
5.4. Centrioles	122
5.5. Collagen	125
5.6. Water and Gibbs Free Energy	130
5.7. Fibonacci Numbers	145
References	152

### **HYPERPOLARIZED LIGHT 155**

6.1. Sun's Radiation	157
6.2. Light in Medicine	159
6.3. Problem Determination and its Conceptual Solution	163
6.4. Light in Medicine	165
6.5. Fibonacci Light Structures vs. Fibonacci Biological Structures	171

6.6. *Engineering Hyperpolarized Light Based on the C<sub>60</sub> Molecule* 188  
*References* 194

**APPLICATION OF HYPERPOLARIZED LIGHT IN MEDICINE** 197

7.1 *Effects of Hyperpolarized Light on Biophysical Skin Status* 199  
7.2 *Medical Cases* 212  
    7.3.1 *Hyperpolarized Light Applied to Burns* 212  
    7.2.2 *Hyperpolarized Light Applied In the Treatment of Lichenification* 215  
    7.2.3 *Hyperpolarized Light Applied in the Therapy of Burn Wounds* 217  
    7.2.4 *Hyperpolarized Light Applied in Psoriasis* 220  
    7.2.5 *Hyperpolarized Light Applied in Acne Treatment* 225  
    7.2.6 *BIOPTON Hyperpolarized Light Applied in the Therapy of Bronchial Asthma* 228  
    7.2.7 *Hyperpolarized Light Applied to Spondylolisthesis* 230  
    7.2.8 *Hyperpolarized BIOPTON Light Applied in the Lumbar Painful Syndrome* 233  
    7.2.9 *Hyperpolarized Light Applied in the Treatment of Chronic Venous Insufficiency* 236  
7.3 *Effect of Hyperharmonized Light on the Modification of EEG Signals* 241

**EPILOGUE** 249

8.1. *Time Phenomenon and Biological Time* 251  
8.2. *Biological Systems as Light Beings* 252  
8.3. *Full Moon Phenomenon* 256  
8.4. *Light model of Embryogenesis* 268  
8.5. *Energies <sup>11</sup>E<sub>3</sub> and <sup>11</sup>E<sub>4</sub>* 277  
8.6. *Entropy Force and the Life Phenomenon* 281  
*References* 286

**INDEX** 289

*About the Author* 300

*Collaborating Authors in Chapter VII* 301

*Glossary* 304

*Abbreviations and Notation* 309

*SI prefixes and units* 310

*General constants* 312





## *Preface*

This book stems from the need to present systematically new findings and technical solutions from the domain of physics and biomedical engineering by the author and the scientific community from the past thirty years of investigating light, nanotechnologies and biomedicine. Of course, the main goal of the monograph is the application value of presented findings and technical solutions in the medical practice, because physicians applying light therapy should be acquainted with physical foundations of light, and with biophysical characteristics of molecules and tissues that light interacts with. Expected results cannot be achieved without the cooperation between biologists, physicians and engineers, because *without medicine, technology is blind, medicine without technology is feeble*.

The monograph *Hyperpolarized Light: Fundamentals of Nanobiomedical Photonics* is divided into eight chapters: Introduction; Light: What is a Photon?; Matter: What is an Electron?; Light-Matter Interaction; Fibonacci Phenomena in Biology; Hyperpolarized Light; Application of Hyperpolarized Light in Medicine, and Concluding Remarks: *Epilogue*.

The Introduction presents problems and challenges of the contemporary world, starting with light as viewed by ancient civilizations, describing embryogenesis as the process of formation of three primitive germ layers: *ectoderm*, *endoderm* and *mesoderm* (from which the organism is formed). The organism generates consciousness in interaction with the environment, in a similar way as, from the RGB color model, spectrum of all colors originates ending with white color, significant only for the human brain, because there is no white photon in nature. Finally, the mechanism of the *tally* is described as a principle according to which we wish to treat tissues and the organism with light.

Chapter II treats the light phenomenon and the principal question: *what is a photon?* The reader will find here many interesting facts about light, from the aspect of classical physics, and from the view of quantum mechanics as well. In order to approach the answer, we had to go back not only to Maxwell and to his elegant unification of electricity and magnetism, but to Kaluza and Klein, and their idea of the unity between electromagnetism and gravitation in the five-dimensional space. Travelling this road, we encounter Planck, Einstein and Penrose and their invaluable contributions, but what will present

the photon and the light phenomenon in an original way is Hamming's investigation of unit spheres in multidimensional space, relevant in coding and information theory. Thus, beside mass, energy and other categories, information has a role in contemporary physics as well. Although we still do not know what a photon is, these new findings enabled us to comprehend that by using light and its polarization, it is possible to construct five-dimensional memory devices, to realize the levitation phenomenon at the nano and pico level, and to organize photons within light in a new way.

Chapter III, discussing matter, will draw no less attention and curiosity of the reader, investigating yet another enigma of nature, the electron. Presented is the knowledge evolution since electron's discovery in 1897 to date. Excitements afforded by Thomson, Luis de Broglie and Schrödinger regarding the electron can be matched by the effect of a good action motion picture. However, you will experience additional thrills when studying at the same time the electron and an ordered group of electrons in an object with icosahedral symmetry, the size of only one nanometer (billionth part of the meter), forming a sphere that rotates billion times in a second, all this taking place in a crystal, i.e., in a solid. Due to the spheric  $\pi$ -electron cloud, we observe a phenomenon similar to levitation; bodies are close to each other at minute distances, without external force needed for their separation. This nanomaterial of very unusual characteristics is used to generate a new light structure containing spatio-temporal information.

Chapter IV discusses basic principles of the light-matter interaction using the Poincaré and Bloch spheres. Elements of the classical and quantum field theory are presented, and collisions between light and valence electrons. The interaction between the linearly polarized light and the carbon nanomaterial containing the  $C_{60}$  molecule will also be discussed. It is demonstrated that the interaction between the linearly polarized light and the  $C_{60}$  molecule generates polarized light no longer linearly polarized (vertical polarization). It is a combination of the vertical and the horizontal polarization, so that gradual curvature of the polarization plane takes place resulting in the space-energy structural organization of photons according to the „sunflower seed” principle- according to the Fibonacci law. We named thus obtained light the hyperpolarized light (neither horizontally, nor vertically polarized, that is, both vertically and horizontally polarized). It can be viewed almost as an ancient phenomenon, as expressed by Heraclitus „Only one thing is wise, to be and not to be called by the name of Zeus“; today we recognize it as the quantum bit, that is a *qubit*.

Structure analysis of particular biomolecules and reexamining their functions brought new insights into biomolecular information processes described in Chapter V. Clathrin is a biomolecular structure responsible for the release of neurotransmitters at presynapses in the brain. It can be found in other tissues as well, where it performs secretion functions. This biomolecule has icosahedral symmetry, therefore, energy values  $T_{1g}$ ,  $T_{2g}$ ,  $T_{1u}$ ,  $T_{2u}$ , and their vibration modes, are determined by the Fibonacci law. The same is true of microtubules having multiple functions in the cell's cytoplasm; transport of matter from one place to another, cell shape determination, participation in cell division, etc. In the extracellular space, there is collagen whose peptide planes oscillate according to the Fibonacci law. However, biological water was a complete surprise: water's hydrogen bonds also oscillate according to the Fibonacci law. Therefore, more than 70% of body

matter oscillates according to the Fibonacci law. Consequently, a logical need arises to organize photons' structure (light) according to the same pattern as biological structures, to achieve a more efficient effect of light on tissue (mutual recognition between light's energy-structure and the structural-energy pattern of biomolecules, i.e., the realization of the effect „structured light meets structured matter“<sup>1</sup>).

Chapter VI describes hyperpolarized light, phenomenon unknown by science until now, based on the interaction between the linearly polarized light and the  $C_{60}$  molecule. Molecules of  $C_{60}$  are incorporated into the PMMA material, approximately 2 mm thick, 94% transparent in the domain of visible light, of arbitrary diameter (we obtained 50 mm, 100 mm and 150 mm). The nanophotonic material was characterized, and it was experimentally established that the  $C_{60}$ @PMMA material, with respect to PMMA, generates, under the influence of linearly polarized energy of visible light of 2.4 J/cm<sup>2</sup> per minute, paramagnetism of the order 10 nT. Light output from the nanophotonic filter is organized according to the „sunflower seed“ pattern, owing to its interaction with icosahedral symmetry of the  $C_{60}$  molecule and its haphazard rotation of  $1.8 \times 10^{10} \text{ s}^{-1}$  (performing a „bang-bang“ effect, i.e., „twisting“<sup>2</sup>).

Chapter VII, marked by Faraday's maxim „theory leads, experiment decides“, presents examples of hyperpolarized light application in medical practice. A study is described involving 32 examinees, and several case studies of asthma, psoriasis, acne, wounds, neurodermatitis, eczema, lumbar syndrome, etc. are discussed. In the above study, biophysical modifications on the skin were investigated after treatments with hyperpolarized light lasting from 8 to 10 minutes. The study was performed on a self-controlled group, by recording biophysical skin status of the arm's left and right side (contralaterally) with opto-magnetic imaging spectroscopy before and after treatment. It was demonstrated that hyperpolarized light has a positive effect on the improvement of the biophysical skin status (collagen, elastin, water, etc). In some cases (asthma, psoriasis, etc.) several treatments were performed (5–10) and it was demonstrated unquestionably that improvement of 25%–40% was registered in all cases.

Concluding remarks on the five-dimensional foundations of the unity of electromagnetism and gravitation are given in Chapter VIII. The foundation of this unity was established by relating nanogravitation dynamics at the Earth's surface, generated by the Solar system bodies, and the experiment performed at Grenoble with cold neutrons, where it was demonstrated that Earth's gravitational field is quantized. The quantum value of the gravitational field on Earth's surface at Grenoble was 1.4 peV, equivalent to the value of 110pg, which we obtained using nanogravitation approach. If the unity of the classical and quantum gravitation on the Earth's surface exists, this should be reflected on the formation of biomolecules in water, and on the origin of life. Calculations demonstrate that the intermolecular interactions based on hydrogen and Van der Waals bonds can be „disconnected“ or „connected“, i.e., it is possible to perform an orchestration of biomolecular interactions under the influence of micro and nano gravitation. The „full Moon“ phenomenon is also investigated, proposing an explanation for the excited state

---

1 Science, Vol. 337, 2012, pp.1054–1055.

2 Nature Physics, 25. December 2005; doi:10.1038/nphys192.

and behavior of some individuals during this period, based on the synergy of Moon's gravitation and Sun's light reflected off the Moon, i.e., on the synergy of gravitons and photons as a Möbius effect in  $N(-2_s)$ . Calculations are given of the external influence of the electric, magnetic, gravitational, and thermal effects. It is demonstrated that biological systems are the fourth „nano overtone“ of the grand unifying theory of all interactions ( $GUT \sim 10^{-35}$  m :  $\sim 10^{-9} \times 10^{-9} \times 10^{-9} \times 10^{-9}$  m).

On this occasion, I wish to express my gratitude to the medical team of the ZEPTEP MEDICAL general practice department from Belgrade: Dr. Biljana Lučić, Dr. Jelena Simić, Dr. Danijela Mitrović, Dr. Đuja Lazić, Dr. Aleksandra Ignjatović, Dr. Zlatica Kečić, Dr. Milica Komnenić, Dr. Miloš Mladenović, and Dr. Aleksandar Nešković. Their investigations are included in Chapter VII. By their conscientious and dedicated work they contributed not only to the quality of this publication, but also to the establishment of new therapeutic methods in medical practice. It can be said that they are the pioneers of hyperpolarized light application in medicine.

Without the participation of Tomasz Kukovsky, Zbigniew Soke and Rafael Klisjak in the production of the nanophotonic filter, this work would have been more difficult and delayed for „better times“. Their expert cooperation succeeded in transforming our basic scientific knowledge of polymerization and adding nanomaterials to polymers into a technological procedure for commercial use in the production of nanophotonic filters of  $1280 \times 1050$  mm, as opposed to our research solutions of the size 10 mm – 15mm. Special credit for the organization and realization of the production of experimental, larger dimension samples, and later to the production of nanophotonic filters, goes to Srđan Balaban.

It has taken 25 years of investigation and patience, with all ups and downs, to realize the idea of nanophotonics and hyperpolarized light. The skies echoed already in 2000, when Ljuba Latinović and Prof. Dr. Milan Skrobić, ardent supporters of nanotechnology application in medicine, contributed decisively to a new beginning. In 2002, the idea was initially supported, first by Philip Zepter, and then by Vibor Mulić, today's protagonists of the application of hyperpolarized light in medicine.

Dane Bjelopetrović from the USA, who exhibited incredible belief in Fibonacci laws and the application of this principle in biomedical engineering in the period 2006–2011, financed, while he could, part of the research and patenting of the application of light and water in cosmetics and in medicine. The idea to apply light in cancer diagnostics was financed by the Ministry of Science and Technological Development of the Republic of Serbia during 2005–2016, and light implementation in cosmetics in the period 2008–2012 by *MySkin*, USA. The most deserving for this is Aleksandar Obradović, who, without hesitation, gave moral and material support and was the driving force of this research.

I am also indebted to Prof. Đuro Kurepa, renowned mathematician, who had encouraged me, since 1990, to work in a new mathematical field—time physics of the  $C_{60}$  molecule. Another two mathematicians deserve my gratitude: Professor Zlatko Mamuzić and Professor Ljubomir Ćirić, who introduced me enthusiastically into mathematics, realm of ideas and creative imagination, improving thus significantly this monograph.

With my virtuous acquaintance Prof. Miloje Rakočević, with whom I am „on bad terms“ since our first meeting in the 1980-ties (although we never engaged in a fight), I exchanged thousands of thoughts on the life phenomenon, Fibonacci, genetic code, and

the golden section. I was introduced to medical science relevant for this monograph, by Prof. Dr. Antonije Škokljević, Prof. Ljubiša Rakić, Prof. Milorad Japundžić, Prof. Dr. Borivoje Stamenović, Prof. Nikola Ilanković, Prof. Radmila Mileusnić, Prof. Vera Gal and Prof. Marija Guć. As biologists and medical experts, at the time when I most needed support (40 years ago), they believed in me (as an engineer) and unselfishly dedicated their time to introduce me in detail to the world of microtubule biology and medicine. I had fruitful discussions on issues of physics, regarding the contents of this book with Abdus Salam, Harold Kroto, Richard Smalley, Sir Roger Penrose, Prof. Stuart Hameroff, and Prof. Zvonko Marić. I worked with my doctoral students Dr. Aleksandar Tomić and Željko Ratkaj for several years on biomolecular information processes and nanogravitation. I had very useful exchange of ideas on biophysics with Prof. Dr. Michael Conrad, Prof. Dr. Felix Hong, Prof. Dr. Dejan Raković, and on the relationship between biophysics and medicine, with Dr. Jadran Bandić.

I had an especially stimulative epistolary dialogue with Prof. Dr. Tom Stonier, author of *Information and the Internal Structure of the Universe*, and with Prof. Dr. Alwyn Scott, author of *Stairway of the Mind*, an extraordinary connoisseur of the soliton phenomenon. Dr. Gen Macumoto, Prof. Masuo Aizawa and Prof. Yukio Kosugi supported my initiation into the mental world of the East, biomedical engineering and nano science. I am infinitely grateful to my professors of Chinese language at the Faculty of Philology in Belgrade, because, in the period 1977–1982, they aided me to enter new, unknown horizons and initiate a path of new conceptual insights.

I am indebted also to all scientists to whom I talked to concerning the subject of this book, and who contributed, directly or indirectly, to my knowledge. Above all, I owe gratitude to my wife Lidija and son Igor, who, by their critical reviews and useful suggestions, improved the quality of this monograph.

November 23, 2017  
Belgrade

*Author*



# 1

## INTRODUCTION





*The hardest thing to see is  
what is in front of one's own eyes*  
GOETHE

## ***1. Light and the Phenomenon of Life***

### ***1.1. Light and Ancient Civilizations***

We can conclude that light had an important role in each stage of civilization development according to preserved documents (pictures, written documents, legends, etc.). Known gods of ancient Egypt (Ra), Greece (Helios) and other ancient civilizations were the gods of the Sun, that is, light. The Bible considers that by the act of creating light, in the process of bringing the world into existence, something new and positive was created as opposed to „darkness“, which, according to the Testament, preceded light. Approximately 60% of information on the outside world is received via the eyesight only (light) - everything else through senses of hearing, touch, smell and taste. Light is, together with water and oxygen (the atmosphere), synonym for biological life on Earth.



Contemporary science considers that biological life on Earth originated in water, under the influence of light (Sun and atmospheric discharges) and Earth's microwave radiation. Of course, other preconditions must have been satisfied, such as gravity, appropriate temperature, atmosphere, etc. The importance of initial conditions for the origin of life is significant. It is compared, within the science of deterministic chaos, to the „butterfly effect“. Chapters on electromagnetic radiation, nanogravitation, quantum gravitation, and the entropic foundations of gravitation will describe in more detail external influences significant for the origin and sustaining of life on Earth.

### ***1.2. Life and Deterministic Chaos***

The science of deterministic chaos (Schuster and Just, 2005), which originated within metrology (Edward Lorenz), established that the dynamic systems, being nonlinear and dissipative, such as, for example, the atmosphere and biological systems, are sensitive to the initial conditions. Lorenz named this extraordinary sensitivity the „butterfly effect“:

flapping of butterfly's wings on a flower in Japan causes a tornado in America after a few days, or in some other part of the planet. The human genome exhibits analogous behavior: the union of paternal and maternal chromosomes determines the characteristics of the newborn being. Therefore, the initial conditions of conception (union of maternal and paternal chromosomes), of embryogenesis (organization of the formation of the human organism, which is, as we shall see in the following chapters, actually a „light being occupied by darkness“), and childbirth (influence of classical and quantum gravitational effects of the environment) are very significant regarding the life and health of the newborn organism. The science of deterministic chaos explains that if the formation of the human organism starts from „two proximal points“, they will be found, after a sufficiently long time, arbitrarily distant from each other, in the next phase becoming close again, finally becoming united. In other words, if the union of the genetic material (chromosomes) is not adequate („two proximal points“), after the embryogenesis, the defect will be concealed and inactive („arbitrarily distant“). However, eventually it will be activated under stress („reestablished proximity“). Therefore, insight into the human genome, embryogenesis and stressogenic factors is of utmost importance for disease prevention, medical diagnostics and therapy. Although, at first sight, everything seems chaotic, Einstein is right in saying: „...dear God does not gamble...“, however we must add: ... *although he throws dice*. However, this dice throwing is the basis of the law of the distribution of large numbers that corresponds to the *law on the conservation of information*, similar to the laws on the conservation of mass, energy, momentum, etc.



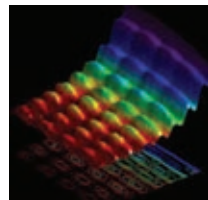
### 1.3. Genetic Material and Light

Chromosomes are cell organelles within the nucleus responsible for the transfer of hereditary features of a given biological species. They were first detected by the German scientist Hofmeister in 1848, yet 40 years later, in 1888, Waldeyer gave them their name.

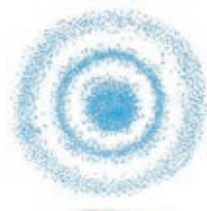
The term *chromosome* originates from the Greek words *chroma* – color and *soma* – body, because by staining biological substrate with specific chemicals, they become visible under the microscope (average size  $20 \times 1.4 \mu\text{m}$ ) with respect to other cell organelles. Essential genetic material, beside the one within the mitochondria, is located within chromosomes. The human genome has 22 pairs (father, mother) and one sex chromosome, X and Y respectively, as the 23<sup>rd</sup> pair. The overall number of nucleotides (carriers of information content) is approximately 3 billion ( $3 \times 10^9$ ). However, at chromosome endings, telomeres are found (red tips in the Figure), structures decreasing with each cell division. The number of information carriers (A-adenine, T-thymine, G-guanine and C-cytosine) corresponds to the space-time characteristics of light propagation. Thus, the thought of St. Augustine „...we do not live in time, we are composed of time“ is increasingly drawing attention of scientists; diagnostics and healing via light is gaining increasing significance.

### 1.4. PHOTON: *the Enigma of Contemporary Science*

What is a photon? Science still does not have the answer to this question. However, much is known about photon characteristics. Based on this insight, many devices have been constructed, used by man in quotidian life, starting with the light bulb and radio, up to the laser. Especially significant is the use of light in medicine, in diagnostics and in therapy as well. Beside ordinary daylight, being mostly diffuse, polarized light (linear, circular, elliptical) is also used for technical and medical purposes. It is known that the photon has a dual, corpuscular-wavelike nature, that is, under certain conditions it behaves like a wave, and otherwise like a corpuscle. However, recent experimental findings demonstrate that the photon exhibits mass-wave duality simultaneously (Piazza, L. et al, 2015), enabling better understanding of the light-matter interaction. The concept of wavelike light dominated until 1905, when Einstein explained the photoelectric experiment and demonstrated that the moving photon has also a corpuscular nature. This discovery awarded him the Nobel Prize in 1921. Asked once what a photon is, he replied that, despite the fact that he devoted most of his time to the study of light, he does not know what a photon is, and added: „it would also be nice to know what an electron is“.



### 1.5. ELECTRON: *„It Would Also Be Nice To Know What an Electron Is“*

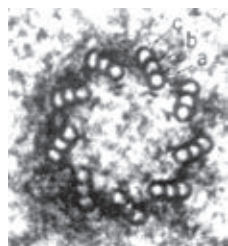
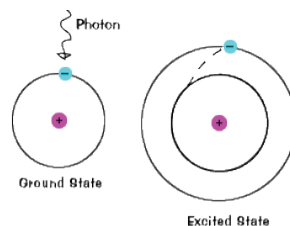


We should ask ourselves what is an electron. Most people think that this question has been resolved, because it seems that the electron is an easier problem than the photon. However, contemporary science still does not have the answer to this question. As in the case of the photon, many of its characteristics have been established; however, the essential answer is still lacking. While light was the subject of human curiosity and investigation since the beginning of time, the electron was discovered in 1897 by the British scientist Joseph John Thomson. At first it was represented as a cloud, filling the entire atom volume, later as a particle orbiting the nucleus at a given distance. The electron has corresponding energy depending on its distance from the nucleus. As Einstein established that the photon has a dual, wavelike-corpuscular nature, Luis de Broglie in 1924, in his doctoral dissertation, demonstrated that the electron has a corpuscular-wavelike nature (he was awarded the Nobel Prize for this discovery in 1929). Today, many devices have been constructed based on the corpuscular-wavelike nature of the electron, such as the scanning tunneling microscope (STM), which records molecules at the atomic scale (Binnig, 1982).

### 1.6. *Light–Matter Interaction*

In the light–matter interaction, photons of various energies interact with valence electrons. In case of visible light, photons interact exclusively with electrons from the

external orbital, leaving electron organization unchanged. However, high-energy photons interact with valence electrons ejecting them from orbitals, thus causing matter ionization. X-rays penetrate deeper into atoms, reaching electrons in internal shells, resulting in the reorganization of electrons within the atom; atoms transit into higher energy orbitals, that is, into the excited state (Weiner and Nunes, 2013). This monograph discusses the interactions of the visible and infrared light of wavelengths between 400 nm and 3000 nm. In order to comprehend the interaction of the VIS-NIR light with tissue, it is necessary to be well acquainted with characteristics of biomolecules, tissues and the organism.

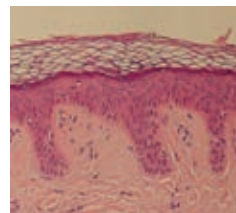


### ***1.7. Biomolecules and Light***

Biomolecules, such as proteins, lipids, fat, etc., constitute about 15% of the total organism mass. The interaction between light and biomolecules is of utmost significance, thus, it is very important to investigate and understand biomolecules. Until now, the absorption characteristic of biomolecules was dominant in selecting the type of light for diagnostics and therapy. It can be said that this was a necessary, although not a sufficient condition for the optimal interaction between light and biomolecules. Beside classical vibration complexes (C-O, C=C, O-H, N-H, etc.) it is necessary to understand vibration modes of the molecule (structure) as a whole. In order to grasp this, we have to know the symmetry group to which a molecule or structure belongs to as a whole. Therefore, this monograph will place special emphasis on the investigation of symmetry features of particular biomolecules such as clathrin, microtubules, collagen, actin, cilia, centrioles, etc. These characteristics will define light adequate to act on biomolecules in order to preserve their organization or improve their impaired structure and functionality. Light and matter structure should have the same type of symmetry, organization, so that, during their interaction, mutual recognition of structural-organizations, „patterns“, occurs, that is they should interact resonantly (Litchinitser, M.N., 2012).

### ***1.8. Biological Tissues and Light***

Epithelial tissues are the first biological structure that light interacts with, in diagnostics or in therapy. Skin is one of the best examples of this interaction, because it is daily exposed to the effects of daylight (diffuse light). Owing to the presence of water in the skin (approximately 70%), blue light penetrates the tissue very slightly, only 5–10  $\mu\text{m}$ , green light penetrates the skin up to the basement membrane (100–150  $\mu\text{m}$ ) and slightly deeper, while the red light penetrates deep into the



dermis, 800–1600  $\mu\text{m}$ , and the infrared light (of wavelength greater than  $\lambda \geq 800 \text{ nm}$ ) up to 0.5–3 cm. The water absorption spectrum is 100–1000 times greater for the red and infrared light than for the blue light. Since, in the Sun's spectrum, participation of the red and infrared light is small compared to the blue, green and yellow spectrum, the origin and sustaining of life on Earth is possible. Otherwise, body temperature would exceed 65°C, preventing the synthesis of nucleic and amino acids into DNA and protein chains. Even in case they were somehow formed under specific local conditions, their denaturation would occur later. Collagen is the protein prevalent in the human organism (40% of all proteins), and plays an important role in the extracellular space, especially in the basement membrane.



### ***1.9. Human Organism and Light***

Depending on age, human organism contains 60% –75% of water. The interaction between water and light is one of the most important phenomena for the diagnostics and therapy of the human organism as a whole (holistic medicine). This is why we need to be well acquainted with the phenomenon of hydrogen bonds, from the aspect of classical physics, and from the view of quantum mechanics as well. Knowing that IR light penetrates the tissue up to 3 cm, the question arises is it possible to transfer, using hydrogen bonds, light signals deeper into the organism. In other words, is it possible to transfer local light effects onto the entire organism or to specific internal organs? The following chapters will demonstrate that it is possible, using hydrogen bonds on one hand, and the system of extra-bioactive body loci, known as the acupuncture points, on the other, to act selectively and holistically on the organism (Koruga, 1984). The significance of hydrogen bonds can be observed in the DNA, because the nucleotides adenine and thymine, i.e., guanine and cytosine, are connected by hydrogen bonds, which are, via the phosphate group within the DNA, related to the hydrogen interactions of water as the external environment. Linus Pauling (twice Nobel Prize winner) was aware of the importance of hydrogen bonds for the human organism. As early as 1938, he stated that the importance of hydrogen bonds for the human organism surpasses the significance of any particular organ, including the brain or the heart (Pauling, 1985). He believed that the origin of many diseases is found at the molecular level, which supports the view that in the future we should focus more on the personal than on the statistical medicine.

### ***1.10. The Light Model of Embryogenesis***

The embryogenesis is probably, after the evolution of the Universe, one of the most complex processes we know. The anatomic-physiological stages in the development of the fetus, from the fertilized ovum to childbirth, are mostly known. They can be divided into three main phases: from the zygote to the formation of the three-layered germ (pre-

embryonal period of development), from the forming of ectoderm, endoderm and mesoderm till the end of the second lunar month (embryonal period), and from the third month until childbirth (fetus period). Based on perfect numbers and Fibonacci numbers, a light model of embryogenesis is developed, i.e., it is demonstrated that the embryogenesis can be represented using the RGB system (color system leading from the black, via blue, green, and red color, to the white). The light model improves the understanding of the interconnectedness between parts of the human organism developed during the embryogenesis (Carlson, 2009). The embryogenesis is one of the key processes for the understanding of the formation of extra-bioactive body loci and channels (acupuncture) representing the flow network of electromagnetic signals (of light), and quantum gravity signals (biological "black hole" effect of 4D space-time, as  $-1_4$ ), Yang (light) and Yin (gravity).



### 1.11. Tally: Challenge for the Light–Matter Interaction

As the essence of the photon and electron is unknown, neither are we aware of the essence of our own existence, i.e., of the life phenomenon. However, we do know many characteristics of the photon and electron, and regarding life, we know that, according to Leibniz, after peace of mind, health is the most important issue. This monograph originated from the need to contribute to as efficient as possible health preservation in a natural way, using light. To achieve this, it is necessary to be well acquainted with structural, energetic, and informational foundations of biomolecules, that is, with organization and regulation mechanisms of the human organism. After we have understood the laws governing the main rules of biomolecules, which are essential as life itself, the next step is to design a device generating structural organization of photons according to the same laws that govern biomolecules' organization, that is, in the way biochemical/physical processes are realized based on Gibbs free energy. Biomolecules are, by their structure and energy, via entropy, related to information. This will enable the newly created light to influence the information states, and thus act on structural-energy-information processes of biomolecules as well. Structuring photons, according to some of biomolecular features, should follow the *tally* principle, the ancient method of recognition, pairing, i.e., identification of ownership (it was used by millers; a farmer would bring a sac of wheat, take a shorter slim stick, notches would be made on the stick, it would be split longitudinally, so that on both parts notches would be visible (see Figure: parts A and B); one half would be kept by the miller, and the other by the farmer, and

when the farmer came to claim the flour, notches on the two sticks would be compared and if they corresponded, the farmer would receive his flour). Chapter VI explains how a light polarization characteristic was applied in order to achieve recognition between light and biomolecules, effecting interaction between matter and light, which, in a natural way, efficiently acts on the organism.

## References

1. Carlson, M.B. Human Embriology and Developmental Biology, Mosby, Philadelphia, 2009.
2. Koruga, Đ. Qi inženjering: Fenomen ekstrabioaktivnih tačaka tela, Poslovna Politika, Beograd, 1984.
3. Koruga, Đ. Fraktalna mehanika: Klasično-kvantni fenomeni u prirodi i biološkim sistemima, Nauka/DonVas, Beograd, 2012.
4. Litchinitser, M.N. Structured Light Meets Structured Matter, *Science*, 337, pp.1054-1055, 2012.
5. Piazza, L., et al. Simultaneous observation of the quantization and the interference pattern of a plasmonic nearfield, *Nature Communication*, 6: 6407, DOI: 10.1038/ncomms7407.
6. Pauling, L., Wilson, E.B. Introduction to Quantum Mechanics: With Application in Chemistry, Dover Publications, New York, 1985.
7. Schuster, H.G. Just, W. Deterministic Chaos: An Introduction, Wiley-VCH Verlag GmbH &Co, Weinheim, 2005.
8. Stonier, T. Information and the Internal Structure of the Universe: An Exploration into Information Physics, Springer-Verlag, London, 1990.
9. Thomson, J.J. Carriers of negative electricity. *Nobel Lecture*, December 11, 1906.
10. Thomson, J.J. Carriers of negative electricity. *Philosophical Magazine*, S.5, Vol. 44, No.269, October 1897.
11. de Broglie, L. Researchers sur la theorie des quanta, *Annales de Physique*, 3, pp.22, 1925.
12. Binnig, G., Rohrer, H., Gerber Ch., Weibel, E. Surface Studies by Scanning Tunneling Microscopy, *Physical Review Letters*, 49 (1), 57-60, 1982.
13. Weiner, J. and Nunes, F. Light-Matter Interaction: Physics and Engineering at the Nanoscale, Oxford University Press, Oxford, 2013.





2

LIGHT

*What is a photon?*



## 2.1. Photon in 3D Space

Today, four basic interactions are known in the 3D space (Huang, 2007): *strong* (acting at a distance of  $10^{-11}\text{m}$  – in the atom nucleus, interaction carrier: *pion* and *kaon*), *weak* (acting at a distance of  $10^{-13}\text{m}$  – radioactive beta decay, interaction carrier *W boson*), *electromagnetic* (acting over arbitrary infinite distances, action intensity decreases with the square of distance, basis of the atomic and molecular interactions, interaction carrier *photon*) and *gravitational* (acting also over arbitrary infinite distances, decreasing with the square of distance, interaction between solids is based on mass, interaction carrier *graviton*). Comparing intensities of the above four interactions, the electromagnetic interaction is  $10^{-12}$  times weaker than the strong interaction, although  $10^2$  times stronger than the weak interaction, and  $10^{28}$  times stronger than gravitation.

The carrier of the electromagnetic interaction in the 3D space is the *photon*, a dual entity, of corpuscular-wavelike character. Photon's spin is 1, it travels with the speed of  $2.99 \times 10^8$  m/s in the vacuum, through water with  $2.24 \times 10^8$  m/s, and in soft biological tissue, such as epidermis, with the speed of  $1.93 \times 10^8$  m/s. These are average values for the photon of wavelength  $\lambda = 550$  nm. For photons of lower wavelength, propagation velocity is decreased, and for higher wavelengths, it is increased. Photon's propagation velocity in solid biological tissues (bones, teeth) is  $1.84 \times 10^8$  m/s. Instead of investigating photon's propagation in the tissue, the same phenomenon can be represented by the refractive index  $n = c/c^*$ , where  $c$  is the photon's velocity in vacuum, and  $c^*$  photon's velocity in the respective medium.

Photon's velocity in vacuum is determined by vacuum characteristics, its permittivity  $\epsilon_0$  (electric characteristics) and permeability  $\mu_0$  (magnetic characteristics), where  $\epsilon_0 = 8.854 \times 10^{-12}$  ( $F \cdot m^{-1}$ ), and  $\mu_0 = 4\pi \times 10^{-7}$  N / A<sup>2</sup>  $\approx 1.2566 \times 10^{-6}$  (H/m). Photon's velocity in vacuum, using these characteristics, is given by the expression:

$$c_0 = \frac{1}{\sqrt{\epsilon_0 \mu_0}} = 2.99 \times 10^8 \left( \frac{m}{s} \right), \quad (2.1)$$

so that the ratio of the *electric field* ( $E$ ) to the *magnetic field* ( $M$ ) of the photon is given by the expression 2.2:

$$\frac{E}{M} = 2.99 \times 10^8 \left(\frac{m}{s}\right), \quad (2.2)$$

Thus, photon's magnetic field in vacuum is billion times ( $10^9$ ) weaker than the electric field, that is, it is a *nano* value (expression 2.3):

$$M = 3.34 \times 10^{-9} E \text{ (kg/As}^2\text{)}, \quad (2.3)$$

In an actual biological environment,  $\epsilon_0$  and  $\mu_0$  are modified by  $\epsilon_r$  and  $\mu_r$ , which are directly related to the refractive index  $n$ . From the expression 2.3, we can conclude that the electric photon field (of light) should be used for diagnostics or treatment of tissue from the aspect of classical phenomena, and the magnetic photon field should be used when we need to act at the quantum level. This is because the value of Planck's constant is:

$$h = 6.626 \times 10^{-34} \text{ (Js)}, \quad (2.4)$$

having as a unit of measure Js (*Joule*  $\times$  *second* = *action*), which can be written as

$$h = F \times d \times t \text{ (Js)}, \quad (2.5)$$

where  $F$  – is action force ( $N$  – Newton),  $d$  – displacement ( $m$  – meters) performed by the action, and  $t$  – time (s – second) of action execution. For example, if the force is of the order  $10^{-12}$  N (*pico Newton*), displacement  $10^{-11}$  m, and time  $10^{-9}$  s, the photon executes the action of  $10^{-32}$  Js in the tissue during the light–matter interaction. This effect is near the quantum action, because  $10^{-34}$  Js is of the order of Planck's constant, although the action of  $10^{-32}$  Js, as we can see, is not a quantum action in matter. If the action is not quantum it must be, based on our present knowledge, classical. However, this is a hypothesis; therefore, this phenomenon should be investigated to determine to which action class it belongs.

As already stated, in the process of interaction with matter, photons interact first with the electron layer called the valence electrons. In order to apprehend what is the effect of the action caused by photons of visible light, we have to know the ratio of the electric force to the magnetic force of valence electrons. Why do we have to know the ratio of forces, and not some other electromagnetic characteristics of valence electrons? The answer lies in the character of the action, because *force* ( $F$  –*force*), *displacement* ( $d$  –*displacement*) performed by this action in a given *time* ( $t$  –*time*) are magnitudes determining action (expression 2.5).

Comparing electronic and magnetic interactions between the charges of two electrons in neighboring atoms in relative motion, as is the case in all molecules, and thus also in biological molecules, can provide the answer. We know that it is difficult to calculate the magnetic interaction between the charged particle, moving with respect to the observer „O“, in the form resembling the electric interaction described by Coulomb's law (interaction of motionless charges). However, the laws of physics can give us the insight into the order of magnitude of the ratio of the magnetic interactions to the electric interactions caused by charges of two atoms, which are related via valence

electrons. Since the two electric charges  $q$  and  $q'$  of valence electrons are actually two connected atoms whose charges in the external electron shell travel with velocities  $v$  and  $v'$  relative to the observer, it can be concluded that the electric force produced by the charge  $q'$  acting on  $q$ , measured by the observer  $O$ , is equal to  $qE$ . The resulting magnetic field  $q'$  can be determined using the equation (Alonso, Finn, 1992)

$$B = \frac{1}{c^2}(vE), \quad (2.6)$$

Consequently, the order of magnitude  $B$  of the magnetic field is defined by  $v'E/c^2$ , and the magnetic force acting on the charge  $q$  is of the order:

$$qvB = \left(\frac{vv'}{c^2}\right) qE, \quad (2.7)$$

$qE$  being the electric force acting on  $q$ . Therefore, the ratio of the *magnetic force* to the *electric force* is  $F_M / F_E = vv' / c^2$ . Since the velocities of charges are much smaller than the velocity of light  $c$ , the magnetic force is negligible with respect to the electric force in many cases of classical mechanics. The orbital speed of valence electrons in the hydrogen atom is  $\sim 2.8 \times 10^6$  m/s, giving the ratio  $F_M / F_E = [(2.8 \times 10^6) \times (2.8 \times 10^6)] / (3 \times 10^8)^2 = (7.84 \times 10^{12}) / (9 \times 10^{16}) = 0.871 \times 10^{-4} = 8.71 \times 10^{-5} \approx 10^{-4}$ . Therefore, the magnetic force is smaller than the electric force by four orders of magnitude. From the aspect of classical mechanics, this is negligible, although from the aspect of quantum mechanics it is very significant, because by four orders of magnitude it is closer to the quantum effect, responsible for conformation modifications in the biomolecules. Therefore, existing quantum action ( $A_q$ ) can be  $6.626 \times 10^{-34}$  Js  $< A_q < 0.871 \times 10^{-30}$  Js. Within this interval ( $10^{-30} - 10^{-34}$ ), from the energy aspect, classical and quantum effects exist simultaneously in the material; classical as electric action and quantum as a magnetic effect. Therefore, if the action  $A$  (*Action*) is greater than  $0.871 \times 10^{-30}$  J<sub>s</sub>, it is classical (based on the electric and magnetic force), and if it equals  $6.626 \times 10^{-34}$  J<sub>s</sub>, the action is a quantum action (quantum with respect to the electric and to the magnetic force).

Understanding these phenomena is of utmost importance for diagnostics and for therapy. For example, in medical practice, sometimes patient's ECG signal displays normal values, but the patient dies of heart disease after a short while (from within half an hour up to several days, as recorded in medical practice). How is this possible? This is possible because the ECG device measures the electric heart activity at the level of tissue and the heart as an organ. However, the problem in these cases was at the level of conformation changes in biomolecules, which are 10–100 000 times smaller, regarding energy, than tissue changes, so that electric signals cannot identify them. Regarding therapy, it is believed that if higher energies were used (while beneath the hazardous level for the organism) the action would have better effects. This is not necessarily so, because if light of intensity and type that could have effect at the tissue and organ level is used this is true, however, the therapy is unsuccessful if the problem is at the level of biomolecules. The electronic states of tissue exceed, for example, 100–1000 times the vibrational and rotational states of biomolecules, so if the problem were at the biomolecular level, classical action of the electric component of light would not produce

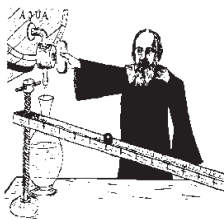
satisfactory results that would otherwise be achieved via the magnetic component of weaker intensity. However, this is necessary although not sufficient knowledge of light diagnostics and therapy (electromagnetic radiation in general), because biological systems, at the level of biomolecules, tissues, organs and the organism, have informational characteristics, not only energy characteristics. How structure, energy and information should be related is explained in Chapters V and VI, where the Fibonacci phenomena in biology and the hyperpolarized light are presented and discussed.

### 2.1.1. Light and Classical Mechanics

Classical mechanics originated in antiquity, around 4 century B.C., at the time of a fundamental turning point in the perception of the world: transition from the mythological, irrational thinking, toward the empirical-scientific, rational thought. In ancient Greece, prominent scholars appear, such as Thales of Miletus (about 624–546 B. C.), Pythagoras (582–507 B. C.), Heraclitus of Ephes (about 540–475 B. C.), Plato (about 427–347 B.C.), and Aristotle (384–322 B. C.), and in the East, Lao Tzu (about 500 B. C.), Buddha (about 300 B. C.), and others. We should bear in mind significant differences between the



*Galileo Galilei*  
(1564-1642)



Eastern and Western thought of the time also valid today; however it is significant that this „revival“ occurred approximately at the same time in the East and in the West. This transformation was not instantaneous - it lasted a few centuries. In ancient Greece, the origin of the contemporary scientific thought, transition from the mythological (irrational) to the empirical (rational) thought took place, while in the East the mythological (imaginary) concept was transformed into the empirical (complex) thought. While in the Western civilizations, the rational negates the irrational, in the East there is the „Aufgehoben“ phenomenon (German concept used by Hegel to denote that something is at the same time *abolished* and *preserved*). In a way, this is analogous to the procedure where, in mathematics, a real number is corresponded to an imaginary number – thus obtaining a complex number, where the imaginary number is preserved, yet it is also transcended, because the complex number is something more than just an imaginary number). The relation between the classical and quantum mechanics is similar (quantum mechanics „abolished“ classical mechanics, but „preserved“ it at the same time). Two basic processes, „East“ and „West“, exist in all people, while in some, depending on the moment one is primarily active, and in others the opposite.

If we wish to understand the fundamental laws of nature, the universal physical constants are the starting point to grasp the laws of nature and to perform the systematization of human knowledge about nature. It is considered that contemporary physics, therefore mechanics as well, begins with Galileo, who, already as a student, discovered the isochronousness of pendulum oscillations, using his own pulse to

measure time (this Galileo's discovery later aided Huygens to construct the astronomical pendulum clock). By introducing *experiment* as the ultimate proof in science, Galileo established a historical turning point, and is rightly considered the founder of the modern mechanics (physics).

Physics, as a theoretical discipline, was conceived much earlier - in the antiquity. The most famous thinkers of ancient Greece that investigated laws of nature (dynamics and statics) were Thales, Pythagoras, Plato, Aristotle, Archimedes (about 287–212 B.C.), etc. Aristotle was Plato's disciple. Later, as an independent thinker he established the *Lyceum*, introduced the concept of physics (Greek φυσική – nature) and was the first to write the book under this title - *Physics* (Aristotle, 1987). His approach was Ptolemaic (geocentric) and metaphysical (behind the visible nature and its dynamics there is an invisible driving „force“). However, the seed of the physics of antiquity is with Thales, the roots are with Plato, and the trunk is with Aristotle (Leartije, 1979, Marić, 1997). Modern physics is just a ramified branch on the trunk of human knowledge. Galileo laid the foundations of the contemporary mechanics as a science by his discovery of the law of free fall, sling (projectile trajectory), oscillatory motion (pendulum), and insight into the motion of planets. He constructed the telescope in 1609 and discovered four main Jupiter's satellites, agglomeration of stars into clouds of the Milky Way, mountains on the Moon, and sunspots. He introduced experiment as the ultimate proof in science, and the concept of inertia in mechanics, investigated the principle of relativity of classical mechanics from the aspect that postulates the equality of the laws of motion in all inertial reference systems. Although, at the beginning, he was a supporter of the Ptolemaic system (according to which the Earth is at the center of the Universe), impressed by arguments of Copernicus, he became his ardent proponent. However, the church inquisition compelled him to renounce this belief.

Sir Isaac Newton (1642–1727), mathematics professor at Cambridge, discovered three laws of motion and the law of gravitation. At the same time as Leibniz, he developed the infinitesimal calculus, leading to the definition of the derivative, and thus to the law that relates trajectory, velocity and acceleration in time. He investigated the light phenomenon, studied scrupulously the Bible (mythological poems of Homer and Hesiod speak of polytheism, while the Bible, as a religious work, which is in Hebrew also a poem, speaks of monotheism. Lao Tzu speaks on the need for a change, on the necessity of *oneness*: „man needs *oneness*, as the fish needs the sea“).

It can be said that the seed of biophysics in antiquity was planted by Hippocrates (around 460–377 B.C.) He investigated the human organism state (healthy /pathological) from the aspect of the laws of nature, as opposed to the widespread mythological belief of the epoch that destiny and state of the human organism depend solely on gods. He wrote *The Canon of Medicine* where he states „human nature belongs to the entirety of nature, and abides by the same laws as the nature itself, because everything is divine and everything is human. Medicine is nothing else than mimesis of nature. Physician is a servant and interpreter of nature“.

When first exploring the physical characteristics of nature and light, most experiments were based on the assumption that light had no special (oriented) characteristics in other directions, so that a light ray was represented by a straight line, and all light

characteristics were investigated in this direction. In other words, light characteristics along other directions were neglected, including the direction orthogonal to the light propagation direction.



David Brewster,  
(1781–1868)



Jean-Augustin  
Fresnel (1788–1827)



James Maxwell  
(1831–1879)

It is hard to say when and who was the first to observe that light has special features in directions orthogonal to the propagation direction, that is who performed the complex analysis of light's wave motion. Basic ideas can be found with Newton and David Brewster (1781–1868), however it is established that Jean-Augustin Fresnel (1788–1827) in 1817 and 1821, discovered light polarization; light characteristic in the directions orthogonal to the light's propagation direction.

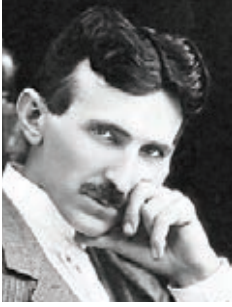
Light is an electromagnetic phenomenon, it consists of two coupled waves, the electric and the magnetic wave, mutually perpendicular, which can be polarized under certain conditions. Light polarization can occur spontaneously during the interaction of light with matter under a certain angle, for example, with smooth surfaces of transparent bodies, or in light traveling through particular crystals. Light polarization, depending on conditions, can be a very complex phenomenon. As an example, if a light vector rotates about the direction of the beam in a plane orthogonal to the ray, while periodically varying its intensity, light is *elliptically polarized*. When there is no change of light intensity, *circularly polarized light* occurs. However, when the light vector does not rotate, but only changes intensity in one direction, it is said that light is *linearly polarized*.

$$\nabla \cdot \mathbf{E} = 0 \quad \nabla \times \mathbf{E} = -\frac{1}{c} \frac{\partial \mathbf{H}}{\partial t}$$

$$\nabla \cdot \mathbf{H} = 0 \quad \nabla \times \mathbf{H} = \frac{1}{c} \frac{\partial \mathbf{E}}{\partial t}$$

Maxwell succeeded, in 1864, to unify the work of Newton, Faraday, Kelvin and Ampère into four differential equations postulating the macroscopic theory of the electromagnetic field. They have the same significance in electromagnetics as Galileo's and Newton's laws in mechanics. This brave approach received experimental confirmation a quarter of a century later, when Heinrich Hertz, in 1888, established the existence of electromagnetic waves. However, one should bear in mind that this is a classic macroscopic theory and therefore cannot describe electromagnetic phenomena in the micro and nano world, at the level of atoms and molecules, the photoelectric effect, atom radiation, Casimir's effect, etc. One of the most important Maxwell's results is based on Faraday's law of electromagnetic induction; he succeeded in uniting time-dependent electric and magnetic fields, and demonstrated that they always exist simultaneously, as the electromagnetic field.



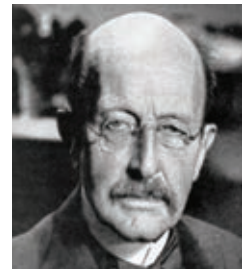


*Nikola Tesla*  
(1856 -1943)

Philosophers say, for example Feuerbach, „the point is to change the world, not to interpret it“. The man who is among the most credited for the transformation of the world regarding electromagnetism is undoubtedly Nikola Tesla. He succeeded, by transforming mechanical work into electromagnetism, to generate the *rotating magnetic field*, to create the alternating current, which could be transported at distance enabling its application in quotidian life. The first realization of this concept was at Niagara Falls, where the mechanical energy of water was transformed into electromagnetic energy. His creative process, based on the visualization of ideas, functioned by recognizing patterns in nature. He was called the „master of lightning“, because in his high-voltage constructions, he produced spark discharges propagating several meters and the phenomenon of electric discharge and lightning. Many famous personalities of the time enjoyed his experiments, among them Mark Twain, who rightly noticed „that thunder is impressive, however the lightning does all the work“. As a poet, he gave priority to light over sound. Tesla is responsible for many inventions based on electromagnetism; however, he is less known for his contributions to mechanics, i.e., mechanical engineering. He is the father of mechanical and electrical engineering unity in the form of synergy. However, he detected the existence of the Earth-Moon barycenter and based on this and some other facts, explained, in 1919, Moon’s rotation much better than astronomers of the time. He had unusual ideas regarding the „hypothetical velocity“, which is meaningful only in the system of absolute units, and is responsible for the phenomenon of biological life on Earth. He was considered a genius, yet also an eccentric, because in everyday life he behaved unconventionally according to the standards of his time (also according to contemporary standards). As an example, everything he did - ate, the way he walked, etc., had to be a multiple of three (Tesla, 1977). If, for example, the number of steps or the number of soup spoons he took, was not a multiple of three, he would repeat the activities, although sometimes this took him several hours. Tesla was an extraordinary creative author, unusual thinker, contemporary even today.

### **2.1.2. Photon, Light and the Origin of Quantum Mechanics**

The end of the 19 century and the beginning of the 20 century brought about the problem of radiation and its explanation in the domain of blue and UV radiation. Classical physics (Rayleigh-Jeans law) could explain this phenomenon in a satisfactory way in the domain of the visible spectrum up to the blue spectrum. As the remaining spectrum could not be explained, this was called the „ultraviolet catastrophe“. However, energy measurements per photon for  $\lambda = 400 \text{ nm}$ ,  $\lambda = 600 \text{ nm}$ ,  $\lambda = 800 \text{ nm}$ , showed that



*Max Planck,*  
(1858-1947)

energies  $E$  in all three cases are:  $4.96 \times 10^{-19}$  J;  $3.31 \times 10^{-19}$  J and  $2.48 \times 10^{-19}$  J. When we multiply  $E\lambda$ , the same values are obtained:  $19.8 \times 10^{-26}$  Jm;  $19.9 \times 10^{-26}$  Jm, and  $19.8 \times 10^{-26}$  Jm.

Since  $c_0 = \lambda\nu$ , this gives:

$$E = \frac{19.86 \times 10^{-26} \text{ Jm}}{\lambda} = \frac{19.86 \times 10^{-26} \text{ Jm}}{2.99 \times 10^8 \text{ m/s}} \times \nu = (6.626 \times 10^{-34}) \times \nu \text{ (J)}$$

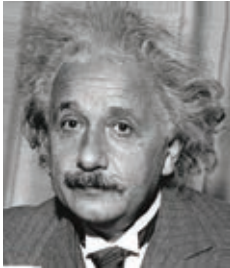
Therefore  $E = h\nu$ , where  $h = 6.626 \times 10^{-34}$  is the universal Planck's constant. Taking into account the number of photons of the same wavelength, energy is obtained as

$$E = n \times h\nu, \quad (2.8)$$

Energy is not continuous, it is executed in „portions“, *quanta*. This discovery opened the door to a new science, the *quantum mechanics*.

Planck realized that probability and indeterminism are at the fundament of this process. He could not accept this possibility entirely, probably because he saw that determinism is not the basis of the law of quantum radiation, and in private life, he was a very religious man. He determined the law of the black body radiation as a function of the wavelength  $\lambda$  and temperature  $T$  in the form:

$$\rho(\lambda, T) = \frac{8\pi hc}{\lambda^5} \frac{1}{e^{\frac{hc}{\lambda kT}} - 1}, \quad (2.9)$$



Albert Einstein  
(1879-1955)

The turning point in the apprehension of light's nature occurred in 1905, when Einstein provided the explanation of the photoelectric effect based on experiment. Starting from Planck's result that the black body radiates energy discontinuously, in energy quanta  $E = h\nu$ , Einstein founded the explanation of the photoelectric effect based on light absorption, on the same principles. Light waves do not propagate in space continuously, as water surface waves, because light energy is not distributed continuously along the wave front, but in „portions“ of light energy  $h\nu$ . It is assumed that in the photoelectric effect, one electron receives energy at the time of interaction only from one photon. During one interaction, the maximum energy that the electron can receive is equal to the energy of the photon quant ( $h\nu$ ). In order for the electron to be ejected from the material sample (metals were used at the time) after the collision with the photon, it has to have at least the energy equal to its output work ( $A_i$ ). If the electron receives from the photon energy smaller than the output work ( $A_i$ ), the photoelectric effect will not take place. Different output work corresponds to different metals - output work ( $A_i$ ) is e.g. for lithium 2.4 eV, for cesium 0.7 eV, etc. When the photon energy is greater than the output work ( $A_i$ ), the electron leaves the metal with a corresponding kinetic energy equal to the difference between the energy of the incident photon and the output work. Generally, it can be assumed that the photoeffect occurs when the photon interacts with the valence electron of the atom (the external shell), and the entire photon energy is transferred to one electron, thus the relation holds:

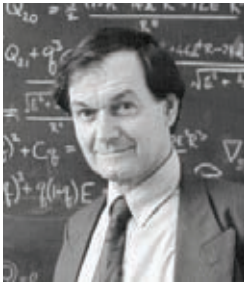
$$h \cdot \nu = E_{ion} + A_i + E_k, \tag{2.10}$$

where  $E_{ion}$  – is the atom ionization energy,  $A_i$  – output work of the electron ejected from the matter,  $E_k$  – kinetic energy of the photoelectron. As there are free electrons found in metals, Einstein disregarded the ionization energy ( $E_{ion}$ ), so that the energy of one photon is equal to the sum of the output work ( $A_i$ ) and the kinetic energy of the electron ( $E_k$ ):

$$h \nu = A_i + E_k, \tag{2.11}$$

This, simplified, Einstein’s equation, holds only for electrons that have received the entire photon energy, that is, for those electrons that have not lost part of their energy passing through metal layers. Regardless of this simplification, these results conform very well to experimental findings. Note that the interaction between the electron and the photon occurs *one-on-one*, so that light intensity does not affect the received energy of the electron, only the number of liberated electrons. It should be noted that the photoelectric effect was observed already by Hertz in 1887, who noticed that electrodes illuminated by ultraviolet radiation discharge a spark more easily.

Einstein was one of the founders, together with Bohr, De Broglie and Schrödinger, of the quantum mechanics, which will be explained in more detail in the next chapter describing the electron. He was awarded the Nobel Prize in 1921 for the photoelectric effect; he demonstrated that during the photoelectric effect energy is exchanged between the electron and the light quantum– the photon.



Sir Roger Penrose  
(1931- )

Within the theory of relativity, which was already initiated in 1887 by Fitzgerald and elaborated by Lorentz in 1899, Einstein formulated, in 1905, the hypothesis that a rigid body of mass  $m$  cannot reach the *velocity of light* and that in the three-dimensional space, for massive bodies, there is no greater velocity than the velocity of light. He introduced the concept of the invariant light velocity, because it remains constant, irrespective of the motion direction and sense of motion of the light source ( $\nu + c = c, c + c + c..... = c$ ). These proposed light features are still being discussed today, and there are scholars who question these results.

In a letter to Max Born, from 1926, Einstein wrote „Quantum mechanics is, undoubtedly, compelling. However, an inner voice tells me that this is not yet *the real thing*. The theory explains a lot, except it does not bring us any closer to the secrets of the *Old Man*. I, myself, am in every way convinced that He does not gamble“.

Penrose has defined a systematization of physics based on the three universal physical constants  $G, h,$  and  $c$ , similarly as Sommerfeld in 1916 determined the fine matter structure ( $1/\alpha = 137.0359$ ) (using electric charge, reduced Planck’s constant, and the velocity of light). Their relationship is defined in the absolute system of units by  $G \times h \times c = 1$  (gravitation, Planck’s constant, and the velocity of light). He started from Galileo’s physics,

because when it is viewed from the aspect of Planck's constant, it represents quantum mechanics, from the aspect of the gravitational constant the classical Newton's mechanics, and from the aspect of the light velocity Einstein's special theory of relativity (Penrose, 1997).

### 2.1.3. Universal Physical Constants: $G$ , $c$ and $h$

#### Gravitational Constant $G$

The gravitational force (attraction) between two bodies having mass  $M_1$  and  $M_2$  is given by the expression:

$$F = G \frac{M_1 M_2}{r^2}, \quad (2.12)$$

where :  $G$  – universal gravitational constant,  $r$  – distance between centers of mass  $M_1$  and  $M_2$ . Using the second Newton's law, force can be written as:

$$\vec{F} = m \vec{a}. \quad (2.13)$$

For a body at Earth's surface, by replacing  $m = M_k$  (sphere),  $a = g$  (acceleration of Earth's gravity  $9.806 \text{ m/s}^2$ ),  $M_z$  – Earth's mass,  $R_z$  – Earth's radius, it has been obtained:

$$g = \frac{F}{M_k} = G \frac{M_z}{R_z^2}, \quad (2.14)$$

thus, the universal gravitational constant is:

$$G = \frac{gR_z^2}{M_z} = \frac{9.806 \times (6.370 \times 10^6)^2}{6 \times 10^{24}} = (6.6 \pm 0.041) \times 10^{-11} \quad (\text{m}^3/\text{s}^2\text{kg})$$

which can be rewritten as:

$$G = (6.6 \pm 0.041) \times 10^{-11} \quad (\langle m / s^2 \mid m^2 / \text{kg} \rangle) \quad (2.15)$$

Using dimensional analysis, we observe that the universal gravitational constant is a synergy of acceleration ( $\text{m/s}^2$ ) as an external action on mass, and the specific surface mass density ( $\text{m}^2/\text{kg}$ ) at the interior of the surface interacting with environment.

#### Velocity of Light $c$

The velocity of light in vacuum was determined by multiple measurements (Galileo was the first to propose the measurement method, Danish astronomer Roemer was the first to succeed in measuring  $c$ , and the measurement corrections were made by the American scientist Michelson) :

$$c = 299\,792\,500 \pm 150 \text{ m/s},$$

while in different mediums light propagates with different velocities and can be, under certain circumstances, equal to zero.

Einstein correlated the velocity of light with mass, so that matter energy is

$$E=mc^2 \tag{2.16}$$

He modified the law on the conservation of momentum ( $m_1v_1+m_2v_2 = const.$ ) into the relativistic form by dividing the classical formula with the factor  $\sqrt{1-(v/c)^2}$ . The formula (2.16) found its experimental confirmation in nuclear reactions, in the so called mass defect. The internal energy of a system composed of mass  $m$  is  $mc^2$  and it is much greater than the energy, which this same mass has when moving with velocity  $v$  in the external three-dimensional space, because  $c$  is greater than  $v$ . The expression  $mc^2$  was confirmed by nuclear reactions; the energy liberated in nuclear reactions was equal to the defect of mass before and after the explosion, i.e.,  $E=(m_1-m_2)c^2 = \Delta mc^2$ , where  $m_1$  is the system mass before the nuclear reaction and  $m_2$  the system mass after the nuclear reaction, that is,  $\Delta m$  is the mass defect of the system. In other words, part of the system mass ( $\Delta m$ ) is transformed into energy, precisely the quantity that we obtain by multiplying with the square of the light velocity. Therefore, Einstein was right when he theoretically predicted the existence of this kind of energy, although many scientists were suspicious regarding the equation  $E = mc^2$ , and his entire work as well. Einstein's opponents challenged his results writing at the time that „a hundred most eminent scientists question Einstein“. It is said that Einstein replied coldly: „if they were right, only one scientist would be enough to challenge my results“. However, since „theory leads, and experiment decides“, after the „Manhattan“ project all involved in this debate were silenced forever, for different reasons: some, because the theory conformed to the experiment, and others, due to the fear of what this result implies. Unfortunately, Hiroshima and Nagasaki testify that this fear was justified.

Now it was possible to see that „mass“ energy and body's kinetic energy conform to the same physical law, because when the expression is expanded into a series according to the binomial formula, we obtain:

$$E_n = \frac{mc^2}{\sqrt{1-\frac{v^2}{c^2}}} = mc^2 + \frac{1}{2}mv^2 + \frac{3}{8}m\frac{v^4}{c^2} + \frac{15}{48}m\frac{v^6}{c^4} + \frac{105}{384}m\frac{v^8}{c^6} + \dots \tag{2.17}$$

The binomial formula of type  $(1-x^2)^{-1/2}$  was rigorously established in 1826 by Niels Henrik Abel, (1802–1829), although Newton already knew of the formula, while instead of the exponent „-1/2“ he used a positive integer or zero. This theorem on the binomial series, was used first by Hendrik Antoon Lorentz (1853–1928), later by Minkowski (Hermann Minkowski, 1864–1909), and finally by Einstein to establish the theory of relativity.

It can be seen that the second term of the series in the expression (2.17) takes the form of the kinetic energy

$$E_k = \frac{1}{2}mv^2 \tag{2.18}$$

and that the ordinary velocity ( $v$ ) and the velocity of light ( $c$ ), as a pair, are present in every term, except in the first and the second. This exception, existing still in formulas we use today, is a good pretext to go back to the roots of physics in the antiquity, because as Plato used to say „one is not One, two is hardly One” (Laertije, 1979), meaning that the energy of mass cannot be characterized only by the velocity  $v$  or by the velocity  $c$ , but by both of them simultaneously.

Einstein did not write the term  $\frac{1}{2}mv^2$  of the series in this form, he used the form  $m(v^2/2)$  (Einstein, 1916), disregarding the essence of the factor  $\frac{1}{2}$ . In this term,  $\frac{1}{2}$  does not refer to the velocity, i.e., to the square of velocity, rather to the rule regarding this term within the energy laws of nature. Formally and quantitatively, what Einstein wrote is true, however essentially and qualitatively it is wrong. In order to obtain true insight, simultaneously with *form* and *quantity*, we should observe the *essence* and *quality*, i.e., the other side of the problem. This associates of the tale of a mathematician and physicist traveling together by bus. During their journey, the mathematician asks the physicist at one moment what does he see on the hilltop, and the physicist replies that he sees a black sheep. The physicist was puzzled why the mathematician asked such a simple question with an obvious answer. Curious as to what the mathematician would answer to this same question, the physicist asked what he sees. The mathematician replied that he sees a sheep whose at least one side is black. The physicist wonders is this not the same answer as his, because it is logical, correct and simple, however then he realizes that his answer, although formally correct, was essentially incomplete, because he disregarded the *other side* of the existence he could not see, only imagine.

The mind, as a complex cognitive machine of the *conscious awareness* and the *subconscious*, leads to the insight of the existence of the other side of expression 2.17, which is:

$$E_n = \left\langle n \left| \begin{array}{l} \text{odd} \\ \text{even} \end{array} \right. \right\rangle! m \frac{v^n}{c^{n-2}} \quad \text{for } n = 0, 2, 4, 6, \dots, \quad (2.19)$$

and when developed into a series, we obtain:

$$E_n = \frac{0!}{!0} mv^0 c^2 + \frac{1}{2} m \frac{v^2}{c^0} + \frac{3}{8} m \frac{v^4}{c^2} + \frac{15}{48} m \frac{v^6}{c^4} + \dots, \quad (2.20)$$

where the first and the second term are quantitatively the same as in the expression 2.17, yet essentially different, meaning that the energy and mass status  $m$  are simultaneously and constantly defined by the speed  $v$  and the speed  $c$ .

We observe that for  $n = 0$ , the zero-th term contains a zero factorial, the right factorial „0!” and the left factorial „!0”, which can be denoted as  $\langle\langle ! \rangle\rangle$ . This is transformed expression 2.17, because in the formula we have a zero factorial and velocity  $v^0$ , (recall the conversation between the mathematician and the physicist; the other side of the sheep is not black- it has white spots). The role of the zero factorial in mathematics, and in mechanics as well (for the first time it appears with  $mc^2$ ) is not clear. The unity resulting from  $v^0$  is also mysterious, yet it can be comprehended because the term  $v^0$  can be written as  $v^0 = v/v = 1$ , giving for  $E_0$ :

$$E_0 = \langle (!) \rangle \frac{mv}{v} c^2. \quad (2.21)$$

The expression 2.21 signifies that there is a momentum  $mv$  within mass  $m$  effected by the velocity inverse to the velocity  $v$  ( $v^0 = 1 = v/v$ ), providing a synergic effect with velocity  $c$  - the invariant of space–time. The momentum defined by the speed  $v$  determines the internal state of mass  $m$ . In other words, mass is transformed into energy via the internal momentum possessed by mass, as a „trigger“ activating  $mc^2$ . The same is true for  $c^0 = c/c = 1$  in the second term of the expression 2.20 (matter is imbued by light-electromagnetism).

The *zero factorial* (it used to be written as  $0!$  which is actually the right zero factorial) is a great enigma of mathematics, and its physical interpretation is still more problematic. The value of the zero factorial is a *unity*, which is very strange. However, if this were not so the „world of mathematics“, as we know it today, would collapse as a „house of cards“. In other words, the equality of the zero factorial to 1 is „artificial“, although why is  $0! = 1$  nobody knows for sure. The factorial is related to the gamma function, which was introduced into mathematics by Leonhard Euler (1707–1783). For example, factorial of number 5 is  $5! = 1 \times 2 \times 3 \times 4 \times 5 = 120$ , and it represents the *right* factorial. Our renowned mathematician Đuro Kurepa (1907–1993) introduced the concept of the *left* factorial  $(!n)$  and proposed the hypothesis that the greatest common divisor of numbers  $n!$  and  $!n$  is number 2 (Kurepa, 1974).

In the equation 1.9,  $n$  factorials are  $0!, 2!, 4!, 6! \dots$ . In  $2!$  we have  $1 \times 2$ , then since 1 is an odd number, and 2 even, we obtain  $\frac{1}{2}$ . For  $4!$  we have  $1 \times 2 \times 3 \times 4$ , so the product of odd numbers is  $1 \times 3 = 3$ , and the product of even numbers is  $2 \times 4 = 8$ , giving  $3/8$ . In  $6!$  we have  $1 \times 3 \times 5 = 15$ , that is  $2 \times 4 \times 6 = 48$ , giving  $15/48$ . Here we encounter the phenomenon of „fracture“ of the factorial into values obtained as the product of odd numbers and the product of even factors of  $n!$ . Due to the fracture of the factorial  $n!$  and the phenomenon of self-similarity, we named this new science *fractal mechanics*. Everything is clear except  $0!$ , and the phenomenon of its fractality. Is this the question of the phenomenon of the ratio of the *left* to the *right* fractal in the term  $E_0$ , i.e.,  $1 = 0!/0 = \langle (!) \rangle$ ? What is the physical interpretation of this phenomenon? Does  $0!/0$  contain the law of the left and the right helix that we encounter in nature and in biology?

We observe that beside the „mass“ energy  $E_0$  and the kinetic energy  $E_2$ , there are terms that define new types of energy directly coupled with them. If we observe energy for  $n = 4$  we obtain:

$$E_4 = \frac{1 \times 3}{2 \times 4} m \frac{v^4}{c^2} = \frac{3}{8} m \frac{v^4}{c^2}. \quad (2.22)$$

For  $n = 6$  we have:

$$E_6 = \frac{1 \times 3 \times 5}{2 \times 4 \times 6} m \frac{v^6}{c^4} = \frac{15}{48} m \frac{v^6}{c^4}. \quad (2.23)$$

Energies  $E_4$  and  $E_6$  are energies at the Earth’s surface resulting from Earth’s motion around the Sun and the galactic motion of the Earth and the Sun, representing the

basis of the „hypothetical velocity“ put forward by Tesla, which „defines the lifeline“ of biological systems (Tesla, 1977, Koruga, 2007).

### Planck's Constant

Planck's constant, as already stated, originated as a result of the „ultraviolet catastrophe“ that occurred at the turn of the 20 century. The black body radiation energy in the domain of the blue and ultraviolet spectrum could not be explained in a satisfactory manner using the Rayleigh-Jeans energy law. Planck succeeded in 1900 to arrive at a satisfactory solution by introducing new hypotheses into classical mechanics (*first hypothesis*: energy of the oscillator changes discontinuously in precisely defined quanta, *second hypothesis*: quantum energy is proportional to the oscillating frequency and has a constant value). By using these hypotheses and fitting to experimental results, he arrived at the law, which is in complete agreement with experimental results across the entire interval of wavelengths and at all temperatures. All absolutely black bodies, at the same temperature, regardless of the atoms of which they consist, exhibit the same spectral curve.

Planck obtained the law of black body radiation in the form:

$$w_{\lambda} = f(\lambda, T) = \frac{2\pi hc^2}{\lambda^5} \frac{1}{e^{hc/kT} - 1} \left[ \frac{W}{m^3} \right] \quad (2.24)$$

where:  $h$  – Planck's constant:  $6.626 \times 10^{-34}$  Js,  $c$  – velocity of light:  $2.99779 \times 10^8$  m/s,  $k$  – Boltzmann's constant:  $1.380662 \times 10^{-23}$  J/K.

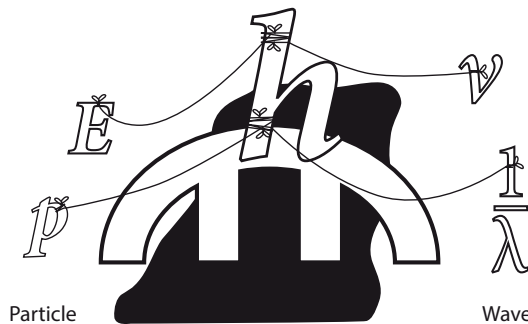
Now energy can be rewritten in the form

$$E = h\nu, \quad (2.25)$$

and momentum as

$$m\vartheta = \frac{h}{\lambda}, \quad (2.26)$$

thus linking the wave and the particle, so that Planck's constant, as the basis of the quantum action, can be considered the „bridge“ between the corpuscular-wavelike characteristic of matter and light.





## 2.2. Systematization of Physics by Penrose

Penrose is one of the world's leading mathematical physicists of today. He systematized physics (mechanics) based on  $G$ ,  $\hbar$  and  $c$  (Figure 2.1). He used the velocity of light as its inverse value ( $c^{-1} = 1/c$ ), which is from the phenomenological aspect, viewed in the absolute system of units, correct. As can be seen from Figure 3.3, two fields remain empty, i.e., two physics. One results from the synergy between classical and quantum mechanics, and the other is the result of synergy of the new physics (still nameless) with quantum field theory and general relativity. In this aspect, Einstein was right when he said that the quantum mechanics of his time „is not yet the *real thing*“.

Penrose affirmed the contribution of antiquity to modern science, by introducing into science the Platonic mathematical world (the world of Truth, Beauty and the Good) beside the physical and the mental world. These three worlds (physical, mental and Platonic) are not absolutely separated, only relatively independent, therefore, they constitute *one world*.

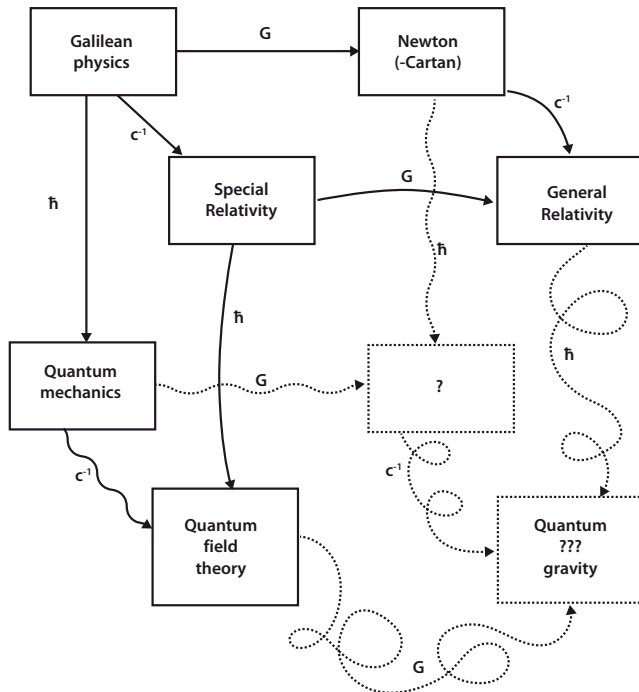


**Figure 2.1** Penrose's systematization of physics from Galileo to date, based on universal physical constants  $G$ ,  $h$ , and  $c$ . It can be observed from the displayed that we have yet to define two sciences, one based on the classical (Newton) and quantum mechanics (Schrödinger), and another based on quantum field theory, general relativity theory and this missing science (which we shall conditionally call fractal mechanics) (Penrose, 1997)

### 2.3. Light, 5D -Space and Fractal Mechanics

It is often said in everyday life, that an object is stable if it has at least three supporting points, which justifies the choice of universal constants  $G$ ,  $h$ , and  $c$  in science systematization. The missing science in Figure 2.1, in the field with question mark, could be fractal mechanics that should unify classical and quantum mechanics. In order to demonstrate this, we have to be acquainted with mathematical foundations of the gamma function.

#### Gamma Function

The gamma function was introduced into mathematics by the Swiss mathematician Euler in 1730, as a generalization of the factorial. Due to the importance of this interesting function for mathematics, it was investigated by Adrien-Marie Legendre (1752–1833), Carl Friedrich Gauss, (1777–1855), Joseph Liouville (1809–1882) and other renowned mathematicians of the 18 century.

Euler denoted the gamma function by  $\Pi(x)$ , while the symbol  $\Gamma(x)$  was introduced by Legendre in 1809. Gauss later accepted the notation  $\Gamma(x+1)$ , indicating that the gamma function satisfies the condition  $f(x+1) = x f(x)$ , giving  $\Gamma(n+1) = n\Gamma(n)$ .

The gamma function is written in the form of an integral:

$$\Gamma(n) = \int_0^{\infty} x^{n-1} e^{-x} dx, \quad (2.27)$$

Thus, for  $n = 1$  we obtain:

$$\Gamma(1) = \int_0^{\infty} x^{n-1} e^{-x} dx = \int_0^{\infty} x^0 e^{-x} dx = -e^{-x} \Big|_0^{\infty} = 1, \quad (2.28)$$

for  $n = 2$ ,  $n = 3$ ,  $n = 4$  and  $n = 5$ ,

$$\begin{aligned} \Gamma(2) &= 1\Gamma(1) = 1 \times 1 = 1! \\ \Gamma(3) &= 2\Gamma(2) = 2 \times 1\Gamma(1) = 2 \times 1 \times 1 = 2 \times 1 = 2! \\ \Gamma(4) &= 3\Gamma(3) = 3 \times 2\Gamma(2) = 3 \times 2 \times 1\Gamma(1) = 3 \times 2 \times 1 = 3! \\ \Gamma(5) &= 4\Gamma(4) = 4 \times 3\Gamma(3) = 4 \times 3 \times 2\Gamma(2) = 4 \times 3 \times 2 \times 1 = 4! \end{aligned}$$

Generally, it can be written:

$$\Gamma(n + 1) = n! \quad (2.29)$$

This implies one of the strangest results in mathematics, because when calculating the value of the function for  $n = 0$ , we obtain

$$\Gamma(0 + 1) = \Gamma(1) = 1 = 0!$$

Until 1974, this symbol was called *factorial*, however, our renowned mathematician Kurepa (Kurepa, 1974) introduced the general concept of the left and the right factorial, and in 2012 we proposed that the *zero factorial* (Koruga, 2012) be defined as:

$$\langle ! \rangle = \frac{0!}{!0} = \frac{\Phi - \phi}{e^{i\pi}(\phi - \Phi)} = \frac{1.61803 - 0.61803}{e^{i\pi}(0.61803 - 1.61803)} \equiv 1, \tag{2.30}$$

So that  $E_0$  in the expression 2.20 becomes:

$$E_0 = \langle ! \rangle mv^0c^2 = \frac{1.61803 - 0.61803}{e^{i\pi}(0.61803 - 1.61803)} \times \frac{mv}{v} \times c^2, \tag{2.31}$$

showing that mass  $m$  includes momentum  $mv$ , moving by the speed inverse to the speed  $v$  in  $mv$  (because  $v^0=1=v/v$ ), providing the synergic effect with speed  $c$  - the invariant of space-time.

In general, the factorial can be written as:

$$n! = n(n-1)!, \tag{2.32}$$

giving:

$$\begin{aligned} 3! &= 3 \times 2! \\ 4! &= 4 \times 3! \\ 5! &= 5 \times 4! \end{aligned}$$

This demonstrates the memorial evolutionary thread of the factorial system; each factorial contains the preceding factorial and itself:  $3! = 2! \times 3$ ,  $4! = 3! \times 4$ , etc.

The gamma function belongs to the category of special transcendental functions significant in number theory.

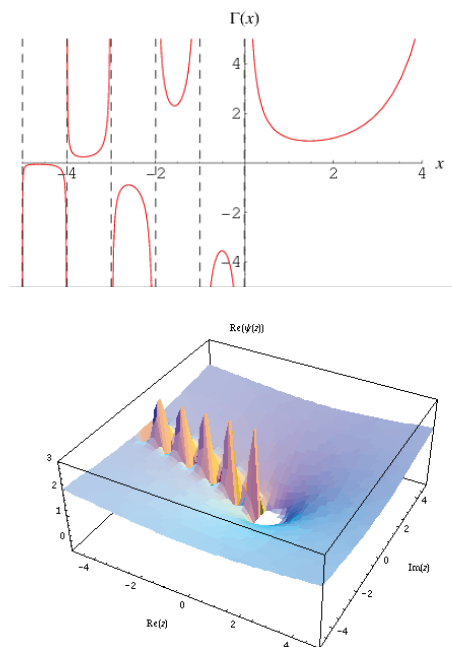
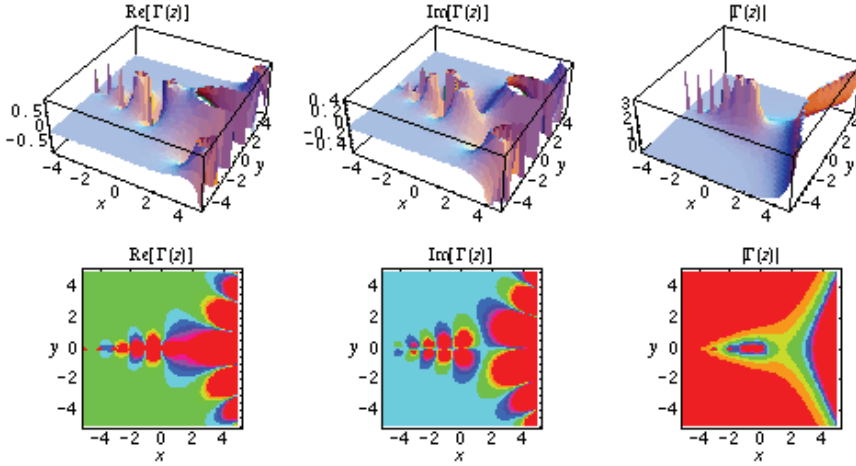


Figure 2.2 Graphical representation of the function  $G(x)$  in the plane (above) and the complex function  $G(z)$  (below).



**Figure 2.3** Three-dimensional representation of the  $G(z)$  function: real, imaginary and complex (above), and in the  $x,y$  plane (below) (Havil, 2003).

### **Gamma Function and Space Coding**

In the  $n$ -dimensional space, the radius is calculated using the Pythagorean distance, which for the Euclidean space has the quadratic form:

$$x_1^2 + x_2^2 + x_3^2 + \dots + x_n^2 = r^2, \quad (2.33)$$

while for the  $n$ -dimensional sphere with the radius  $r^n$ , the sphere volume is:

$$V_n(r) = C_n r^n. \quad (2.34)$$

Calculating  $C_n$  for a surface area, that is, a two-dimensional space,  $n = 2$ , and for volume- the three-dimensional space,  $n = 3$ , is easy, because we know all the constitutional elements of  $V_n$ . For  $n = 2$ ,  $V_2 = C_2 r^2$ , and knowing that circle surface is  $P = r^2\pi$ , we obtain  $C_2 = \pi$ . Similarly for  $n = 3$ , because volume of the sphere is  $V_3 = 4/3 r^3\pi$ , giving  $C_3 = 4/3 \pi$ . What is the value of  $C_1$  or  $C_4$ ? It cannot be deduced in this way; we have to find a general rule to calculate the  $C_n$  value for the  $n$ -dimensional sphere.

A general rule for calculating a space of different dimensions is obtained using the function  $\Gamma(1/2)^n$  (Hamming, 1986):

$$\left[\Gamma\left(\frac{1}{2}\right)\right]^n = \pi^{\frac{n}{2}} = \int_0^\infty e^{-r^2} \frac{dV_n(r)}{dr} dr = C_n \int_0^\infty e^{-r^2} nr^{n-1} dr \quad (2.35)$$

Based on the expression 2.35, the rule for computing unit spheres of the  $n$ -dimensional space is given by the expression:

$$C_n = \frac{\pi^{\frac{n}{2}}}{\Gamma\left(\frac{n}{2} + 1\right)} \quad (2.36)$$

that is:

$$C_n = \frac{2\pi}{n} C_{n-2} \tag{2.37}$$

Based on expression 2.37, and starting from  $n = 2$  and  $n = 3$ , where  $C_2 = \pi$  and  $C_3 = 4\pi/3$ , Hamming obtained, in 1986, values for unit spaces of dimension  $n = 1, n = 4, n = 5, n = 6$  and  $n = 7$ . We can observe, from the Table 2.1, that the maximum value of the unit sphere corresponds to the  $n = 5$  dimension. If the unit sphere had some kind of capacitance, this would be one of the favored cosmic dimensions.

**Table 2.1** *Known values of unit spheres based on expression 2.37 (Hamming, 1986).*

<b>n</b>	<b><math>C_n</math></b>	<b>Value</b>
$2k$	$\pi^k/k!$	$\rightarrow 0$
...	....	.....
7	$16\pi^3/105$	4.724
6	$\pi^3/6$	5.167
5	$8\pi^2/15$	5.263
4	$\pi^2/2$	4.934
3	$4\pi/3$	4.188
2	$\pi$	3.141
1	2	2.000

If we continue calculations of unit sphere values, under the condition that the rule of symmetry holds (symmetry element of inversion), for  $n = 0$ , we obtain  $C_0$  as

$$C_0 = \frac{2\pi}{n_0} \times C_{-2} = 1 \rightarrow n_0 = 2\pi \times \frac{1}{\frac{4\pi}{3}} = 3/2, \tag{2.38}$$

giving the values for the remaining dimensions, as shown in Table 2.2 (further on in text, dimension will be denoted by a capital N, and its dimensionality as Möbius strip by  $n$ ). In mathematics, dimension  $N = 0$  is a point, which is, since the time of Euclid (Euclid „Elements“, 1949), defined as an entity „that has no parts“. However, based on the gamma function, we can observe that this is an entity *whose division is senseless*, implicating the nonlocality phenomenon ( $V_0 = C_0 r^0 = 1 \times 1 = 1$ ), *because* regardless of  $r$ , the entirety of the system is given in the unit sphere  $C_0$ . The universal physical constants for dimension  $N = 0$ , its unit sphere and unit spheres of the remaining dimensions, except dimension  $N = 1$ , are:  $G = 1, h = 1, c = 1$ , that is  $Ghc = 1$  (the idea to use these three universal physical constants for the absolute system of units stems from Planck, Wheeler accepted it in 1975, and in 1994 Penrose). Sphere-packing (especially of unit

spheres) represents the basis of coding, and relates information theory and the entropy physics (information physics).

**Table 2.2** Positive and negative space dimensions as Möbius strip  
(Koruga 2012, adapted from Koruga, 1993).

Dimension N	Unit sphere $C_n$	Dimensi- onality n	Value of the unit sphere through $\pi$	Value of the unit sphere
N = 6	$C_6 = \frac{2\pi}{n} \cdot C_4 = \frac{2\pi}{6} \cdot \frac{\pi^2}{2}$	6	$\frac{\pi^3}{6}$	5.1677
N = 5	$C_5 = \frac{2\pi}{n} \cdot C_3 = \frac{2\pi}{5} \cdot \frac{4\pi}{3}$	5	$\frac{8\pi^2}{15}$	5.2637
N = 4	$C_4 = \frac{2\pi}{n} \cdot C_2 = \frac{2\pi}{4} \cdot \pi$	4	$\frac{\pi^2}{2}$	4.9348
N = 3	$C_3 = \frac{2\pi}{n} \cdot C_1 = \frac{2\pi}{3} \cdot 2$	3	$\frac{4\pi}{3}$	4.1887
N = 2	$C_2 = \frac{2\pi}{n} \cdot C_0 = \frac{2\pi}{2} \cdot 1$	2	$\pi$	3.1415
N = 1	$C_1 = \frac{2\pi}{n} \cdot C_{-1} = \frac{2\pi}{1} \cdot \frac{1}{\pi}$	1	$2\pi^0 = 2$	2.0000
N = 0	$C_0 = \frac{2\pi}{n} \cdot C_{-2} = \frac{2\pi}{3/2} \cdot \frac{1}{4\pi/3}$	3/2	$\frac{1}{\pi^0} = 1$	1.0000
N = -1 <sub>4</sub>	$C_{-1} = \frac{2\pi}{n} \cdot C_{-3} = \frac{2\pi}{4} \cdot \frac{2}{\pi^2}$	4	$\frac{1}{\pi}$	0.3183
N = -2 <sub>5</sub>	$C_{-2} = \frac{2\pi}{n} \cdot C_{-4} = \frac{2\pi}{5} \cdot \frac{15}{8\pi^2}$	5	$\frac{1}{\frac{4\pi}{3}}$	0.2387
N = -3 <sub>6</sub>	$C_{-3} = \frac{2\pi}{n} \cdot C_{-5} = \frac{2\pi}{6} \cdot \frac{6}{\pi^3}$	6	$\frac{1}{\frac{\pi^2}{2}}$	0.2026
N = -4 <sub>7</sub>	$C_{-4} = \frac{2\pi}{n} \cdot C_{-6} = \frac{2\pi}{7} \cdot \frac{105}{16\pi^3}$	7	$\frac{15}{8\pi^2}$	0.1899

Table 2.2 shows that dimensions N=0 and N=1 are independent (although they are inversely related by  $\pi^0$  of their unit spheres), and all the remaining dimensions depend on N=0, because they are created by duplication in N=0 (N=2 has its pair in N=-1<sub>4</sub>, N=3 has its pair in N=-2<sub>5</sub>, etc.).

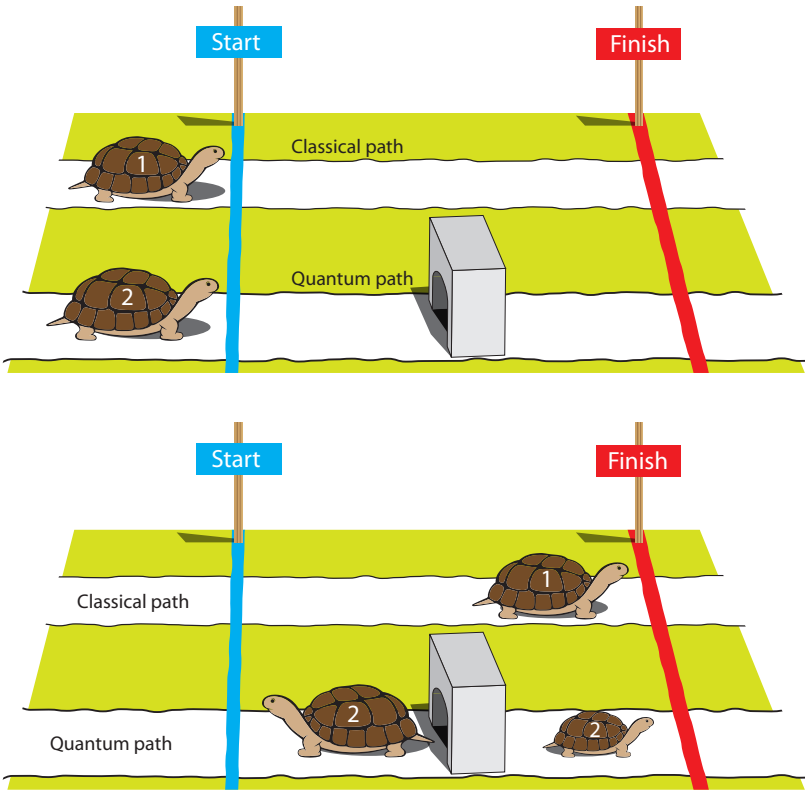


**Figure 2.4** Illustration of the difference between classical and quantum mechanics by the example of two turtles travelling two different paths: one travelling the classical path, and the other taking the quantum path (above). The turtle on the classical path arrives unchanged at the finish (below). However, at the quantum path there is a „quantum tunnel“, duplicating the turtle No. 2. One turtle arrives at the finish slightly modified (it is smaller), while the other, that has returned to the start, is bigger (but is in a reverse position with respect to the turtle that has arrived at the finish).

Therefore, if we observe dimension  $N = 3$ , it is united with dimension  $N = -2_5$ , because it is generated by  $N = 0$  ( $N(3) \times N(-2_5) = N(0)$ , i.e.,  $4.1887 \times 0.2387 = 1$ ). This can be illustrated by Figure 2.4, where two turtles start at the same time from the starting position; one is traveling a classical path (classical mechanics), and the other turtle is taking the quantum path (quantum mechanics). At the finish of the race, the turtle on the classical path remains the same, while the turtle on the quantum path is modified. It is duplicated, because it travelled the quantum tunnel, so the turtle that arrives at the start ( $N = -2_5$ ), with respect to the turtle that has arrived at the „finish“ ( $N = 3$ ) is somewhat larger. This is because the turtle returning to the start position has dimensionality 5 and the turtle at the finish dimensionality 3. At the fundament of this phenomenon

is dimension  $N = 0$  that has fractal dimensionality  $n = 3/2$ . Therefore, physical phenomena which are related to dimension  $N = 0$ , that is dimensionality  $n = 3/2$ , belong to the domain of *fractal mechanics*, as the missing science that should unify classical and quantum phenomena.

From Table 2.2, we observe that the rule holds:

$$N_{(n)} \times (1 - n)N_{(n+2)} = N(0), \quad (2.39)$$

which can be rewritten as:

$$\langle N_{(n)} | (1 - n)N_{(n+2)} \rangle. \quad (2.40)$$

Distribution of the gamma function can be expressed using parameters  $k$  and  $\theta$

$$f(x; k, \theta) = x^{k-1} \frac{e^{-\frac{x}{\theta}}}{\theta^k \Gamma(k)} \text{ for } x > 0 \text{ and } k, \theta > 0 \quad (2.41)$$

With respect to parameters given in the expression 2.41, graphical representation is given in Figure 2.5:

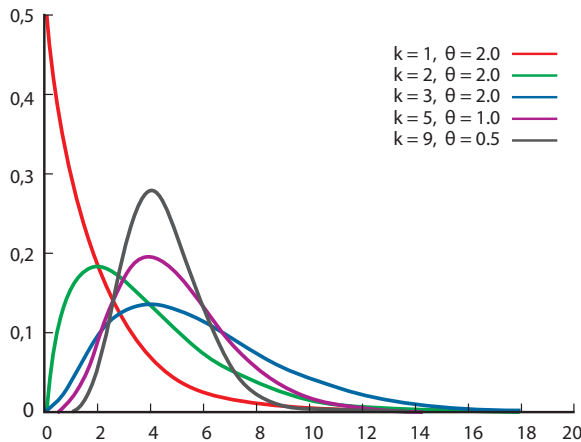


**Figure 2.5** Distribution of the gamma function depending on parameters  $k$  and  $\theta$ .

It can be observed in Table 2.2 that the maximum value of the unit sphere corresponds to  $n = 5$ , therefore, two scenarios are possible for the origin of spaces with lower dimension,  $n < 5$ : (1) that  $n = 5$  was first created from  $n = 0$ , and later on from  $n = 0$  the „smooth“ reduction established  $n = 4$  and  $n = 3$ ; (2) „cascade“ reduction into  $n = 4$  and  $n = 3$ .

Schematic representation of the „cascade“ transformation of dimension  $N = 5$  into lower dimensions is given in Figure 2.6.



**Table 2.3** Space of dimension  $n$  based on the „smooth“ and „cascade“ transformation of dimension  $N = 5$  into lower dimensions.

$nD^5$ values					
$5D^5$	$4D^5$	$3D^5$	$2D^5$	$1D^5$	0
$\frac{8\pi^2}{15}r^5$	$\frac{8\pi^2}{3}r^4$	$\frac{32\pi^2}{3}r^3$	$32\pi^2r^2$	$64\pi^2r^1$	$64\pi^2r^0$
$nD^n$ : values $V^n$ and $P^n$					
$5D^5$	$4D^4$	$3D^3$	$2D^2$	$1D^1$	$0D0$
$\frac{8\pi^2}{15}r^5$	$\frac{\pi^2}{2}r^4$	$\frac{4\pi}{3}r^3$	$\pi r^2$	$2\pi^0r^1$	$\frac{1}{\pi^0}r^0$
$\frac{8\pi^2}{3}r^4$	$2\pi^2r^3$	$4\pi r^2$	$2\pi r$	$2\pi^0 = 2$	$\frac{0!}{\pi^0} = 1$
Ratio $V: nD^5 / nD^n$					
1	$\frac{16}{3}$	$8\pi$	$32\pi$	$32\pi^2$	$64\pi^2$
Ratio $P^{n+1}V_n/V_n$					
$P^6V_5/V_5$	$P^5V_4/V_4$	$P^4V_3/V_3$	$P^3V_2/V_2$	$P^2V_1/V_1$	$P^1V_0/V_0$
$\frac{\pi^3r^5}{8\pi^2r^5} = \frac{15}{8}\pi$	$\frac{\frac{8\pi^2}{3}r^4}{\frac{\pi^2}{2}r^4} = \frac{2}{3}8$	$\frac{2\pi^2r^3}{\frac{4}{3}\pi r^3} = \frac{3}{2}\pi$	$\frac{4\pi r^2}{\pi r^2} = 4$	$\frac{2\pi r^1}{2\pi^0r^1} = \pi$	$\frac{2\pi^0r^0}{\frac{1}{\pi^0}r^0} = 2$
5.8904	5.3333	4.7123	4	3.1415	2

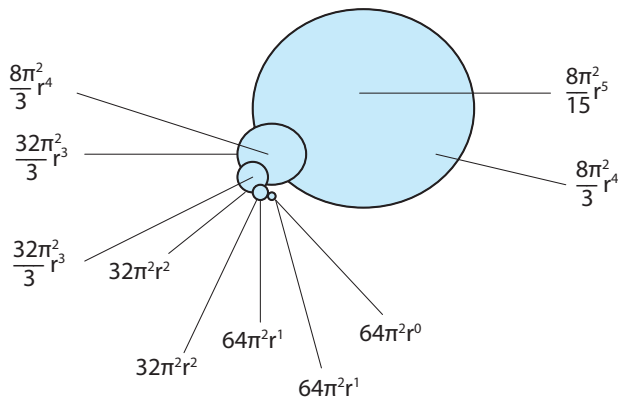


**Figure 2.6** Schematic representation of the „cascade“ transformation of dimension  $N = 5$  into lower dimensions.

### Space-Time Based on the Gamma Function

It is known that Einstein was not taken by the Big Bang theory, thus he did not consider this approach in his work. However, Hawking and Penrose showed that the general theory of relativity results in a possibility that the Universe originated with Big Bang, although the theory cannot forecast what was created by the Big Bang. Einstein's general relativity theory transformed the passive *space* and *time* into active factors of the Universe dynamics, by demonstrating (together with Hilbert) that what we consider to be a gravitational field is actually a curvature of space–time.

According to the physics of the four-dimensional space–time described with

$$x_1^2 + x_2^2 + x_3^2 - [(ct)]^2 = 0 \quad (2.42)$$

we observe that time  $t$  is a cofactor of the fourth dimension together with the speed of light  $c$  (dimensionally  $c \times t = s \times (m/s) = m$ ). According to the results from Table 2.2 we can describe the four-dimensional space–time in the form:

$$x_1^2 + x_2^2 + x_3^2 + [(-1_4)]^2 = 0 \quad (2.43)$$

and the five-dimensional space–time as:

$$\begin{aligned} x_1^2 + x_2^2 + x_3^2 + [(-1_4)]^2 + [(-2_5)]^2 &= 0 \\ x_1^2 + x_2^2 + x_3^2 - [(ict)_4]^2 - [(i\kappa\nu)_5]^2 &= 0 \end{aligned} \quad (2.44)$$

where  $i = \sqrt{-1}$  (*rotator*),  $\kappa$  is the space–time code (*scenario* – resembling DNA in biological systems, where according to the DNA *scenario*, an organism is created from the fertilized ovum), of dimension  $ms$  (direct unity of space and time, i.e., spacetime),  $\nu$  is the frequency  $s^{-1}$ .

According to quantum field theory (Ryder, 1985), the dimension of mass  $m$  can be calculated using the expression 2.45:

$$d_m = \frac{n}{2} - 1, \quad (2.45)$$

giving for  $n = 5$  :

$$d_m = \frac{n}{2} - 1 = \frac{5}{2} - 1 = \frac{5-2}{2} = \frac{3}{2}, \quad (2.46)$$

Value  $3/2$  is the value of dimensionality for  $n = 0$ , so that mass in a three-dimensional space is represented by dimension  $n = 0$ , through the reduction of  $n = 5$  into  $n = 3$ . According to Hawking, and based on the gamma function (expression 2.11), „information on quantum states in a space-time domain can be coded at the domain boundary being two dimensions smaller“. Mass, with characteristic  $3/2$  (fractal mass), is a direct reduction entity of dimension  $n = 5$  into  $n = 3$ , since both of them, as space, originated from  $n = 0$ . The reduction of the space of dimension  $n = 5$  into  $n = 3$  originating from  $n = 0$ ,

can be written in the form  $| 0 \uparrow 5 \downarrow 3 |$ , that is: from the dimension  $N = 0$  dimension  $N = 5$  is created, which is reduced to dimension  $N = 3$ .

Another reduction entity of the  $N = 5$  dimension space into  $N = 3$  is indirect, via  $N = 4$ , and corresponds to the photon (light). Photon is today one of the biggest enigmas of science. When, 55 years ago, Einstein was asked what a photon is, he replied: „Many physicists think that they know what is a photon, while I, who devoted most of my time to the study of light, do not know what a photon is. It would also be nice to know what an electron is“. A satisfactory answer is sought constantly, especially based on direct measurements.

However, based on the formula 2.45, photon, as a reduction entity of  $N = 5$  into  $N = 4$ , has a reduction mass of dimension  $d_m = (n/2) - 1 = 4/2 - 1 = 1$  (photon), resulting in its feature of a vibrating „string, cylinder“ (similarly to chords on the guitar or violin). Therefore, photon’s duality of wave and particle is natural. This can be written in the form  $| 0 \uparrow 5 \downarrow 4 \downarrow 3 |$ , that is  ${}^{3/2}[\uparrow \downarrow_1 \downarrow]$ , because  $d_m(4) = 1$ .

The diameter of the photon string is of Planck’s length  $l_p = 1.6163 \times 10^{-35}$  m, and string length ( $l_{ph}$ ) is the product of time since the creation of  $N = 5$  from  $N = 0$  (Planck’s time,  $5.35 \times 10^{-43}$  s) until the establishment of a reduced mass with transition time of  $N = 5$  into  $N = 4$  ( $137.438 \times 10^9$  s). This time corresponds to the phase transition (about 300 000 years after the transition  $n = 0 \rightarrow n = 2 \rightarrow n = 3 \rightarrow n = 4 \rightarrow n = 5$ ), i.e., to the time when light, as a 5D phenomenon, was established as a new entity, and, through dimension reduction, penetrated into the 3D space filled with mass  ${}^{3/2}[\uparrow \downarrow]_m$  of separated electrons and protons. The minimum value of the photon string, i.e., the wavelength, is:

$$l_{p_h} = (t_p \times t_R) \times c = (5.35 \times 10^{-43} \times 1.37 \times 10^{11}) \times 2.997 \times 10^8 = 2.2 \times 10^{-22} \text{ (m)} \quad (2.47)$$

and the maximum string frequency is  $\nu = 1.4 \times 10^{30} \text{ s}^{-1}$ . The photon string can vibrate with various frequencies, depending on its energy given by Planck’s relation  $E = h\nu$ .

In order to organize the mass  ${}^{3/2}[\uparrow \downarrow]_m$  (which was in the form of electrons and protons in 3D) and create more complex structures (atoms), light (photons) was captured. This capturing reestablished the unity of dimensions  $N = 0$  and  $N = 1$  resembling their original state (attraction). While the original unity of  $N = 0$  and  $N = 1$  was direct, now in a repulsive state it is indirect in  $N = 4$ , via the transformed dimensions from  $n = 0$  and  $n = 1$  of *photons* (wavelike-corpuseular entities with electromagnetic characteristics  $\lambda$ ) and of *mass* (corpuseular-wavelike entity with  $\lambda$ , having mass (De Broglie’s) wavelength  $\Lambda$ ).

## 2.4. Five-Dimensional Light Nanotechnology

The idea of the existence of the *fifth dimension* is about 100 years old. Even before Einstein published his general relativity theory in 1915, Finish scientist Gunar Nordstrom published in 1914 a paper entitled *On the Possibility of Simplification and Unification of the Electromagnetic Field and the Gravitation Field* (Nordstrom, 1914), where he attempted the unification of electromagnetism and gravitation by adding to Maxwell’s



Gunar Nordström  
(1881–1923)



Theodor Kaluza  
(1885–1954)

tensor theory of electromagnetism a scalar gravitation theory. This was not a very adequate solution, so that his idea, although revolutionary at the time, was later forgotten.

A breakthrough regarding the idea of five-dimensionality was made by Theodor Kaluza from the University u Königsberg, Germany (today Kaliningrad, in Russia), when, in 1919, he sent to Einstein his paper entitled „On the Problem of Unity in Physics“ (Kaluza, 1919). Kaluza started from the decomposition of five coordinates  $x^i$  into four  $x^\mu$  and one  $x^5$ , which implied the decomposition of the metric tensor  $g_{ij}$  into three groups:  $g_{\mu\nu}$ ,  $g_{\mu 5}$  and  $g_{55}$ . The idea was to describe the graviton and photon with ten components  $g_{\mu\nu}$  of the metric tensor (gravitation) and four components  $g_{\mu 5}$  (electromagnetism). Since the Riemann metric tensor (mathematical basis of Einstein’s gravitation theory) can be formulated in arbitrary many dimensions, this was used by Kaluza to transform Einstein’s four-dimensional gravitation theory with electromagnetism, into a five-dimensional theory. With respect to Einstein’s and Maxwell’s theory, his theory had a „small addition“:  $g_{55}$ . This supplement shocked Einstein, because it resulted in  $g_{55} = -1$ , leading to multiples of the fifth dimension („the cylindrical condition“), so that Einstein’s gravitation theory was at the same time transcended and preserved (Hegel’s *Aufgehoben*). In other words, Kaluza proposed an elegant solution, where Einstein’s and

Maxwell’s field are emerged in Kaluza’s five-dimensional metric field. Einstein was shocked by the elegance of the solution, that is, by the idea that by adding another dimension to the four-dimensional gravitation, electromagnetism and gravitation can be united. If gravitation is a four-dimensional phenomenon, does this mean that light is a five-dimensional phenomenon? Planck’s radiation law points also to this solution, because the wavelength ( $\lambda$ ) is of the fifth degree  $\lambda^5$  (Expression 2.24), so that space metrics of light  $m^5$ , corresponds to the five-dimensional physical space. Kaluza considered that light occurs as a perturbation at the surface of the five-dimensional sphere caused by its wrinkling, dynamic folding („prominences and depressions“). However, no one knew the size of this sphere. Oscar Klein, the Swedish physicist, improved Kaluza’s theory in 1926, postulating that the fifth dimension is curled (closed in a circle, resulting from Kaluza’s condition of „cylindricity“) at the quantum level, so that quantum mechanics could be the explanation. After calculations were performed, the sphere size was obtained at the level of Planck’s length ( $1.6162 \times 10^{-35}$  m). This is corroborated by experimental findings that the elementary charge is  $q = 1.602 \times 10^{-19}$  C and that the gravitational constant is  $G = 6.674 \times 10^{-11} \text{Nm}^2\text{kg}^{-2}$ , so that, based on small perturbations (of the metric tensor) associated with electromagnetic field (Klein-Gordon equation), we obtain:



Oscar Klein  
(1894–1977)

$$\frac{cq}{2\sqrt{G}} = \frac{h}{r_5} \tag{2.48}$$

where  $r_5 \approx 10^{-35}$  m. Consequently, the radius of the fifth dimension has to be of the order of Planck's length, in order to generate elementary charge obtained from the experimental measurements. Because we still cannot measure  $10^{-35}$  m (today, the most accurate measurement is of the order  $\sim 10^{-18}$  m), this is indirect evidence that the fifth dimension, based on the Kaluza–Klein approach, is of the order of Planck's length.

However, we can see in Table 2.2 that the fifth dimension occurs at two instances, in  $N = 5$  and in  $N = -2_5$ . The Kaluza–Klein approach refers to the fifth dimension which is given as  $N = 5$ . Nevertheless, we have demonstrated that the fifth dimension exists as  $N = -2_5$  solution, and it is directly coupled with  $N = 3$ , through  $N = 0$ . In other words, dimension  $N = 3$ , by itself would be „nothing“. However, in this way it is not „empty“ because it is impregnated by  $N = -2_5$ , so there exists „something“. Therefore, our three-dimensional space is filled with five-dimensional contents reduced by two dimensions. Could this finding be used for a technological solution? The answer is positive; one possible solution is to take three entities having a space characteristic (unit in meters) e.g., the light wavelength. Two dimensions are missing that should represent the „reduction“ of light. These can be two types of light polarization, horizontal ( $\leftrightarrow$ ) and vertical ( $\updownarrow$ ). In this way, we correspond features of  $N = -2_5$  to light as an ordered set of 5D entities (photons).

The first technological realization of the five-dimensional light nanotechnology as  $[-2_5]$  (Table 2.2) was realized in 2009 by the Australian scientists (Zijlstra et al, 2009) from the Swinburne University of Technology. This nanotechnologic solution was obtained independently from the results of our investigations that were published for the first time in 1991 (Koruga, 1991), and subsequently in 1993 (Koruga et al, 1993). They used golden nanorods (45nm –65nm) to provide the orthogonality of data input/output in the 3D space in all directions, and in two orthogonal polarized directions. For their solutions, they used light with three wavelengths: 700 nm, 840nm, and 980 nm, and two orthogonal polarizers for three lights (which is equivalent to the horizontal and vertical polarization). They succeeded in constructing an optical multipixel system of information capacity of  $10^{12}$  bits  $\text{cm}^3$  (1 Tbit  $\text{cm}^{-3}$ ).



**Figure 2.7** The first five-dimensional memory of 1 Tbit/cm<sup>3</sup>, based on the use of three wavelengths and two polarized lights (Zijlstra et al, 2009).

## 2.5. Five-Dimensionality of Light and Levitation

If our 3D space is filled with „something“ like  $\langle -2_5 \rangle$  objects (five-dimensional, at the level of Planck's length), is it possible, by localization of a very small 3D space, to provoke this contents, so that we would have the impression that we have „created“ the photon? Beside this photon creation illusion („creation illusion“ because it is already present, although minute and dark, so that it cannot be seen) the levitation phenomenon should also occur, because in  $\langle -2_5 \rangle$  we have a minus, negativeness, opposite to gravitation as positive in  $N = 3$ . Since the Kaluza–Klein theory unified electromagnetism and gravitation at the level of Planck's length, and the above described phenomenon was determined, it would be expected that in a very small space (distance) the levitation effect occurs that could be experimentally measured. As is known, Planck's length is very small ( $\sim 10^{-35}$  m) so that there has to be a large number of  $\langle -2_5 \rangle$  entities in this small space. Today, it is technologically feasible to construct two nano/pico smooth plates, best of gold, with perfect one-atom smoothness (uniformly level) and place them in a vacuum at a very low temperature (only a few K). The experiment should be an improved variant of the experiments measuring Casimir's force (Munday, 2009). Of course, all positive features of previous experiments should be respected, yet all „ill-defined conditions“ resulting from the influence of material and measuring circumstances during experiment should be eliminated.

The levitation caused by  $\langle -2_5 \rangle$  is a method to eliminate the influence of the gravitation force. The levitation possibility has been confirmed by experiment, although it has not been explained adequately. We offer an explanation of the levitation effect based on the interaction between gravitation ( $N = 3$ ) and electromagnetism ( $N = -2_5$ )

$$\frac{N(3)}{N(-2_5)} \begin{pmatrix} \downarrow \\ \uparrow \end{pmatrix} \quad (2.49)$$

As the interaction intensity between two masses regarding gravitation and magnetism decreases with the square of distance in 3D, in the synergy, the interaction between the macroscopic  $mg$  and the five-dimensional unit sphere  $(8/15)\pi^2$  (Table 2.2) will be inverse. Consequently, for the absolute unit system (holding for all unit spheres because they have all originated from the zero-th dimension, except the one-dimensional space)  $Ghc = 1$ , that is  $1/G = hc$ , this interaction is defined with inverse square of distance ( $d^2$ ), because the levitation takes place in the three-dimensional space.

$$mg = \frac{8hc\pi^2}{15d^2} \quad (2.50)$$

Therefore, the maximum distance ( $d$ ) can be calculated between two unit plates to create the levitation effect of the upper plate (body) of  $1 \mu g$

$$d = \pi \sqrt[2]{\frac{8hc}{15mg}} = \sqrt[2]{\frac{8 \times (6,626 \times 10^{-34}) \times (2,99 \times 10^8)}{15 \times 9,81 \times 10^{-6}}} \approx 100 \text{ pm.} \quad (2.51)$$

However, a body having Planck’s mass  $2 \times 10^{-8} \text{ kg}$  levitates at a distance of approximately 1 nm from the base plate.

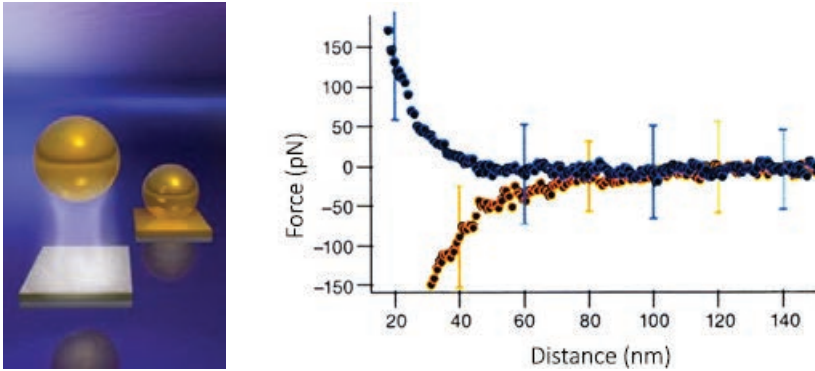


**Figure 2.8** Levitation of a golden ball interacting with silicon plate (left). Experimental result of attractive repulsive forces in the levitation process (right). It can be seen that the levitation effect, under these conditions, occurs at a distance of approximately 32 nm, and that it is maintained up to 140 nm (Munday et al, 2009).



This phenomenon can be applied to cogwheels at the micro-nano level, because the repulsive material characteristic prevents contact between cogwheels, eliminating friction.

The described approach is in very good agreement with the phenomenon observed by Casimir (Hendrik Brugt Gerhard

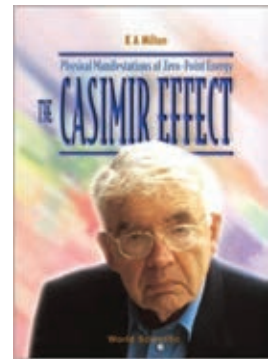
Casimir, 1909–2000) known as Casimir’s force.

If we compare the expression for Casimir’s force acting on two plates at a close distance with surface A at a distance L, with expression (2.50):

$$F_{cas} = \frac{hc\pi A}{480L^4} \tag{2.52}$$

we observe the difference in „coefficients“ between expressions 2.52 and 2.50 due to a different approach: one macroscopic, phenomenological (Casimir), depending on the surface and thus on body mass, and another, ours, which is the result of the interaction between gravitation and electromagnetism as a five-dimensional phenomenon, therefore depending only on mass.

Researchers succeeded in maintaining the aluminum foil at the height of 500 nm. A successful experiment was performed with a golden ball interacting with a silicon plate.



Hendrik Casimir (1909-2000)

## 2.6. „He does not gamble“

Einstein's opinion on the quantum mechanics incompleteness was mentioned, and regarding this, his position that *He* (meaning the Creator of the Universe, and not the religious God, because he was actually *an atheist believer*) does not gamble. At the beginning, when all four interactions known today (strong, weak, electromagnetic and gravitation) were united, there was no light. Light was generated during their separation, although it could not immediately propagate through the established Universe, because electrons and protons absorbed the energy of the electromagnetic field  $E/M = 3 \times 10^8$  m/s, which is also the velocity of light. Only when electrons and protons started to form atoms of hydrogen and helium, light absorption decreased, and subsequently stopped; light began to „flow“ (this moment is called the phase transition of cosmos; it occurred approximately 300 000 years after the origin of the Universe).

No one comprehends the nature of our existence, what we do know is that events take place, although we are unaware if it is *hazard* or *determination*, or both in a combination (bifurcation processes). From our viewpoint, by the creation of  $N = 3$  and its pair  $N = -2_5$  from  $N = 0$  (with synergy of  $N = 1$ ) the process depicted in Figure 2.9 is established.

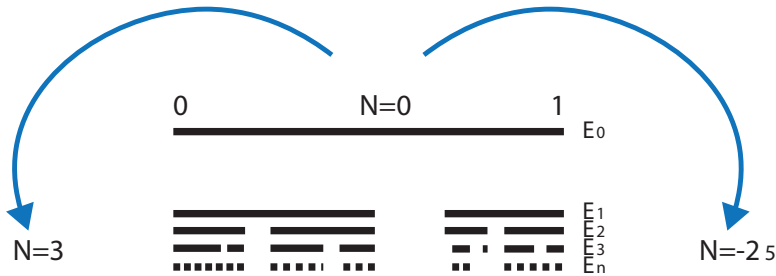


**Figure 2.9** Information content of dimension  $N = 0$  is mapped into two dimensions  $N = 3$  and  $N = -2_5$ . Mapping from the original state  $E_0[0,1]$  into  $N = 3$  and into  $N = -2_5$  is not the same regarding contents and is arbitrary (random). In the first step, not everything is mapped, a portion remains unmapped. In the second step, what is allocated to  $N = 3$  is mapped only within its own dimension (randomly), and the same goes for the dimension  $N = -2_5$ . In the following phase, a similar process takes place continuing until the  $n$ -th mapping.

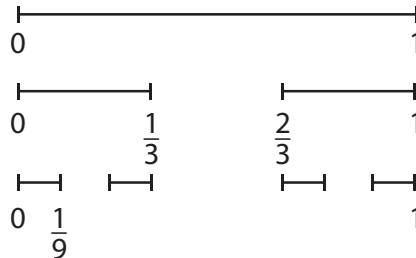


**Figure 2.10** Generation of Cantor's triadic set from the segment  $[0,1]$ .





Georg Cantor  
(1845-1918)

We can establish, from Figure 2.9, the ruling principle of Cantor’s dyadic-triadic random perturbation set, which will be further discussed.

Georg Cantor, (1845–1918), German mathematician, born in Russia of the time, was the founder of set theory, and among many sets he described, one is of special significance for fractal mechanics, known as the Cantor’s *triadic set* ( $T$ ). Scientists have since developed different variants of this set, yet two are most noted: the *uniform* and the *random* Cantor’s triadic set.

In mathematics, it is considered that, based on the Cantor-De-dekind axiom, all real numbers can be represented by a one-to-one correspondence with points of a line, where points 0 and 1 are fixed, including the segment  $[0,1]$  as the *measure* unit. Resulting from this axiom, Cantor’s *uniform triadic set* can be constructed

by corresponding to an arbitrary sequence

$$a_1, a_2, a_3 \dots a_n$$

composed of 0 or 1 in the form of a set  $\{0,1\}_{1(N)}$ , a real number

$$\sum_{n=1}^{\infty} (2a_n) \cdot 3^{-n} \tag{2.53}$$

that will be mapped on the set  $T$  (triadic set).

To simplify the investigation of the triadic set and the above mapping, observe the creation of the triadic set from the segment  $[0,1]$  of all real numbers  $0 \leq x \leq 1$  in the following way (Fig. 2.11): segment  $[0,1]$  is divided into three equal segments. After eliminating the middle interval of size  $1/3$ , two segments  $[0,1/3]$  and  $[2/3,1]$  remain, each  $1/3$  long. In the second step, the procedure with remaining segments is the same as with the first one, that is, each segment is divided into three equal segments, and the middle interval is eliminated (so that the end-points of eliminated intervals  $1/3, 2/3$  in the first step, and likewise all the remaining end-points of eliminated intervals in the next steps, always belong to the set). In the next step, we shall have four left over segments:  $[0,1/9], [2/9,3/9], [6/9,7/9]$  and  $[8/9,1]$ , in the succeeding step eight segments, and so on. We observe that, in the first step, interval  $1 \times 1/3$  long is eliminated, in the second step  $2 \times 1/3^2$ , in the third step  $4 \times 1/3^3$  etc., which can be written in the form:

$$\frac{2^0}{3^1} + \frac{2^1}{3^2} + \frac{2^2}{3^3} + \frac{2^3}{3^4} + \frac{2^4}{3^5} + \dots + \frac{2^n}{3^{n+1}} = \frac{2^0}{3^1} \sum_{n=0}^{\infty} \left(\frac{2}{3}\right)^n = \frac{2^0}{3^1} \cdot \frac{1}{1 - \frac{2}{3}} = 1. \tag{2.54}$$

We observe that no number of the set  $T$  was eliminated, therefore, the triadic set  $T$  is located on the segment  $[0,1]$  in a manner that those intervals which do not belong to the set  $T$ , but whose endpoints are in  $T$ , have the overall length equal to 1, the same

length as the segment  $[0,1]$  itself. Due to this characteristic, the *measure* of the set  $T$  equals 0, although its cardinal number is equal to the cardinal number of the entire linear continuum ( $2^{\aleph_0} = c_1$ ) of the real line  $R^1$  (Dauben, 1990, Kurepa, 1951). Therefore, the *length* of the triadic set is 1, although its *measure* is 0.

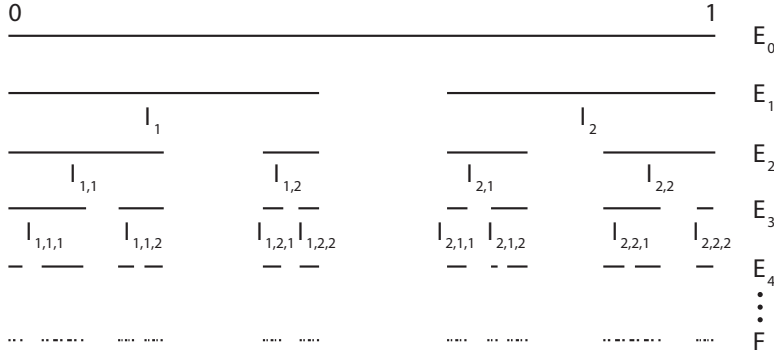


**Figure 2.11** Random Cantor's triadic set ( $T_R$ ); the ratio of two of set's intervals in  $I_1 (i_1 \dots i_k)$  corresponds to the same statistic distribution as the statistic similarity that exists in the ratio of intervals in  $I_2 (i_2 \dots i_k)$  (Falconer, 1990).

This result seems even more paradoxical than the result in mathematics stating that the space has the same number of points as any segment of the real line  $R^1$ . This result, by its paradox, surpasses the result in the number theory regarding the *zero factorial*  $(0!) = 1$ . However, this Cantor's result „established the harmony we think of when we speak of spaces of different dimensions, which are, concerning the question of the number of points, all mutually identical“ (Kurepa, 1951). Namely, the triadic set  $T$ , with *measure* 0, has the same number of points as the entire space. However, there is no one-to-one and mutually continuous mapping between spaces, therefore, neither between the triadic set and the multi-dimensional space, although they all have the same number of points.

It is customary to write  $1/3$  instead of  $2^0/3^1$ , which is quantitatively the same, therefore this set is called the *triadic set* ( $T$ ), although it would be more appropriate to call it a *dyadic-triadic set* ( $DT$ ), because in the numerator we have *dyads*, and in the denominator *triads*.

**Random Cantor's Dyadic-Triadic Set**

In the *uniform* dyadic-triadic Cantor's set, presented above, all the intervals in each step were identical, equal to  $1/3$ . For fractal mechanics, beside the significant mapping  $N = 0$  into  $N = 3$  and  $N = -2_5$ , and understanding the uniform Cantor's dyadic-triadic set, *the random Cantor's dyadic-triadic set*,  $DT_R$ , is very important, where intervals are not equal within the same step, neither is the inequality of intervals regularly repeated in the steps. The interval length is random and varying. In a sufficiently large number of steps,  $DT_R$  exhibits statistical self-similarity, so that in the end two unequal segments with probability  $p = 1$  perform self-mappings, the set itself has Hausdorff's dimension. In other words, the  $DT_R$  set is a fractal:  $dim_H T_R = s$ ,  $s$  is the value satisfying the condition that ratios of the *left* to the *right* intervals ( $I_1$  and  $I_2$ ) in each step  $E_n$  are random variables

$C_1$  and  $C_2$ , transforming the set  $DT_R$  into the fractal state with probability  $p = 1$ , which can be written in the form (Falconer, 1990):

$$E(C_1^S + C_2^S) = 1 \tag{2.55}$$

**Fractal Dimension of the Cantor’s Dyadic-Triadic Set**

Dimension is, in general, an intuitive concept formed in our *mental world* based on the perception of the *physical world*. We have a mental perception of three-dimensionality of our physical world, however, as is known, we are a natural codogenic entity in which, based on reduction, „information of quantum states of space-time was recorded“, thus we perceive the physical world with two dimensions less than it actually has. We perceive the *physical world* as 3D, because our mind is  $-2_5$  (five-dimensional). Since the Universe (*physical world*) and our *mental world* are of the same dimension, Einstein’s statement „it is most incomprehensible that the Universe is comprehensible“ becomes understandable.

Concerning the *physical world*, we are accustomed to dimensions as integral numbers 1, 2, 3, 4... However, question arises does a system of closed points or broken lines, given on a sheet of paper (2D quasi-space), have a dimension smaller than 2D since it is composed of points (0D quasi-objects) and/or lines (1D quasi-objects). Covering any space with objects of lesser dimension, results in the fact that the object has smaller dimension than the space it is located in.

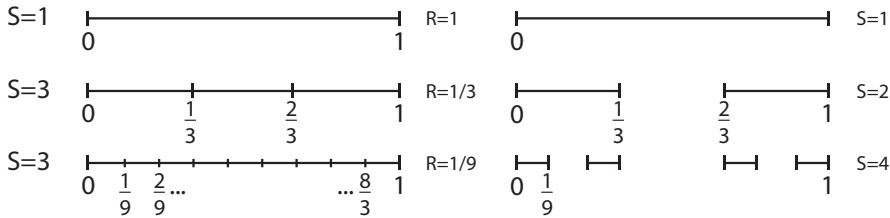


**Figure 2.12** Procedure to determine the Hausdorff’s dimension on the unit segment (left) and creation of Cantor’s dyadic-triadic set (right) with elements used for the definition of Hausdorff’s dimension (Falconer, 1990).

Observe the *segment* [01] (Fig. 2.12) as an 1D object (we write for simplicity 1D object, although we have in mind that the segment, drawn on a sheet of paper, is actually a *quasi* 1D object), we want to cover it with small  $s$ -dimensional spheres of diameter  $R$ . We need  $S$  spheres, and the total number of spheres needed for complete covering depends on the dimension of the object we wish to cover. If  $R$  is smaller, a larger number of spheres  $S$  is needed. If the number of spheres  $S(R)$  grows according to the rule  $1/R^D$  Hausdorff’s dimension ( $D_H$ ) of the object is calculated as follows as  $R$  decreases:

$$D_H = - \lim_{R \rightarrow 0} \frac{\ln S(R)}{\ln R} \tag{2.56}$$

Using the expression 2.56 let us try to determine Hausdorff’s dimension of Cantor’s dyadic-triadic set (Fig. 2.12 *right*). In the first step, it is possible to cover the initial seg-

ment with a two-dimensional sphere (circle) of diameter 1, while for the covering of the object after the first step, 2 spheres are needed, each of diameter  $R = 1/3$ . In the third step, 4 spheres (circles) are needed, each of diameter  $R = 1/9 = (1/3)^2$ .

After  $n$  steps, we obtain  $S = 2^n$  spheres (intervals) of diameter (length)  $R = (1/3)^n$ . After infinitely many (yet countable) repeated procedures, we obtain Cantor's triadic set. Since, according to Hausdorff's procedure, it is necessary to determine the rule according to which the number of spheres  $S(R)$ , needed for the covering of intervals, varies as a function of their diameter  $R$ , the limit of the given value is computed when  $R$  approaches zero. In each step  $n$ , we obtain  $S = 2^n$  spheres (segments), and the value of the diameter is decreased according to the formula  $R = (2^0/3^1)^n$ , so that, based on the expression 2.56, Hausdorff's dimension of the Cantor's dyadic-triadic set, with accuracy of eight decimal digits, is:

$$D_H = - \lim_{R \rightarrow 0} \frac{\ln S(R)}{\ln R} = - \lim_{\substack{R \rightarrow 0 \\ n \rightarrow \infty}} \frac{\ln 2^n}{\ln \left( \frac{2^0}{3^1} \right)^n} = \frac{\ln 2}{\ln 3} = 0,630929754. \quad (2.57)$$

Therefore, value 0.630929754 is Hausdorff's dimension of the *DT* set and it is less than 1, which reflects the „representation“ of points (0D objects) and lines (1D objects) in a given set. Since Cantor's *DT* set is „point-like“, it is also called „Cantor's dust“ (Mandelbrot, 1977). We observe that „dust particles“ of the set are not *monads* (self-isolated objects), they are entities establishing ordering, mutually related and „connected“. Cantor's „dust“ is not yet visually represented, except in the form of points on the real line, because „dust“ can create arbitrary shapes. However, there is an essential limitation in the construction of such a figure: the interrelationship of all the elements constituting the system must be 0.6309 and its measure 0 (a void, not *nothingness*, rather *darkness*, from which *everything* originates).

## 2.7. Photon and Light

To recapitulate contemporary knowledge on what is a photon and what is light; we do know that photon has a dual nature, corpuscular-wavelike, it is the carrier of electromagnetic interactions in nature, it has two components, electric and magnetic, mutually orthogonal, it carries energy depending on the wavelength, has spin 1, travels with velocity  $2.99 \times 10^8$  m/s in vacuum, when passing through different mediums it is slowed down, it can be absorbed, reflected or scattered during interaction with matter.

If photons are of the same wavelength, we say that light is monochromatic, and if photons of different wavelengths constitute light, it is polychromatic. As the orthogonality of the electric and magnetic field can take different positions in space (from  $0^\circ$  to  $360^\circ$ ), when this position is arbitrary, we say that light is diffuse. When orthogonality is not arbitrary, but fixed, it is said that light is linearly polarized.

However, when orthogonal vectors of the electric and magnetic field rotate, light is circularly polarized, and if the electric and magnetic waves do not have the same common wave point (there is a small displacement), it is said that light is elliptically polarized. About light types, and new possibilities to create hyperpolarized light, more details in Chapter VI. We finalize our presentation of the photon with the dilemma put forward by Richard Feynman: „Quantum electrodynamics resolves the wavelike-corpuseular dualism by claiming that light is composed of particles (as Newton considered at first), however this big step forward is paid by the return to the situation when we can only calculate the *probability* that the photon will hit a target (detector), meaning that there is no adequate model explaining how this is happening“ (Feynman, 1985).

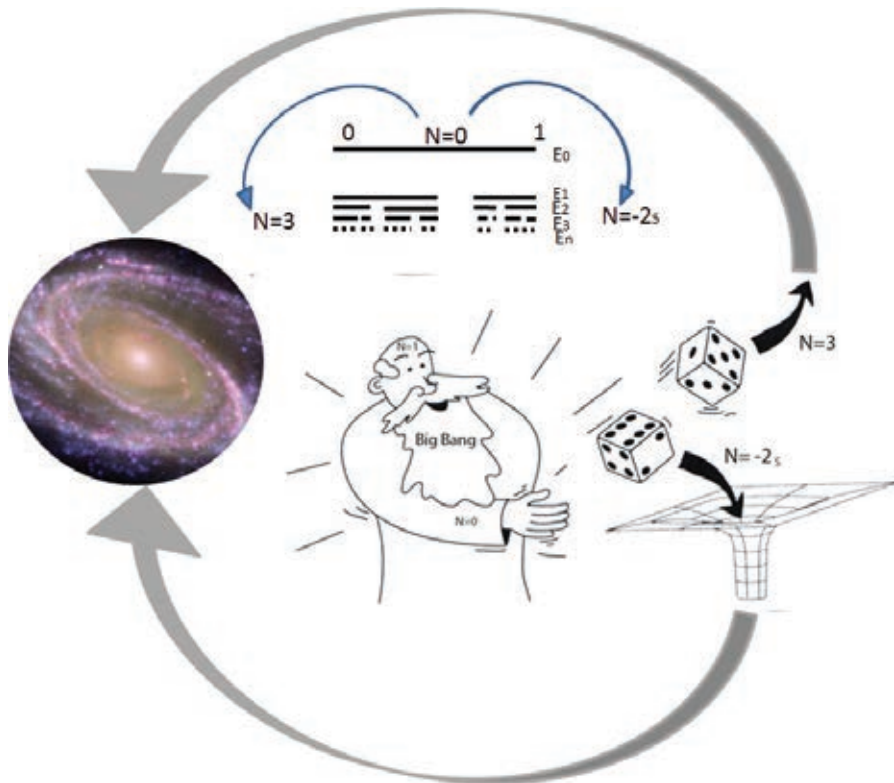


**Figure 2.13** „He does not gamble, although he throws „light“ ( $N = 3$ ) and „gravitational“ ( $N = -2$ ) dice, in such a way that the process is performed with probability 1, because light and gravitation establish a direct unity in the fifth dimension at the level of Planck's length  $2.28 \times 10^{-35}$  m. Therefore, the Universe, as a macroscopic object, must reach the value  $10^{35}$  m, which will lead to a complete and direct unity  $10^{-35} \times 10^{35} = 1$  ( $\langle (-2_s) \times \langle 3 \rangle = \langle 0 \rangle$ ) of light and gravitation in the space-time continuum, as opposed to the present state where space and time, light and gravitation are separated. This will create new possibilities for technological progress, because the conditions will be created to construct levitating devices (wingless aircraft), operate without scars („five-dimensional surgical knife“ that leaves no wounds) and other – unexpected innovations.

Our 3D universe is part of a surface in a 4D space. Black holes are quantum tunnels that lead us into the "volume" of the 4D space that is nothing but a surface entity of the 5D space of Planck's length,  $10^{-34}$  m (see text on pages 40-42 and Figures 2.6 and 2.14). Our 3D universe is a combination of a 3D space (*as itself*) and the presence of mass, energy and time as a reduction of 5D into 3D. The DNA code, and other information entities in 3D, are properties of 5D into 3D. Energy and time are a reduction of the 4D repulsion into 3D, while mass is the unity of reduced 4D and 0D (attraction) into 3D ( $E = !0/0! mv^0c^2$  and  $x^2+y^2+z^2 - (ict)^2 = 0$ ).

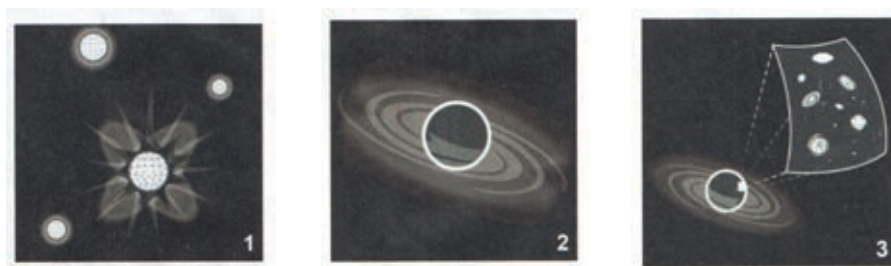


**Figure 2.14** *The star that dies in 4D (1) different than ours (quantum field), has formed a black hole (2), the horizon of the 4D black hole event is our 3D universe (3).*

## References

1. Alonso, M., Finn, J.E., Physics. Addison Wesley, Harlow, 1992.
2. Aristotel, Fizika. Sveučilišna Naklada Liber, Zagreb, 1987.
3. Einstein, A., Relativity: The Special and General Theory. Crown Publishers, New York, 1916.
4. Euklidovi elementi, Prva knjiga (prevod Anton Bilimović). Naučna knjiga, Beograd, 1949.
5. Falconer, K, Fractal geometry: Mathematical Foundations and Applications. John Wiley & Sons, Chichester, 1990.
6. Feynman, R.P., QED: The strange theory of light and matter. Princeton University Press, Princeton and Oxford, 1985.
7. Hamming, R.W., Coding and Information Theory. Prentice Hall, Englewood, 1986.
8. Havil, J., Gamma: Exploring Euler's constant. Princeton University Press, Princeton, 2003.
9. Huang, K., Fundamental Forces of Nature. World Scientific, New Jersey, 2007.
10. Kaluza, Th., Zum Unitatsproblem der Physik. Sitzungasberichte Preussische Akademie der Wissenschaften, 966-772, 22. Dezember 1921.

11. Koruga, D., From Geometrical Fractal Theory to Fractal Mechanics, 613-618. Eds. Sumarac, D and Kuzmanovic, D., Proceedings of the 1st International Congress of Serbian Society of Mechanics, Kopaonik, 2007.
12. Koruga, D., Neurocomputing and consciousness. Neural Network World, Vol.1, No.1, pp.32-38, 1991.
13. Koruga, D., Hamerof, S., Withers, J., Loutfy, R., Sundareshan, M., Fullerene C60: History, Physics, Nanobiology, nanotechnology. North-Holand (Elsevier), Amsterdam, 1993.
14. Koruga, Đ., Teslina „Hipotetička brzina“: Fenomen života i sinergija klasično-kvantnih dejstava, st. 31-52, u knjizi, urednici Benišek, M.M., Pokrajac, S., Koruga, Đ., Tesla: Vizije, delo, život. Mašinski fakultet, Univerziteta u Beogradu, 2007.
15. Kurepa, Đ., On the left factorial function !n. Mathematica Balkanica, 1, 147-153, 1974.
16. Leartije, D., Životi i mišljenja istaknutih filozofa. BIGZ, Beograd, 1979.
17. Mandelbrot, B., The Fractal Geometry of Nature. W.F. Freeman and Company, New York, 1983.
18. Marić, I., Platon i moderna fizika. Društvo filozofa i sociologa Crne Gore, Nikšić, 1997.
19. Munday, J. N., Capasso, F., Parsegian V. A, Measured long-range repulsive Casimir–Lifshitz forces. Nature 457, 170-173, 2009.
20. Nordstrom Gunar, Über die Möglichkeit, das Elektromagnetische Feld und das Gravitationsfeld zu vereiningen. Physikalische Zeitschrift, 15, 504-506, 1914.
21. Penrose, R., The Large, the Small and the Mind. Cambridge University Press, Cambridge, 1997.
22. Planck, M., Eight Lectures on Theoretical Physics, Dover Pub. Inc., Mineola, New York, 1998.
23. Roychoudhuri, C., Kracklauer, Creath, K., The nature of Light: What is a Photon? CRC Press, Boca Raton, 2008.
24. Rayder, L.H., Quantum field theory. Cambridge University Press, Cambridge, 1985.
25. Tesla, N., Moji pronalasci. Školska knjiga, Zagreb, 1977.
26. Zijlstra, P., Chon, W.M.J, Gu, M. Five-dimensional optical recording mediated by surface plasmons in gold nanorods. Nature, Vo. 459, pp. 410-413, 2009





# 3

## MATTER

*What is an electron?*



*One thing I have learned in a long life:  
that all our science, measured against reality,  
is primitive and childlike,  
and yet it is the most precious thing we have.*  
EINSTEIN

### **3.1. Basic Knowledge about the Electron**

Toward the end of the 19 century, it was thought that everything that ought to be known was already discovered. A kind of self-satisfaction reigned, not without reason, because a considerably coherent macroscopic (classical) picture of the world had been created based on the concept of atom as an indivisible particle; from Copernicus and Galileo to Newton and Kepler regarding gravitation and the „celestial sphere“, from Faraday, Volta and Ampère to Maxwell and Tesla in the domain of electromagnetism, from Darwin and Avogadro to Mendel and Mendeleev regarding the life phenomenon. However, there were researchers whose questioning spirit was alive (like Faraday, Hertz, Röntgen, and others) challenging the imagination of the coming giants of science who would dramatically change the scientific worldview.

One of the turning points was the discovery of the subatomic particle and its charge; enter „his highness“ – the *electron*. This name was put forward in 1881 by Johnstone-Stoney, who calculated the value of the smallest electric charge  $q_0$  based on Faraday's experiments in electrolysis. The electric charge produced during the extraction of a gram-atom of substance was  $Q = 96.400 \text{ C/mol}$ . However, the number of atoms per mol was not precisely determined, instead it was taken to be  $1.44 \times 10^{24} \text{ mol}^{-1}$  (what we call today Avogadro's number,  $N_A = 6.022 \times 10^{23} \text{ mol}^{-1}$ ). Based on the results obtained from experiments in extracting oxygen from a solution, it was calculated:

$$q_0 = \frac{Q}{N_A} = \frac{96400}{1.44 \times 10^{24}} = 0.67 \times 10^{-19} \text{ (C)}, \quad (3.1)$$

which was an excellent result for the time (today we know that this value is equal to  $1.602 \times 10^{-19} \text{ C}$ ).

In 1897, the 40 year old Joseph John Thomson (who as a 14 year old enrolled the University of Manchester), announced that he discovered a charged particle whose mass is a thousand times smaller than the hydrogen mass. This caused a disturbance in the scientific community of the time, because it had shaken the several decades lasting lethargy based on the belief that most of the important scientific discoveries have already been made.

Thomson had, during his stay at Cambridge, where he was appointed professor in 1884, and where he remained until 1897, worked on the clarification of the cathode ray tube radiation phenomenon.

The rays were visible, however, it was obvious that they were not the rays of the everyday visible light. A serious scientific discussion was initiated about this phenomenon. In order to resolve the „scientific Gordian knot“, Thomson decided to accept Faraday’s advice „theory leads, experiment decides“ and took to experimenting. He measured the particle’s mass ( $9,1 \times 10^{-31} \text{kg}$ ) and realized that it was 1830 times smaller than the hydrogen’s mass (at the time only atoms of the Mendeleev’s periodic system of elements were known, protons and neutrons were not even a concept). He determined experimentally that the particle (or as he called it the „corpuscle“) carried negative charge and that it filled the entire atom volume (Thompson, 1897).

Now there was a more complete picture of the electron, because aside from its charge, its mass was also determined. These two experimentally obtained values consolidated the knowledge foundation. However, this was not the end because Becquerel (1852–1908) discovered radioactivity in 1896, enabling Rutherford (1871–1937) to discover that there is a mass with *positive charge* at the atom center only fifteen years later (1911). However, the greatest surprise was the insight that there is *empty space* within the atom measuring approximately 10000 diameters of the positive electric charge. This meant that the negative charge does not fill the entire atom, instead it orbits at a distance from the positive charge. Rutherford was astonished by his own discovery, as was the scientific community of the time.

Bohr improved Rutherford’s atom model and proposed that the energy within the atom is emitted and absorbed in quantum leaps when the electron moves between orbitals. The first phase of Bohr’s theory (proposed in 1913) is based on the hypothesis that the electron orbits a circular path under the condition that the centripetal force and Coulomb’s electrostatic force are equal:

$$\frac{m_e \times v^2}{r} = \frac{1}{4\pi\epsilon_0} \frac{Ze^2}{r^2}, \quad (3.2)$$

and that the condition is satisfied that the *momentum* ( $L$ ) of the electron is equal to an integral multiple of the constant  $\hbar (h/2\pi)$ , i.e.,  $m_e v r = n\hbar$ . Bohr intuitively selected the angular momentum of the electron, and not its energy, to be quantized. This approach enabled him to



Joseph John  
Thomson (1856-1940)



Niels Bohr,  
(1885-1962)



Yin-Yang symbol on the cover page of the book by Nils Bohr explaining the nature of the particle-wave relationship.

calculate the orbitals  $r_n$  where it was probable that the electron could be found within the hydrogen atom for various energy states:

$$r_n = 4\pi\epsilon_0 \frac{\hbar^2}{m_e e^2} \times n, \quad (3.3)$$

where  $n = 1$  yields  $r_1 = 52.91772 \text{ pm}$  called Bohr's radius, usually denoted as  $a_0$ .

Bohr considered that the corpuscular-wavelike nature of matter is synergic, that is, that it represents its synergic state, so that he put the Chinese symbol *Yin-Yang* on the cover page of his book illustrating direct unity of the particle and its wave.

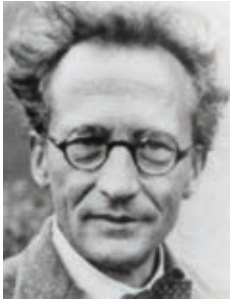


*Louis de Broglie,*  
(1892-1987)

De Broglie assumed, starting from the insight of light duality (wave/particle), that dualism is a general characteristic of matter, not only of light. Combining  $E = mc^2$  and  $E = h\nu$  he demonstrated that each particle has a „matter wave“ of wavelength inversely proportional to the momentum:

$$\lambda^* = \frac{h}{mv}, \quad (3.4)$$

also written as  $h = p \times \lambda^*$ , that is  $h = mv$ . The duality characteristic is more pronounced as the particle (body) becomes smaller, so electron, proton or molecule cannot be considered localized as a particle at only one location. Instead they have their wavelike „extension“ in space. However, it should be noted that  $\lambda$  and  $\lambda^*$  are not of the same nature, and that the nature of De Broglie's waves remains to be discovered. Today, literature does not differentiate between  $\lambda$  and  $\lambda^*$ , however, it would be more correct to write  $\lambda^* = \Lambda$ , as proposed by Khun and Forsterling in 2000.



*Erwin Schrödinger,*  
(1887-1961)

De Broglie's relation indicates that the electron, on its circular orbiting about the nucleus, will form a stationary wave only in case the perimeter of the circle is equal to an integral multiple of the electron's wavelength

$$2r\pi = n \frac{h}{mv}, \quad (3.5)$$

that is,  $mvr = n\hbar$ , which indicates that the permanence of electron's orbit results from the character of the wave motion of the electron within the atom.

Schrödinger, at Einstein's suggestion, developed the wave function of the electron based on De Broglie's concept of the corpuscular-wave nature of matter and its energy state using the Hamiltonian. Hamiltonian is an operator written as

$$H = -\frac{\hbar^2}{8\pi^2 m_e} \nabla^2 + V, \quad (3.6)$$

where  $V$  – is the potential energy, and  $(nabla)$  – the Laplace operator of the form:

$$\nabla^2 = \frac{\partial^2}{\partial x^2} + \frac{\partial^2}{\partial y^2} + \frac{\partial^2}{\partial z^2}. \quad (3.7)$$

If we consider that for the wave function  $\psi$

$$H\psi = E\psi, \quad (3.8)$$

then for the stationary wave, the equation is as follows:

$$\frac{d^2\psi}{dx^2} = -\frac{p^2}{\hbar^2}\psi. \quad (3.9)$$

For a free particle, we have  $E_k = E = p^2/2m$ , so that based on the previous expression, the equation is obtained:

$$\frac{d^2\psi}{dx^2} + \frac{2mE_k}{\hbar^2}\psi = 0. \quad (3.10)$$

A bound particle moves in the field of potential force, characterized by the potential energy  $E_p$  and the kinetic energy  $E_k$ , thus  $E_k = E - E_p$ , so we obtain the equation:

$$\frac{d^2\psi}{dx^2} + \frac{2m}{\hbar^2}(E - E_p)\psi = 0 \quad (3.11)$$

known today as the Schrödinger's wave function.

Schrödinger's equations have the same significance in quantum mechanics today as Newton's laws in the classical mechanics. However, one should bear in mind that science has not discovered all the characteristics of *the quantum*, and that further breakthroughs in this area are not only possible but necessary.

Werner Heisenberg (1901–1976) introduced the uncertainty principle into quantum systems according to which an experiment cannot determine both the position of the particle and its energy in the system simultaneously, only one of them.

Since the electron moving between two walls of width  $l$ , can be located anywhere with probability proportional to  $\psi^2$ , Heisenberg determined that the product of the electron's position uncertainty  $\Delta x$  and the momentum uncertainty  $\Delta p$  along the  $x$ -axis corresponds to the value of the Planck's constant, that is:

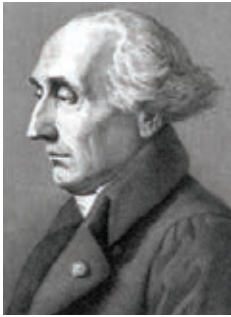
$$\Delta x \cdot \Delta p_x = h. \quad (3.12)$$

This demonstrates that at least two „pictures“ are necessary in order to characterize a quantum entity. The first refers to the *wave-particle* attributes, and the second to the *position-momentum* properties.

In the 1970-ties, Yoichiro Nambu proposed that elementary particles be observed not as pointwise structures (such as electrons, quarks, etc.), as the until then proposed forms, but as vibrational-rotational 1D (one-dimensional) objects, known today as strings or superstrings (he was awarded the Nobel Prize in Physics in 2008 for the discovery of the mechanism of spontaneous broken symmetry in subatomic physics).

He was inspired for this idea by Pythagoras and the musical string chords. Today, this is a scientific approach explaining elementary particles (according to this theory there are 496 elementary particles), gravitation, general relativity theory, etc. Beside positive aspects, string theory has its limitations, it is only a transitive (auxiliary) solution, because it deals with quasi 1D objects, not with real 1D objects. When a theory is developed where the real 1D physical entity will be implemented, we shall be at a threshold of a new scientific progress that will be much closer to the *Theory of Everything*.

### 3.2. Lagrangian and Hamiltonian



Joseph Louis  
Lagrange (1736-1813)

For the understanding of similarities and differences in the calculation of energy and system states between the classical and quantum physics, two functions are especially important: the *Lagrangian* and the *Hamiltonian*. Both functions are implemented in discrete systems and are named after their authors, Lagrange and Hamilton.

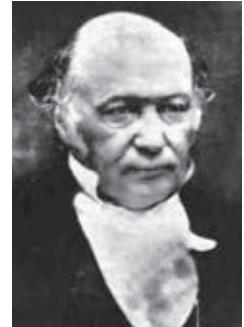
Lagrange was a famous French mathematician, founder of mathematical analysis, which he dissociated from geometry. He made significant contributions to the variation calculus, numerical analysis, the number theory, and the theory of algebraic equations. Lagrange introduced the notation  $f'(x)$  based on the theorem bearing his name, which refers equally to mathematical analysis and to the group theory, and is also known by his interpolation polynomial  $L_n(x)$  resulting from the general interpolation theory.

The Irish mathematician Hamilton (William Rowan Hamilton, 1805–1865) investigated differential geometry, mathematical analysis, partial differential equations, and mechanics.

The *generalized coordinates* define uniquely system position—the number of independent generalized coordinates is :  $s = 3N - k$ ,  $N$  –is the number of system points,  $k$  – the number of holonomic constraints. They are denoted by  $q$ . From the definition, follow the characteristics: two conditions must be satisfied – the point radius vectors must be unique,

$$\vec{r}_i = \vec{r}_i(q_1, q_2, \dots, q_s, t); \quad (i = 1, 2, 3, \dots, N)$$

and independent, which is established by the condition that the derivatives of the vector projection along the coordinates (denoted by  $x_i$ ) satisfy the condition:



William Hamilton  
(1805–1865)

$$\begin{vmatrix} \frac{\partial x_1}{\partial q_1} & \dots & \frac{\partial x_1}{\partial q_s} \\ \frac{\partial x_s}{\partial q_1} & \dots & \frac{\partial x_s}{\partial q_s} \end{vmatrix} \neq 0$$

Point velocities as functions of generalized coordinates, kinetic energy and generalized forces are:

$$\begin{aligned} \vec{r}_i &= \sum_{j=1}^s \frac{\partial \vec{r}_i}{\partial q_j} \dot{q}_j + \frac{\partial \vec{r}_i}{\partial t}, & T &= \sum_{i=1}^N \frac{m_i}{2} (\dot{\vec{r}}_i)^2 = T(q, \dot{q}, t), \\ Q_j &= \sum_{i=1}^N \vec{F}_i \frac{\partial \vec{r}_i}{\partial q_j}, & (j &= 1, 2, \dots, s) \end{aligned}$$

Lagrange's differential equation of motion can be written in the form:

$$\frac{d}{dt} \left( \frac{\partial T}{\partial \dot{q}_j} \right) - \frac{\partial T}{\partial q_j} = Q_j; \quad (j = 1, 2, \dots, s) \quad (3.13)$$

If the forces are potential, then:

$$Q_j = \sum_{i=1}^N \nabla_i U \frac{\partial \vec{r}_i}{\partial q_j} = - \frac{\partial U}{\partial q_j}, \quad (j = 1, 2, \dots, s), \quad (3.14)$$

If the generalized, potential, and dissipative forces are present then:

$$\frac{d}{dt} \left( \frac{\partial L}{\partial \dot{q}_j} \right) - \frac{\partial L}{\partial q_j} = Q_j^d; \quad (j = 1, 2, \dots, s) \quad (3.15)$$

thus  $L = T - U$  if the dissipative forces depend on the velocity

$$Q_j^d = - \frac{\partial D}{\partial \dot{q}_j}, \quad (j = 1, 2, \dots, s), \quad D = \sum_{i=1}^N \frac{k_i}{2} (\dot{\vec{r}}_i)^2$$

where  $D$  is Rayleigh's dissipative function.

The generalized system energy is:

$$H = \sum_{j=1}^s \frac{\partial L}{\partial \dot{q}_j} \dot{q}_j - L; \quad H = H(q, p, t); \quad p_j = \frac{\partial L}{\partial \dot{q}_j},$$

where  $p$  is the generalized impulse. This formula does not contain linear members of the generalized velocity, while the *total* energy does. If the radius vectors of position do not depend explicitly on time, these energies are numerically identical (a system with stationary relations). Also holds:

$$H = \sum_{j=1}^s \frac{\partial L}{\partial \dot{q}_j} \dot{q}_j - L = T + U, \quad (3.16)$$



This is a *Hamiltonian*, its *advantage* - equally treats generalized impulses and coordinates, enabling compatibility when applied to statistical and quantum mechanics:

$$H^{(op)} = -\frac{\hbar^2}{2m} \frac{\partial^2}{\partial x^2} + V(x) \quad (3.17)$$

There is another, *formal, difference* between the Lagrangian and the Hamiltonian: Lagrange's *equation* is a system of  $s$  differential equations of the second order with respect to  $s$  generalized coordinates  $q$  as functions of time.

*Hamilton's equation* is a system of  $2s$  differential equations of the first order with  $s$  generalized coordinates and  $s$  generalized impulses as functions of time. They are also called canonical equations (they describe the *laws of conservation*).

Quantum mechanics originated as a step forward from the classical physics, first by Planck's black body radiation law in 1900, then by Einstein's papers from 1905, by the Bohr (1913) – Sommerfeld (1916) atom model and the Schrödinger's wave equation (1925), which unites particles and waves, links statistics and probability with determination of state.

Today, there are about ten theories of quantum mechanics, all having their place due to different mathematical models they employ and application in particular boundary cases.

After the successful application of quantum mechanics to the atom nucleus and Pauling's discovery of the protein structure 1950, Frohlich (1969) applied quantum mechanics to biomolecules as polymers, while Heisenberg and other leading quantum physicists foresaw a prominent future in its application to biophysics.

### 3.3. Tunneling Electrons

The electron tunneling phenomenon is viewed in the context of Schrödinger's quantum-mechanical interpretation of the electron. In classical mechanics, the kinetic energy cannot be negative, i.e., the total energy  $E$  cannot be less than the potential energy  $V$  ( $E - V \geq 0$ ). However, the already mentioned Schrödinger's quantum-mechanical equation

$$\frac{\hbar^2}{2m} \cdot \frac{d^2\psi}{dx^2} + (E - V)\psi = 0 \quad (3.18)$$

leaves the possibility that  $E - V < 0$ , i.e., that the kinetic energy has a negative value.

If the solution to the equation 3.18 is sought in the form  $\psi = Ae^{kx}$ , then the magnitude  $k$  can take both positive and negative values, giving the equation solution:

$$\psi = A \exp\left[+\sqrt{\frac{2m(V-E)}{\hbar^2}} \cdot x\right] + B \exp\left[-\sqrt{\frac{2m(V-E)}{\hbar^2}} \cdot x\right] \quad (3.19)$$

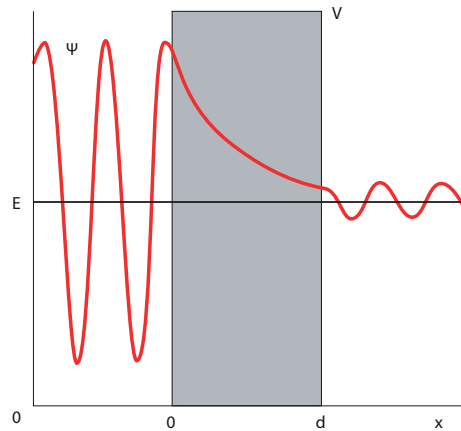


**Figure 3.1**  
Tunneling barrier,  
the barrier  
potential, and  
a proposed wave  
function for  
the particle.



Gerd Binnig (1947- )

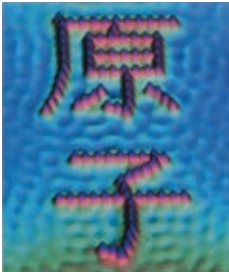


**Figure 3.2** In the 1990-ties, Japanese scientists wrote the word „atom“ with atoms using the STM.

As shown in Figure 3.1, left and right of the barrier, the positive kinetic energy produces oscillatory processes, while within the barrier region the process is exponential. From the aspect of classical physics, the barrier is impenetrable because the particle does not have enough energy to pass through the region  $0 < x < d$ .

In quantum mechanics, however, the value of the wave function does not decrease to zero instantaneously, so that there is a probability that a particle can pass through the barrier, i.e., be *tunneled*. A rough approximation of the expression 3.19 for  $x = d$ , while  $B = 1$ , according to Bohr's electron interpretation, gives the probability of tunneling:

$$P_{(T>)} \approx \exp \left[ -2d \sqrt{\frac{2m(V-E)}{\hbar^2}} \right]. \quad (3.20)$$

Expression 3.20 shows that the probability of a particle tunneling decreases sharply with: (1) barrier thickness, (2) particle mass (3), and with decrease of the  $V-E$  energy, compared with values demanded by classical physics for the particle to transit the barrier. If we consider that an electron with energy  $E-V=1\text{eV}$  should pass through the barrier of 0.2 nm, we obtain the probability of electron tunneling 0.13. However, if we observe proton tunneling, then the probability is  $10^{-38}$ , meaning that tunneling electrons, as small particles, is much more probable than proton tunneling, proton having 1836 times greater mass than the electron.

Quantum mechanics and the tunneling phenomenon have great significance for the solid-state physics, physical chemistry, nuclear physics, and biology. Electron tunneling can be elastic or plastic. In elastic tunneling, electron energy remains the same after tunneling, while in plastic tunneling energy is decreased after tunneling.

Gerd Binnig succeeded in 1981, together with his colleagues from the IBM laboratory in Zurich, to construct the first device based on electron tunneling for which he was awarded the Nobel Prize in 1986. Using the scanning tunneling microscope (STM) they succeeded to characterize the material surfaces with atom resolving power. The STM also enables manipulation of single atoms and construction of arbitrary structures. This is Richard Feynman's dream come true, who forecast this possibility in 1959. This was a technological confirmation that quantum mechanics, as defined by Schrödinger, „works“ (Binnig, 1982).

The tunneling current is created as the difference  $\Delta N = N_1 - N_2$ , where  $N_1$  is the number of electrons tunneling from the electrode 1 toward the electrode 2,  $N_2$  number of electrons tunneling from the electrode 2 toward electrode 1 after the bias voltage  $U$  has been applied at the connection. The symbols have the following meaning:  $v_z$  – velocity of electrons along the direction of the  $z$ -axis;  $n(v_z)dv_z$  – number of electrons per unit of volume with the  $z$  component of velocity between  $v_z$  and  $v_z + dv_z$ ;  $D(E_z)$  – probability that the electron with energy  $E_z = (mv_z^2)/2$  tunnels through the potential barrier  $V(z)$ ;  $f(E)$  – Fermi-Dirac distribution function; and  $E_{11} = m(v_x^2 + v_y^2) / 2$ . Now we can write for  $N_1$  and  $N_2$  (Wiesendanger, 1994):

$$N_1 = \frac{m}{2\pi^2\hbar^3} \int_0^{E_{\max}} D(E_z) dE_z \int_0^\infty f(E) dE_{II} \quad (3.21)$$

and

$$N_2 = \frac{m}{2\pi^2\hbar^3} \int_0^{E_{\max}} D(E_z) dE_z \int_0^\infty f(E + eU) dE_{II} \quad (3.22)$$

that is,

$$\Delta N = \int_0^{E_{\max}} D(E_z) \left\{ \frac{m}{2\pi^2\hbar^3} \int_0^\infty [f(E) - f(E + eU)] dE_{II} \right\} \quad (3.33)$$

The probability of electron tunneling through the potential barrier is:

$$D(E) = \exp \left\{ - \frac{2 \cdot (2m)^{1/2}}{\hbar} \int_{S_1}^{S_2} [E_{F_1} + \phi(z) - E_z]^{1/2} dz \right\}, \quad (3.34)$$

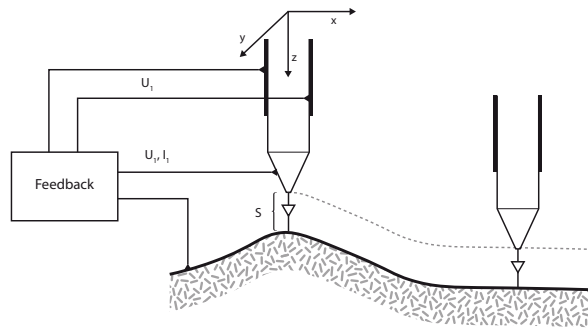


**Figure 3.3** Schematic representation of the constant current mode during the STM apparatus operation (Wiesendanger, 1994).

where  $E_{F1}$  – is Fermi's energy,  $\phi(z)$  – average value of the potential barrier above the Fermi level. However, for more accurate calculations it would be necessary to take into account that electron tunneling does not take place in an absolute vacuum; the process takes place in an environment at temperature  $T$ , and mutual interaction of metal electrodes affects electron tunneling. Regardless of the above approximations, the expression 3.34 has practical value.

The basic principle of STM operation is given in Figure 3.3. The sample under examination is placed on the pad, the sample itself must be a semiconductor or conductive material (for non-conductive materials the AFM – Atomic Force Microscopy is used, a technique that exploits the elasticity forces of material and a specially constructed tip). The STM has two operation modes: constant current mode or constant distance mode. Figure 3.3 represents an example of the STM operation based on the constant current mode: when the tip follows the sample surface these fine displacements are transferred to the crystal structures whose dilatation, via the piezoelectric attributes of crystals, generates currents of very small intensity. They are amplified and conducted into the apparatus for recording scanning lines, which are processed by software to produce the processed image on the display.

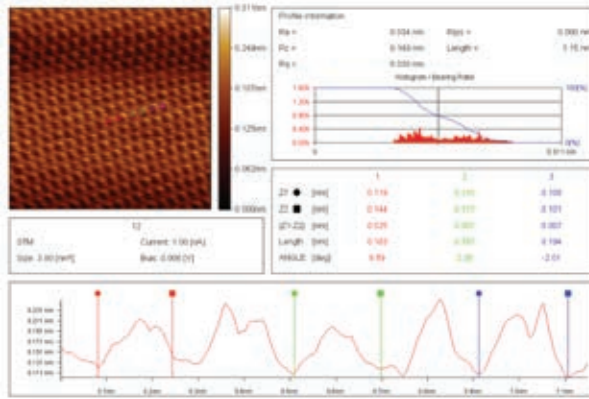


**Figure 3.4** The STM image of carbon atoms configuration in graphite realized at the NanoLab, of the Mechanical Engineering Faculty at the University of Belgrade, in 2005 on the JEOL Nanoprobe JSPM-5200 apparatus. As seen from the diagram, none of the atoms (at the given moment) are the same due to the interaction between them (atoms would all be the same if they were in the vacuum and separated from each other).

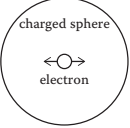
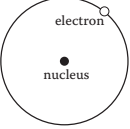
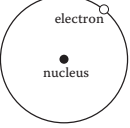
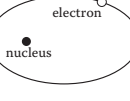
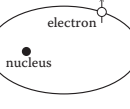
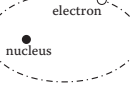
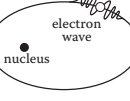
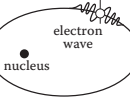
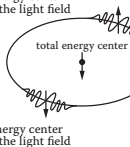
The tunneling current  $I$  can be written as a first order form, time dependent perturbation equation:

$$I = \frac{2\pi e}{\hbar} \sum \left\{ f(E) [1 - f(E_e + eU)] - f(E_V + eU) [1 - f(E_\mu)] \right\} \cdot |M_{\mu V}|^2 \delta(E_V - E_\mu) \quad (3.35)$$

where:  $f(E)$  – is Fermi's energy;  $U$  – bias voltage;  $M_{\mu V}$  – matrix of tunneling elements of unperturbed electron states  $\psi_\mu$  (of the tip apex) and  $\psi_V$  (of the sample surface);  $E_\mu(E_V)$  – state energy  $\psi_\mu(\psi_V)$  when there is no tunneling (Wiesendanger, 1994).

### 3.4. Electron Models in Physics

**Table 3.1** *Electron models of the hydrogen atom as scientists change their view on this phenomenon.*

Electron in the HYDROGEN atom	DESCRIPTION
	<p><b>1897 J.J. Thomson:</b> Electron is a subatomic corpuscle filling a sphere with uniform positive charge. Atoms of order number <math>Z</math> are positively charged bonding the electron with electric forces.</p>
	<p><b>1911 E. Rutherford:</b> Electron is a three-dimensional corpuscular, negatively charged particle in the nuclear atom model. In the proposed planetary model, the electrons rotate at a great distance from the positively charged nucleus on exactly defined circular paths. The overall negative electron charge is equal to the positive nucleus charge.</p>
	<p><b>1913 N. Bohr:</b> Electron is a point-like three-dimensional charged particle on a circular path. Each orbit has a different energetic level. Electrons do not emit energy while moving on stationary paths. When the electron transits from a path of a higher energy level to a path of a lower energy level, it radiates electromagnetic radiation (<math>h\nu</math>) equal to the difference of energies of these two energy levels.</p>
	<p><b>1916 A. Sommerfeld:</b> Electron orbits a quantized elliptical orbital. The electron position is defined by the radius of the orbital and the azimuth angle. Electron mass depends on its velocity along quantized orbitals.</p>
	<p><b>1925 S. Goudsmit:</b> Besides moving along elliptical orbitals, electron rotates about its own axis (spin). As the electron is negatively charged, it has a proper magnetic field. Electron has its own momentum and a proper magnetic moment, which explains the splitting of atomic levels.</p>
	<p><b>1925 W. K. Heisenberg:</b> Electron is not considered from the aspect of the classical formalism (Poisson notation); the concept of uncertainty is introduced according to which the product of two related quantities cannot exceed the Planck constant (electron's position and its velocity cannot be determined at the same time).</p>
	<p><b>1926 E. Schrödinger:</b> Electron is considered from the aspect of wave mechanics (De Broglie, 1923), according to which paths of particular electrons within the atom are not described classically spatially and temporally, but are determined based on probability. Therefore, particular electron energy levels within the atom are given only as average values of the distribution of the electron charge cloud with respect to the nucleus. The solution of the Schrödinger's equation gives the electric charge distribution around the nucleus.</p>
	<p><b>1928 P. Dirac:</b> The electron is a quantum-mechanical object whose motion can be described relativistically. This approach forecast the existence of the <i>positron</i>, a particle having the same mass and spin as the electron, but opposite charge. Using relativistic theory for electron motion, the best conformity to spectral lines for the hydrogen atom was demonstrated.</p>
	<p><b>1978 H. Salhofer:</b> The electron is at the same time a quantum-mechanical (microscopic) and an electrodynamic (macroscopic) entity (Maxwell-Dirac isomorphism – MDI). There are two electromagnetic fields with energy centers symmetrically distributed on „Keplerian“ electron orbitals (antipodal action).</p>

The table 3.1 summarizes, with short comments, major electron models from Thomson (1897) to Salhofer (1978) proposed by scientists and accepted by the scientific community (Lakhtakia, 1996). An interesting model was put forward by von Hippel in 1959, however, it went considerably unnoticed (von Hippel, 1959). In this model the wave packet of the electron, orbiting about the hydrogen nucleus, generates a wave packet, this packet at one moment decays, to be created again.

According to the scenario of contemporary physics, the electron, within the system of elementary particles, belongs to the group of *leptons* having mass of 0.511 MeV (rest mass  $9.109 \times 10^{-31}$  kg), electric charge of  $1.602 \times 10^{-19}$  C, radius of  $2.818 \times 10^{-15}$  m (classical electron radius is calculated from the relation  $r_e = e^2/m_e c^2$ , however according to the working hypothesis of Dehmelt  $r_e \approx 10^{-22}$  m), and spin  $\frac{1}{2}$ . Compton's electron wavelength is  $\lambda = h/m_e c = r_e/\alpha = 2.426 \times 10^{-12}$  m, so that based on the basic hydrogen atom radius, Bohr's radius of  $0.529 \times 10^{-10}$  m and proton size  $0.887 \times 10^{-15}$  m (proton is approximately three order greater than the electron,  $\sim \pi$ ), we can conclude that our classical perception of the electron which as a „ball“ circles about the atom nucleus is far from the truth. It is much more probable that it is a highly organized „energy package“ („nebulas“), as seen in Table 3.1 in Salhofer's model (Zettili, 2009 and Allosso, 1992).

### Electron Spin and Matter Structure



**Figure 3.5** Illustration explaining spin: spin 1 – the „ace“ has to rotate by  $360^\circ$  in order for the picture to coincide with itself ( $1 \times 1 = 1$ ), spin 2 – the „queen“ should rotate by  $180^\circ$  because „up“ and „down“ are the same ( $2 \times 1/2 = 1$ ). However, spin  $\frac{1}{2}$  is hard to grasp, because two rotations are necessary in order for the card to coincide with itself ( $1/2 \times 2 = 1$ ) (Hawking, 2001)

As seen from the Table 3.1, the concept of *spin* was introduced into the microworld in 1925 (Goudsmit and Uhlenbeck) with the idea that it refers to the electron's rotation about its own axis. Spin value denotes the number of rotations about electron's axis: 0 – particles as points look the same from all directions of observation, 1 – particles looking different from wherever observed (rotation of  $360^\circ$  about electron's axis is necessary in order for the picture to be the same), 2 – symmetric particles with the symmetry axis at  $180^\circ$  (observed as same from the front and from the back, i.e., during a  $360^\circ$  rotation they are observed twice),  $\frac{1}{2}$  – a two-fold rotation of  $360^\circ$  is necessary in order for the picture to be observed as the same. Strange indeed! And it is precisely this feature that the electron has. It seems that spin has no analogue in the classical world- rather it is an internal degree of freedom of the quantum-mechanical object. In order to illustrate the spin phenomenon, Hawking used a deck of cards (Hawking, 2001).

Spin dimension corresponds to action, so it is expressed as the product of Dirac's constant  $1.055 \times 10^{-34}$  Js ( $h/2\pi$ ) and the spin quantum num-

ber. It is not easy to grasp what the spin is (it was introduced in physics in order to eliminate the calculation problems with infinities). However, experiments show that spin, or something like it, exists (it was introduced in order to explain experiments and eliminate infinity – thus we could equally agree that it exists or we could agree that it does not exist, as the popular saying goes „who knows better, let him/her decide“). The spin sign denotes spin direction. All particles can be divided into two groups: *fermions* and *bosons* based on their spin.

Fermions have a half integer spin (1/2, 3/2 etc.) and determine the matter structure (such as electrons, protons, etc.), while bosons are particles of force transferring interactions, with an integral spin 0, 1, 2... (such as photons, gravitons, etc.). The boson and the fermion differ also with respect to Pauli’s exclusion principle (two particles cannot have the same quantum state at the same moment in time), which holds for fermions (electron), but does not hold for bosons (photon and graviton).

### Electron: Atom Structure

Electrons in atom orbitals are not independent from each other, because they carry negative charge and by their motion about the atom nucleus produce a magnetic field. Electron orbitals and their spin are related, coupled by the electric and magnetic field. Since in the vector model, each orbit and each spin are represented by a vector of the corresponding impulse momentum, according to Russell and Saunders (1925) singular spins are coupled separately into the overall spin momentum, and separate orbital momenta into the total orbital momentum (spin momentum is of much higher intensity). The vector of the overall momentum is obtained by their addition. However, we shall see in Chapter VI that, under certain conditions, the spin and the orbital calculation of coupling can be expressed differently, leading to new phenomena having their own cognizing and application values.

Table 3.2 Quantum numbers, their values and meaning.

Symbol	Name and value	Meaning
n	Principal quantum number $n = 1, 2, 3, 4, 5...$	Sequence number of the atom’s electron shell determines the electron’s distance from the nucleus and its energy
l	Orbital quantum number $l = 0, 1, 2, 3... n-1$	Determines the electron impulse momentum $\frac{h}{2\pi} \sqrt{l(l+1)}$
m	Magnetic quantum number ... -3, -2, -1, 0, +1, +2, +3... (from -l to +l)	The value of the projection of the electron impulse momentum onto the direction of the magnetic field $\frac{h}{2\pi} m$
s	Quantum number of the electron spin $s = 1/2$	Determines the spin momentum $\frac{h}{2\pi} \sqrt{s(s+1)}$
$m_s$	Magnetic quantum number of the electron spin $m_s = 1/2$ ili $m_s = +1/2$	Projection of the spin onto the direction of the magnetic field $+\frac{1}{2} \frac{h}{2\pi}$ , $-\frac{1}{2} \frac{h}{2\pi}$

Therefore, in electrons with spin  $\frac{1}{2}$ , we have pairing of two electrons per atom shell. As is known, the atom is defined with four quantum numbers:  $n$ ,  $l$ ,  $m$  and  $s$  (Table 3.2). The rule is well known and is presented for a certain number of atoms in Figure 3.6.

**Table 3.3** Determining the atom shell configuration using four quantum numbers.

n	l	m	m <sub>s</sub>		Number of electrons	Configuration	Shell
			+1/2	-1/2			
1	0	0	+1/2	-1/2	2	1s <sup>2</sup>	K
2	0	0	+1/2	-1/2	8	2s <sup>2</sup> p <sup>6</sup>	L
	1	+1	+1/2	-1/2			
		0	+1/2	-1/2			
		-1	+1/2	-1/2			
3	0	0	+1/2	-1/2	18	3s <sup>2</sup> p <sup>6</sup> d <sup>10</sup>	M
	1	+1	+1/2	-1/2			
		0	+1/2	-1/2			
		-1	+1/2	-1/2			
	2	+2	+1/2	-1/2			
		+1	+1/2	-1/2			
		0	+1/2	-1/2			
		-1	+1/2	-1/2			
		-1	+1/2	-1/2			
		-2	+1/2	-1/2			

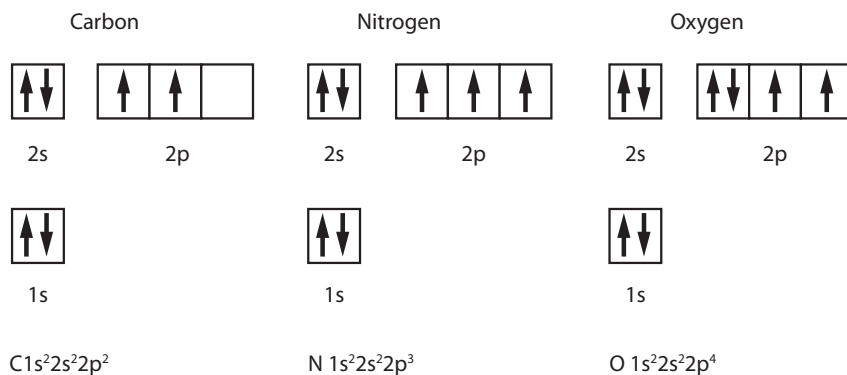


**Figure 3.6** Example of filling shells and pairing electrons ( $\uparrow\downarrow$ ) in the carbon, nitrogen, and oxygen atom.



## ***Electron: Interatomic and Intermolecular Interactions***

The electron not only determines the structure of atoms and their bonding by covalent bonds in creating molecules, but determines the interaction between molecules as well. A more detailed explanation of these interactions is listed in Table 3.4 that follows, and we start with the Van der Waals interactions.

### ***Van der Waals Interactions***

The Van der Waals interactions are the basic forces of matter, discovered in 1873 by Johannes Diderik van der Waals (1837–1923), while working on his doctoral dissertation on real gases.

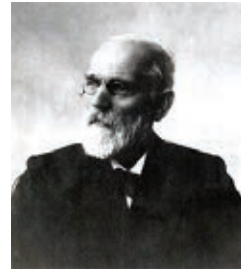
Measuring interatomic and intermolecular forces is a mechanical-electromagnetic (physicochemical) process. As the absorption of the infrared (IR) radiation is, in principle, the same process as the transfer of energy from one mechanical oscillator to another one (resonance), mechanotronics at the nano level is a completely natural phenomenon. The basic precondition is that all entities participating in the energetic process oscillate with the same frequency, or that the frequency of one oscillator is equal to an integral multiple of the frequency of the other oscillator. After resonance, in the system that has received energy, the oscillation amplitude is increased, while the frequency remains unchanged.

The absorption of electromagnetic radiation is a quantum process occurring in most molecules within the IR spectrum with energies of 8 to 50 KJ/mol; it corresponds to the differences between vibrational energy levels. The relation between mechanical and electromagnetic phenomena of interactions between two atoms or two molecules is given by the expression:

$$\nu^* = \frac{1}{2\pi c} \sqrt{\frac{k}{\mu}}, \quad (3.36)$$









where  $\nu^*$  is the wave number ( $cm^{-1}$ ),  $c$  – the velocity of light,  $k$  – constant of the bonding force and  $\mu$  – reduced mass:  $(m_1+m_2)/(m_1 \times m_2)$  (the wave number  $\nu^*$  is still, out of habit, calculated by chemists in  $cm^{-1}$  and not in  $m^{-1}$ ).

Table 3.4 shows that the electromagnetic forces define completely the character of intermolecular interactions, and thus the behavior of biological fluids and solid tissues in the human organism. The gravitation forces govern mostly the macroscopic phenomena (at the level of the organism and organs), however, in certain cases they act coupled with electromagnetic forces (capillary phenomena, viscosity, etc.). However, the quantum gravitation represents a new challenge for the understanding of the behavior of biomolecules and changes in their conformational states. Today, the entropic gravitation is increasingly investigated; it could be associated with biomolecular information processes.



*Johannes Diderik  
van der Waals  
(1837-1923)*

Table 3.4 Survey of the basic intermolecular interactions.

Name	Schematic representation	$E = f(r)$
Ion-ion		$\frac{1}{r}$
Ion-dipole		$\frac{1}{r^2}$
Dipole-dipole		$\frac{1}{r^3}$
Ion-induced dipole		$\frac{1}{r^4}$
Dipole-induced dipole		$\frac{1}{r^5}$
Induced dipole-induced dipole		$\frac{1}{r^6}$
Hydrogen bonds	Network of dipole moments 	$\approx \frac{1}{r^2}$
London interactions	Interaction between temporary dipoles of nonpolar, but polarized bodies 	$\approx \frac{1}{r^6}$

For a completely accurate investigation of these phenomena, it would be necessary to use quantum mechanical principles (quantum electrodynamics), however, it was established that the electrostatic approach, using adequate approximations, provides comparatively accurate results in good conformity with experiments that can be relatively quickly applied in the realization of a biomedical device.

### ***Nonpolar Interactions***

In the aim to grasp the description of intermolecular forces in a nutshell, the *potential of interaction* concept was designed related to force by the expression  $F = -dw(r)/dr$ . Having in mind the differential relation of  $w(r)$  and force, that is, the work performed

by that force, the function  $w(r)$  is often called *free energy* or *available energy* to perform work. Throughout the 19 century, there persisted a belief that it is possible to formulate an expression for the law of the force that would include all intermolecular interactions, something like Newton's law of gravitation. Various expressions were proposed for the interaction potential in the form:

$$w(r) = -\frac{Cm_1m_2}{r^n} \quad (3.37)$$

where  $m_1$  and  $m_2$  denote the masses of the molecule related to the force by the relation:

$$F = \frac{dw(r)}{dr} = \frac{d}{dr} \left( -\frac{Cm_1m_2}{r^n} \right) = -n \frac{Cm_1m_2}{r^{n+1}}. \quad (3.38)$$

In this model, the values of the exponent  $n$  were envisaged as the 4<sup>th</sup> or 5<sup>th</sup> power, while in the case of Newton's gravitation law, the exponent takes the value 1, thus the  $C$  constant would be equal to the gravitational constant, meaning that the law of the force would be identical to Newton's law of gravitation:

$$w(r) = -\gamma \frac{m_1m_2}{r} \quad F = -\gamma \frac{m_1m_2}{r^2}, \text{ where } g = 6.67 \times 10^{-11} \text{ N/m}^2\text{kg}^2.$$

However, it turned out that the solution is not as simple as that. On the other hand, the mistake was not substantial. Namely, the degree of dependence was the principle that could explain relatively short distances at which the intermolecular forces act. However, for a more accurate explanation it was necessary to include molecule polarity, i.e., molecule's electromagnetic character, as the main determinant of the description.

A general expression for the determination of the law on the intermolecular interactions is:

$$w(r) = -\frac{C}{r^n}. \quad (3.39)$$

Based on this expression, the total energy of the molecule interaction with all other molecules in the neighborhood is calculated, from the molecule radius  $\sigma$  to the distance  $L$ , obtaining the expression:

$$E(r) = \int_{\sigma}^L w(r) dV = -\frac{4\pi C\rho}{(n-3)r^{n-3}}, \text{ for } n > 3, L \gg \sigma.$$

It turned out that most molecular interactions have the characteristic  $n > 3$ , namely that they are of short range.

In parallel with these conclusions, the concept of capillary phenomena and surface tension was developed, resulting in the inference that the same forces are responsible for the cohesion in solids and in fluids. The final outcome of these investigations is that these forces of short range can also generate mechanisms of macroscopic phenomena (forming the drop shape, reactions of water with detergents and lipids, etc.). One of the first successful applications of the concept of molecular interactions at the macroscopic level was the equation of state for the real gas by Van der Waals:

$$\left(P + \frac{a}{V^2}\right)(V - b) = RT . \quad (3.40)$$

In this expression, a term  $a/V^2$  was added to pressure, representing the contribution of attractive Van der Waals forces.

In 1903, Mie proposed the following expression for the interaction potential, which for the first time included the attractive and the repulsive component:

$$w(r) = -\frac{A}{r^n} + \frac{B}{r^m} . \quad (3.41)$$

This expression is still used today, and in the special case of Mie potential, when  $n = 6$  and  $m = 12$ , we obtain the expression for the Lenard-Johns potential:

$$w(r) = -\frac{A}{r^6} + \frac{B}{r^{12}}$$

where values of constants  $A$  and  $B$  for the interaction of two atoms are  $A = 10^{-77} \text{ Jm}^6$ ,  $B = 10^{-134} \text{ Jm}^{12}$ .

Contemporary perceptions of the intermolecular interactions are based on the Helman-Feynman's theorem, according to which all intermolecular forces can be determined based on the solution of the Schrödinger's equation determining the spatial configuration of electrons. The intermolecular interactions are then determined as classical electrostatic interactions. However, the *exact* solutions to the Schrödinger's equation are not easy to obtain, even in case of the simplest molecules, such as a pair of hydrogen atoms. Therefore, we shall initiate a classification of intermolecular interactions from the electrostatic aspect, although they have the same basic mechanism of creation. We shall distinguish short and long range interactions, ionic interactions, covalent interactions, Van der Waals interactions, solution interaction, hydrogen bonds, etc.

This classification influenced numerous scientific disciplines where first some classes were imposed as the most relevant, then the corresponding terminology accepted, different for each discipline, but pointing to, basically, the same phenomena.

In the investigation of intermolecular forces, we can distinguish two major cases: interaction in the vacuum and interaction in a medium (most often in a liquid medium – solution). As the significance of investigating interactions in vacuum is mostly theoretical, it is necessary to investigate the intermolecular interactions compared with the thermal motion of matter most concisely described by  $kT$ , ( $k$  – Boltzmann's constant  $1.38 \times 10^{-23} \text{ JK}^{-1}$ ,  $T$  – temperature K).

In a large number of cases, it is necessary to investigate whether the observed interaction can „overpower“ the entropic influence of the thermal motion. This criterion actually, indicates prevalently the stability of intermolecular interactions in the „standard environment“, always at a certain temperature and in thermal motion.

The average translational kinetic energy of molecule is  $3kT/2$ , composed of rotational and vibrational components, which we shall not investigate here, but which are present in all aggregate states of matter. Therefore, it is necessary to compare constantly all further deliberations with the thermal energy parameter.

### 3.5. Classification of Intermolecular Forces

Intermolecular forces can be classified into three classes. This classification is neither exact nor comprehensive. It serves as an introductory overview of classical physics insights without the use of the quantum mechanics approach, which are nevertheless very useful.

The first class of intermolecular forces results from *purely electrostatic*, *Coulomb* interactions including interactions of concentrated charges (ions), dipoles, quadripoles, etc. The second class represents *polarization* forces resulting from the *induction* of the polarized state in atoms and molecules (otherwise nonpolar) due to the presence of the external electric field. The third class includes forces of *quantum-mechanical* nature that result in the generation of *covalent* or *chemical* bonds, and repulsive forces which balance the attractive forces at short range.

At the same time with this classification, we shall investigate strong interactions belonging to the first and the third class, and afterwards we shall devote attention to weaker forces including several interactions of polar and polarized molecules.

#### **Strong Interactions: Covalent Bonds and Coulomb Interactions**

Covalent bonds are formed primarily in elements belonging to the middle groups of the periodic system of elements. They act at distances of 0.1 nm – 0.2 nm, representing thus forces of very short range. The strength of some covalent bonds is: C ≡ N approximately 870 (kJmol<sup>-1</sup>), C=O approximately 690 (kJmol<sup>-1</sup>), C=C about 600 (kJmol<sup>-1</sup>), O-H around 460 (kJmol<sup>-1</sup>), C-H around 430 (kJmol<sup>-1</sup>), keeping in mind that 1 kJmol<sup>-1</sup> is approximately 0.4 kT.

The Coulomb attraction force between two charged atoms or ions is undoubtedly the strongest interaction, stronger than many chemical forces (bonds). The interaction potential (free energy) of this interaction is:

$$w(r) = \frac{Q_1 Q_2}{4\pi\epsilon_0 r} = \frac{z_1 z_2 e^2}{4\pi\epsilon_0 r} \quad (3.42)$$

where  $\epsilon_0$  is the relative dielectric constant of vacuum (in case of interaction in a medium,  $\epsilon_r$  is the dielectric constant of the medium where the reaction occurs), while  $r$  is the distance between two interacting charges,  $z$  ion valence and  $e$  the elementary electric charge equal to the electron charge  $e = 1.602 \times 10^{-19}$  C. Based on free energy, we obtain the expression for the Coulomb force:

$$F = -\frac{dw(r)}{dr} = \frac{Q_1 Q_2}{4\pi\epsilon_0 r^2} = \frac{z_1 z_2 e^2}{4\pi\epsilon_0 r^2}$$

When this free energy is compared to the thermal energy, expressing it as a multiple of  $kT$ , the following ratio is obtained for the case of monovalent ions Na<sup>+</sup> and Cl<sup>-</sup> (their summed ion radius is 0.276 nm):

$$w(r) = \frac{-(1.602 \cdot 10^{-19})^2}{4\pi(8.854 \cdot 10^{-12})(0.276 \cdot 10^{-9})} = -8.4 \cdot 10^{-19} \text{ J} \quad (3.43)$$

which, compared to the thermal energy that at the temperature of 300 K equals  $kT = (1.38 \times 10^{-23}) (300) = 4.1 \times 10^{-21} \text{ J}$ , gives approximately 200  $kT$  per ion pair in the vacuum, resembling energies of covalent bonds.

Coulomb interactions are responsible for the creation of bonds in ion compounds (crystals) and the calculation of the overall interaction energy, denoted by  $\mu^i$ , in case of the monovalent ions of sodium and chlorine and the inter-ion distance of  $r = 0.276 \text{ nm}$ , is obtained as the sum of all mutual interactions of the cubic crystalline lattice:

$$w(r) = \frac{z_1 z_2 e^2}{4\pi\epsilon_0 r} = \frac{(1)(-1)e^2}{4\pi\epsilon_0 r} = \frac{e^2}{4\pi\epsilon_0 r}$$

$$\mu^i = -\frac{e^2}{4\pi\epsilon_0 r} \left[ 6 - \frac{12}{\sqrt{2}} + \frac{8}{\sqrt{3}} - \frac{6}{2} + \dots \right] = -\frac{e^2}{4\pi\epsilon_0 r} [6 - 8,485 + 4,619 - 3 + \dots] =$$

$$= -1,748 \frac{e^2}{4\pi\epsilon_0 r} = -1,47 \cdot 10^{-18} \text{ J} \quad (3.44)$$

By multiplying this value with Avogadro's number, we obtain the molar energy value:

$$U = -N_0 \mu^i = (6.02 \cdot 10^{23})(-1.47 \cdot 10^{-18}) = 880 \text{ kJmol}^{-1}$$

The action range of Coulomb forces in ion compounds is somewhat smaller because the attraction forces of opposite ions in non-neighboring positions of the lattice are weakened by the effect of the repulsive forces of neighboring ions. Regardless, they maintain a considerably greater action range than covalent forces (bonds).

## Interactions between Polar Molecules

Most molecules have neither a shortage nor a surplus of charge, however, there exists an imbalance caused mainly by the differences in electronegativity between atoms in the molecule. As an example, the glycine amino-acid does not have a surplus/shortage of electrons when it is isolated in a neutral surrounding. However, in a polar environment, such as water, an acid group and a base group are created becoming the origin of polarity.

Polar molecules whose quantity of positive charge is equal to the quantity of negative charge are called *zwitterions*, while in the case of an imbalance of charge such ions are called *bipolar ions*.

The dipole moment of a polar molecule is defined as the product of the quantity of the disbalanced charge and the distance between poles:

$$u = ql.$$

For example, considering water, it is possible to calculate the dipole moment knowing the dipole moment of the O-H bond and the angle between two O-H bonds:

$$u_{H_2O} = 2 \cos\left(\frac{1}{2}\theta\right)u_{OH} = 2 \cos(52.25^\circ) \cdot 1.51 = 1.85D$$

Permanent dipole moments occur only in asymmetric molecules, not in single atoms.

### ***Ion - Dipole Interaction***

Figure 3.7 presents a model of the ion- dipole interaction. According to the expression for the Coulomb free energy of interaction, we can write that the overall energy is the sum of particular interactions between ions and dipole ends.

In accordance with the notation from the Figure, we have:

$$w(r) = -\frac{Qq}{4\pi\epsilon_0\epsilon} \left[ \frac{1}{AB} - \frac{1}{AC} \right] \quad (3.45)$$

where distances  $AB$  and  $AC$  are determined by the relation:

$$AB = \left[ \left( r - \frac{1}{2}l \cos \theta \right)^2 + \left( \frac{1}{2}l \sin \theta \right)^2 \right]^{1/2}$$

$$AC = \left[ \left( r + \frac{1}{2}l \cos \theta \right)^2 + \left( \frac{1}{2}l \sin \theta \right)^2 \right]^{1/2}.$$

At distances far greater than the dipole length, we can introduce an approximation:

$$AB \approx \left( r - \frac{1}{2}l \cos \theta \right)$$

$$AC = \left( r + \frac{1}{2}l \cos \theta \right).$$

By substituting these expressions into the starting equation, we finally obtain the expression for free energy:

$$w(r) = w(r, \theta) = -\frac{(ze)u \cos \theta}{4\pi\epsilon_0\epsilon r^2}.$$

If the concept of field  $E(r)$  is introduced, this expression can be simplified as:

$$w(r) = w(r, \theta) = -\frac{(ze)u \cos \theta}{4\pi\epsilon_0\epsilon r^2} = -uE(r) \cos \theta.$$

As a result of the approximations introduced above, the expression error is increased when the distance between the ion and the dipole becomes close to the dipole length. Quantitative analysis of this expression, in case of the interaction between the sodium

ion  $\text{Na}^+$  ( $z = 1$ ,  $a = 0.095$  nm) and the dipole moment resulting from the water molecule ( $a = 0.14$  nm,  $u = 1.85$  D), with maximum interaction energy (300 K), will be:

$$w(r, \theta = 0^\circ) = -\frac{(1.602 \cdot 10^{-19})(1.85 \cdot 3.336 \cdot 10^{-30})}{4\pi(8.854 \cdot 10^{-12})(0.235 \cdot 10^{-9})^2} = -1.6 \cdot 10^{-19} \text{ J} = 96 \text{ kJmol}^{-1} = 39 \text{ kT} \quad (3.46)$$

These attraction forces between water and positive ions are responsible for the hydrophilic, hydrophobic and absorption reactions. The experimental value obtained for this interaction conforms extremely well to the theoretical result and equals  $100 \text{ kJmol}^{-1}$ . Similar is the case with other theoretical/experimental results: for the  $\text{Li}^{+1}$  ion ( $a = 0.068$  nm) the theoretic value is  $50 \text{ kT}$  ( $125 \text{ kJmol}^{-1}$ , experimental value is  $142 \text{ kJmol}^{-1}$ ), for small bivalent cations  $\text{Mg}^{2+}$  ( $z = 2$ ,  $a = 0.065$  nm) and  $\text{Be}^{2+}$  ( $z = 2$ ,  $a = 0.030$  nm) we have values  $100 \text{ kT}$  and  $150 \text{ kT}$ .

Aggregates of water molecules, formed in the immediate vicinity of the ion, create a *primary hydration shell* that represents a local selforganization of water at the molecular level. This phenomenon does not exist only in the first shell; it results in the formation of multilayer shells, which are far less stable, having a shorter life cycle. For the  $\text{K}^+$ ,  $\text{Na}^+$  and  $\text{Li}^+$  ions, this time is approximately  $10^{-9}$  s, for the  $\text{Ca}^{2+}$  ion it is  $10^{-8}$  s, for  $\text{Mg}^{2+}$  :  $10^{-6}$  s, for  $\text{Fe}^{2+}$  :  $10^{-3}$  s, etc.

## Interactions between Two Dipoles

Similarly to the procedure used to obtain the expression for the ion-dipole interaction, we describe the interaction dipole-dipole in the following way:

$$w(r) = w(r, \theta_1, \theta_2, \phi) = -\frac{u_1 u_2 \cos \theta}{4\pi\epsilon_0 \epsilon r^3} [2 \cos \theta_1 \cos \theta_2 - \sin \theta_1 \sin \theta_2 \cos \phi] \quad (3.47)$$

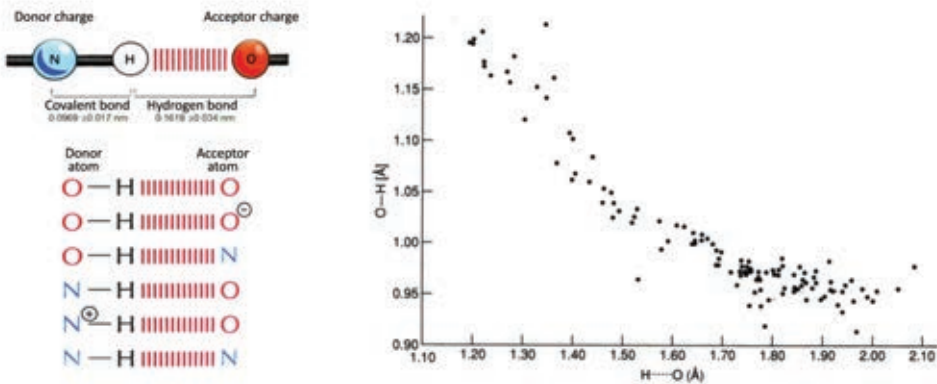


**Figure 3.7** Six basic types of hydrogen bonds in biological systems, three with oxygen and three with nitrogen as donors, i.e., four with oxygen and two with nitrogen as acceptors (left), and the relationship between the O-H covalent bond and the H...O noncovalent bond (right).



It can be seen from the above equation that the interaction maximum occurs when the dipole directions are collinear:

$$w(r) = w(r, 0, 0, \phi) = -2u_1u_2 / 4\pi\epsilon_0\epsilon r^3. \quad (3.48)$$

On the other hand, the minimum interaction occurs when the dipoles are parallel to each other, then energy equals half of the maximum energy. Calculations indicate that the interactions of the type dipole-dipole are not so strong and that, already at distances of 0.35 nm in vacuum, they become weaker than the energy  $kT$ .

The exception are hydrogen bonds, which are a special case of strong dipole-dipole bonds formed between the atoms  $O^{\frac{3}{4}}N^+$ ,  $N^{\frac{3}{4}}N^+$  and  $F-H^+$  due to the very small radius of the hydrogen atom which brings these atoms much closer resulting in increased interaction intensity.

### ***Interactions with Polarization***

Polarization represents the induction of additional dipole moments, and is caused by the action of local electric fields on atoms (ions). All atoms and molecules can be polarized. The degree of polarization is determined by the size of the *induced dipole moment* occurring in the field  $E$ :

$$u_{ind} = \alpha E. \quad (3.49)$$

The polarization coefficient of an atom per molecule  $\alpha$  is obtained from the condition that the force induced by the field action must be in equilibrium with the force resisting the action of the external field:

$$F_{ext} = eE, \\ F_{int} = \frac{e^2}{4\pi\epsilon_0 R^2} \sin \theta \approx \frac{e^2 l}{4\pi\epsilon_0 R^3} \approx \frac{e}{4\pi\epsilon_0 R^3} u_{ind}.$$

Therefore:

$$u_{ind} = 4\pi\epsilon_0 R^3 E = \alpha_0 E$$

Resulting in the degree of polarization:

$$\alpha_0 = 4\pi\epsilon_0 R^3. \quad (3.50)$$

### ***Interactions between Ions and Nonpolar/Polar Molecules***

This reaction type is reduced to the induction of a dipole in a nonpolar molecule. The ion electric field of intensity:

$$E = \frac{ze}{4\pi\epsilon_0\epsilon r^2} \quad (3.51)$$

induces, in a nonpolar molecule, a dipole with moment:

$$u_{ind} = \alpha E = \alpha ze / 4\pi\epsilon_0\epsilon r^2.$$

The interaction energy of such a pair (ion – induced dipole) can be generalized in cases of polar and non-polar molecules by including the constant  $\alpha_0$  for the case of polar molecules (this constant equals zero in case of non-polar molecules):

$$w(r) = -\frac{(ze)^2}{2(4\pi\epsilon_0\epsilon)^2 r^4} \left( \alpha_0 + \frac{u^2}{3kT} \right). \quad (3.52)$$

### ***Dipole – Induced Dipole Interactions***

The interaction between a nonpolar and a polar molecule is analogous to the interaction ion – induced dipole, with the exception that the field of polarization results from the dipole and not from a constant electric charge. Bearing in mind that two different molecules have different dipole moments  $u_1$  and  $u_2$ , and corresponding polarization coefficients  $\alpha_1$  and  $\alpha_2$ , the total free energy of this pair will be:

$$w(r) = \frac{(u_1^2\alpha_{02} + u_2^2\alpha_{01})}{(4\pi\epsilon_0\epsilon)^2 r^6}. \quad (3.53)$$

### ***Van der Waals Interactions***

The theory of Van der Waals interactions represents unification and generalization of all investigated interaction types with an additional element – the *dispersion* interaction. The dispersion interaction resembles the gravitation force because it acts between *all* atoms and molecules, regardless of charge and polarization.

Dispersion forces probably contribute most to intermolecular interactions, because they are always present, unlike other interaction types whose presence can depend on the molecule's characteristics. Essentially, they are forces of long range (from 0.2 to over 10 nm) and can be both attractive and repulsive. The origin of these forces is quantum-mechanical and can be explained in sum as the current value of the interaction of each electron forming a dipole with proton. Although it can be argued that the average value of these interactions should tend to zero, this is not so – their intensity is considerable – approximately 1 kT.

If we take into account all three components of the Van der Waals forces (induction force, orientation force and dispersion force), we can conclude that all three are inversely proportional to the third power of distance in the following way:

$$w_{vdw}(r) = -\frac{C_{vdw}}{r^6} = -\frac{[C_{ind} + C_{ori} + C_{disp}]}{r^6} = \frac{\left[ (u_1^2\alpha_{02} + u_2^2\alpha_{01}) + \frac{u_1^2 u_2^2}{3kT} + \frac{3\alpha_{01}\alpha_{02}h\nu_1\nu_2}{2(\nu_1 + \nu_2)} \right]}{(4\pi\epsilon_0\epsilon)^2 r^6} \quad (3.54)$$

### 3.6. Do We Need a New Electron Model?

We observe From Table 3.1 that the electron model, regarding hydrogen, ends with two electromagnetic (light) packets, which are symmetrical with respect to the center of total energy (Salhofer, 1978). This is a very interesting and significant solution for our approach to the model of reality, especially regarding the interaction between light and matter (Chapter II). We are interested in biological structures where hydrogen is present in about 63% compounds, carbon 9.5%, oxygen 25.5%, and all the other elements with 2% of the total number of atoms (1.8% is nitrogen, phosphorus and sulfur, and 0.2% all the other elements). The electron model is especially interesting regarding carbon, for two reasons: because the biological life is based on carbon polymers, and because the nanophotonic material we intend to use for the construction of a device used in bio-medical engineering should be based on carbon.

Carbon atoms are organized as 3D objects (diamond), 2D quasiobjects (graphite, if it is a monolayer then it is graphene), 1D quasiobject (nanotube) and 0D quasiobject (fullerene). For „2D, 1D and 0D“ objects we used the term „quasiobjects“ because they resemble but are not of this dimension, they are 3-dimensional objects. Fullerene, the  $C_{60}$  molecule, especially significant for our research, belongs to the class of 0D quasiobjects. The 0D structures act like celestial macroscopic bodies acted upon by gravitation- they take the shape of a sphere. However, reality is completely different, they have one „quasi-center of gravitation“ based on electromagnetic interactions and icosahedral symmetry.

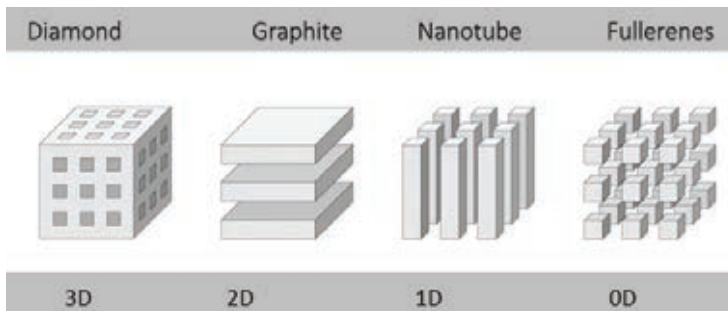


**Figure 3.8** *The real carbon 3D crystal structure is the diamond, graphite is something between a 2D and a 3D structure because it is layered. Nanotubules are quasi 1D structures, as are the fullerenes- 0D molecular crystal structures.*

The STM method is important for the identification of surface energy concentration of the  $C_{60}$  molecule. The NMR spectroscopy is used to determine its rotation speed. Based on these experimental data, a working hypothesis was postulated about a new model of the electron as a spatio-temporal entity.

The first experimental result obtained by the NMR method demonstrated that the  $^{13}C$  NMR spectrum of the crystalline  $C_{60}$ , at room temperature, is composed of a relatively narrow line, which confirmed the most important postulate about the  $C_{60}$  structure; that all 60 atoms are equivalent, i.e., the structure of a truncated icosahedron had been confirmed (Tycko, 1991, Heiney, 1991).

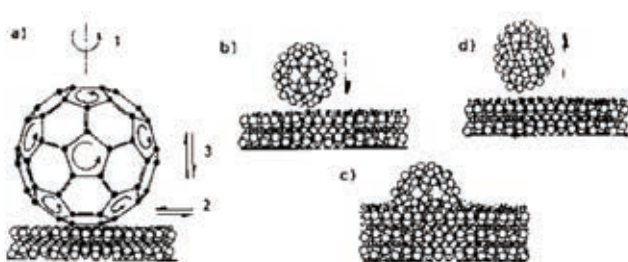


**Figure 3.9**  $C_{60}$  is a molecular crystal with icosahedral symmetry, however, several  $C_{60}$  molecules form a cubical crystalline lattice, based on point symmetry (left). 60  $\pi$ -electrons of each  $C_{60}$  molecule cause the repulsive forces to be formed keeping the molecule at a distance, there is no friction, so that the  $C_{60}$  molecule rotates randomly („twisting“) with the velocity of approximately  $3 \times 10^{10} \text{ s}^{-1}$  (average). Due to this high velocity rotation on the support, it moves alternatively to the left and to the right, forward and then backward. These effects cause it to hop (we call it *punctum saliens* – a hopping point). Only when it falls into a „mouse trap“, a slight defect on the supporting pad, and is immobilized, it is possible to take an image by STM or AFM or by MFM (Koruga, et al., 1993a).

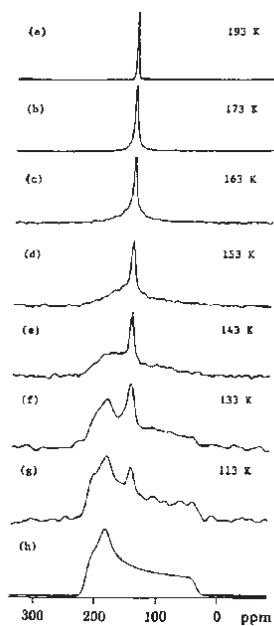


**Figure 3.10** The  $^{13}\text{C}$  NMR spectrum of the solid  $C_{60}$  (a)-(g), and the simulation of the graph shape with an anisotropic chemical shift (h) (Johnson, 1992).

The  $^{13}\text{C}$  NMR spectra obtained at lower temperatures demonstrate that the nature of molecular dynamics of  $C_{60}$  changes at 260K. This result conforms to the results of calorimetric studies and the diffraction of X-rays. A sharp NMR peak, as a result of the isotropic rotation of  $C_{60}$  is obtained in the range of high temperatures over 190 K. Below 190 K the peak is gradually flattened and transformed into a shape typical of the axially symmetric tensors of the chemical shift when the molecule rotates about an axis. Below 100 K, the rotation speed is sufficiently small, so that it is possible to determine the tensor elements based on the NMR graph form [13].

The phase transition is experimentally confirmed as a discontinuity in the temperature dependence spin – lattice time relaxation  $T_1$  (Figure 3.10). Using the theoretical model according to which the basic mechanism spin – lattice relaxation ( $T_1$ ) is the anisotropy of the chemical shift

$$\frac{1}{T_1} = \gamma^2 B_0^2 \left[ \frac{2}{3} A^2 \frac{\tau_A}{(1 + \omega^2 \tau_A^2)} + \frac{2}{15} S^2 \frac{\tau_S}{(1 + \omega^2 \tau_S^2)} \right] \quad (3.56)$$

where A and S originate from the symmetrical ( $\sigma_S$ ) and the antisymmetrical ( $\sigma_A$ ) tensor component of the chemical shift ( $A^2 \approx 1.4 \times 10^{-10}$ ,  $S^2 = 3.17 \times 10^{-8}$ ), the rotation correlation times  $\tau_A$  and  $\tau_S$  can be calculated ( $\tau$  is the time for the molecule to rotate by the angle  $\theta = 1$  rad) based on experimentally obtained relaxation time values and the shift tensor. The phase transition occurs at 260 K. The full line represents the low temperature phase between 193 K and 243 K. The discontinued line corresponds to experimental results obtained in the high temperature phase, over 263 K (Johnson, 1992).

The rotation diffusion constant  $D$  is related to correlation times  $\tau_A$  and  $\tau_S$  by the expression:

$$1/6D = \tau = \tau_S = \tau_A / 3. \quad (3.57)$$

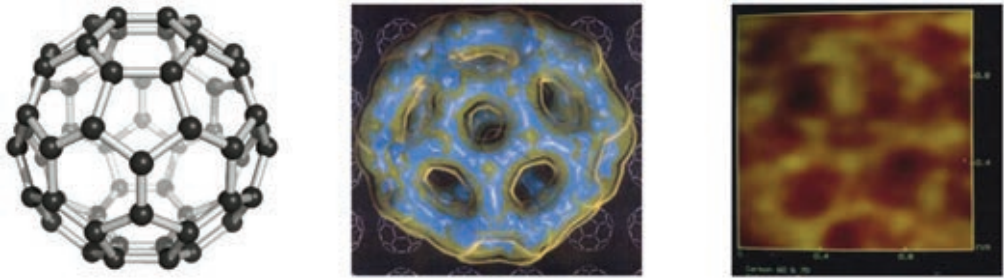


**Figure 3.11** The theoretical model of the  $C_{60}$  molecule from 1985, immediately after it was discovered by Kroto, Curl, and Smalley of Rice University, USA (left); the  $C_{60}$  molecule model based on quantum-mechanical calculations from December 1991, cover page of *Science* (middle); the first STM image of the  $C_{60}$  molecule, April 1992, NanoLab, Faculty of Mechanical Engineering, University of Belgrade (right). It is striking that all three images of molecules are more than similar, and the most interesting fact is that quantum theory and experiment coincide completely (Koruga, et al., 1993<sup>b</sup>).

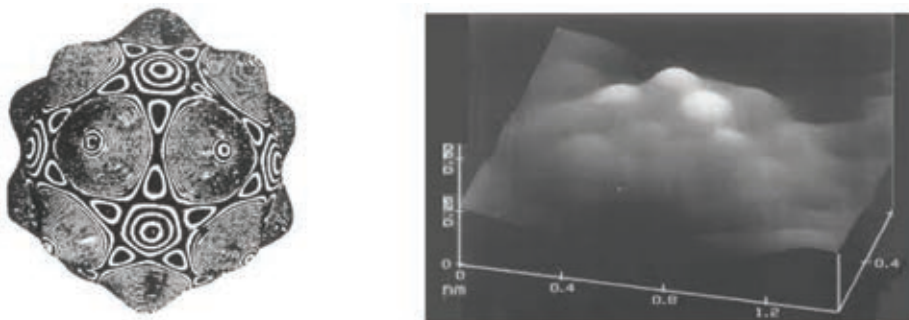
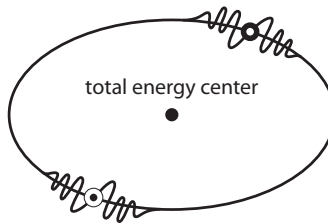


**Figure 3.12** Molecule  $C_{60}$  is a dynamic structure with vibrating carbon atoms generating surface energy in pentagons (left); the same effect was identified by using the STM (April 1992, NanoLab, Faculty of Mechanical Engineering, University of Belgrade) (Koruga, et al., 1993<sup>b</sup>).

For solid state  $C_{60}$  at temperature  $T = 283$  K, coefficients of diffusion in solid state and in fluid state were obtained as  $D = 3 \times 10^{10} \text{s}^{-1}$  and  $D = 1.8 \times 10^{10} \text{s}^{-1}$  respectively. The rotation phenomenon of the  $C_{60}$  molecule is still unexplained, it is assumed that it is caused by space-time coupling of electrons in the hexagonal and pentagonal lattices (concentration of electronic, vibrational and rotational energy), the isotropic environment of the  $\pi$  electron cloud, and marked symmetry of the  $C_{60}$  molecule.

If the classical radius of the electron, as a 3D object, is calculated from the relation  $mc^2 = e^2/4\pi\epsilon_0 r$ , we obtain  $r_e \sim 10^{-16}$  m. On the other hand, we have seen (Chapter II) that the elementary charge is of the order of Planck's length  $r_e \sim 10^{-35}$  m. Thus we conclude that for the electron, as an  $N = 3$  object, the value is  $r_e \sim 10^{-16}$  m, and for the  $N = -2_5$  object  $r_e \sim 10^{-35}$  m.

Electron as an  $N=3$  object



Electron as an  $N(-2)_5$  object

**Figure 3.13.** Electron as a three-dimensional object ( $r_e \sim 10^{-16}$  m) as a five-dimensional object ( $r_e \sim 10^{-35}$  m) and the center of total energy in resonant relationship with  $N = 0$  [ $N(3) \times N(-2_5) = N(0)$ ].

The above presentation introduced the *photon* (spin 1, belongs to the boson family, velocity  $\sim 3 \times 10^8$  m/s, rest mass 0, has mass in motion (depending on wavelength)) and the *electron* (spin  $+1/2$  or  $-1/2$ , belongs to the fermion family, velocity of valence electrons  $\sim 2 \times 10^6$  m/s, mass  $1.602 \times 10^{-31}$  kg, size in  $N = 3$ ,  $r_e \sim 10^{-16}$  m, and as an  $N = -2_5$  object  $r_e \sim 10^{-35}$  m).

As can be seen, both electron attributes, in the  $N(3)$  and in the  $N(-2_5)$ , belong to the system  $N(3) \times N(-2_5) = N(0)$ , so that their interaction can be investigated from the classical aspect or the five-dimensional aspect. It is precisely this electron attribute that enables the light–matter interaction to be observed and investigated from both of these aspects.

## References

1. Alonso, M., Finn, E.J., Physics. Addison-Wesley, Harlow, 1992.
2. Avouris, Ph. ed., *Atomic and Nanometer-Scale Modification of Materials Fundamentals and Application*. NATO ASI Series, Kluwer Academic Pub, Dordrecht, Boston, London, 1993.

3. Binnig, G., Rohrer, H., Scanning Tunneling Microscopy. *Helvetica Physica Acta*, 55, 726-735, 1982.
4. Frolich, H., Quantum mechanical concepts in biology, in *Theoretical Physics and Biology*. Ed. Marois, M., North Holland, Amsterdam, 1968.
5. Hawking, S., *The Universe in a Nutshell*. Bantam Books, New York, 2001.
6. von Hippel, A.R., *Molecular science and molecular engineering*. MIT Press/Wiley, New York, 1959.
7. Johnson, D.R., Yannoni, S.C., Dorn, C.H., Salem, R.J., Bethune, S.D.,  $C_{60}$  Rotation in the Solid State: Dynamics of a Faceted Spherical Top. *Science*, vol. 255, 1235-1238, 1992.
8. Khun, H., Forsterling, H-D., *Principles of Physical Chemistry*. John Wiley & Sons, Chichester, 2000.
9. Koruga, D. S. Hameroff, J. Withers, R. Loutfz, M. Sundershan, *Fullerene  $C_{60}$ : History, Physics, Nanobiology, Nanotechnology*. North-Holland, Elsevier, Amsterdam, 1993<sup>a</sup>.
10. Koruga, D. et.al., *Fullerene Science and Technology*, 1 pp. 93-100, 1993<sup>b</sup>.
11. Lakhtakia, A. (ed.), *Models and modeleres of hydrogen*. World scientific, Singapore, 1996.
12. Springford, M., *Electron: a centenary volume*. Cambridge University Press, Cambridge, 1997.
13. Russell, H.N., Saunders, F.A., New Regularities in the Spectra of the Alkaline Earths. *Astrophysical Journal*, vol. 61, pp. 38-42, 1925.
14. Thomson, J.J., Cathode Rays. *Phil.Mag.*, S.5, Vol. 44, No. 269-316, 1897.
15. Wiesendanger, R., *Scanning Probe Microscopy and Spectroscopy*. Cambridge University Press, Cambridge, 1994.
16. Zettili, N., *Quantum Mechanics: Concept and Applications*. John Wiley and Sons, Chichester, 2009.





# 4

## LIGHT-MATTER INTERACTION



Artist, design! Do not converse in vain!  
 Create your poetry as a light breeze!  
 GOETHE

### 4.1. Poincaré Sphere (light)

Henri Poincaré formulated in 1892 the concept of a *virtual sphere* that is used to represent light polarization graphically. This virtual sphere is known today under his name. Light can have different polarizations; linear (vertical and horizontal), elliptical (right-hand or left-hand) and circular polarization (right-hand or left-hand). These polarizations correspond graphically to different locations on the surface of the Poincaré sphere (Figure 4.1). Information on the state of polarization corresponds to different points on the Poincaré sphere.



Henri Poincaré  
 (1854–1912)

To define the light sphere, Poincaré used circular polarization based on the propagation of the relative wave magnitude for the left-hand and right-hand circularly polarized component, using the difference of their phase shift. The Poincaré sphere can be used interactively to understand various types and states of light polarization.

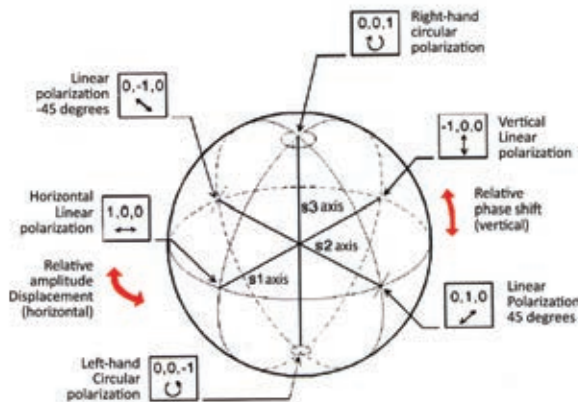
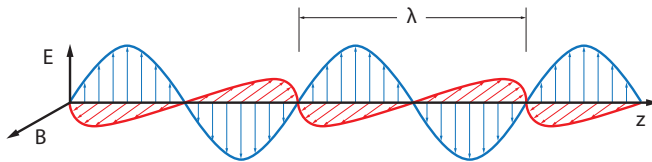


Figure 4.1 Poincaré sphere with layout and interdependence of basic linear and circular polarizations.

Poincaré is also known by his 1904 conjecture (regarding the topology of the three-dimensional sphere) which was one of the most intriguing unsolved mathematical problems, until a couple of years ago, when it was solved by the Russian mathematician Gregory Perelman.

Light consists of a stream of photons which, as electromagnetic waves, propagate in vacuum or in another homogenous isotropic medium in the form of an electric field (vector) and a magnetic field (vector) travelling in the direction orthogonal to the direction of wave propagation (Figure 4.2). Therefore and are vector quantities, not scalars (temperature is a scalar), meaning that they have *intensity*, *direction*, *sense* and *point of application*. Another important feature is that and are always mutually orthogonal. A simplified representation of the photon wave with electric (E) and magnetic (B) field, and wavelength ( $\lambda$ ) is given in Figure 4.2.



**Figure 4.2** Electric (blue) and magnetic (red) field of photons propagating along the  $z$ -axis. Wavelength is denoted by  $\lambda$  (m), depending on the wavelength magnitude it can be expressed in pm, nm,  $\mu\text{m}$  or mm units. Chemists use the wave number  $\lambda^* \text{cm}^{-1}$  instead of the wavelength, denoting the number of waves per unit centimeter.

The electric field ( $\vec{E}$ ) of photons is defined by the expression 4.1 as a vector quantity:

$$\vec{E}(z, t) = \begin{bmatrix} e_x \\ e_y \\ 0 \end{bmatrix} e^{i2\pi(z/(\lambda/n)-t/T)} = \begin{bmatrix} e_x \\ e_y \\ 0 \end{bmatrix} e^{i(kz-\omega t)} \quad (4.1)$$

where:  $e_x$  and  $e_y$  are complex numbers (denoted as  $a+ib$ ) along the  $x$  and  $y$  axes defining amplitudes,  $e$  is the base of the natural logarithm (value 2.728...),  $i$  is the imaginary unit ( $\sqrt{-1}$ ),  $\pi$  is the Ludolph number (3.14...),  $z$  is the value (variable) of the coordinate along which the photon wave is propagating,  $\lambda/n$  is the photon wavelength in the medium it travels in ( $n$  is the refraction index of the medium),  $t$  is the time of wave propagation,  $T$  is the wave period ( $T=1/\nu$  where  $\nu$  denotes the frequency). Sometimes the wave number  $k=2\pi n/\lambda$  and the angular (circular) frequency  $\omega=2\pi\nu$  are used in equations.

$$\text{ELECTRIC FIELD} \quad \nabla^2 \vec{E} = \mu_0 \epsilon_0 \frac{\partial^2 \vec{E}}{\partial t^2}$$

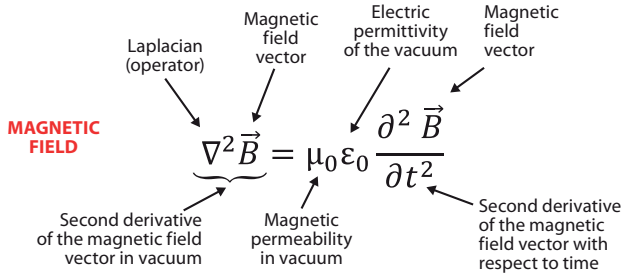
Diagram illustrating the equation  $\nabla^2 \vec{E} = \mu_0 \epsilon_0 \frac{\partial^2 \vec{E}}{\partial t^2}$  with labels:

- $\nabla^2$ : Laplacian (operator)
- $\vec{E}$ : Electric field vector
- $\mu_0$ : Magnetic permeability in vacuum
- $\epsilon_0$ : Electric permittivity of the vacuum
- $\frac{\partial^2 \vec{E}}{\partial t^2}$ : Second derivative of the electric field vector with respect to time

The magnetic field ( $B$ ) of the photon, similarly to the electric field, is defined by the expression 4.2:

$$\vec{H}(z, t) = \begin{bmatrix} h_x \\ h_y \\ 0 \end{bmatrix} e^{i2\pi(z/(\lambda/n)-t/T)} = \begin{bmatrix} h_x \\ h_y \\ 0 \end{bmatrix} e^{i(kz-\omega t)} \quad (4.2)$$

where  $h_x$  and  $h_y$  are complex numbers denoting the wave phase in the directions of  $x$  and  $y$ . The rest of the notation has the same meaning as in the previous expression.



Taking into account the Lorentz transformations, all light transformations can be rewritten in matrix format, including rotations, where  $Z(\delta)$  are rotations about the  $z$ -axis,  $B(\mu)$  are translations in the direction of the  $z$ -axis, while  $R(\theta)$  are rotations about the  $y$ -axis and  $S(\lambda)$  translations in the direction of the  $x$ -axis.

$$Z(\delta) = \begin{pmatrix} e^{i\delta/2} & 0 \\ 0 & e^{-i\delta/2} \end{pmatrix} \rightarrow \begin{pmatrix} 1 & 0 & 0 & 0 \\ 1 & 0 & 0 & 0 \\ 0 & 1 & \cos \delta & -\sin \delta \\ 0 & 0 & \sin \delta & \cos \delta \end{pmatrix}$$

$$B(\mu) = \begin{pmatrix} e^{\mu/2} & 0 \\ 0 & e^{-\mu/2} \end{pmatrix} \rightarrow \begin{pmatrix} \cosh \mu & \sinh \mu & 0 & 0 \\ \sinh \mu & \cosh \mu & 0 & 0 \\ 0 & 0 & 1 & 0 \\ 0 & 0 & 0 & 1 \end{pmatrix}$$

$$R(\theta) = \begin{pmatrix} \cos(\theta/2) & -\sin(\theta/2) \\ \sin(\theta/2) & \sin(\theta/2) \end{pmatrix} \rightarrow \begin{pmatrix} 1 & 0 & 0 & 0 \\ 0 & \cos \theta & -\sin \theta & 0 \\ 0 & \sin \theta & \cos \theta & 0 \\ 0 & 0 & 0 & 1 \end{pmatrix}$$

$$S(\lambda) = \begin{pmatrix} \cosh(\lambda/2) & \sinh(\lambda/2) \\ \sinh(\lambda/2) & \sinh(\lambda/2) \end{pmatrix} \rightarrow \begin{pmatrix} \cosh \lambda & 0 & \sinh \lambda & 0 \\ 0 & 1 & 0 & 0 \\ \sinh \lambda & 0 & \cosh \lambda & 0 \\ 0 & 0 & 0 & 1 \end{pmatrix}$$

Only photons having a vertical electric component pass through the vertical polarizer in case a lamp is used as a light source emitting diffuse light (Figure 4.3). This is usually about 20% -30% of light. Analogously, only those photons having a horizontal electric component pass through the horizontal polarizer. However, this depends on the light incidence angle (Figure 4.5a). It is characteristic of the linear polarization that its horizontal component equals zero in case the light incidence angle is Brewster's.

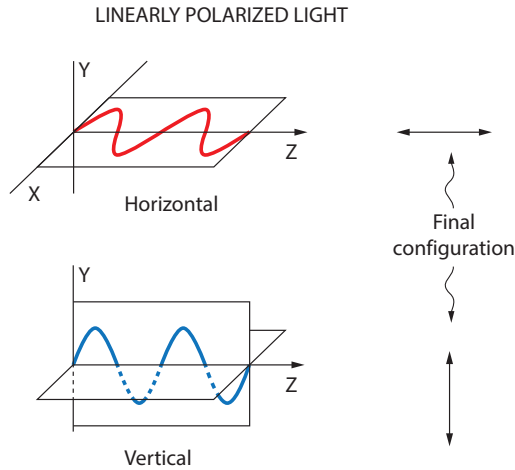


**Figure 4.3** Representation of two types of linearly polarized light—vertical and horizontal, using the standard notation, according to the final configuration of the light wave.

Vertically polarized light (diffuse light that passed through the vertical polarizer) passes through the analyzer having a vertical slit. However, if we observe the third case in Figure 4.4, we can see that vertical linearly polarized light does not pass through the horizontal analyzer.

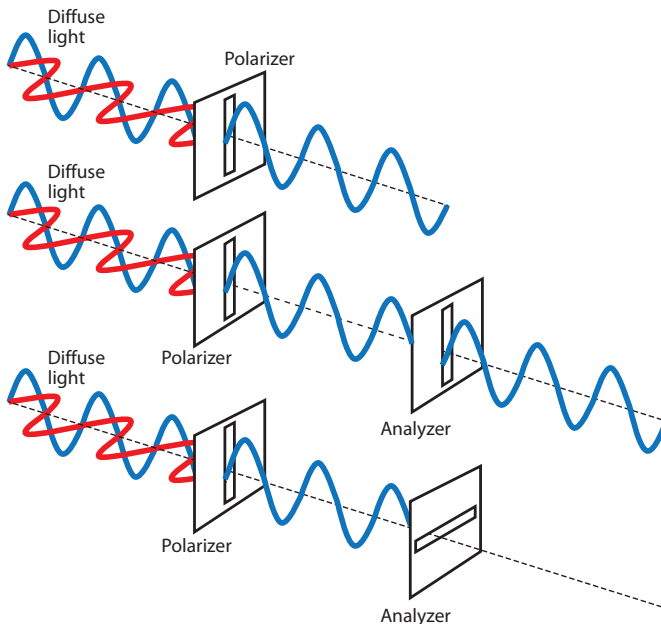


**Figure 4.4** Transforming diffuse light into vertical linearly polarized light and testing its polarization with the horizontal analyzer.

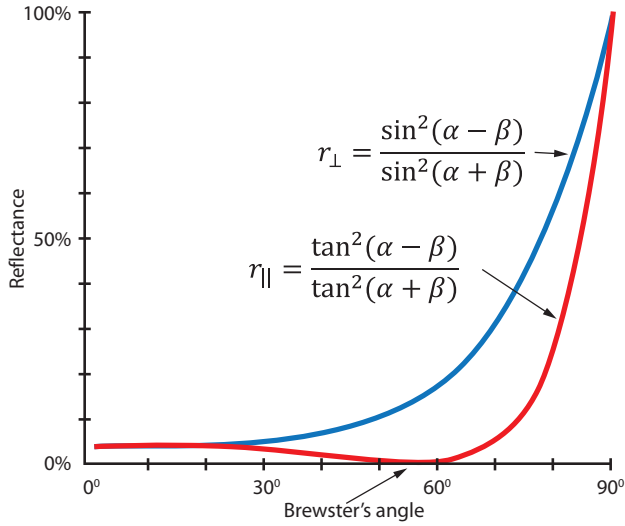


**Figure 4.5a** The relation between the vertical ( $r_{\perp}$ ) linearly polarized light and the horizontal ( $r_{\parallel}$ ) linearly polarized light ( $\alpha$  is the angle of specular reflection - the incidence angle equals the reflection angle,  $\beta$  is the angle of refraction—the angle of light refraction in the medium). If diffuse light passes through a filter, efficiency depends on the incident light and the medium (for water at the room temperature 53.1°, for skin 53.6°). If we wish to generate linearly polarized light using a mirror (as in the BIOPTRON lamp) then the efficiency of transforming diffuse light into polarized light can reach 95%.

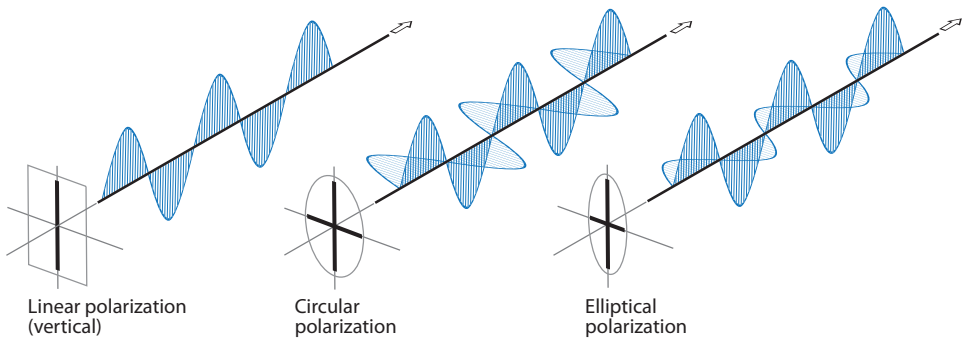


**Figure 4.5b** Comparison of linearly polarized light, circularly polarized light and elliptically polarized light.

The implementation of various polarization types depends on the purpose of light application in diagnostics and in therapy. In diagnostics, the linearly polarized light is used for the characterization of tissue, based on valence electrons and intermolecular

bonds under the Brewster's angle, because the reflected light from the tissue is exclusively vertical linearly polarized. Analysis of the energy balance in the interaction light-biological tissue enables classification of tissue as healthy, inflammatory, precancerogenic or cancerogenic. In therapy, the linearly polarized light is used to act upon linearly organized structures, primarily on their dipole moments. If the structure is twisted or entangled, the linearly polarized light acts like a "comb", straightening twisted, decoupling entangled, similarly as a comb does with hair. If in the process, a coincidence of electronic absorption energies occurs, light could affect not only structures but also biochemical processes (especially in membranes and mitochondria, which are highly organized structures with defined energy processes). In general, linearly polarized light affects biological structures that form "liquid crystals" (linearly ordered biomolecules such as collagen, muscular actin-myosin complexes, etc). Circular polarization is applicable in optically active biomolecules (having left and right orientation), and in the determination of the secondary protein structure ( $\alpha$ -helix). The elliptical polarization (where a phase shift occurs between the electric and the magnetic field oscillations, thus having different amplitudes at a given moment) can be adequate for cylindrical biological structures forming liquid crystals with a varying dipole moment.

## 4.2. Bloch Sphere (electron)

The quantum-electronic Bloch sphere was defined in 1946 for fermions, spin-1/2 particles, such as electrons. Equations defining this sphere follow from the time-dependent Schrödinger's equation (Chapter III) for a system of two levels, i.e., states. Using the Hamiltonian, Bloch sphere can be defined with smaller modifications, so that Pauli's matrix is included as part of the Bloch vector defining the sphere. If we compare Figure 4.6, representing the Bloch sphere, with Figure 4.1, representing the Poincaré sphere, we can see that there is a one-to-one correspondence between notations for light and for the electron.

In the Bloch sphere, "north" and "south" pole are defined by the characteristic that electron has two orientations " $\uparrow$ " (up, "north") and " $\downarrow$ " (down, "south"). However, since this is the consequence of the fourth quantum number (Chapter III), this determination defines the quantum bit (*qubit*) denoted by  $|0\rangle$  and  $|1\rangle$ . Comparative analysis of Poincaré and Bloch spheres yields the following relations:  $[0,0,1]$ - the right-hand circular polarization is equivalent to " $\uparrow$ " - that is  $|0\rangle$ ,  $[0,0,-1]$ - left-hand circular polarization is equivalent to " $\downarrow$ " - that is  $|1\rangle$ .  $[0,0,-1]$  - to the vertical linearly polarized light corresponds the superposed state  $[(1/\sqrt{2})|0\rangle - i|1\rangle]$ , and  $[0,0,1]$  - to the horizontal linear light polarization corresponds the superposed state  $[(1/\sqrt{2})|0\rangle + i|1\rangle]$ .



Felix Bloch  
(1905–1983)



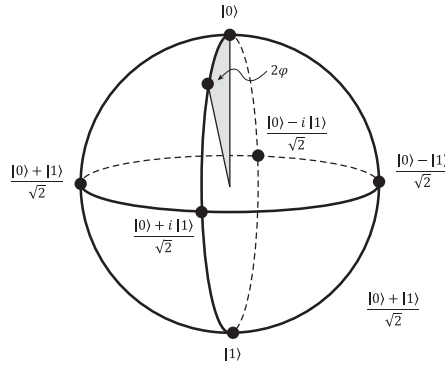


Figure 4.6 Bloch sphere with two basic  $|0\rangle$  and  $|1\rangle$ , and four superposed states.

The initial state is defined with the wave function:

$$\Psi(0) = \frac{1}{2}(|\uparrow\rangle + |\downarrow\rangle)$$

However, completely temporally dependent wave function is given by the expression:

$$\Psi(t) = \frac{1}{2}(|\uparrow\rangle + e^{-i\omega t}|\downarrow\rangle)$$

In case of the electron,  $\omega$  should be Larmor's frequency for the electron spin  $\omega_L$ . Since the system is orthogonal, follows  $\omega_L t = \pi$ , i.e.,  $t = \pi/\omega_L$ . The uncertainty principle, being defined as:

$$\Delta t = \frac{\pi h^*}{2E}$$

gives the energy  $E = \frac{1}{2} \omega_L$ , where  $h = h/2\pi$  (Dirac's constant).

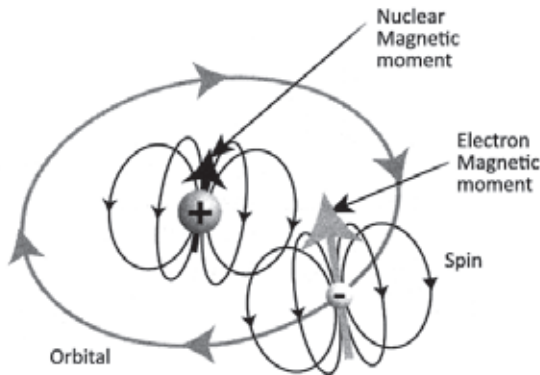


Figure 4.7 The atom has two basic magnetic moments, the nuclear magnetic moment (spin) and electron's magnetic moment (spin and orbital). In this case, we observe only the electron moment, because light interacting with matter interacts with the electrons first.

### 4.3. Larmor's Determination of the Magnetic Moment of the Electron

Larmor was a productive scientist, especially in the implementation of Lorentz transformations and electron quantum states. He was a supporter of the *ether* hypothesis and an ardent opponent of Einstein's relativity theory. He determined fairly well the quantum states of the electron and proton, which are today the foundations of the EPR (electronic paramagnetic resonance) and the NMR (nuclear magnetic resonance). He calculated:



Joseph Larmor  
(1857–1942)

$$\omega_{\text{electron spin}} = \frac{2\mu_e B}{h^*} = 1.7608 \times 10^{11} \text{ s}^{-1}, \text{ thus } \nu = \frac{\omega}{2\pi} = 28.025 \text{ GHz}.$$

$$\omega_{\text{proton spin}} = \frac{2\mu_p B}{h^*} = 2.6753 \times 10^8 \text{ s}^{-1}, \text{ giving } \nu = \frac{\omega}{2\pi} = 42.5781 \text{ MHz}.$$

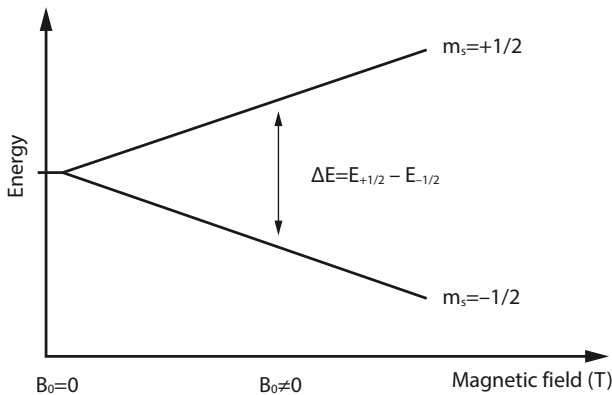


**Figure 4.8** Electron precession under the influence of the external magnetic field (left). Electron states "↑" and "↓" are basic states when the electron is not exposed to the external magnetic field  $B_0 = 0$  (Faraday cage). However, in an external magnetic field, the energy of the electron spin increases making it possible to obtain the precession signal of matter (first adequate signals are obtained with external magnetic field of 0.4 T, very good at 1.5 T and excellent at > 3 T).

The NMR and the EPR provide valid images of soft tissues enabling quality diagnostics. However, the electron, like the photon, remains the enigma of contemporary science. Their characteristics are discovered daily, expanding our knowledge and their implementation possibilities in medicine.

## 4.4. Light-Water Interaction

One of the most important interactions, regarding biological life, is between light and water, because biological systems and man specifically, contain 60%-75% of water, depending on age. It is considered that biological life originated in water under the influence of atmospheric discharges. Maintaining constant body temperature would be impossible without water in the human organism with its heat capacitance.

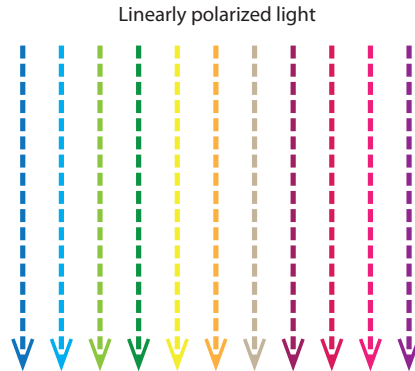


**Figure 4.9** Photon organization in linearly polarized visible light (photons of the same wavelength are regularly structured in the plane and give light energy of 1.8-2.6 J/cm<sup>2</sup> per minute for the application in biological systems). In interaction with charged matter forming dipole moments (water molecule:  $\mu_{\text{H}_2\text{O}} = 6.16 \times 10^{-30}$  cm; 20 water molecules:  $\mu_{20\text{H}_2\text{O}} = 10.4 \times 10^{-30}$  cm; collagen 300 nm long:  $\mu_{\text{coll.}} = 4.95 \times 10^{-26}$  cm; microtubules 300 nm long:  $\mu_{\text{MT.}} = 5.42 \times 10^{-25}$  Cm; membrane biomolecules per lipid:  $\mu_{\text{memb.}} = 4.85 \times 10^{-30}$  Cm, with potential of +275 mV etc.), linearly polarized visible light functions like a "comb", it organizes structures.

In order to understand the interaction between linearly polarized light and water, it is necessary to know the basic physical characteristics of the water molecule. We shall focus on one feature, the dipole moment of the water molecule, as a relevant characteristic for the interaction with linearly polarized light. The dipole moment of the water molecule is  $\mu_{\text{H}_2\text{O}} = 6.16 \times 10^{-30}$  Cm, or 0.001 J/T or 1.8546 D (where 1 Debye =  $3.3 \times 10^{-30}$  Cm). Several other characteristics will be presented relevant for respective calculations: Gibbs free energy  $\Delta_f G^\circ = -237.24$  kJ/mol, electric conductivity  $0.05501 \pm 0.0001$   $\mu\text{S/cm}$ , water molecule as a diamagnetic  $-0.91 \times 10^{-5}$  (magnetic susceptibility).

For example, a biological structure, with a dominantly positive charge on the surface, does not interact with water molecules adequately, because biochemical processes acting pathologically are taking place in the vicinity. In this case, vertical linearly polarized light will act, according to the Poincaré-Bloch correspondence  $[-1, 0, 0] \leftrightarrow [(1/\sqrt{2}) | 0\rangle - i | 1\rangle]$ , on the superposed electronic state of water molecules (coupled with the state of the dipole moment) organizing the water molecules to interact with biomolecules in an optimal way.

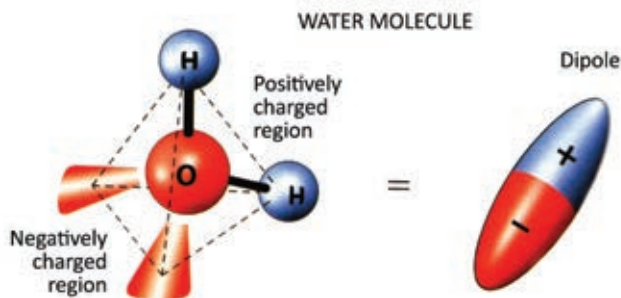


**Figure 4.10** Water molecule with positive and negative charge (region near the oxygen molecule is negatively charged, while the region near the hydrogen molecule is positively charged).

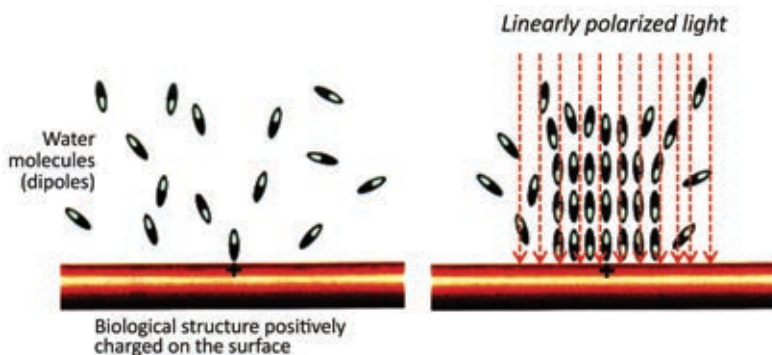


**Figure 4.11** Water molecules (dipoles) are of random structure in the presence of a biomolecule having mainly positive charge on its surface (left). Under the influence of the vertical linearly polarized light, water molecules become regularly structured and generate an electromagnetic effect on the biomolecule necessary for its normal functioning (right).

Collagen is another example of the linearly polarized light action on biomolecules. Collagen is one of the most important proteins; there are about 28 collagen types, however, all are composed of six amino acids. This is one of the rare proteins where the entire secondary structure is an  $\alpha$ -helix. Collagen fibers play an important role in the basement membrane (the energy barrier between the "external" and the "internal" world). The epidermis is exposed unprotected to external influences. It is organized into four basic layers (*stratum corneum*, *stratum granulosum*, *stratum spinosum*, and *stratum basale*). In the *stratum granulosum* there are, beside other structures, the lipid-water layers only 50-80 nm thick. If the lipid layer is not adequately structured, water loss occurs (water perfuses to the surface and evaporates, process known as TEWL – *trans-epidermal-water-loss*). Nevertheless, as stated before, vertical linearly polarized visible light can aid the organization of the lipid layer structure and significantly improve water conservation in the epidermis.

## 4.5. Interaction of Collagen and Microtubules with Linearly Polarized Light<sup>1</sup>

Collagen is the protein most frequently found in the organism; it is composed mainly of two amino acids: *glycine* and *proline*. It forms triple helices, mutually connected by hydrogen bonds, giving it stiffness, while the amino acid ends are made of glycine and located in the external space between the three helices. Collagen is the connective structure of the skin, bones and the connective tissue.

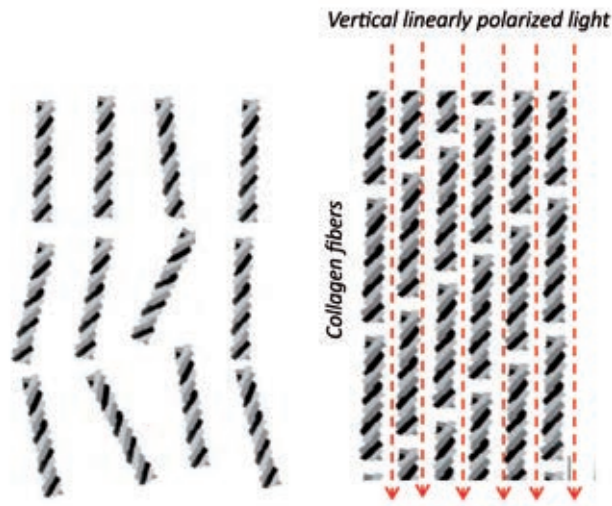


**Figure 4.12** Random structure of collagen filaments (left) and their organization (right) under the influence of vertical linearly polarized light acting as a “comb” on collagen fibers having properties of “liquid crystals” (structures in the water, oriented and periodically duplicated, are called liquid crystals).

Lateral chains of amino acids are part of a 3D-structure - stabilizing the entire formation of protein molecules. Bonds include covalent bonds as a bridge between two sulfur atoms, hydrogen bonds, and bridges between salts as a hydrophilic interaction. Collagen represents a triple helical structure; it is an extracellular protein highly resistant to extension, functioning as such in the connecting tissue.

Collagen of *Type I* accounts for approximately 90% of all collagens. Its mass is 285 000 Daltons, width 0.14 nm, length about 300 nm. Although, it is formed of only three polypeptide chains, in mammals alone it occurs in 17 genetically different peptide structures, with 10 variations of collagen. Collagen denoted as  $\alpha 1(I)$  of the total 1042 units contains 1011 units made of three amino acids: Gly -Pro -Hyp.

<sup>1</sup> This Chapter is an integral part of the Project BIOPTRON K3, 2002.-2004. (Ref. 6)

Oscillation frequencies of amino acids in a sequence were calculated, and the analysis produced:

- the first triplet has *primary* frequencies:  $\omega=(1.34 - 2.05 - 2.49)10^{11}(s^{-1})$ ;
- in the next step they are redistributed as:  $\omega=(5.37 - 5.12 - 4.99)10^{11}(s^{-1})$ , and this ratio is maintained for all units until the end of the series;
- oscillation change is resonant because the leap is proportional to primary frequencies, for Gly residue 3 times, for Pro residue 3/2 times and for Hyp once:

$$\Delta\varpi_1 = 3 \cdot 1.344821 \cdot 10^{11} = 4.034314 \cdot 10^{11} (s^{-1})$$

$$\Delta\varpi_1 = \frac{3}{2} \cdot 2.051660 \cdot 10^{11} = 3.077335 \cdot 10^{11} (s^{-1})$$

$$\Delta\varpi_1 = 1 \cdot 2.496456 \cdot 10^{11} = 2.496456 \cdot 10^{11} (s^{-1})$$

This is the beginning of an increment series, and the ratio of the highest to the lowest frequency increment is:

$$\frac{\Delta\omega_{MAX}}{\Delta\omega_{min}} = 1.616 \approx \Phi$$

Later, this ratio increases to 2.91, giving a more complex relation within  $\phi$  and  $\Phi$  values. The initial ratio of frequency increments is:  $\Delta\omega_1 / \Delta\omega_2 / \Delta\omega_3 = 4 / 3 / 2.5 = \Phi / 1.20 / 1$ . For the last triplet the (final) ratio of frequency increments is:

$$\Delta\omega_1 / \Delta\omega_2 / \Delta\omega_3 = 2.7 / 1.6 / 1 = e / \Phi / 1,$$

which is possible iff (if and only if) De Moivre's law exists ( $(\cos x + i \sin x)^n = \cos(nx) + i \sin(nx)$ )

The ratio of the initial to the final increment is expressed according to the binary principle, since:

$$\left(\frac{\Delta\omega_I}{\Delta\omega_F}\right)_1 / \left(\frac{\Delta\omega_I}{\Delta\omega_F}\right)_2 / \left(\frac{\Delta\omega_I}{\Delta\omega_F}\right)_3 = 143.6 / 184.3 / 257.4 = (2^2 2^6) / (2^2 2^7) / (2^2 2^8)$$

The total frequency increment is:

$$\Delta\omega_1 = 865.0595 \cdot 10^{11} (s^{-1})$$

$$\Delta\omega_2 = 658.846 \cdot 10^{11} (s^{-1})$$

$$\Delta\omega_3 = 533.626 \cdot 10^{11} (s^{-1})$$

Consequently, the ratio of the maximum to the minimum increment is again  $\Phi$ .

The total frequency increment is  $e^{2\pi} \times 10^{11} (s^{-1})$  or  $e^{2\pi-1}$  times. Since energy has to be added, it is obvious that *complex space* is more adequate for this representation, because in the energy loss expression, the multiplier in the exponent is  $i$ , that is, coding has the

form:  $e^{(2\pi-1)}$ . In the expanded form (De Moivre's formula), when  $n=1/2$  then for  $x=2\pi$  formula results in  $-1$ , as  $i^2$  and for  $x=0$  the result is  $+1$ , as  $i^4$ , energy loss is represented within the factor multiplying the imaginary unit.

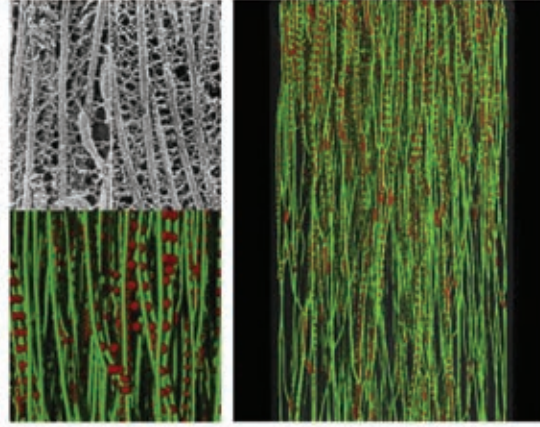


**Figure 4.13** Microtubules (MT), similarly to collagen, represent biological structures, which, from the physical aspect, can be investigated as liquid crystals. Vertical linearly polarized light can act on their macroscopic organization.

Oscillatory processes in *microtubules*, where energy is considerably lower, behave similarly. For example, for a microtubule of 75 elements and 13 proto-filaments, there are six frequencies having increments:

$$\Delta\omega_{11} = (9.65404 - 9.40652)10^{11} = 0.2475 \cdot 10^{11} (s^{-1})$$

$$\Delta\omega_{12} = (14.25767 - 14.09124)10^{11} = 1.6643 \cdot 10^{11} (s^{-1})$$

$$\Delta\omega_{21} = (3.87334 - 3.22059)10^{11} = 0.65275 \cdot 10^{11} (s^{-1})$$

$$\Delta\omega_{22} = (10.89518 - 10.68056)10^{11} = 0.21462 \cdot 10^{11} (s^{-1})$$

$$\Delta\omega_{31} = (6.30411 - 6.077198)10^{11} = 0.22691 \cdot 10^{11} (s^{-1})$$

$$\Delta\omega_{32} = (14.52192 - 14.42486)10^{11} = 0.09706 \cdot 10^{11} (s^{-1})$$

The ratio of the asynchronous to the synchronous increment is (successively by pairs) 6.7244, 3.04142, and 2.33785, giving as average  $4.03456 \approx 2^2$ .

Considering possible light action (electromagnetic) on microtubules, we present main frequencies appearing as portions in the increment:

$$\Delta\omega = (9.7 - 21.5 - 22.7 - 24.7 - 65.3 - 166.4) \cdot 10^9 (s^{-1}) \text{ or}$$

$$\Delta\nu = (1.54 - 3.42 - 3.6 - 3.95 - 10.4 - 26.5) \cdot 10^9 (Hz).$$

Average increments are:

$$\Delta\bar{\omega} = 5.1719 \cdot 10^{10} (s^{-1})$$

$$\Delta\bar{\nu} = 8.23 \cdot 10^9 (Hz)$$

i.e., approximately 9 GHz, representing a signal with an adequate electron magnetic moment.

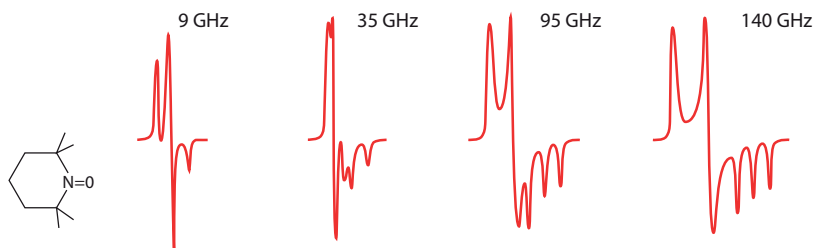


**Figure 4.14** Signals of different frequencies for the identification of the magnetic moment of the electron of a given structure based on Larmor's approach to the interaction between electromagnetism and matter.

Energy has to be increased to effect each leap, meaning that during formation of the microtubule chain, or something else, energy which the system *can* accept has to be added. Per each leap, i.e., per each succeeding unit (amino acid), it is necessary to add absorption energy increased by the amount:

$$Q = \Delta\bar{\omega} \cdot \hbar = 5.17 \cdot 10^{10} \cdot 1.05 \cdot 10^{-34} (J) = (5.4285/1.6) \cdot 10^{-5} (eV) = 0.0000339(eV)$$

A sequence composed of  $N$  elements, where each successive element, starting with the second, has with respect to the previous an increment equal to  $Q$ , requires the energy:

$$Q_S = \{Q[1 + 2 + 3 + \dots + (N - 3) + (N - 2) + (N - 1)]\} = \frac{(N - 1)N}{2} Q$$

For a collagen composed of 1042 amino acids, this is 18.386 eV. Knowing the number of these elements, the total energy necessary for their forming is easily calculated.

**Table 4.1** Oscillating frequencies of CNH (a) and OCC (b) and their ratio.

	$\omega_1$ ( $10^{13} s^{-1}$ )	$\omega_2$ ( $10^{13} s^{-1}$ )	$\nu_1$ ( $10^{13} Hz$ )	$\nu_2$ ( $10^{13} Hz$ )	$\omega_1 / \omega_2$
H: (a) C-N-H	22.3830	6.5470	3.5640	1.0425	3.419
O: (b) O-C-N	8.7866	4.3535	1.3990	0.6932	2.000
a/b	5/2	3/2	5/2	3/2	



**Table 4.2** Oscillating frequencies of the O and H atoms in the hydroxyl chain of collagen.

Atom block	NHOC	NHOCC	NHOCC + NHOC	
No. of atoms in the block	4	5	5 + 4	
No. of OH sequences	1	1	2	
No. of OH bonds in sequence	113	43	51	51
$[\omega_O - \omega_H]10^{10} (s^{-1})$	9.547	20.240	10.591	9.505
First pair	54.500	161.430	61.180	54.600
Last pair				
$\omega_O / \omega_H$	1.5311	1.6294	1.1695	1.5311
First pair	1.0208	1.0642	1.0234	1.0208
Last pair				
$[\omega_N - \omega_1]/(N-1), 10^{10} (s^{-1})$	23.426	62.282	52.034	52.933
Oxygen (O):	23.028	58.920	51.022	52.031
Hydrogen (H):				
Wave velocity (m/s)	44.1	93.5	48.9	43.9
initial	254.8	748.9	285.3	254.8
maximum				

**Table 4.6.** Oscillating frequencies of the O and H atoms in the hydroxyl chain of the quasibeta helix E-cadherine and wave velocities.

Atom block	NHOCC + NHOCNCC		NHOCC + NHOCNCC		NCCNHOCC + NHOC	
No. of atoms in the block	5 + 7		5 + 7		8 + 4	
No. of OH sequences	2		2		2	
No. of OH bonds in sequence	5	5	5	5	5	5
$[\omega_O - \omega_H]10^{10} (s^{-1})$	64.646	82.695	61.520	78.027	75.620	92.890
First pair	119.280	154.910	109.210	142.310	198.640	196.480
Last pair						
$\omega_O / \omega_H$	1.6068	1.2229	1.6021	1.2196	1.2846	1.1763
First pair	1.0699	1.0758	1.06667	1.0726	1.0968	1.0942
Last pair						
$[\omega_N - \omega_1]/(N-1), 10^{10} (s^{-1})$	413.781	436.488	395.714	417.430	477.225	415.584
Oxygen (O):	400.123	418.434	383.792	401.360	446.471	389.686
Hydrogen (H):						
Wave velocity (m/s)	298.7	382.0	284.2	360.5	349.4	429.1
initial	714.1	716.3	660.2	661.6	917.7	907.7
maximum						

## 4.6. Experiments: Interaction between Light and the Amniotic Fluid

The amniotic fluid is a clear, transparent liquid between amnions and the embryo. It can become *clouded*, greenish, often due to fetal meconium, which is a sign of fetal suffering. It protects the embryo from impact and infection, enabling its motility. The amniotic fluid is mainly formed in the amnion, placenta and the umbilical cord. Creation and resorption dynamics of the amniotic fluid correspond to embryo's needs (Cunnungham, 1997).

The amniotic fluid composition depends on the gravidity stage. At the beginning, it is influenced only by the mother, while later it also contains products of fetal excretion. At the end of the gestation, in the amniotic fluid, epithelium cells of the fetal skin are also found, hair and vernix flakes, desquamated amnion cells, granulations of meconium, salts of the uric acid, electrolytes, vitamins and ferments.

The amniotic fluid volume increases until the 34<sup>th</sup> week of gestation, when it starts to decrease. Increased volume of the amniotic fluid is called polyhydramnion, often linked to some fetal congenital anomaly, especially of the central nervous system or the gastrointestinal tract. Decreased volume of the amniotic fluid, oligohydramnion, can be linked to various malformations of the heart, central nervous system, genitourinary tract or to chromosome aberrations.

Volume of the amniotic fluid at the beginning of the second trimester is approximately 50 ml and it does not differ from the fetal plasma by its composition. At the end of gestation, the liquid volume is from 1000ml up to 1200 ml, when it is composed mostly of fetal urin. In postponed pregnancy, the volume of amniotic fluid decreases. In case the fetus is endangered intra uterus, meconium is discharged and the amniotic fluid becomes clouded, green and saturated with bilirubin and urobilinogen (Gnyton, 2006).

Only recently has it been realized that the amniotic fluid has considerable clinical significance, because it can be used to determine prenatally the fetal karyotype and the maturity of lungs in fetus. It is considered that the amniotic fluid supports the maturing of fetal lungs and the digestive tract. The amniotic fluid is a good sound conductor, so that the fetus can hear sounds of his mother and of himself, as well as sounds from the external environment. Fetus behavior has been examined under the influence of various sound types, especially music, and it was demonstrated that sound affects the fetus. Stem cells can also be isolated from the amniotic fluid that can be differentiated into cells of other organ systems, playing a significant role in the therapy of certain diseases. The sensitivity of the amniotic fluid to external effects is very important for the protection of the fetus and for the determination of its sensitivity to external influence after birth.

Using the opto-magnetic method to determine the effect of the electric and magnetic component of matter based on the sensitivity of structures to light effects, four samples of amniotic fluid were taken during childbirth and immediately after labor (at the Gynecologic-Obstetric clinic „Narodni front“ in Belgrade), and immediately

transferred to NanoLab. Imaging of the amniotic fluid samples was performed by the FΩF-1 device (Fractal Opto-magnetic Fingerprint). The device consists of a digital Sony camera, light source based on white diffuse light generated with a LED diode of 5000 candela intensity (Figure 1-left and Figure 2-left), diodes of the light source are placed at an angle giving reflected polarized light (Figure 1-right and Figure 2-right). In the first case, the digital image was obtained by using white light containing the electric and the magnetic component, while in the second case, the image of the same area was obtained using the electric light component, a second after the first image. Using the software package (DΩC -1: Digital Opto-magnetic Convolution) performing subtraction of the image 4.15 from the image 4.16 (pixel by pixel) and the convolution of the light recording, a spectroscopic magnetic „print“ of the amniotic fluid was obtained in the form of a diagram (Figure 4.15, normal amniotic fluid, and Figure 4.16, clouded amniotic fluid), as a result of the difference between changes obtained by the analysis of the image in the red (R) and the blue (B) channel. The green channel was not considered, because Maxwell's RGB color model relating Red-White-Blue provides all wavelengths necessary for the analysis of the convolution image (Koruga, 2006 and Koruga, 2008).

Hydrogen bonds of liquid molecules participate in the organization of clusters (up to 60 molecules per cluster), thus, the electromagnetism of the visible light can adequately characterize the energy dynamics of the structure. The grid of the water cluster has an optical and acoustic oscillatory mode, enabling registration of acoustic influence (speech, music, noise, etc.) on the clustered liquid in the optical spectrum (Pain, 2002).

Four types of water were taken as samples (18.2 MΩ, aqua purificata - two times distilled water, „aqua-viva“, and tap water) their ingredients determined, and two samples of amniotic fluid: normal and clouded. Each sample was divided into six equal parts and examined under the same conditions (in an area isolated from sound and light, under constant temperature of 18°C). All six liquids were examined under the same conditions in six different situations: *silence* (less than 5 dB), *white noise* (sound of uniform intensity in a given range), *conversation* (agreeable voice speaking words introducing the listener into a relaxed state), *Bach's music* (violin concerto), *noise* (American army sergeant shouting at a private), and *rock* (aggressive music).

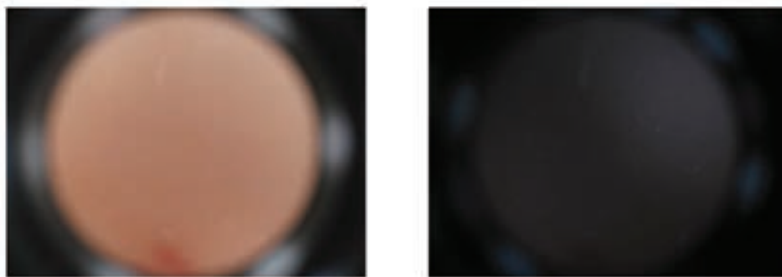


**Figure 4.15** Image of amniotic fluid (normal) taken by the digital camera: white diffuse light (left) and reflected polarized light from the same light source type as the diffuse light (right).

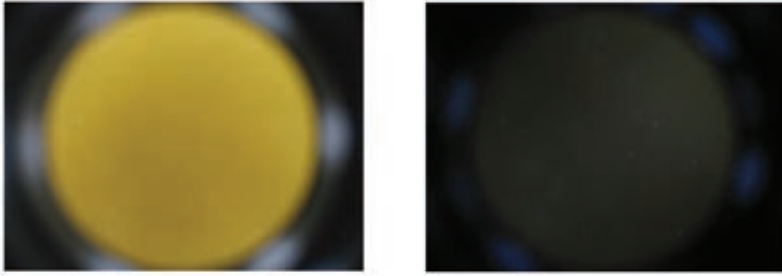


**Figure 4.16** Image of the amniotic fluid (when the fetus was suffering) taken by the digital camera: white diffuse light (left) and reflected polarized light of the same light source type as the diffuse light (right).

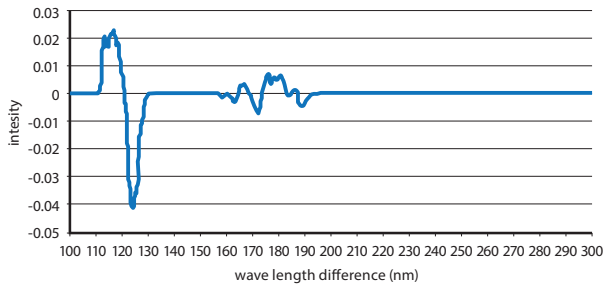


**Figure 4.17** Opto-magnetic „print“ of the normal amniotic fluid based on the convolution of images: white light (W) minus reflected polarized white light (P) of the same light source for the red (R) and blue (B) channel.

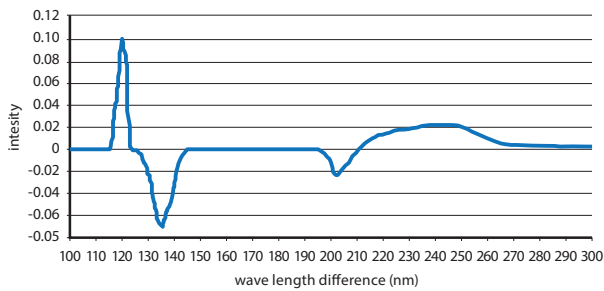


**Figure 4.18** Opto-magnetic „print“ of the clouded amniotic fluid (fetus suffering) based on the convolution of images: white light (W) minus reflected polarized white light (P) of the same light source for the red (R) and blue (B) channel.

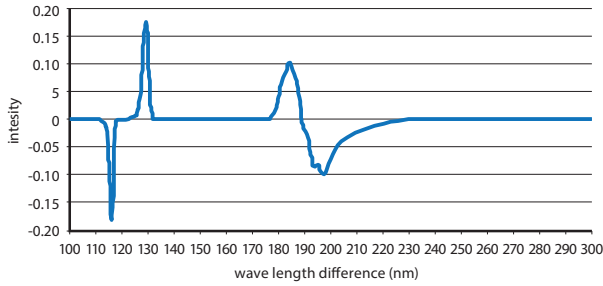


**Figure 4.19** Opto-magnetic „print“ of drinking water (tap water) based on the convolution of images: white light (W) minus reflected polarized white light (P) of the same light source for the red (R) and blue (B) channel.

Systematic research results are displayed in Figures 4.20-4.24. It is evident that the demineralized (02) and drinking water (03 and 04) display a completely different response with respect to the amniotic fluid (05 and 06).

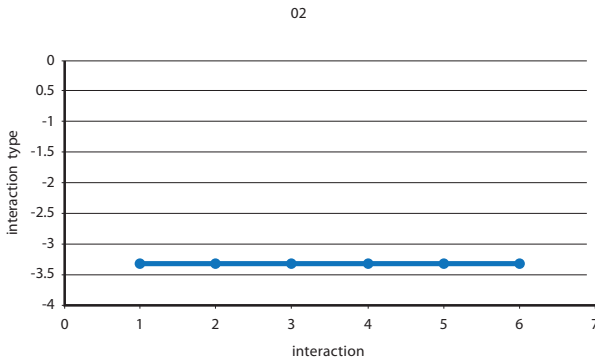


**Figure 4.20** Systematization of six types of acoustic effects on distilled water (1-silence, 2-white noise, 3-conversation, 4-Bach’s music, 5-noise and 6-rock. All six effects are in the interval [-3.5, -3]. Not only do all six effects belong to one type of action, they are all very coexistent within one type.

**Figure 4.21** Systematization of six types of acoustic effects on the water “aqua viva” (1-silence, 2-white noise, 3-conversation, 4-Bach’s music, 5-noise and 6-rock. All six effects are within the interval [-3.5, -3]. Five effects (1, 2, 3, 4 and 6) are highly coexistent, there is only a slight difference in effect 5.

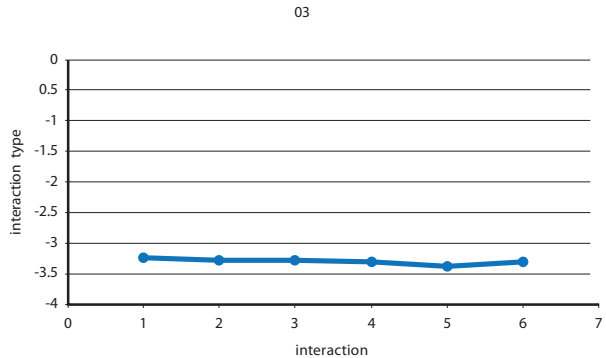


**Figure 4.22** Systematization of six types of acoustic effects on the drinking water, tap water (1-silence, 2-white noise, 3-conversation, 4- Bach's music, 5-noise and 6-rock. All six effects are within the interval  $[-3.5, -3]$ . All six effects belong to the same type of action, except that effects 1, 2 and 6 can be classified into one subgroup, and effects 3,4 and 5 into another subgroup.

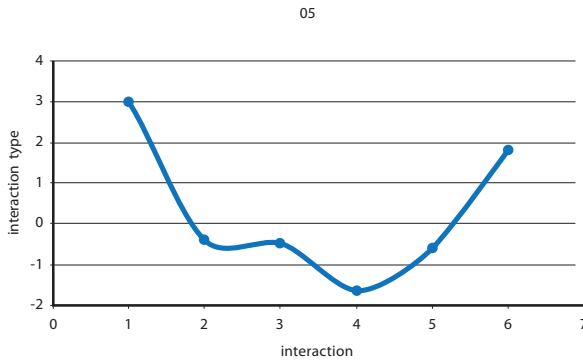
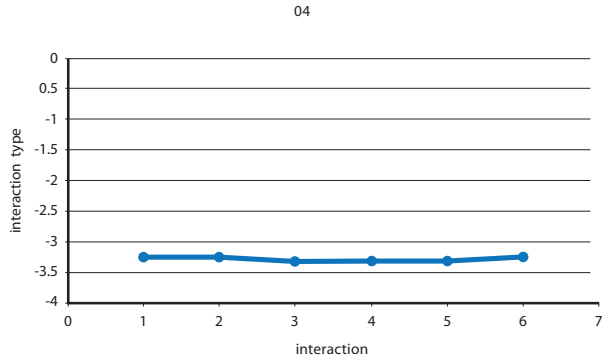
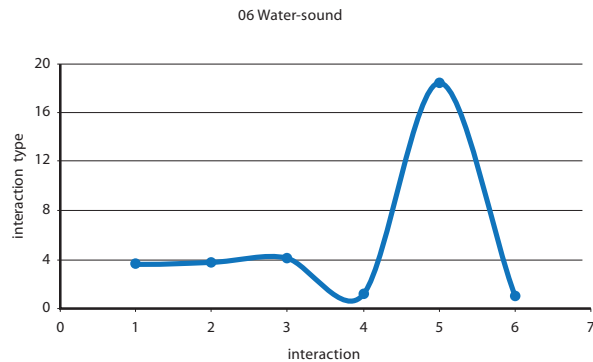


**Figure 4.23** Systematization of six types of acoustic effects on the amniotic fluid (1-silence, 2-white noise, 3-conversation, 4-Bach's music, 5-noise and 6-rock. Two effects are in the interval  $[0,3]$ , and the remaining four in the interval  $[0,-2]$ .

**Figure 4.24** Systematization of six types of acoustic effects on the clouded amniotic fluid (1-silence, 2-white noise, 3-conversation, 4-Bach's music, 5-noise 6-rock. Two effects are in the interval  $[0,4]$ , three effects are at the endpoints of the fourth interval, while the effect 5 (noise) is in the interval 18.



Dynamic water structures and water dynamics are complex processes, which, in spite of considerably sophisticated measurement and diagnostic tools, have not been sufficiently investigated. Water organization into clusters and its structure organization in the equilibrium and in the nonequilibrium states remain unknown. However, measurements and observed behavior, such as this by using optical-magnetic fingerprinting,

point to the fact that water is a highly organized structure with memory elements. For example, normal amniotic fluid is sensitive to *silence* and *loud music* from the ambient where the pregnant woman lives. Clouded amniotic fluid is sensitive to sound, and extremely sensitive to *noise* and *emotional stress*, indicating that the fetal environment is acoustically very unfavorable. This is caused by intensified (memory type) energy states which, through resonant processes, were dominant before the experimental treatment. In other words, water remembers previous influence and energy states via stochastic dynamics (energy distribution and memory based on the number „e“, because „e“ is at the foundation of the quantum state of matter and light) of formation and deconstruction of clusters. Memory of the previous cluster energy distribution and the establishment of a resonant relationship with the current one, give the system a boost, which is manifested in hydrogen bonds.

Therefore, it can be recommended to pregnant women to carefully choose the acoustic ambient they dwell in, because it affects the embryo and can be a very significant factor in fetal development during embryogenesis, and in the „post memory effect“ after childbirth as well.

## References

1. Cunningham, et al. Williams Obstetrics. 20th edition. Appleton and Lange, 1997.
2. Guyton, A.C. and Hall, J.E. Textbook of medical Physiology, Elsevier-Saunders, Philadelphia, 2006.
3. Janković-Ražnatović, S., Dragojević-Dikić, S., Rakić, S., Nikolić, B., Plesinac, S., Tasić, L., Perišić, Ž., Sovilj, M., Adamović, T., Koruga, Đ., Fetus Sound Simulation: Cilia Memristor Effect of Signal Transduction, BioMed Research International, Vol. 2014, Avicle ID 273932, 6 pages, <http://doi.org/10.115/2014/273932>
4. Koruga, Đ., Tomić, A., Method and algorithm for analysis of light-matter interaction based on spectral convolution. Patent PCT/US2008/050438.
5. Koruga, Dj., Tomić, A., Ratkaj, Ž., Matija, L., Classical and quantum information channels in protein chain. *Materials Research Forum*, Vol.518:491-496, 2006.
6. Koruga, Đ., Janković, S., Tomić, A. and Kojić, D., Investigation speech influence on biophysical properties of amniotic fluid, in book *Speech and Language*, Eds. Jovičić, S. and Sovilj, M., Institute for experimental phonetics and speech pathology, pp.246-255, Belgrade, 2008.
7. Pain, H.J., *The Physics of Vibrations and Waves*. John Wiley, West Sussex, 2002.
8. Koruga, Đ., Tomić, A., Ratkaj, Ž., Projekat BIOPTRON. Zepter International, Beograd 2002.





# 5

## FIBONACCI PHENOMENA IN BIOLOGY



Chapter IV described water properties, which constitutes 65% –70% of the human organism, and characteristics of its dipole moments, which enable water to be linearly „ordered“. We shall see that *collagen fibers*, constituting 40% of all proteins, are linearly organized biomolecules in the extracellular space, similarly to *microtubules* in the intracellular space. Therefore, using the linearly polarized light of adequate intensity we can act on biological structures with a dipole moment. However, the linearity of mentioned biomolecules is only one of its characteristics. The vertical linearly polarized light can be applied to reestablish the linearity of their compromised organization.

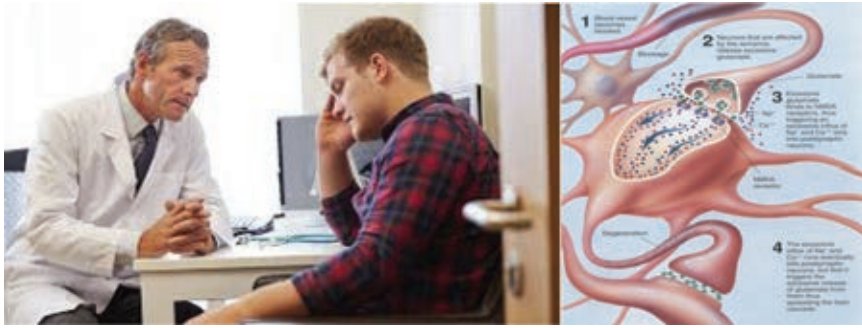
Beside the above biomolecules, this Chapter will be investigating another biomolecule, the *clathrin*, and processes influenced by the Gibbs free energy.

## 5.1. Clathrin

When we have a headache, feel sleepy, or have a mental or a motoneuronal functional disorder, in most cases the cause is one of the neurotransmitters: *serotonin* (5-HT), *acetylcholine* (ACh), *melatonin*, *catecholamine*, *GABA* etc.

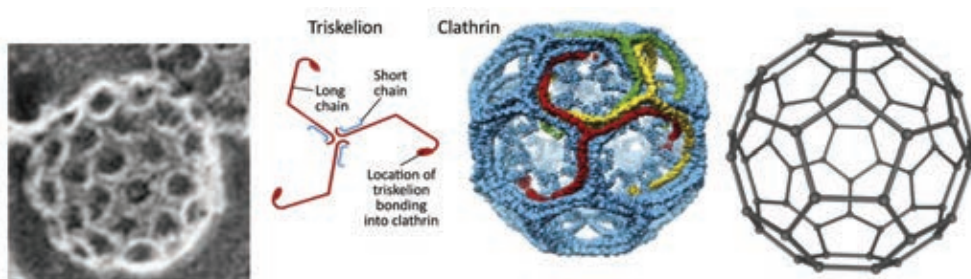
For example, *serotonin*, colloquially known as the hormone of happiness, is formed from the amino acid tryptophan, by the oxidation of this amino acid into the 5-oxytryptophan, and its decarbonization. It has a very important regulatory function in the organism; it is stored in the presynaptic vesicles, in clathrin. When the action potential acts on the presynaptic termination, the depolarized presynaptic membrane interacts with vesicles (clathrin), opens them and the contents (neurotransmitter) is released into the intersynaptic space to activate the postsynaptic membrane (Figure 5.1, right).

The catecholamine group includes three compounds: *dopamine*, *noradrenalin* and *adrenaline*, originating from the amino acid tyrosine. They are released at the sympathetic peripheral nerve terminations, synapses, and various zones of the central nervous system (CNS). Catecholamines are accumulated in secretory vesicles – in clathrin.



**Figure 5.1.** Many functional processes of the CNS depend on the quantity and dynamics of neurotransmitter secretion. Secretion dynamics depends on the functionality of the secretion vesicle (clathrin) where many neurotransmitters are stored.

Clathrin is a complex protein structure, composed of two main protein chains: the „light“ chain (25 000 D) and the „heavy“ chain (190 000 D). The overall molecular mass is about 215 000 D (Dalton: 1D ~weight of an atom of hydrogen), the size is 20 to 80 nm. Human chromosome 17 is responsible for the synthesis of the „heavy“ chain, and chromosome 22 for the synthesis of the „light“ chain. These two protein chains form a more complex structure called the triskelion (trimer). It was discovered in 1969 by the Japanese scientists Kamaseki and Kadota using the electron microscope (Kamaseki, 1969), and extracted for the first time in 1975 by Barbara Pears. Clathrin is found in many human tissues as a carrier of substances such as neurotransmitters. It also clears the cell debris into the extracellular space. The triskelion forms pentagons and hexagones, so the clathrins in the CNS, composed of 36 triskelions, form 12 pentagons and 20 hexagons, while in other tissues they are made of 12 pentagons and a varying number of hexagons (Figure 5.2). Clathrin of the CNS is the most perfect symmetrical structure that can exist in nature based on the law of point symmetry. This is the icosahedral symmetry group (dual to dodecahedron) whose energy states  $T_{1g}$ ,  $T_{2g}$ ,  $T_{1u}$  and  $T_{2u}$  are determined by the ordered quadruple  $\Phi$ ,  $-\Phi$ ,  $\phi$ ,  $-\phi$  (1.61803..., -1.61803..., 0.61803..., -0.61803).



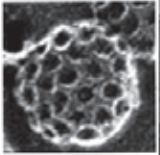
**Figure 5.2.** Microscopic image of clathrin (left), triskelion shape and the network of 36 triskelions forming clathrin with 12 pentagons and 20 hexagons. Schematic structure with pentagons and hexagons (right) is displayed.

Table 5.1 displays the interdependence of symmetries (of a structure or a process) and the energy eigenvalues (of a structure or a process) determined by the electronic, vibrational, rotational or translational energies. Table indicates that for symmetric transformations  $C_5$ ,  $C_5^2$ ,  $S_{10}$  and  $S_{10}^3$  we have:

$$\frac{1}{2} (1 + \sqrt{5}), \frac{1}{2} (1 - \sqrt{5}), -\frac{1}{2} (1 + \sqrt{5}), -\frac{1}{2} (1 - \sqrt{5}). \tag{5.1}$$

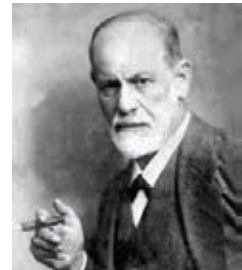
**Table 5.1** Dependence between symmetry and energy eigenvalues of a structure or process with icosahedral symmetry (dual to dodecahedron).

Table of the icosahedral symmetry group

$I/I_h$	$E$	$12C_5$	$12C_5^2$	$20C_2$	$15C_2$	$i$	$12S_{10}$	$12S_{10}^3$	$20S_6$	$15\sigma$	III	IV	
$A_g$	1	1	1	1	1	1	1	1	1	1	$(R_x, R_y, R_z)$	$x^2 + y^2 + z^2$	
$T_{1g}$	3	$\frac{1}{2}(1 + \sqrt{5})$	$\frac{1}{2}(1 - \sqrt{5})$	0	-1	3	$\frac{1}{2}(1 - \sqrt{5})$	$\frac{1}{2}(1 + \sqrt{5})$	0	-1		$(2z^2 - x^2 - y^2, x^2 - y^2, xy, yz, zx)$	
$T_{2g}$	3	$\frac{1}{2}(1 - \sqrt{5})$	$\frac{1}{2}(1 + \sqrt{5})$	0	-1	3	$\frac{1}{2}(1 + \sqrt{5})$	$\frac{1}{2}(1 - \sqrt{5})$	0	-1			
$G_g$	4	-1	-1	1	0	4	-1	-1	1	0			
$H_g$	5	0	0	-1	1	5	0	0	-1	1			
$A_u$	1	1	1	1	1	-1	-1	-1	-1	-1	$(x, y, z)$		
$T_{1u}$	3	$\frac{1}{2}(1 + \sqrt{5})$	$\frac{1}{2}(1 - \sqrt{5})$	0	-1	-3	$-\frac{1}{2}(1 - \sqrt{5})$	$-\frac{1}{2}(1 + \sqrt{5})$	0	1		$(x(x^2 - y^2), y(y^2 - x^2), z(x^2 - y^2), xyz)$	
$T_{2u}$	3	$\frac{1}{2}(1 - \sqrt{5})$	$\frac{1}{2}(1 + \sqrt{5})$	0	-1	-3	$-\frac{1}{2}(1 + \sqrt{5})$	$-\frac{1}{2}(1 - \sqrt{5})$	0	1			
$G_u$	4	-1	-1	1	0	-4	1	1	-1	0			
$H_u$	5	0	0	-1	1	-5	0	0	1	-1			

## 5.2. Microtubules

The scientist who first observed fibrous cell structures under the microscope was Sigmund Freud. During 1879–1881, he worked as a student at the Ernst von Brucke laboratory, in the Institute for Physiology of the Vienna University, where he performed experiments during the summer. He succeeded in recording the cytoskeleton structures, and among them, as the largest, the microtubules. It can be said that in the beginning Freud was a cytologist. However, he became known to the scientific community as a psychiatrist and by his investigations of subconscious mind mechanisms.



Sigmund Freud  
(1856–1939)

Microtubules did not attract attention until, in 1974, the New York Academy of Sciences organized the first scientific meeting on the subject, with the emphasis on the structural and biochemical aspects of microtubules. This topic aroused interest of researchers all over the world, so the same Academy organized in 1986 a scientific conference on the dynamic aspects of microtubules (Soifer, 1986). It was demonstrated that microtubules have an important role in biology, in intracellular transport, cell shape definition, and as the main compound of the cell mitotic spindle. Microtubules also create more complex structures such as cilia, flagella, and centrioles (Dustin, 1984).

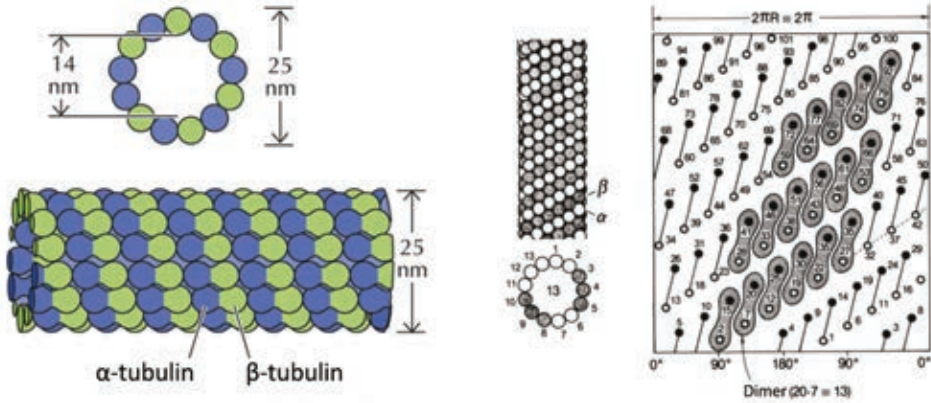


**Figure 5.3.** Schematic presentation of the microtubular configuration (MT) with 13 protofilaments, of the inner diameter 14 nm, outer diameter 25 nm, random length (from several nm to several tenths of  $\mu\text{m}$ ) depending on cell type (left). When the microtubular cylinder is flattened in the plane (right), we obtain the packing sequence of subunits of  $\alpha$  and  $\beta$  tubulin, which form a dimer. The packing sequence is such that the dimer always has the value 13, as the number of protofilaments in MT ( $15 - 2 = 13$ ,  $20 - 7 = 13$  etc.).

The structural (spatial) packing of  $\alpha$  and  $\beta$  tubulin into a protofilament of 13 subunits complies to the rule 1, 2, 3, 5, 8, 13..., followed by 4, 6, 7, and ending with 9, 10, 11 and 12. From this sequence we observe the ratios  $1:2 = 0.500$ ,  $2:3 = 0.666$ ,  $3:5 = 0.600$ ,  $5:8 = 0.625$ ,  $8:13 = 0.615$ ,  $13:21 = 0.619$ , seeing they oscillate between 0.5 and 0.66 and that the convergence point belongs to the category of number  $\phi = 0.61803$ . Observing inverse ratios, we have  $2:1 = 2.000$ ,  $3:2 = 1.500$ ,  $5:3 = 1.666$ ,  $8:5 = 1.600$ ,  $13:8 = 1.625$ ,  $21:13 = 1.615$ , and the convergence point belongs to the category of number  $\Phi = 1.61803$ . Since microtubules are structured as thirteens, the biophysical characteristics (dipole moments, temperature, magnetism, etc.) that depend on microtubules are within the limits  $1.615 \leq \Phi \leq 1.625$ .

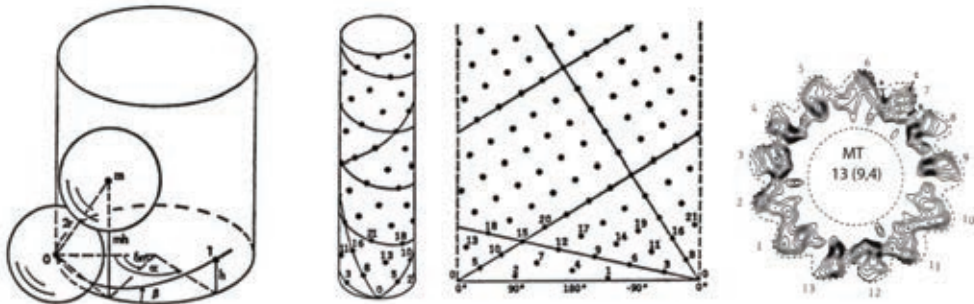


**Figure 5.4.** Packing of unit spheres ( $\alpha$  and  $\beta$  tubulin) on the cylinder surface according to the sequence 1,  $a$ ,  $a+1$ ,  $2a+1$ ,  $3a+2$ ,  $5a+3$ +... For  $a = 2$ , we obtain 1, 2, 3, 5, 8, 13, and the divergence is  $\phi^2$ . There are seven types of packing of 13 subunits, the example 13 (9.4) is on the right (Ericson, 1973).

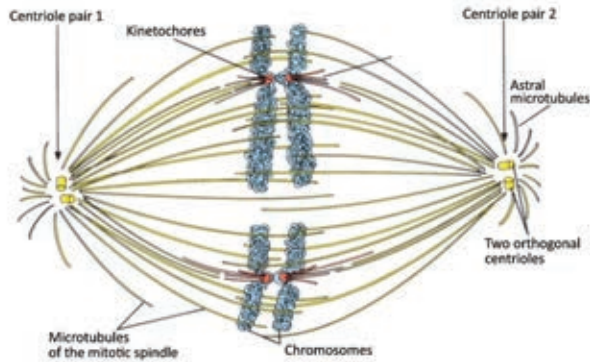


**Figure 5.5.** *Function of microtubules and centrioles in cell division. There are four types of microtubules in the mitotic spindle: mitotic spindle microtubule, astral microtubules, kinetochoral microtubules and microtubules within centrioles. Since the cell division is one of the most important processes in reproducing biological systems, learning about microtubules is an important task in diagnostics and in therapy.*

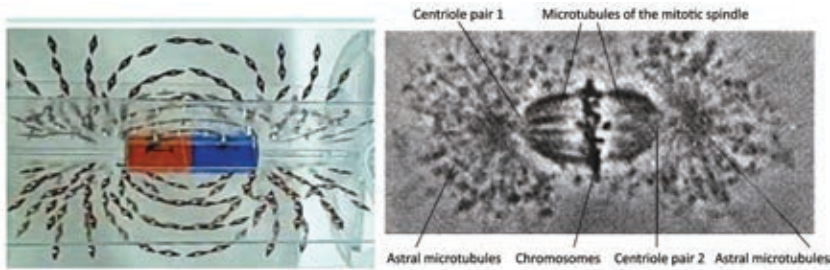


**Figure 5.6.** *Classical magnet with magnetic lines of force between the north and the south pole (left) and the distribution of microtubules along magnetic lines of force during cell division. Centrioles have the role of poles, and the „astral“ microtubules are present as the result of the law of magnetism.*

### 5.3. Cilia and Flagella

Cilium is an important biological organelle found primarily in epithelium tissues of internal organs, but also in ocular structures such as the „cilial muscle“ controlling mechanical properties of cornea movement. They are composed of nine microtubule doublets with 13 and 10 protofilaments. The organization of the structure and its dynamics is fascinating (Figure 5.8, right). For example, the role of cilia in lung function (Figure 5.7, left): when, by inhalation, microparticles enter the lung, the cilia attempt to eliminate them mechanically from the lung surface, to enable the gas exchange of oxygen and carbon dioxide. In smokers, this process is hampered because the nicotine glues cilia restricting their function.

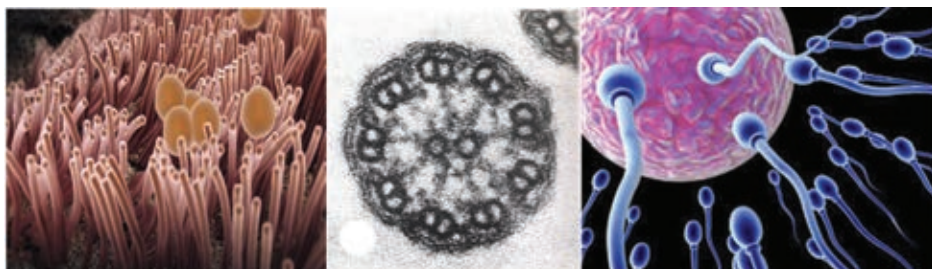


**Figure 5.7.** Cilia of the lung epithelium interacting with microparticles (left). Cilium diameter is about 240 nm, the length is about 10–30  $\mu\text{m}$ . Cilium cross section with 20 microtubular protofilaments, organized into doublets. The cilium does not have central microtubules, as opposed to the flagellum in spermatozoids (right).

The flagellum resembles the cilium by its cross section, it is somewhat longer, has two microtubular protofilaments and, at its root, has a chemical motor generating the propeller motion of the flagellum ending, as opposed to the „bang-bang“ motion of cilia. The first unicellular organisms, such as *Paramecium*, were covered by cilia, and *flagellate* had flagella.

The spermatozoid has a flagellar structure (Figure 5.7, right). Its motility actually depends on the functional state of the microtubule. The ovum fertilization depends on the spermatozoid motility and its ability to penetrate the ovum membrane. The flagellar spermatozoid structure at the root of the spermatozoid head is transformed into a centriole. The centriole, together with the genetic material (22 + X + Y chromosomes), enters the ovum and is united with ovum's genetic material. There are two curiosities regarding the spermatozoid genetics. The first is that of all chromosomes, the Y chromosome is the smallest, and its shape gives the impression of being damaged. However, its genetic material is perfect (sequences of A, T, C, G numbering 59 million), is of palindrome character, i.e., it is read the same backward and forward, like *radar*, *level*, *rotor*. Thus, it is necessary to know only half of the genetic material in order to know the entire genetic sequence. This „perfect“ relation between the *half* and the *whole* (*half=whole*) is especially significant in science and information technologies. The question remains whether this type of „perfection“ is the reason that the Y chromosome is the only one that does not cause any type of cancer. All other chromosomes are responsible for multiple cancers (for example chromosome 1 is responsible for breast cancer, colon cancer, prostate cancer, brain tumor, etc., and chromosome 19 for thyroid cancer, ovaries cancer, colon cancer, and leukemia/ B-cell lymphoma). Another curiosity concerns the Bible story that „the woman originated from man's rib“. It is considered that this is an error of translation from Hebrew. Namely, „rib“ and „half“ are pronounced identically (like *sole* and *soul*). However, if we were to say „woman was created from man's half“, this makes sense, because man has the XY pair of sex chromosomes, and the woman has the XX sex chromosomes (so  $\frac{1}{2}$  of male's chromosome pair, the X chromosome, is taken to create the female pair of sex chromosomes XX). Again, in a different way, this is a „perfect“ relation between the *part* and the *whole* (the male is the *part*, and the female is the *whole*). Plato, of course was unaware of this, when he wrote „one is not *One*, two is hardly *One*“.



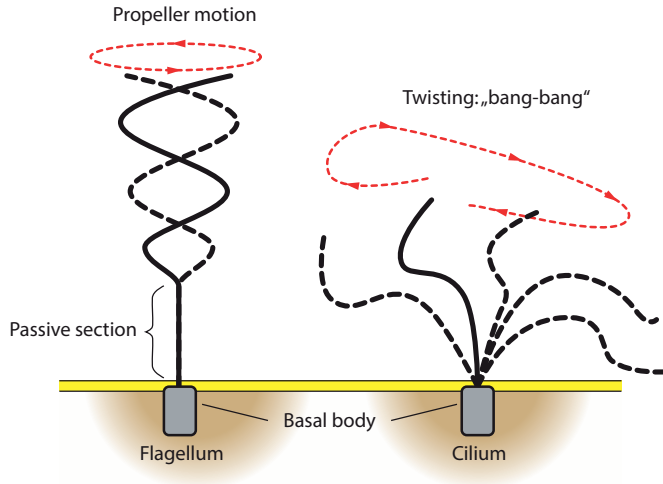


**Figure 5.8.** Schematic representation of the flagellum (with propeller motion) and cilium with twisting „bang-bang“ motion. When this motion is locally variable, but synchronized as a whole, as in a microorganism, then such coordinated undulation is a very complex process.

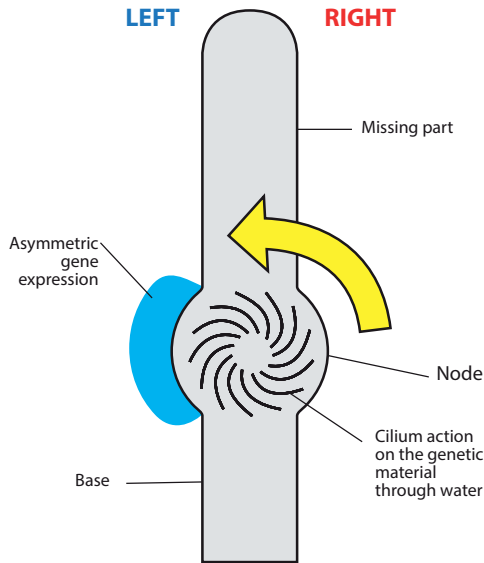


**Figure 5.9.** Development of a body part: at the center of action cilia act upon the genetic material via the water in the extracellular space and give a signal to the sonic structures  $FGF8$  and  $TGF\beta$ , which act on the asymmetry of gene expression. We are all somewhat asymmetric as a result of this action. Due to frequent ultrasound examinations of pregnant women (once a month), left-handed children are born in 85% cases.

## 5.4. Centrioles

There is similarity, but also a significant difference between the cilium/flagellum and the centriole. Left and right centriole orientation was observed (Figure 5.10). Within the cell (cytoplasm), they are always perpendicular and in a pair. Their orthogonality is caused by their classical-quantum electric and magnetic properties. This is an obvious example how the quantum effects of the electrical and the magnetic fields of microtubules are realized macroscopically (orthogonality must be maintained, because, one centriole primarily generates the electrical field, while the other one generates the magnetic field).

Centriole's diameter is approximately 300 nm, length about 450 nm. It is composed of 27 microtubules ( $9 \times 3$ ), where 9 are with 13 protofilaments, and 18 with 10 protofilaments (total 297).

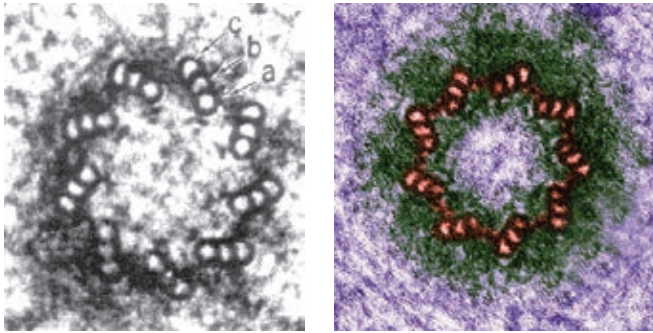


**Figure 5.10.** *Left and right centriole organization: the microtubule a has 13 protofilaments, while microtubules b and c have 10 protofilaments each (left). The angle of angulation of the microtubule triplet is  $222.5^\circ$ , that is  $360^\circ \times 0.61803 = 222.5^\circ$  (Dustin, 1984).*

The centriole is the central enigma of molecular biology. What are the physical processes behind such a beautiful geometric figure, inciting not only a feeling of beauty but of sublime, because it resembles galaxies („a cosmic New York“)? This is the question we tried to answer 30 years ago. I discussed this with many biologists, but no satisfactory answer was found; the majority displayed the attitude: it is a structure having a so and so function. Most of them were satisfied with this answer. Why is it so was not of much interest to them from the professional viewpoint (because they were taught so); however, some expressed interest to find out.

Our model is based on the following mathematical and physical premises: for a random point having coordinates  $x, y, z$ , uniformly distributed within a sphere of radius  $r$ ; the mathematical expectation of the point distance from the center of the sphere should be determined. The task is reduced to calculating the mathematical expectation of a function of a three-dimensional random variable, and the result is:

$$M(r) = \frac{3}{4\pi r^3} \int_0^{2\pi} d\theta \int_0^\pi \sin\varphi d\varphi \int_0^r a \times a^2 da = \frac{3}{4} r$$

Thus, the accumulation of points is at the  $\frac{3}{4}$  of the sphere radius from its center.

Therefore, we have solved the first part of the problem, but we do not know why the points accumulate in nine loci on the diameter of  $\frac{3}{4} r$ . In order to answer this question, we encapsulate into the existing sphere ( $S_0$ ) of radius  $r$ , a sphere ( $S_1$ ) of radius  $r_1 = \frac{1}{2} r$ , and observe the ratio of the circumference of the cross section—circle of sphere  $S_1$  and the circle  $S_2$  of radius  $r_2 = \frac{3}{4} r$ . The perimeter of the circle of the sphere  $S_1$  cross section is  $O_{S_1} = 2 (r/2)\pi$ , and  $O_{S_2} = 2 \frac{3}{4} r\pi$ , which yields:

$$\frac{O_{S_2}}{O_{S_1}} = \frac{2\pi \frac{3r}{4}}{2\pi \frac{r}{2}} = \frac{3}{2}$$

As the radius  $r_1$  divides the circle  $S_1$  into 6 equal parts, if the circle  $S_2$  is divided by  $r_1$ , we have:

$$O_{S_2} [f_{(r_1)}] = \frac{3}{2} \times 6 = 9$$

meaning that on the circumference of the circle of radius  $r_2 = \frac{3}{4} r$  there are 9 characteristic loci of point accumulation.

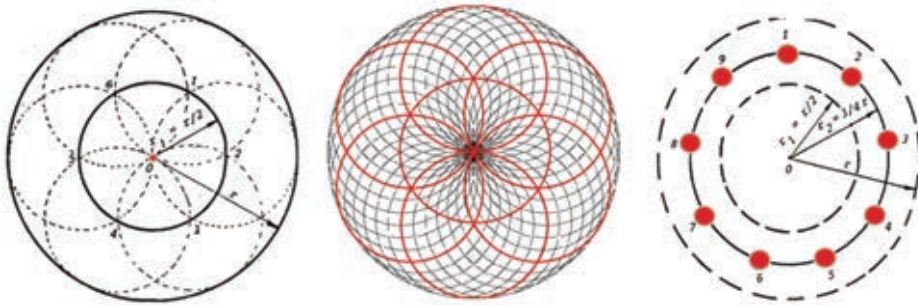


**Figure 5.11.** Cross section of the sphere ( $S_0$ ) of radius  $r$  through its center, with the cross section of sphere ( $S_1$ ) of radius  $r_1 = 1/2 r$ . The circle ( $k_1$ ) of radius  $r_1$  is divided into 6 equal parts. Each point of the divided circle  $k_1$  circumference becomes the center of six circles (1, 2... 6) passing through the center 0 (left). When the structure has icosahedral (dodecahedral) symmetry as in Table 5.1, left and right „lines of electromagnetic twisted force“ are created from the center (middle). When there is a systemic symbiosis between structure and energy, mass points are organized as enneads (nines), displayed in Figure (right).

From the viewpoint of physics, this means that if we have structures with magnetic characteristics (such as microtubules, Figure 5.6) and their magnetic field oscillates and is twisted within limits  $r_1$  and  $r$ , then the structure, as the carrier of magnetism, is distributed into 9 units along the circumference  $\frac{3}{4} r$ .

Now we are faced with another problem, why is each of the 9 units structured as a triplet. Since the ordered triple of each of nine units is oriented under the angle of  $222.5^{\circ}$ , which is  $0.61803$  of  $360^{\circ}$ , this means that  $\phi$  ( $0.61803\dots$ ) is generating this rule to establish a unity with  $\Phi$  ( $1.61803\dots$ ), because  $\phi \times \Phi = 1$  (similarly as the electric and the magnetic

field are always mutually perpendicular,  $\phi$  and  $\Phi$  are always coupled regarding the structural-energetic-information system unity). In this case, the cross section is observed in a plane, i.e., surface, so that the unity of  $\phi$  and  $\Phi$  synergy should be observed as second powers. The sum of their second powers is 3, i.e.,  $\phi^2 + \Phi^2 = 3$  ( $0.61803^2 + 1.61803^2 = 3$ ).

We conclude that the centrioles are organized as ordered triplets of nines because, via the electromagnetism of microtubules, they are establishing an oscillating process according to the  $\phi$  and  $\Phi$  law, as displayed in Figure 5.12 (*middle*).

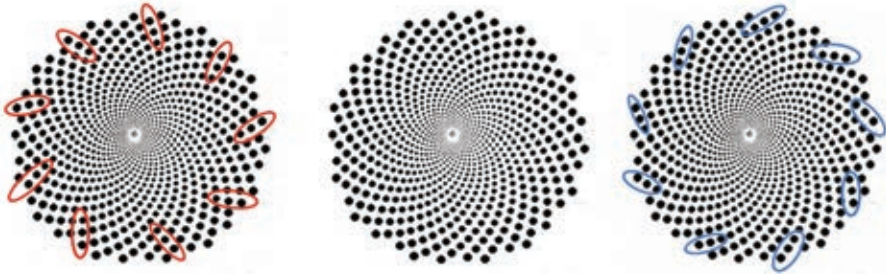


**Figure 5.12.** Discrete two-dimensional representation of the icosahedral energy eigenvalues  $T_{1g}$ ,  $T_{2u}$ ,  $T_{1g}$  and  $T_{2g}$ , where the peripheral angle (of each point on the circle circumference) is 222.50 (*middle*). We observe a left and a right orientation, where the three last points represent microtubular protofilaments forming centrioles.

Since the values generating  $\phi$  and  $\Phi$  are discrete, the curves oriented from the center (Figure 5.11, *left* and *right*) are also pointwise structures generating the law of icosahedral symmetry. This proves that in centrioles, the energy and structure are symbiotically coupled according to the icosahedral (dodecahedral) symmetry.

Knowledge of structural and dynamic properties of centrioles is of utmost importance for the understanding of cell functions, primarily regarding cell division. When the system is unstable and the symmetry is impaired, within the cell cycle, three or more centriole pairs are formed (Figure 5.13, *left*), causing the distribution of chromosomes' (genetic) material to be chaotic and accelerated. This process leads to cancerogenic disorders.

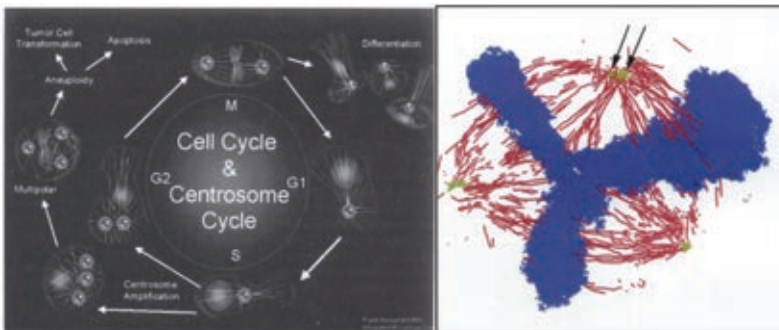


**Figure 5.13.** Cell cycle leading to normal cell differentiation (two pairs of centrioles), into cell death, or to cancer (three or more pairs of centrioles) (Pollard, 2002).

## 5.5. Collagen

Collagens (there are 28 presently known types) are proteins that originated and developed during evolution. Collagen represents about 30% of dry body mass, and the most important collagens are found in the skin, bones, cartilage, smooth muscles, dentin, etc. The most important collagens are those in the basement membrane (type VII) and the reticular lamina of the basement membrane (type I and III, and somewhere type IV). Type I collagen is prevalent (85%–90% of all collagens) and is found in most tissues.

Schematic representation of the procollagen structure, collagen molecules, collagen microfibrils, collagen fibers and the collagen macroscopic fibers is displayed in Figure 5.13. The main amino acids composing collagen are: glycine (35%), proline (15%) and hydroxy-proline (10%), constituting 60% of collagen; all other amino acids constitute 40% of collagen. The procollagen molecule is 265–300 nm long, of 1.5 nm diameter, with a 8.6 nm helix. This is one of the rare proteins whose secondary structure is a 100%  $\alpha$ -helix.

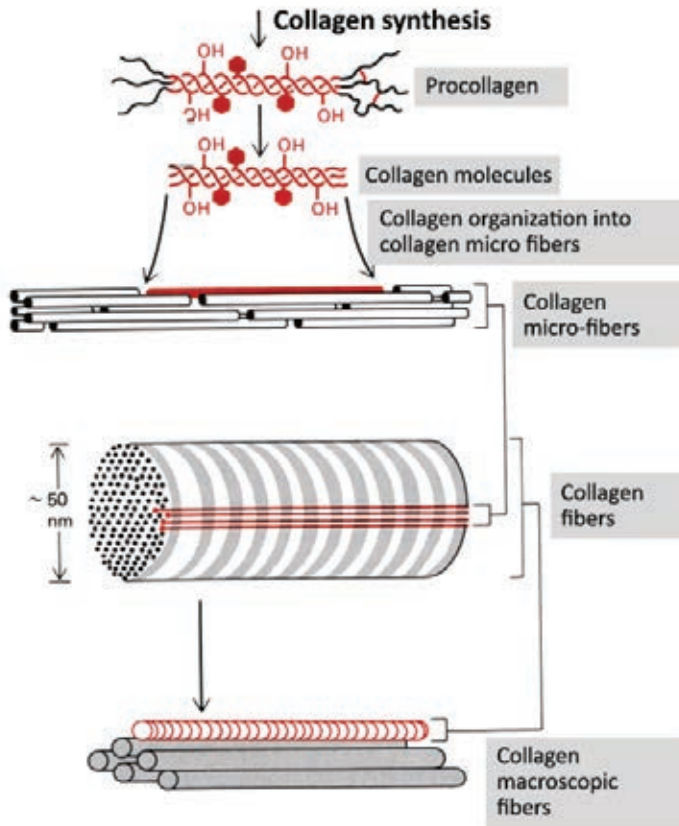


**Figure 5.14.a** Various collagen organization forms, from the procollagen of diameter 1.5 nm to the macroscopic collagen fibers of diameter 150–200 nm (Nossal, 1991).

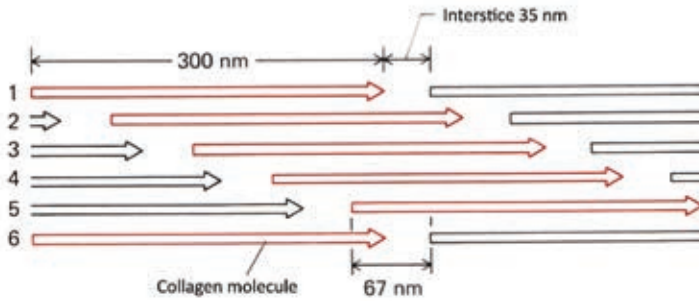


**Figure 5.14.b** Schematic representation of several collagen molecules organized into a microcollagen fiber. Due to oscillatory processes of peptide planes in the collagen molecule, there are interstices of 35 nm, so that a collagen fiber can oscillate to the left and to the right 1 to 10 nm overall.

Let us demonstrate that collagen is energetically and/or structurally determined by  $\phi$  and  $\Phi$ . Since their relation is determined by the „golden“ triangle ( $\phi^2 + \Phi^2 = 3$ ), we shall investigate the oscillatory processes of the ordered triple of peptide planes of the collagen molecule. Oscillations of the first three peptide planes of the collagen molecule are: the first–  $8.650595 \times 10^{13} \text{ s}^{-1}$ , the second–  $6.58846 \times 10^{13} \text{ s}^{-1}$  and the third–  $5.33626 \times 10^{13} \text{ s}^{-1}$ . Calculating the ratio of the first and the second to the third, we obtain 1.6, 1.20, 1, meaning that the relation of the first and the third peptide is equal to  $\Phi$ . In the last three peptide planes, ratios are 2.7, 1.6 and 1. Therefore, the oscillatory signal is transferred from the molecule beginning to the molecule end; at the beginning, the first peptide plane had the value 1.6, and the second peptide plane has the same value at the end. It is interesting to note that the signal transfer is analog with base  $e$ , and signal energy is about 0.35 eV, which is approximately  $2800 \text{ cm}^{-1}$  (wave number) or  $3570 \text{ nm}$  (wavelength).

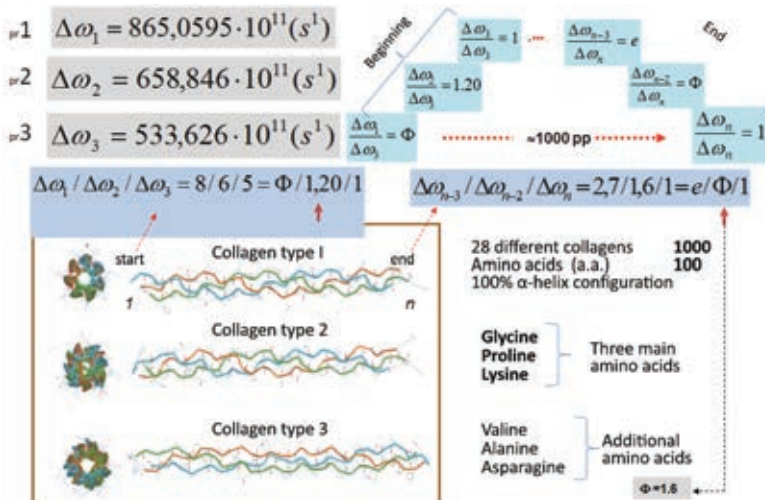


**Figure 5.15.** Oscillation of the collagen molecule having base  $\Phi$  and the transfer of this signal with base  $e$ , via the  $\alpha$ -helical organization of collagen.

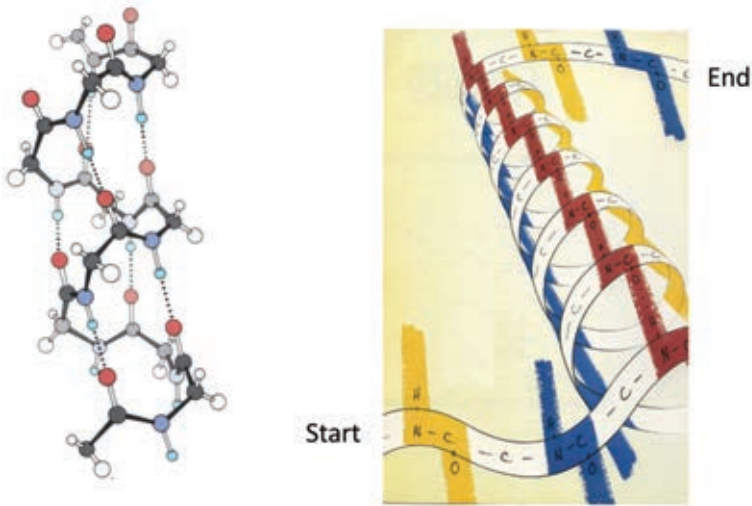


**Figure 5.16.** The  $\alpha$ -helical organization (secondary structure) of collagen: from the molecule „beginning“ (the first three peptide planes) the vibration signal is transferred through the  $\alpha$ -helical structure, via hydrogen bonds O...H (pointwise bonds–Figure left, red, blue or yellow line–Figure right), to the end of the molecule according to bases  $\Phi$ .

Regarding the organization of macroscopic collagen fibers (Figure 5.17), there is a reversible transition in packing fibers from the form (a) into form (b) and vice versa. This transition from one form into another provides for the elasticity/stiffness of collagen, because the form (a) is transformed into form (b) under pressure, but as soon as the pressure is lifted, as collagen fibers are in biased voltage states, it returns into form (a). This basic biased voltage state of collagen fibers in form (a) is structured into a pentagram, enabling the oscillatory process in state (a) to be established according to the  $\phi$  law, that is the  $\Phi$  law, because there is an inverse relation of pentagonal structures  $\phi = 1/\Phi$  (Figure 5.17b).

Penrose first predicted that collagen fibers may be organized as quasicrystals. A quasicrystalline structure in alloys was first discovered experimentally by Den Schectman (Schectman, 1984). It is interesting to note that Schectman waited 35 years for recognition, he received the Nobel Prize for the discovery of quasicrystals in 2011. For 20 years his main opponent was Linus Pauling, two-times Nobel Prize winner, who even on one occasion cynically remarked: „...there is no such thing as quasicrystals, there are only quasiscientists“. We know today that not only do quasicrystals exist in the solid state, but liquid crystals exist as well (which, with respect to the classical crystals, are a kind of quasicrystals), notably present in biological systems. Schrödinger was the first to propose that organized structures in the form of crystals are at the foundation of biological systems, and that the genetic material is an aperiodic crystal (Schrödinger, 1943). In classical crystals, the basic unit („crystal cell“) is repeated, while in the genetic material (DNA), we observe aperiodic repetition of A, T, C, G, although the ribose and the phosphorus group are periodically repeated.

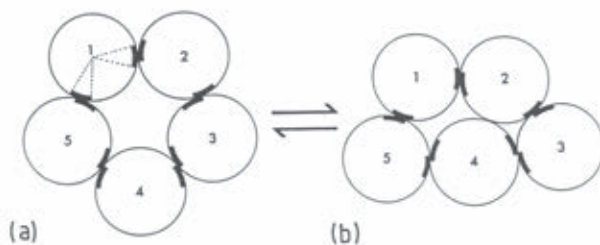


**Figure 5.17.a** (a) Organization of collagen fibers into pentagons, bias-voltage state with the  $\phi$  and  $\Phi$  characteristic, and collagen shape that endures high pressure strain (b). Depending on external influence there are reversible processes between states (a) and (b).

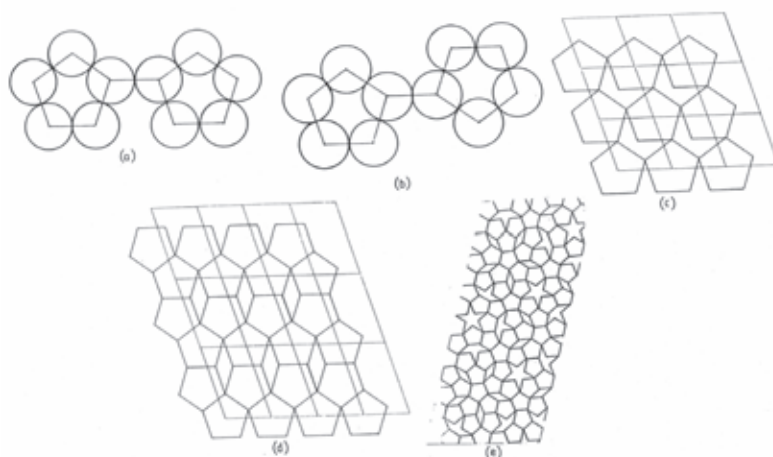


**Figure 5.17.b** Pentagonal bases of the collagen fibers organization (a and b), elementary unilayer lattice of pentagonal fibers (c), double layer organization of pentagon fibers (d) and a multilayered form of collagen fibers organization having the quasicrystalline property with characteristics  $\phi$  and  $\Phi$  (e).

Quantitative energy values of the hydrogen bond  $N-H \cdots O = C$  are determined in the collagen of type I, which includes polypeptide planes of amino acids glycine and proline. These findings can explain the physical basis of the collagen stability, having a very important structural role in connecting tissues. Numerous experiments on collagen were conducted: infrared spectroscopy, quartz piezogravimetry, and differential scanning calorimetry. Results indicate that bonding 3–4 water molecules as internal hydration of collagen leads to a conformation reorganization of the triple helix and the reinforcement of hydrogen bonds. Hydration enthalpies of Poly (Gli-Pro-Pro) and of collagen are -10.9 and -12.2 kJ/mol, respectively. The hydrogen bonds  $N-H \cdots O = C$  are -7.6 and -6.0 kJ/mol in the Poly (Gli-Pro-Pro) and collagen, respectively. These findings can be used to assess the influence of energies of various interaction types on the overall energy stabilization of the natural triple collagen helix and Poly (Gli-Pro-Pro).



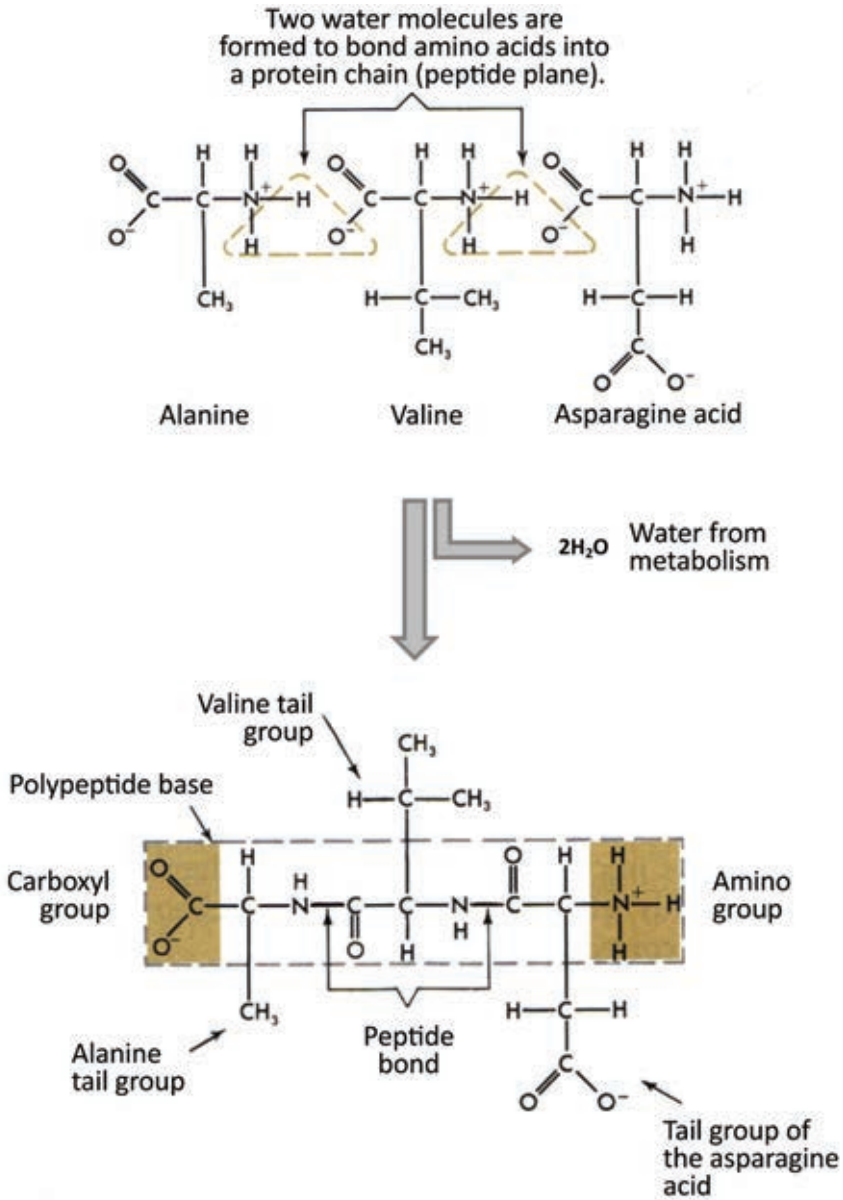


**Figure 5.18.** When two amino acids engage in interaction to form a peptide plane (belonging to the protein chain), in order to achieve a covalent bond (N-C), a water molecule is formed, because two atoms of hydrogen from the amide group of the first amino acid and one atom of oxygen from the carboxyl group of the second amino acid are paired to form a water molecule (Figure above). At the same time a peptide bond is established (middle Figure), i.e., a peptide plane. Thus, water originating from metabolism accounts for approximately 10% of the overall water in the organism (Mathews, 1990).

## 5.6. Water and Gibbs Free Energy

Water, compared to other natural polymolecular structures, has more than 30 „anomalies“. We intentionally use the term „anomaly“ (under quotes) because compared to, for instance, 100 structures exhibiting one type of behavior, water behaves differently. One such example is that all materials („inanimate nature“) contract in cold, and expand in heat. Water behaves differently; liquid water has greater density than ice, thus ice floats. This means that its volume per  $\text{cm}^3$  is greater than the volume of liquid water. Water expands at lower temperatures, and contracts at higher temperatures. Paradoxical (at first sight), but such is the reality. If it were not for this „anomaly“, biological form of life probably would not exist. Water effected a breakthrough and created life, aided by external factors, primarily light, heat, and gravitation.

Water within cell makes up for about 70% of the cell's contents, the remainders are other chemicals, mostly proteins (15%) (Figure 5.19). As the protein synthesis takes place within the cell cytoplasm, the cell water contains approximately 20% of metabolic water. The organism as a whole contains approximately 72% water, the rest being dry matter. Lungs, blood and the brain are most abundant with water. With age, the water percentage decreases in every organ, mostly within skin (from 70% to 60%).

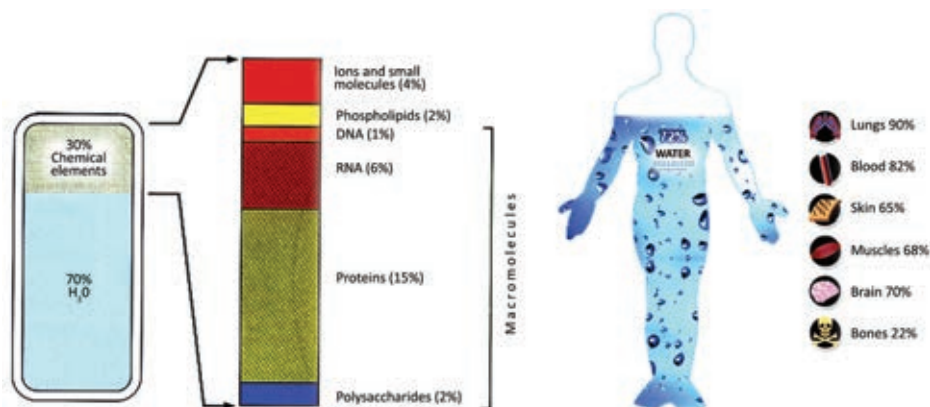


Figure 5.19. Water content (percentage) in the cell (left) and in the human organism (right) (Pollard, 2002).

An interesting fact, of which we are not even aware (and yet have to learn how to utilize it), is that water is made of two chemical elements (atoms) that originated at different times and by different processes. Hydrogen was created as a cosmic phenomenon, i.e., it was created by the Universe, while oxygen originated in the stars (much, much later). The oxygen in the water we drink and incorporate into our tissues was actually once a constitutive part of a star that exploded; its cooled parts formed afterwards cold celestial bodies.

What is the origin of water on Earth? There is no positive answer at present. There are different hypotheses, but not one serious theory which would explain water presence on Earth. However, such as we are, we are the „children“ of the Solar system. We live in a warm oasis at approximately  $25^{\circ}\text{C}$  (about 300 K), while the interplanetary and

interstellar space is at  $-267^{\circ}\text{C}$  (only 6 K). Recall the voice of the stewardess „...Ladies and gentlemen we are flying at the altitude of 11000 m, outside, temperature is  $-50^{\circ}\text{C}$ ...“. If we were not in a plane, there would be no life up there for us. Water, by its high thermal capacity can protect us only within a very small temperature range and for a short time.

The water molecule is composed of two hydrogen atoms and one oxygen atom, connected by *covalent* hydrogen bonds. The strength of the covalent bond O-H is 460 kJ/mol (4.77 eV), while the strength of the noncovalent bond O...H ranges from 10 to 60 kJ/mol (0.09–0.48 eV) depending on the  $\text{pK}_w$ , temperature and the organization of water molecules- in open chains or closed clusters. Two (dimer) or more water molecules (trimer or longer water chains) engage in interaction via *noncovalent* hydrogen bonds. The basic reaction is  $2\text{H}_2\text{O} \leftrightarrow [\text{H}_3\text{O}]^+ + [\text{OH}]^-$ , where  $K_w = [\text{H}_3\text{O}]^+ \times [\text{OH}]^-$ , and  $\text{pK}_w = -\log_{10}K_w$ .

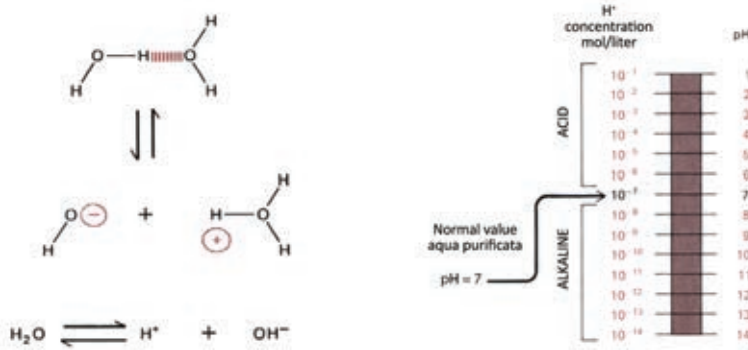


**Figure 5.20.** Basic interaction of water molecules via the noncovalent hydrogen bonds and the process of water autoionization (left). Depending on the ratio of  $[\text{H}_3\text{O}]^+$  to  $[\text{OH}]^-$  ions, water as a medium where chemical reactions take place, and which actively participates in these reactions itself, can be neutral ( $[\text{H}_3\text{O}]^+ = [\text{OH}]^-$ ), acid (more  $[\text{OH}]^-$ ) or alkaline (more  $[\text{H}_3\text{O}]^+$ ) (Mathews, 1990).

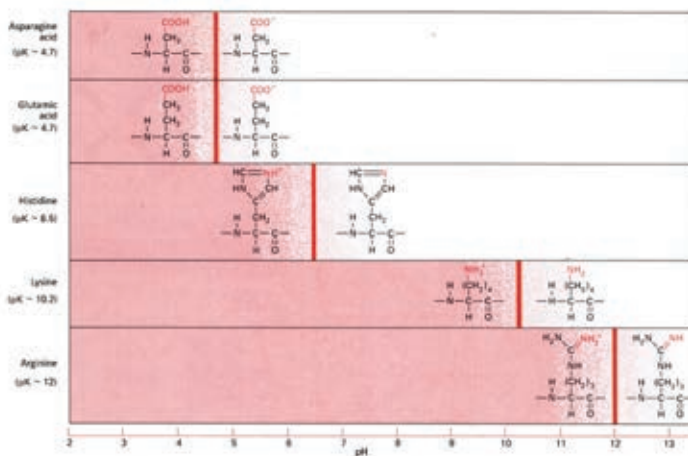


**Figure 5.21.** Dependence of the amino acid charge on the pH value of the environment (Mathews, 1990).

This determines the pH value of the water environment where biochemical reactions take place. This value determines whether the amino acids (their „tails“) entering the protein composition will be positively charged, negatively charged or neutral (Figure 5.21). Depending on the charge that amino acids introduce into the protein, it will have corresponding dipole moments, which is especially significant for the interaction between light and biomolecules. It is established that our vascular system should be slightly alkaline, pH = 7.356, for the body to function harmoniously, that is, to be healthy. However, in the stomach, where food is digested, the medium is very acid, pH= 2-4. Some pH values are: saliva 6–7, bile 7–8, small intestine 8–9, colon 7.5–8, extracellular liquid and arterial blood 7.4, venous blood 7.5, intracellular liquid 6–7.4, and urine 4.5–8.

The free energy of a physicochemical process is the energy capable of performing work. The second law of thermodynamics on the conservation of energy states that, in spontaneous chemical reactions, free energy is decreased giving a *negative*  $\Delta G$ . In the equilibrium state, no further change of the free energy occurs, thus  $\Delta G = 0$ . In this case, the closed system has the least amount of free energy, and all the components are of 1 mol/liter concentration. When the biochemical reaction approaches the equilibrium state, the free energy is increasingly being transformed into heat or into disorder (entropy). It sounds paradoxical, but in the equilibrium state the system is in the greatest „disorder“ (therefore we say that entropy is the measure of disorder).

If we observe the process of water molecule autoionization, the equilibrium constant follows from the expression defining free energy  $\Delta G = -RT \ln K$ :

$$\frac{[\text{H}_2\text{O}]}{[\text{H}]^+ [\text{OH}]^-} = e^{-\Delta G^0/RT} = e^{-\Delta G^0 \times \frac{1,50}{2,00} f(T)}$$

where:  $e$  – base of the natural logarithm 2.7128,  $\Delta G^0$  – free energy of the equilibrium state (all components in the reaction have the concentration of 1 mol/liter),  $R$  – universal gas constant 0.001987 cal/degreeK/mol,  $T$ – temperature in Kelvin.

**Table 5.2** Ratio of free energies of the AB complex and the sum of components A+B for a given equilibrium constant.

Equilibrium constant $\frac{[\text{AB}]}{[\text{A}][\text{B}]} = K$	Free energy of the AB complex decreased by the sum of free energies of components A+B (kcal/mol)
$10^5$	- 7.1
$10^4$	- 5.7
$10^3$	- 4.3
$10^2$	- 2.8
10	- 1.4
1	0
$10^{-1}$	1.4
$10^{-2}$	2.8
$10^{-3}$	4.3
$10^{-4}$	5.7
$10^{-5}$	7.1

Thus, for example, the RT value between 1.50–2.00, as  $f(T)$  of water in process forming, is within limits  $-20^{\circ}\text{C}$  to  $+52^{\circ}\text{C}$ . However, significant RT values are  $25^{\circ}\text{C}=298.15\text{ K}$  (room temperature),  $37^{\circ}\text{C}=310.15\text{ K}$  (body temperature) and  $36.7^{\circ}\text{C} = 309.85\text{ K}$  (optimal body temperature). We observe that the equilibrium constant depends on  $\Delta G^0$  and on temperature. For  $T=25^{\circ}\text{C}$  the product is  $RT=0.001987 \times (273.15+25)=0.001987 \times 298.15=0.592484$  ( $1/RT = 1.6878$ ), for  $T=37^{\circ}\text{C}$   $RT=0.61633$  ( $1/RT = 1.622507$ ), and  $T=36.7$  gives  $RT=0.61567$  ( $1/RT = 1.6242$ ). Since in microtubules  $1.615 \leq \Phi \leq 1.625$ , the value 1.622 is within limits of the operating process. This difference, i.e., the ratio  $1.61803/1.625=0.9961$  indicates that the biochemical processes are not perfect, they occur within narrow limits  $\pm 0.003\%$  ( $1.615/1.625=0.006\%$ ). However, if biochemical processes exceed these limits, the organism defends itself by raising the body temperature to  $37.8\%$  ( $0.001987 \times T=0.61803$ , giving  $T=311.7\text{ K}$ , i.e.,  $37.8^{\circ}\text{C}$ ), because the ideal value is  $RT=0.61803$  (that is  $1/RT =1.61803$ ).

The equilibrium constant for body temperature of  $37.8^{\circ}\text{C}$  ( $309.8\text{ K}$ ) is given by the expression:

$$\frac{[\text{H}_2\text{O}]}{[\text{H}^+][\text{OH}^-]} = e^{-\Delta G^0 \times 1.624}$$

therefore, any aberration (such as body temperature higher than  $37.8^{\circ}\text{C}$ ) demands that  $1/RT$  be brought to the operating value of the organism 1.624. If the body temperature is between  $36.7^{\circ}\text{C}$  and  $37.8^{\circ}\text{C}$ , it is best to let the organism itself fight the biological physicochemical problem, but if the limit  $38.7^{\circ}\text{C}$  is exceeded, it is necessary to take adequate steps to lower the temperature to the limit value.

The rate of water molecules interaction, primarily of noncovalent hydrogen bonds and of the reorganization of dipole moments, is within limits 1–100 ps, while the macroscopic dynamics and the conformation changes of biomolecules occur within microseconds ( $\mu\text{s}$ ).

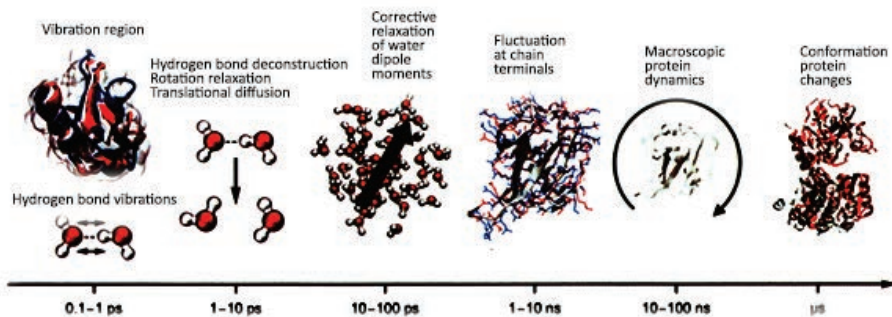


Figure 5.22. *Hydrogen bond vibration value is 0.1–1 ps, while the deconstruction of hydrogen bonds is within 1–10 ps. The dipole moments are reorganized within 10–100 ps, while the macroscopic dynamics is of the order  $10^{-8}$  s.*

Water that we drink, and water in the human organism, is not the same because of the conditions under which the water is found. Water in the glass is under the atmospheric conditions and within the macroscopic volume, while in the organism, it is in the micro and nano volume where complex biological physicochemical processes occur interacting with water.



**Figure 5.23.** Water in a glass and water within the organism are of the same chemical composition, but are under different conditions, thus having different properties. Water in a glass is a classical liquid (it interacts with the glass, the space is macroscopic, temperature about 25°C). In the organism, it is highly elastic (because it is located in a biological environment where strong electric discharges occur per unit of length and volume, temperature is 37°C, the space is microscopic and nanometric, therefore the  $pV = RT$  has to be modified by action of van der Waals forces on nano scale).

In order to determine the features of biological water, let us examine an experiment performed in 2012 by the researchers in Netherlands (Fuchs, 2012). They took two dishes of diameter 60 mm, 30 mm deep, keeping the distance of 10 mm between dishes. Then electric current of 15 kV was introduced into 66 g of deionized water. Before activation, water conductivity was  $0.055 \mu\text{Scm}^{-1}$ , after activation with the given voltage it became  $0.4\text{--}1.0 \mu\text{Scm}^{-1}$  (Figure 5.24).

The experiment was recorded with a camera in the domain of the visible light and in the domain of IR light by a spectrometer in the interval of  $3\text{--}12 \mu\text{m}$ . Regarding hydrogen bonds, the  $3\text{--}4 \mu\text{m}$  domain was observed, and regarding fundamental vibrations of water molecules, the domain of  $8\text{--}12 \mu\text{m}$ . Water temperature was 22°C. After voltage of 15 kV was applied, a water bridge formed between two dishes. The dishes were then separated to a distance of 3 cm and the water bridge survived. A Canon 300D camera recorded the visual phenomenon of the „water bridge“ as shown in Figure 5.25. At the same time, the IR spectrometer measured the radiation of the „water bridge“ at 22°C.

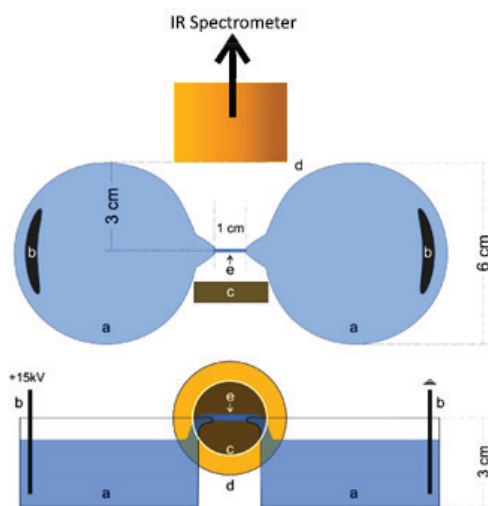


**Figure 5.24.** Experimental setup for the formation and measuring of the „water bridge“ using 66 g of deionized water in two dishes at a distance of 1 cm (Fuchs, 2012).

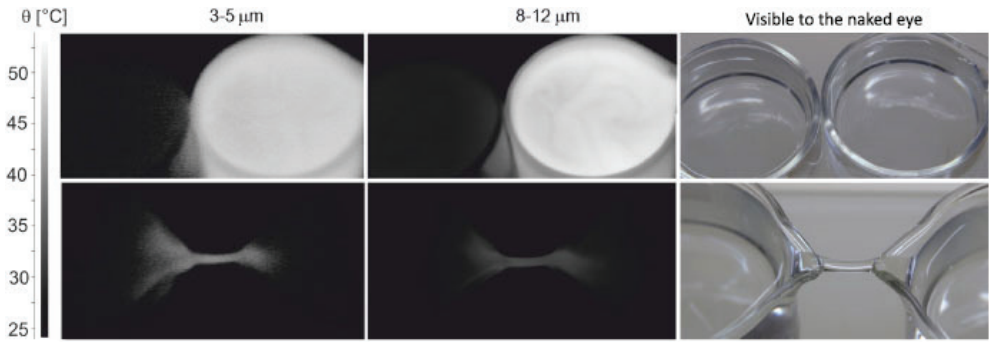


**Figure 5.25.** *Measuring the emission spectrum of the „water bridge“ using the IR spectrometer in the intervals 3–5  $\mu\text{m}$  and 8–12  $\mu\text{m}$  and a Canon 300D camera in the domain of the visible spectrum (Fuchs, 2012).*

In Figure 5.25 (*above*), we observe that water in the right dish is excited (white), while in the left dish water is not excited and the IR spectrometer does not register its presence. When the dishes are separated at 3 cm apart, water in the „water bridge“ „shines“ (*below*).

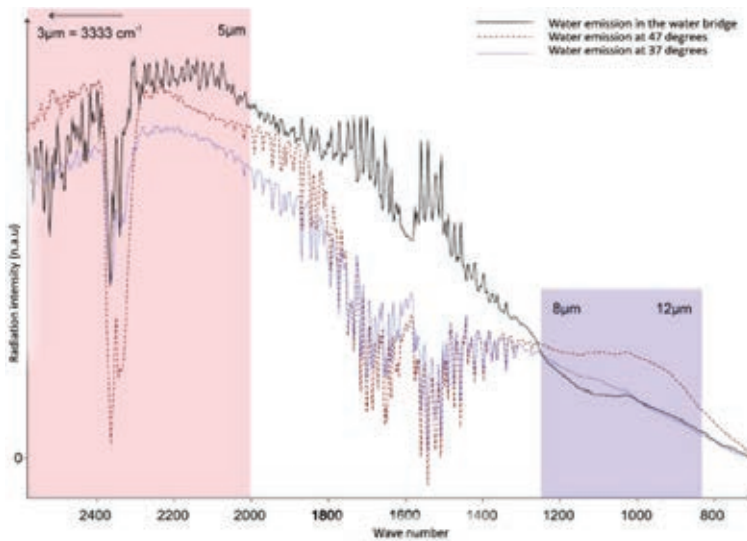


**Figure 5.26.** *Coincidence of the spectrum of the „water bridge“ at temperature of 22°C and of water at temperature 37°C is in the domain 10–14  $\mu\text{m}$  of fundamental vibrations of water molecules (Fuchs, 2012).*

When we compare the spectra of the „water bridge“ emission at 22°C, water at 47°C, and water at 37°C, we observe that in part of the domain of fundamental vibrations 10–14  $\mu\text{m}$ , the spectrum of the „water bridge“ and the water spectrum at 37°C coincide. Water in the „water bridge“ is in the form of a liquid crystal, thus it can create a bridge that does not collapse under the influence of gravitation. This strongly supports the

conclusion that most of the water in the human organism, at the temperature of 36.7 °C, is in the form of liquid crystals. The experiment can be considered an indirect proof of this idea, because while in the „water bridge“, voltage per centimeter length on the average was about 10 kV/cm, in the human organism this value, transformed from mV and nm into kV and cm, is 50–300 kV/cm (Tyner, 2007).

Let us observe the interaction between two isolated water molecules via noncovalent hydrogen bonds as displayed in Figure 5.27.

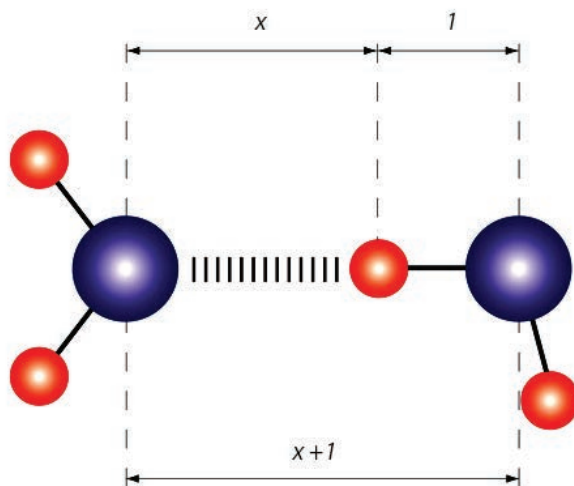


**Figure 5.27.** The interaction between two isolated water molecules via noncovalent hydrogen bonds, where „1“ denotes the value of the covalent hydrogen bond, „x“ is the variable distance between hydrogen atoms of one molecule and the oxygen atom of the other water molecule. The expression „x+1“ represents the distance between centers of oxygen of two water molecules.

The covalent hydrogen bond is  $0.0984 \pm 0.0025$  nm, and this will be declared in our model as unity („1“), a point of reference with respect to the noncovalent hydrogen bond. In other words, we shall observe a change of the noncovalent hydrogen bond „x“ (as the *larger part* of the system „x+1“) with respect to „1“ (as the *smaller part* in the system „x+1“). Since the water molecules spontaneously organize and deconstruct themselves, i.e., they have the property of selforganization (selfcontrol), based on a stable covalent hydrogen bond „1“, the ratio „x“ to „x+1“ should be as „1“ to „x“ (the *larger part* with respect to the *whole* is related as the *smaller part* to the *larger part*). Based on the regular ratio of *parts* to the *whole* and the ratio between *parts*, the proportion is obtained  $x : (x+1) = 1 : x$ , giving  $x^2 = x + 1$ , namely  $x^2 - x - 1 = 0$ . Solutions of this quadratic equation are  $x_1 = 1.61803$ , which is  $\Phi$ , and  $x_2 = -0.61803$ , which is  $-\phi$ . Therefore, we observe that, for two molecules to organize themselves spontaneously into a dimer, the noncovalent hydrogen bond should be  $1.61803 \pm 0.025$  greater than the covalent hydrogen bond. Thus, the oscillation process occurs within limits 1.59303 and 1.64303 of the value of the covalent hydrogen bond.





the double value of the covalent hydrogen bond, they engage in a hydrogen noncovalent bond. It is known that the convergence point of this sequence is  $\Phi$ .

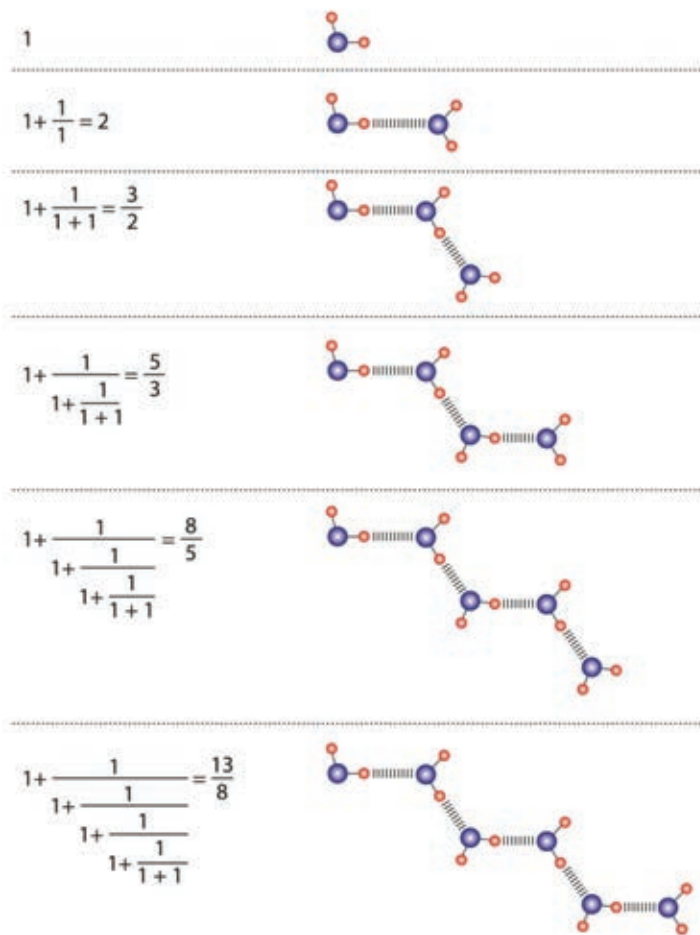


**Figure 5.29.** A possible organization of water molecules into chains with numbers converging to  $\Phi$ . Water molecule chains maintain the same values when the chain configuration is changed, i.e., if at the second or third water molecule bonding starts upward, and after a molecule or two downward (Koruga, 2008).

A diagram representing values of water molecules organization into chains is displayed in Figure 5.30, indicating that the establishing noncovalent hydrogen bond is the longest in a water dimer, equal to two lengths of the covalent hydrogen bond. When the bond is established and stabilized, the noncovalent hydrogen bond oscillates between values 1.615 and 1.625.

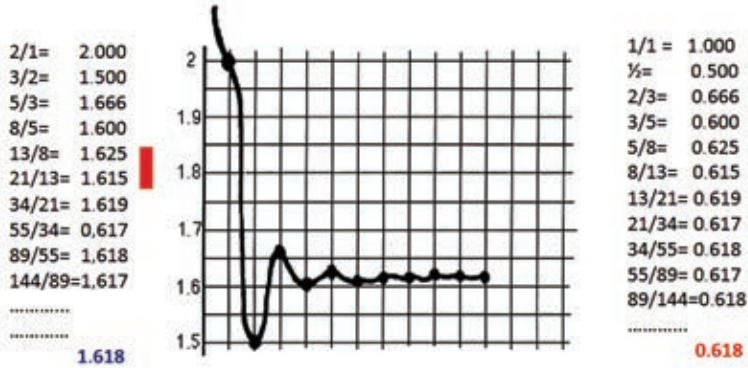


Figure 5.30. Convergent series of water molecules organization into chains. The diagram shows a series converging to 1.618, that is  $\Phi$ .

The question is what is the chain length of stable water molecules? The system determinant provides the answer. The number of molecules where the determinant of noncovalent hydrogen bonds is equal to zero gives a stable chain. A chain of 3, 4, 5...8 water molecules would not be stable, it would be created and destroyed within a few *ps*. However, for a chain of nine water molecules (not beginning with a *monomer* or *dimer* water molecule, but with a *trimer*) the determinant of such a system equals zero:

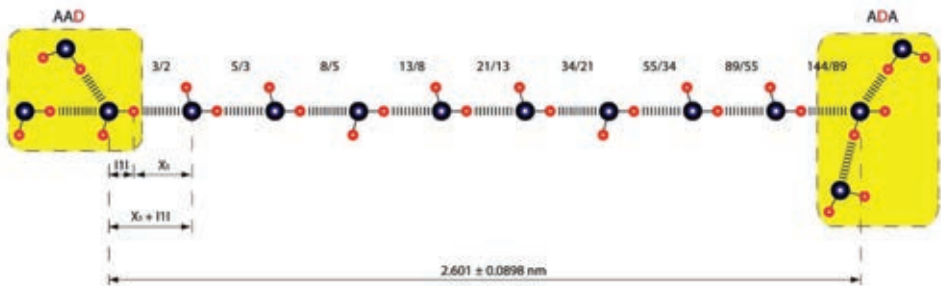
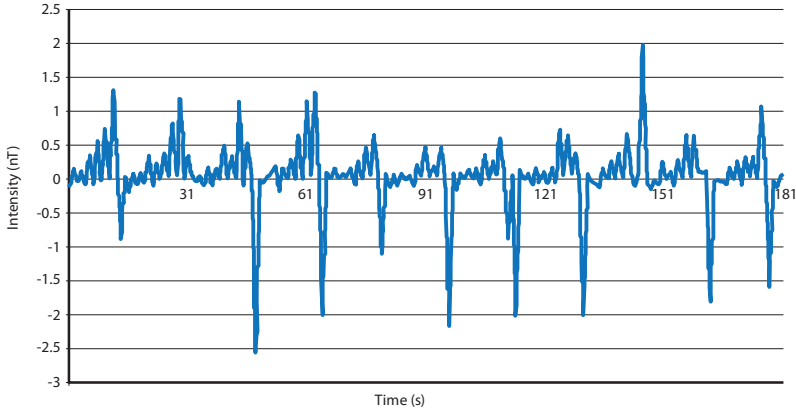


Figure 5.31. A stable hydrogen chain of nine water molecules (linear „ennead“), where the end molecules are ADA (acceptor –donor –acceptor), and the other ending is AAD (acceptor –acceptor –donor), so that a signal is transferred across hydrogen bonds from left to right (the determinant  $3 \times 3$  of 3, 5, 8, 13, 21, 34, 55, 89, 144 is equal to zero).

In order for the hydrogen chain to start forming spontaneously from a monomer (one water molecule) 16 water molecules must be excited creating a system 1, 2, 3, 5, 8, 13, 21, 34, 55, 89, 144, 233, 337, 610, 987 and 1597. The determinant ( $4 \times 4$ ) of this system is equal to zero.

Water molecules can be organized not only into hydrogen chains, which are the necessary condition for the creation of a linear crystalline („gel“) water state, but also

into 3D clusters. Only together, water chains (1D) and clusters (3D) give different characteristics to water as compared to water organized into dimers, trimers... up to the „enneadic“ structures.



**Figure 5.32.** Diagram of paramagnetic/diamagnetic water properties (18.2 MΩ) during a three-minute period. Paramagnetism (positive peaks) occurs as a result of unpaired electrons in water clusters. Diamagnetism is the result of absence (sporadic presence) of unpaired electrons. The diagram shows formation of clusters with small paramagnetic amplitudes. Clusters are deconstructed into dimers and trimers of water molecules, and are again organized into clusters afterwards. However, when they are organized into larger clusters (1–2 nT), and then deconstructed into monomers, the diamagnetic peaks are much more pronounced, up to -2.5 T (experiment performed at the Geomagnetic Institute of the Republic of Serbia, using two coupled protonic magnetometers based on the Overhauser effect, Koruga, et al., 2008).

The calculation of cluster size based on paramagnetism is performed according to the formula: *magnetic force* of unpaired electrons equals the product of the electron mass and its *radial acceleration* (*magnetic force = mass × radial acceleration*), which is for one electron written as:

$$e \times \vartheta \times B = \frac{m \times \vartheta^2}{r}$$

so that the radius  $r$  of a cluster which, by the motion of  $n$  unpaired electrons, generates a magnetic field  $B$  is:

$$r = n \frac{m \times \vartheta}{e \times B}$$

Electron's charge and mass are known, and the cluster velocity of uncoupled electrons is equal to the inverse value of the velocity of light ( $v_{light}/v_{cluster} = 1$ ) based on the inversion of the electric and magnetic field (expressions 2.2 and 2.20, in Chapter II). In this way, a water cluster can be established (temporally limited, but stable) based on noncovalent

hydrogen bonds (expressions 2.2 and 2.20, in Chapter II). Velocity is  $3 \times 10^{-8}$  m/s, while the intensity of the magnetic field is obtained from the diagram. For  $n = 10$ ,  $e = 1.6 \times 10^{-19}$  C,  $m = 9.1 \times 10^{-31}$  kg,  $\vartheta = 3 \times 10^{-8}$  m/s and  $B = 1.3$  nT, the cluster radius is  $1.29 \times 10^{-9}$  m, that is 1.29 nm. Having in mind that the largest value of the Van der Waals radius of water molecule (including noncovalent and covalent hydrogen bonds) is 0.355 nm, we observe that for the cluster organization of water molecules, about 20–30 water molecules can be packed into a radius of 2.58 nm.

Small water clusters (2–10 molecules):	0.1–1.0 nT
Middle size water clusters (10–50 molecules):	1.0–10.0 nT
Large water clusters (50–100 molecules)	10.0–50.0 nT
Extra large water clusters (> 100 molecules)	> 50.0 nT

Paramagnetic/ diamagnetic water properties (200 ml, aqua purificata 18.2 MΩ – twice electro deionized), are displayed on the diagram of Figure 5.32, under the following conditions: temperature 20°C, Earth’s magnetic field 47.500 nT ( $4.7 \cdot 10^{-5}$  T), humidity 45%, atmospheric pressure 1 bar. However, when the same water is exposed to the influence of the oscillatory magnetic field (starting from 100 mT) according to the  $\Phi$  law, we obtain a diagram as in the Figure 5.33.

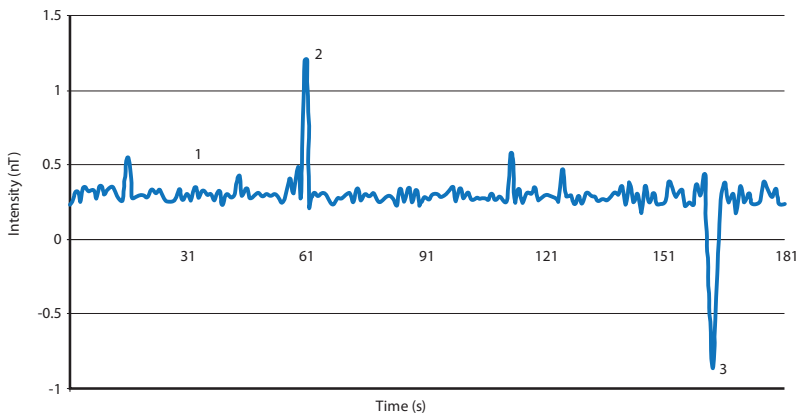


**Figure 5.33.** A diagram of the paramagnetic/diamagnetic water properties exposed to the oscillatory magnetic field oscillating according to the  $\Phi$  law. Three phenomena are observed compared to the diagram from Figure 5.22: water has relatively stable paramagnetic properties at 0.2 nT (region 1). After being for 60 s exposed to the oscillatory magnetic field, a prominent peak occurs (region 2) equal to 1.2 nT, which decreases to 0.2 nT until the 162 s of stimulation, when a sudden transformation occurs into diamagnetism (region 3). After 3 s, water returns to a stable paramagnetic value of 0.2 nT (Koruğa, 2008).

The diagram in Figure 5.33 indicates that it is possible to organize water molecules into stable clusters (paramagnetism 0.2 nT) under the influence of an oscillatory magnetic field according to the  $\Phi$  law that can organize water molecules into clusters (Figure 5.29). This is the domain 1 on the diagram. However, we observe that there are another two characteristic regions- 2 and 3, where in the first case paramagnetism is dominant, and in the second case diamagnetism. In case of *peak 2* (paramagnetism), it can be concluded that the cluster is deconstructed from the value 1.2 nT and is stabilized as a smaller cluster of 0.2 nT. However, it is very hard to explain *peak 3* when water becomes a diamagnetic, and is stabilized afterwards as a paramagnetic, without oscillating about the zero value it starts to oscillate as in Figure 5.32. *Peak 3* indicates strongly the possibility that water, in the form of nano clusters, has the property of a *memristor* (a type of memory at the nano level).

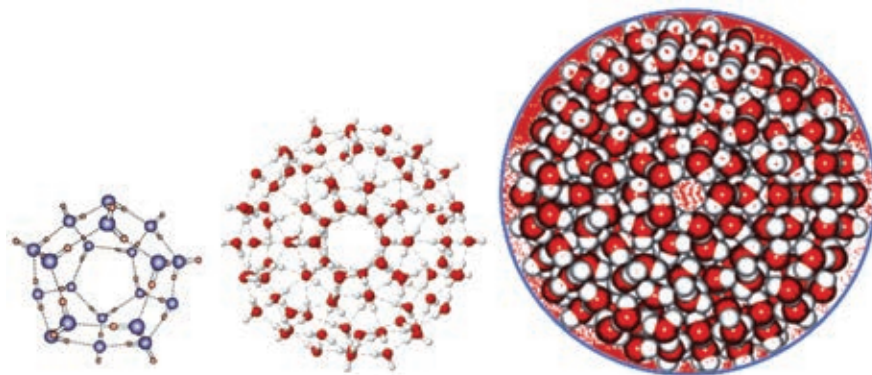


**Figure 5.34.** A cluster of 20 water molecules (left) experimentally confirmed (Sang and Xu, 2010), is organized into a dodecahedron with a symmetry dual to the icosahedral symmetry (it includes only 12 pentagons). Hypothetical water clusters with 100 water molecules (middle) and with 280 (right) water molecules with icosahedral symmetry (12 pentagons and 26 hexagons) (Chaplin, 2008).

Using another method, aquaphotonics (Tsenkova, 2009), we investigated the clusterization of doubly deionized water (18.2 M $\Omega$ ) by an infrared spectrometer in the domain 900 nm –1700 nm, before and after magnetization with an oscillatory magnetic field according to the  $\Phi$  law. As observed in Figure 5.35, pure water (aqua purificata – before) has a basic state at the level of zero according to all 12 coordinates (water is in a maximum state of monomers and dimers). Immediately after water was exposed to the oscillatory magnetic field ( $\Phi$ ), it became structurally organized into clusters (coordinate values: S4 at 1.488 nm (2.6 n.a.u) and V1, V2 at 1.517 nm (2.7, but at the same time it also acquired an organization of multilayered spheres, „water shell“ – (H<sub>2</sub>O)<sub>20</sub> @ (H<sub>2</sub>O)<sub>100</sub> @ (H<sub>2</sub>O)<sub>280</sub> : 20 molecules are within 100 molecules, and 100 molecules within 280 water molecules) at 1.360 nm. We cannot conclude with certainty what form of water shells is present, but one of the more probable candidates is the (H<sub>2</sub>O)<sub>20</sub> cluster.

Magnetized water was observed daily. Variations were not significant until the eighth day. At the end of the seventh day, within 24 hours a spontaneous reorganization of

magnetized water occurred, one part became „free water“ (monomers and dimers), with significant presence of OH groups (Figure 5.36). In this water, „water spheres“ were formed with concentric shells, on both wavelengths: 1382 nm and 1360 nm. Why did, after the seventh day, spontaneous water reorganization occur is presently unexplained. It is obvious that present scientific knowledge about water is not sufficient to explain these phenomena completely. We shall cite Faraday again: „theory leads, and experiment decides“, adding that in our case the experiment leads and represents a very challenging task for the scientific theory. Actually, everything points to the conclusion that for the explanation of the water experiment it is not sufficient to use knowledge of the classical and quantum theory separately. It is necessary to find a new approach based on their unity (German concept of *Aufgehoben* – something at the same time transcendent and preserved), which is by itself a difficult task.

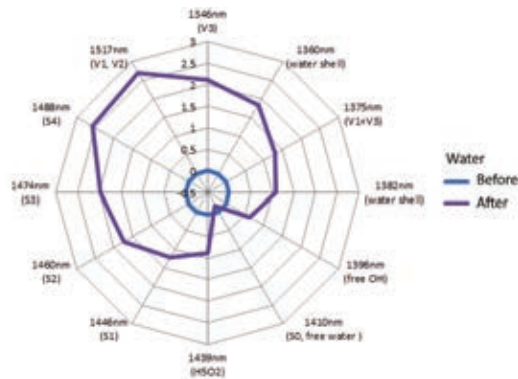


**Figure 5.35.** A spectroscopic diagram of water (18.2 MΩ) before and after its clusterization under the influence of the oscillatory magnetic field  $\Phi$  (infrared spectroscopy in the 900–1700 nm domain).

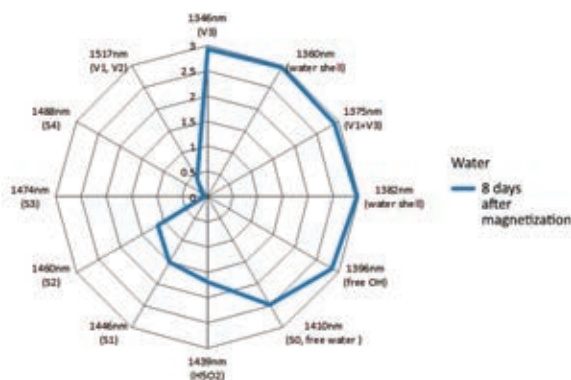


**Figure 5.36.** Spectroscopic diagram of water 8 days after its magnetization (18.2 MΩ) before and after its clusterization under the influence of the oscillatory magnetic field  $\Phi$  (infrared spectroscopy in the 900–1700 nm domain).

The experimental research demonstrates that ordinary water („tap water“) has on the average, due to the presence of ions and the dynamics of creation and deconstruction of water clusters, a magnetic activity at the level of approximately 0.15 nT (that is 250 pT). Due to an unbalanced ratio of diamagnetic to paramagnetic elements in the water, the magnetic oscillatory process is considerably non-uniform, and frequent „magnetic discharges“ are present. World manufacturers of energetic water filters (USA, Japan, S. Korea, etc.) have succeeded to an extent in balancing the ionic composition of the filtered water, in decreasing the frequency of the „magnetic discharges“ and, improving partially its magnetic properties, upgrading thus the level of magnetized water to about 0.28 nT. However, this is insufficient, because the lower magnetism threshold of the drinking water should be about 0.46 nT, and the upper limit is 4.67 nT (according to magnetic properties of human tissue and their interaction with Earth’s magnetic field). An investigation of 18 bottled waters, commercially available in Serbia, demonstrated that none satisfies this biophysical requirement. However, by treating them with adequate devices and varying parameters (different parameters for each water brand) the magnetic energy value can be upgraded to a certain level, without changing water’s chemical composition. Some waters are more easily clustered than others implicating different technical solutions.

How water influences the functionality of proteins is displayed in Figure 5.37. Protein configuration in its basic state is displayed in Figure 5.37 (left). When the water molecule deconstructs the noncovalent hydrogen bond of the ground protein state, as displayed in Figure 5.37 (right), the protein is in an excited state (modified configuration) and its basic function is impaired. This example indicates the importance of water, beside free energy and pH value, in the most elementary biological interactions.

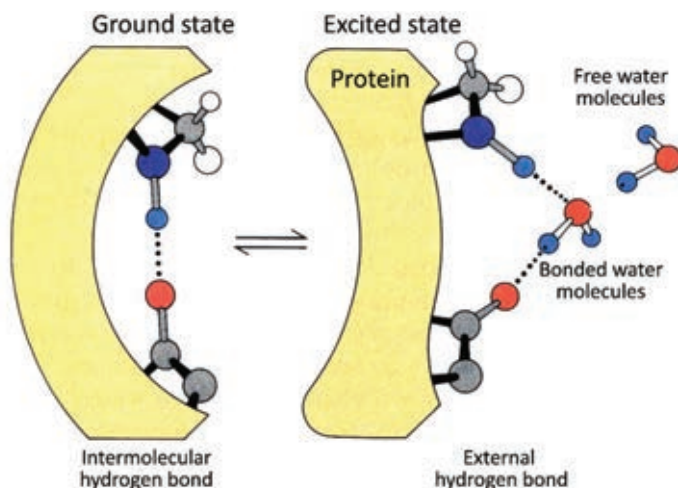


**Figure 5.37.** Modification of protein’s conformation state under the influence of water molecules (change of the hydrogen bond character: from one internal noncovalent hydrogen bond, under the influence of a water molecule two external hydrogen bonds are established) (Nossal, 1991).



The above examples of clathrin, collagen, microtubules, cilia, centrioles, and water demonstrate that these structures are organized according to the icosahedral/dodecahedral symmetry. For corresponding energy states of organized structures, such as  $T_{1w}$ ,  $T_{2w}$ ,  $T_{1g}$  and  $T_{2g}$ , rules are given according to  $\phi$  and  $\Phi$ . In literature, they are known as the Fibonacci numbers and the law of the golden section, so we are going to present the importance of Fibonacci for contemporary science. To express right away his significance, let us say that until the year 1204, Roman numerals were used (in the Western world), and Fibonacci introduced the Indian-Arabic number system, which is today the foundation of science.



Leonardo  
de Pisa Fibonacci  
(1170–1250)

### 5.7. Fibonacci Numbers

By observing a biological process – growth of rabbit population, Fibonacci arrived at the discovery of a special class of numbers, belonging to the set of natural numbers  $\Phi$  (1.61803...) and  $\phi$  (0.61803...). Why do we say natural numbers? Because they are a beautiful and sublime complex structure. These numbers belong to the *mathematica naturalis* – they are at the foundation of nature (Greek φυσικ), i.e., of physical reality, as opposed to *mathematica instrumentalis*, as the instrument of the mind

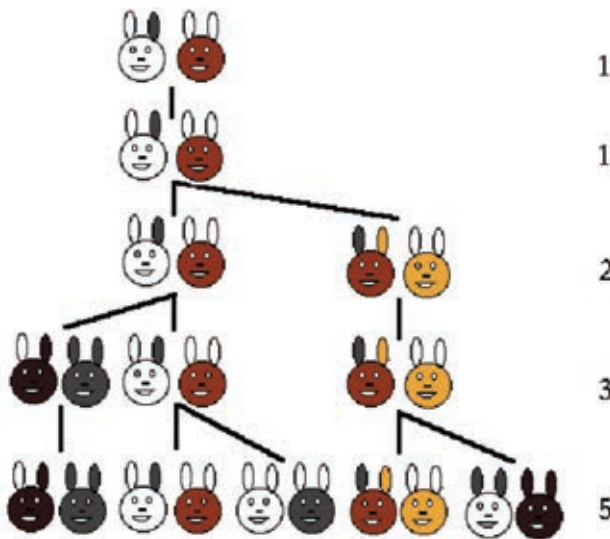


Figure 5.38. Schematic representation of rabbit reproduction and the generation of Fibonacci numbers based on number pairs.

which is self-sufficient. Fibonacci published this discovery in 1202 in his book *Liber Abaci*. Here is what his contemporaries said of him: „... Leonardo from Pisa, known as Fibonacci, played an important role in the revival of the ancient mathematics and made a significant contribution by his approach. His *Liber Abaci* introduced the Hindu-Arabic positional decimal number system and the usage of Arabic numerals into Europe, which incited a renaissance in science“. It is important to note that Roman numerals, used previously in Europe, had a very limited scientific application.

Numbers  $\Phi$  and  $\phi$  can be determined in several ways, and we shall demonstrate three methods. The first is by observing the reproduction of rabbits, as did Fibonacci (*mathematica naturalis*). Let us take the first pair of rabbits (the first „1“) that reproduced, during this time there is only one pair (the second „1“). A new pair follows from this pair, so that now there are two pairs („2“). The original pair continues to reproduce (while the new pair is coming of the age for reproduction) and produced another pair, so that now three pairs exist („3“). This process continues and the original pair produces yet another new pair, but now the first new pair has come of the age for reproduction, so that now we have five pairs („5“), etc. (Vajda, 1989).

Another approach is via a series of numbers created in our mind (*mathematica instrumentalis*): 0, 0!, 1, 2, 3, 5, 8, 13, 21, 34, 55, 89, 144... These numbers are put into proportion: the smaller number ( $n$ ) to the next larger number ( $n+1$ ), then inversely, the larger number ( $N$ ) to the preceding smaller number ( $N-1$ ). It should be noted that we introduced 0! as a logical transition between 0 and 1, i.e., there is no repetition of 1, as is usually denoted (0, 1, 1, 2, 3...).

$\frac{0!}{0} = \infty$	$\frac{0}{0!} = 0$
$\frac{1}{0!} = 1$	$\frac{0!}{1} = 1$
$\frac{2}{1} = 2$	$\frac{1}{2} = 0.5$
$\frac{3}{2} = 1.5$	$\frac{2}{3} = 0.666$
$\frac{5}{3} = 1.666$	$\frac{3}{5} = 0.6$
$\frac{8}{5} = 1.6$	$\frac{5}{8} = 0.625$
$\frac{13}{8} = 1.625$	$\frac{8}{13} = 0.615$
$\frac{21}{13} = 1.615$	$\frac{13}{21} = 0.619$
$\frac{34}{21} = 1.619$	$\frac{21}{34} = 0.617$
.....	.....
$\frac{\sqrt{5}+1}{2} = 1.61803$	$\frac{\sqrt{5}-1}{2} = 0.61803$

The third approach is by using quadratic equations. The first quadratic equation

$$x^2 + x - 1 = 0,$$

gives  $x_1 = -1.61803$  and  $x_2 = 0.61803\dots$ , while the quadratic equation

$$x^2 - x - 1 = 0$$

yields the solutions  $x_1 = 1.61803$  and  $x_2 = -0.61803\dots$ , which makes four solutions:  $-\Phi$ ,  $\Phi$ ,  $\phi$ ,  $-\phi$  that can be graphically represented as an ordered quadruple:

- $\Phi$	$\phi$
- $\phi$	$\Phi$

However, Binet generalized Fibonacci's series in the form

$$F_n = \frac{(1 + \sqrt{5})^n - (1 - \sqrt{5})^n}{2^n \sqrt{5}}$$

as represented in Figure 5.39.

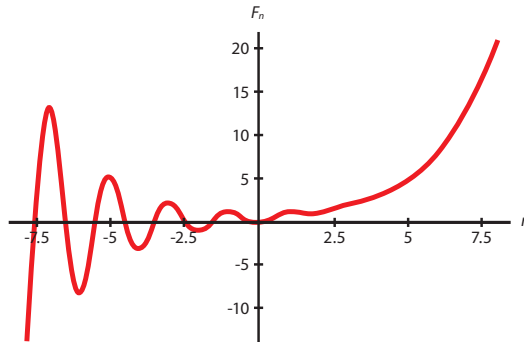


Figure 5.39. Binet's generalized solution of the Fibonacci series.

Beside observing the phenomenon of rabbit reproduction and creating a completely new number system, Fibonacci made a significant contribution to mathematics by introducing the Indian-Arabic number system into mathematics of the Western civilization.

There are many examples of Fibonacci numbers application and realization (leaf distribution on tree branches, the principle of minimum resistance, pyramids of Egypt, temples of ancient Greece, proportions of the human body, the periodic system of elements, genetic code, etc.), but Pascal's triangle and chess are the two most elegant examples of the application of Fibonacci numbers in mathematics and science in general.

Pascal's triangle is displayed in Figure 5.40, and as we can see, it is bounded from the left and from the right by ones- „1“. When we calculate sums (along lines), we observe that a series of numbers is generated (*right*) 1, 1, 2, 3, 5, 8, 13..., which are actually Fibonacci numbers.

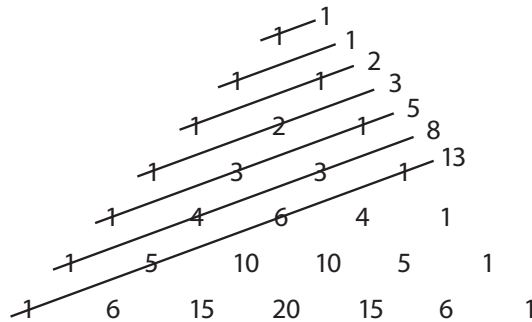


Figure 5.40. Pascal's triangle and Fibonacci numbers.

In order to show that Fibonacci numbers are at the basis of chess, let us demonstrate this on a chessboard. It is general knowledge that the *potential* of each piece depends on its mobility on the chessboard, thus the *queen* is the strongest chess piece, because it can perform more moves from each field than any other piece.

In order to determine a *numerical expression* for the *potential* of each chess piece, we can take the following approach (Figure 5.41):

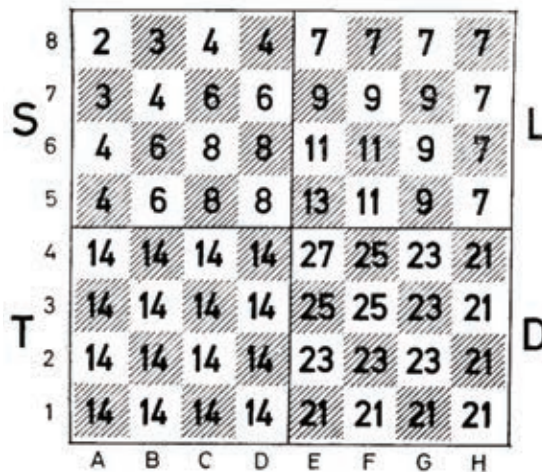


Figure 5.41. Chessboard and „piece potentials“.

Letters **K**, **B**, **R**, **Q** denote respectively: Knight, Bishop, Rook, and Queen.

For each of these pieces only a quarter of a field was used because positions are the same in all four fields, so the same numbers in the remaining  $\frac{3}{4}$  of the field are symmetrically distributed.

If we term the sum of all numbers on the entire board the *potential* of the piece corresponding to this sum, and denote it with the corresponding letter, we obtain:

$$\begin{aligned} K &= 336, B = 560 \\ R &= 896, Q = 1456. \end{aligned}$$

It is easily observed that  $Q = R + B$ , which is not unusual, because the *queen* also moves like the *rook* and the *bishop*.

However, the relation  $R = B + K$  is more surprising leading to proportions:

$$Q : R = R : B \quad \text{and} \quad R : B = B : K$$

Since it holds:

$$Q - R = B \quad \text{and} \quad R = B + K$$

we arrive at the conclusion that the values  $Q, R, B$  and  $R, B, K$  are related via the Fibonacci numbers, because:

$$\begin{aligned} Q : R &= 1456:896 = 1.625 = 13/8 \\ R : B &= 896:560 = 1.600 = 8/5 \\ B : K &= 560:336 = 1.666 = 5/3. \end{aligned}$$

All three ratios coincide, exactly to the decimal, with ratios between two Fibonacci numbers. What about the *king* and the *pawn*? The *king* has the potential 8, and the *pawn* potential 5 (1 field forward, 1 field to the left, 1 field to the right, 2 fields ahead when bypassing opponent's pawn). Therefore, the ratio *king: pawn* = 8/5. Having all this in mind, and when we introduce a correction factor for the ratio *Queen = Rook-Bishop* (the *queen* is one piece and it takes up one field, and the *rook* and *bishop* are two pieces and take up two separate fields— situation is not the same) we arrive at the conclusion that the *potential* of chess is given as the complete solution to the law of Fibonacci numbers.

Note that all the numbers of the decimal number system can be generated by  $\Phi$  and  $\phi$  in the following way:

$$\begin{aligned} \Phi - \phi &= 1 \\ \Phi + \phi^2 &= 2 \\ \Phi^2 + \phi^2 &= 3 \\ \Phi^3 - \phi^3 &= 4 \\ (\Phi + \phi)^2 &= 5 \\ 2(\Phi^2 + \phi^2) &= 6 \\ \Phi^4 + \phi^4 &= 7 \\ 2(\Phi^3 - \phi^3) &= 8 \\ 3(\Phi^2 + \phi^2) &= 9 \\ 2((\Phi + \phi)^2) &= 10 \\ \Phi^5 - \phi^5 &= 11 \\ \dots\dots\dots \\ \Phi^6 + \phi^6 &= 16 \\ \dots\dots\dots \\ (\Phi^3 + \phi^3)^2 &= 20 \\ \dots\dots\dots \end{aligned}$$

Beside positive integers, it is possible, by using Fibonacci numbers  $\phi$  and  $\Phi$ , to generate *zero* and *negative* numbers. Having this in mind, the question is whether water

organization, with its infinite possible combinations, can generate an initial information potential for the realization of a primitive „computing machine“. Does this mean that each human cell is a „small computer“ system based on a network of covalent and non-covalent hydrogen bonds (Figure 5. 42)? From the aspect of complexity, the „hydrogen bond networks“ of the cell, and of the organism as a whole is more universal (but also more primitive, because it is possessed also by unicellular organisms without neurons, but with a molecular network of cytoskeletons and hydrogen bonds) than the neuronal network. This opens many questions, above all incites a reexamination of our „dogmas“ regarding biological information processes and the life phenomenon based on the interaction between light and water.

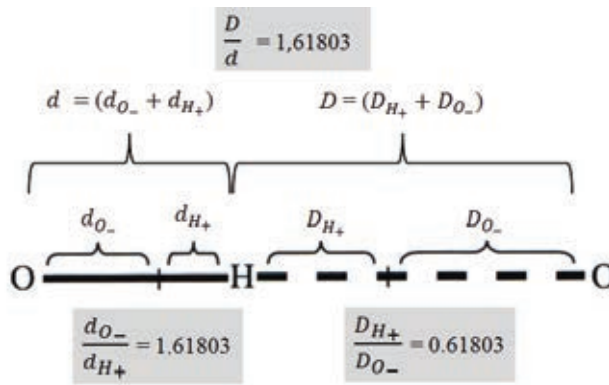


**Figure 5.42.** Fibonacci „molecular machinery“ of covalent and noncovalent hydrogen bonds capable not only to generate processes and information transfer, but also to reestablish impaired processes, effecting adequate external action, into normal, natural, harmonized processes. The hydrogen bonds are, actually, one of the best examples of the Yin-Yang concept, the concept of an ordered quadruple: big Yin ( $d_{O-}$ ), small yin ( $d_{H+}$ ), big Yang ( $D_{O-}$ ), small yang ( $D_{H+}$ ).

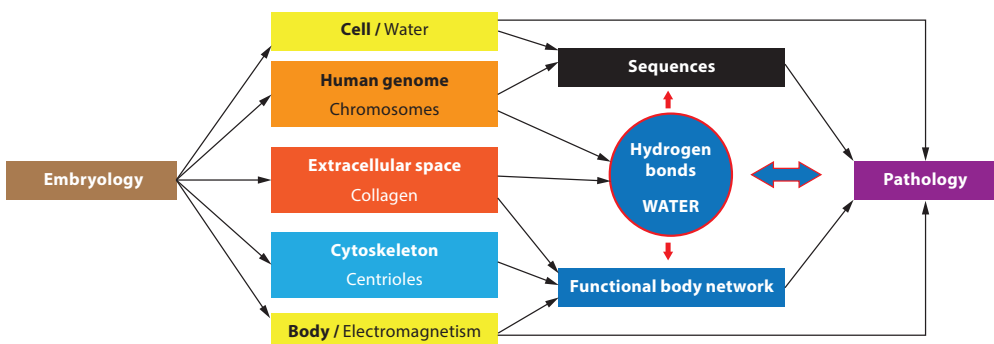


**Figure 5.43.** Main systemic elements where Fibonacci structures and processes dominate. They will be the backbone of a novel approach in the prevention, screening, monitoring, diagnostics and therapy based on the interaction between light (electromagnetism) and tissue (biomolecules, cells and organs).

Future medicine, turning toward personal medicine, will increasingly implement knowledge of human organism functioning based on Fibonacci structures (DNA, water, hydrogen bonds in biomolecules, etc.), and knowledge from embryogenesis. Significant elements of such an approach are displayed in Figure 5.43.

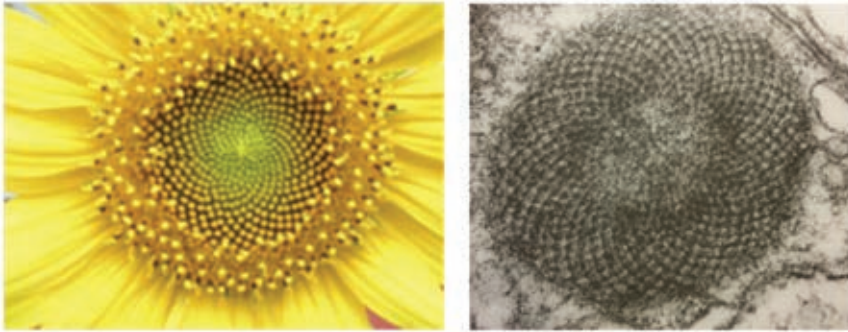
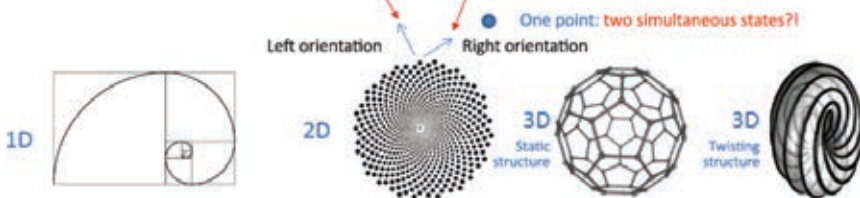


**Figure 5.44.** The sunflower seed (left), one of the most obvious examples of the realization of Fibonacci numbers in nature (realized in 2D), and the toroidal organelle (realized in 3D) within eye cells for night vision (rods) enabling hyperpolarization of the cell (right). These two examples demonstrate the realization of Fibonacci numbers as the *mathematica naturalis* in nature and in biological systems.

**Table 5.3.** Icosahedral symmetry group that determines the energy states ( $T_{1g}$ ,  $T_{2g}$ ,  $T_{1u}$  and  $T_{2u}$ ) of structures and processes according to Fibonacci numbers.

$Ih$	$E$	$12C_5$	$12C_5^2$	$20C_3$	$15C_2$	$i$	$12S_{10}$	$12S_{10}^5$	$20S_6$	$15\sigma$
$A_g$	1	1	1	1	1	1	1	1	1	1
$T_{1g}$	3	$\frac{1}{2}(1 + \sqrt{5})$	$\frac{1}{2}(1 - \sqrt{5})$	0	-1	3	$\frac{1}{2}(1 - \sqrt{5})$	$\frac{1}{2}(1 + \sqrt{5})$	0	-1
$T_{2g}$	3	$\frac{1}{2}(1 - \sqrt{5})$	$\frac{1}{2}(1 + \sqrt{5})$	0	-1	3	$\frac{1}{2}(1 + \sqrt{5})$	$\frac{1}{2}(1 - \sqrt{5})$	0	-1
$G_g$	4	-1	-1	1	0	4	-1	-1	1	0
$H_g$	5	0	0	-1	1	5	0	0	-1	1
$A_u$	1	1	1	1	1	-1	-1	-1	-1	-1
$T_{1u}$	3	$\frac{1}{2}(1 + \sqrt{5})$	$\frac{1}{2}(1 - \sqrt{5})$	0	-1	-3	$-\frac{1}{2}(1 - \sqrt{5})$	$-\frac{1}{2}(1 + \sqrt{5})$	0	1
$T_{2u}$	3	$\frac{1}{2}(1 - \sqrt{5})$	$\frac{1}{2}(1 + \sqrt{5})$	0	-1	-3	$-\frac{1}{2}(1 + \sqrt{5})$	$-\frac{1}{2}(1 - \sqrt{5})$	0	1
$G_u$	4	-1	-1	1	0	-4	1	1	-1	0
$H_u$	5	0	0	-1	1	-5	0	0	1	-1



We have seen in this Chapter that many biological structures (clathrin, collagen, microtubules, cilia, centrioles, water, etc.), almost 75% of the human organism, are actually Fibonacci structures, because they are organized according to the laws of the icosahedral (dodecahedral symmetry). Their electronic, vibrational and rotational energies ( $T_{1g}$ ,  $T_{2g}$ ,  $T_{1u}$  and  $T_2$ ) are determined by Fibonacci laws. Also, one of the most important processes in biochemical reactions, the Gibbs free energy is determined, via the universal gas constant and temperature, by the Fibonacci number  $\Phi$ .

This chapter demonstrated that important structures and processes are established according to the laws of icosahedral symmetry described by Fibonacci numbers and their structural elements. As the biological physicochemical processes are not perfect (they do not occur according to  $\phi$  and  $\Phi$ , but according to a member of a series that generates them: 3/5, 5/8, 8/13... or vice versa), it is necessary to find an adequate electromagnetic action (light) enabling prevention (maintaining adequate existing relationships in the organism) and treatment of morbid changes.



**Figure 5.45:** *Natural phenomena of Fibonacci spiral in stormy sunsets in Oludeniz, Turkey, 2018.*



## References

1. Chaplin, M.F., Water structure science. <http://www.lsbu.ac.uk/water/>
2. Gilli, G., Gilli, P. *The Nature of the Hydrogen Bond: Outline of a Comprehensive Hydrogen Bond Theory*. Oxford University Press, Oxford, 2009.
3. Gulrajani, R.M., *Bioelectricity and Biomagnetism*. John Wiley and Sons, New York 1998.
4. Dustin, P., *Microtubules*. Springer-Verlag, Berlin, 1984.
5. Eisenberg, D., Kauzmann, W., *The structure and properties of water*. Oxford University Press, Oxford, 1969.
6. Ericson, R.O., Tubular packing of spheres in biological fine structures. *Science*, 181: 705-781, 1973.
7. Fuchs, C.E., et al., Investigation of the mid-infrared emission of a floating water bridge. *J. Phys D: Appl phys* 45: 475401 (10pp) 2012.
8. Havelka, D., Cifra, M., Calculation of the Electromagnetic Field Around a Microtubule. *Acta Polytechnica*, 49 (2-3): pp.58-63, 2009.
9. Heyrovská, R., Dependence of the length of the hydrogen bond on the covalent and cationic radii of hydrogen, and additivity of bonding distances. *Chemical Physics Letters*, 432: pp. 348-351, 2006.
10. Jeffrey, A.G., *An Introduction to Hydrogen Bonding*. Oxford University Press, New York, 1997.
11. Kamaseki, T., Kadota T., The vesicle in a basket. *J. Cell Biol*, 42:202-220, 1969.
12. Koltz, M.I., *Introduction to Biomolecular Energetics*. Academic Press, Orlando, 1986.
13. Koruga, Dj., Hameroff, S., Withers, J., Loutfy, R., Sundereshan, M., *Fullerene C<sub>60</sub>: History, Physics, Nanobiology, Nanotechnology*. North-Holland, Amsterdam, 1993.
14. Koruga, Dj., Golden mean harmonized water and aqueous solution, PCT/US2008/052946 Patent, International publication number WO 2008/097922 A2, 2008.
15. Matija, L. Nanotechnology: artificial versus natural self-assembly (Reviewing paper). *FME Transactions*, 32, 1-14. 2004.
16. Mathews, C. K., van Holde, K.E., *Biochemistry*. The Benjamin/Cummings Pub. Co., Redwood City, 1990.
17. Nossal, R., Lecar, H., *Molecular and Cell Biophysics*. Addison-Wesley, Redwood City, 1991.
18. Pollard, T.D. Earnshaw, W.C., *Cell biology*. Saunders, Philadelphia, 2002.
19. Sang, R-L., Xu, L., Reversible formation of regular pentagonal dodecahedral (H<sub>2</sub>O)<sub>20</sub> in 2D metal-organic framework. *Cryst Eng Comm* 12, pp. 1377-1381, 2010.
20. Schectman, I.A, Blech, D., Cahn, J.W., Metallic phase with long-range orientational order and no translational symmetry. *Phys Rev Lett*, 53 (20)1951-1953, 1984.

21. Shigemitsu, T., Electromagnetic Fields, Biophysical Processes, and Proposed Biophysical Mechanism. pp.193-220, in Book Kato, M., (Ed.), *Electromagnetics in Biology*. Springer, Tokyo, 2006.
22. Tsenkova, R., Introduction Aquaphotonics: dynamic spectroscopy of aqueous and biological systems describes peculiarities of water. *J. Near Infrared Spectroscopy*, 17, pp. 303-313, 2009.
23. Tuszynski, A.J., *Molecular and Cellular Biophysics*. Chapman and Hall/CRC, Boca Raton, 2008.
24. Vajda, S., *Fibonacci and Lucas numbers, and the Golden section: Theory and application*. Ellis Horwood Ltd, New York, 1989.
25. Westerhoff, H.V., van Dam, *Thermodynamics and control of biological free energy transduction*. Elsevier, Amsterdam, 1987.

# 6

## HYPERPOLARIZED LIGHT



*One oriented toward itself is condemned to die,  
A world that cannot reproduce and cre-  
ate a new one is a dead world.*  
DR. ARTHUR JANOV  
(Primal Scream)

## **6.1. Sun's Radiation**

Tissue exposure to diffuse (DL) or monochromatic (laser, LS) light can have positive and negative effects, depending on the energy (wavelength, that is frequency:  $E = h\nu$  and  $c = \nu\lambda$ ) and exposure time. The basic action principle is absorption of energy necessary for the functioning of a given structure. When wavelength is adequately defined (specific energy density and stimulation duration), good partial and local effects can be expected. However, if adequate light source and adequate therapy duration are not selected, adverse side effects are possible.

The most obvious example is daylight 1050 W/m<sup>2</sup> (105 mW/cm<sup>2</sup>), with the Sun at zenith. The sunlight is diffuse and polychromatic across the range of 290 to 3200 nm, the UV radiation participates 5% within 100 to 400 nm (UVC radiation, 100–280 nm, is stopped by the ozone layer and only 0.1% reaches the Earth's surface; the UVB radiation, 280–320 nm, constitutes 2% of the overall UV radiation, and the rest 97.9% is the UVA radiation, 320–400 nm). The visible spectrum is 39%, from 400 to 780 nm, it is mostly infrared radiation– 56% in the range 780–3200 nm. Short exposure to the UVA radiation is beneficial for melanogenesis and vitamin D<sub>3</sub> synthesis (improving calcium use in the organism, especially significant for children and persons suffering from osteoporosis), however, prolonged exposure is harmful and causes premature aging (impaired skin, appearance of freckles on the face and hands), photoallergic reactions, immuno-suppression, skin cancer and melanomas.

After a few minutes of sunbathing (depending on the time of the day and skin type) skin redness can appear, an inflammatory process can occur when skin absorbs an excessive dose of radiation energy. The energy quantity that causes uniform, clearly pronounced redness during 24 hours is called the MED – *Minimum Erythematol Dose*. MED value for persons with light complexion is within the range of 20–70 mJ/cm<sup>2</sup>.

Regarding correction of impairments at the molecular level (of one molecule type), the monochromatic coherent light (laser) has advantage over diffuse light, when frequency and treatment duration are adequately selected. However, in case of multimolecular tissue dysfunction, with adequate choice of wavelength, power, and treatment duration, diffuse light is more adequate. Compared to hunting, the relationship between

the carbine and shotgun (double-barrel, buckshot); carbine can kill with one bullet one game, while the shotgun – buckshot can hit one or several game if they are close together (probability of game kill is higher if 100 bullets are used, than with one shot).

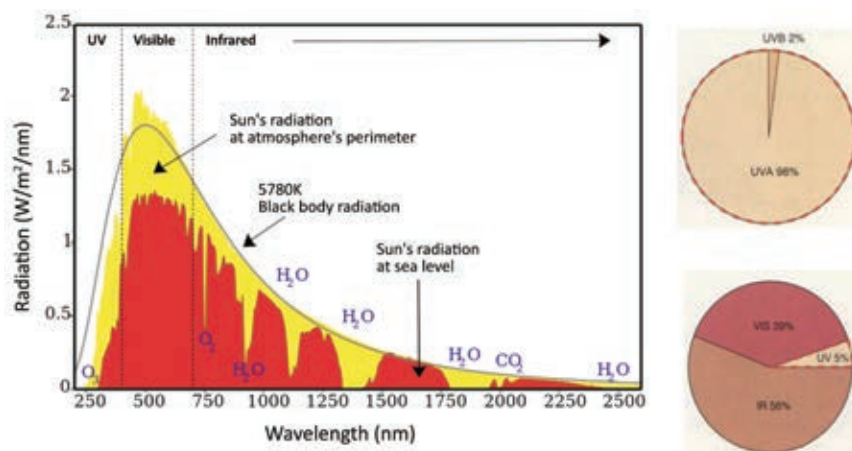


**Figure 6.1** Normalized spectrum of Sun's radiation per nanometer ( $W/m^2/nm$ ) reaching Earth's atmosphere (yellow) and Earth's surface (red). Wavelengths up to 280 nm are absorbed by ozone ( $O_3$ ). Molecular oxygen ( $O_2$ ) absorbs at about 750 nm, water at 1700 nm, 1300 nm, 1850 nm, and 2500 nm. Total radiation reaching Earth's surface is: UV – 5%, (98% is UVA and 2% UVB), VIS – 39% and IR – 56%.

Everything said of diffuse and laser light holds for linearly polarized light (LPL), while the LPL has an advantage- it acts on biomolecules not only by absorption, but also structurally-organizationally on the tissue, since LPL energies are distributed in planes. Broken and distorted biological structures, which are linearly organized when functioning normally (liquid crystals, collagen, microtubules, lipids in membranes, mitochondrial internal organization, and linear organization of water dipole moments), that should be „linearized“, will be reestablished in a normal functional state (like a comb makes a nice hairstyle of tangled hair) under the influence of LPL, with appropriate selection of the light spectrum and light energy in time.

Diffuse and laser light regulate electronic absorption energies, i.e., energies of valence electrons, at the 1.0–3.5 eV level ( $1eV = 1.602 \times 10^{-19} J$ ). However, vibrational, rotational and translational energies escape these actions, because they are 100, 1000, and even 10000 times smaller than electronic energies, respectively.

An obvious example of the significance of vibrational and rotational energies is heating food using water, not on a classic stove, but in a microwave oven. Water absorption degree of blue light is the smallest, it increases with wavelength up to 3  $\mu m$ , and then decreases again. Why is this wavelength important for water? The answer is simple: because this is the rotational water mode about the axis of symmetry of  $C_{2v}$ . Therefore, applying energy with frequency of approximately  $9.5 \times 10^{13} Hz$  ( $\sim 0.4 eV$ ) stimulates the rotation of the water molecules, their rotation causes friction and mutual collision of molecules, creating

heat that warms food. A similar process occurs in chemotherapy, when material is locally introduced into morbid tissue sensitive to certain frequencies, heat is generated during stimulation, and morbid cells (along with some healthy cells) are „destroyed“.

Light, whether diffuse, polarized or laser, is used to treat biological structures and tissues according to their absorption characteristics. The linearly polarized light has an advantage with respect to other two light types, because it structurally organizes („comb“ principle) the linear order of water molecules via the water dipoles, collagen fibers and microtubules, linear process of ATP production in mitochondria, etc. However, particular biomolecules (water, clathrin, microtubules, collagen, etc.), structures (centrioles, cilia, etc.) and processes based on free Gibbs energy possess a specific organization, which is structurally influenced by the icosahedral and dodecahedral symmetry, and functionally by the Fibonacci laws.

Chapter V demonstrated, on the example of water, that the Fibonacci law is the thread that links „inanimate matter“ and „animate matter“. Water in a glass can be considered „inanimate“ matter, while this same water, when we drink it, becomes „animate matter“ in our organism. In this Chapter, we demonstrate that the Fibonacci laws can determine „technical matter“ through light, thus establishing a *nature–man–technology* relationship (based on the Fibonacci laws, that is, on icosahedral/dodecahedral symmetry). This brings us closer to Tesla’s idea that „there is no inanimate matter, because in the entire infinite Universe everything moves, vibrates, everything is alive“, not randomly and chaotically, but organized, as Tesla says: „... he who understands the magnificence of number three, will understand the mechanism of the Universe“ (Tesla, 1977).

## 6.2. Light in Medicine

The aim of nanophotonics is to aid prevention and preservation of the functional status of tissues, organs and the human organism. A dysfunction should be eliminated, that is, impaired function of biomolecule, tissue, organ or the organism restored.

Three basic light types: diffuse, polarized (linearly or circularly) and laser light are used today in medicine.

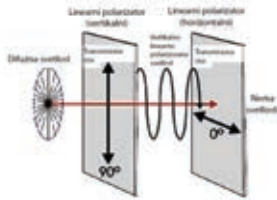
### *Three Basic Light Types in Medicine*

#### *Diffuse Light*



- Polychromatic (photons of various wavelengths)
- Multi directional (random scattering)
- Incoherent (not in phase, neither spatially nor temporal)
- EM components are mutually orthogonal, but their orientation is random.

## Linearly Polarized Light



- Polychromatic (photons of various wavelengths)
- Photons of the same wavelength are organized in a plane
- Incoherent (not in phase, neither spatially nor temporally)
- Vertical or horizontal polarization is possible

## Laser Light



- Monochromatic (photons of the same wavelength)
- Directed (high energy per  $mm^2$ )
- Coherent (in phase spatially and temporally)
- Vertical or horizontal polarization is possible

## Diffuse Light in Medicine



*Lupus vulgaris*

The Nobel Prize for physiology and medicine in 1903 was awarded to Niels Ryberg Finsen „in recognition of his contribution to curing disease, especially *lupus vulgaris*, with directed diffuse light in the UVA domain, by which he opened a new road in medicine”.

The first successful medical application of artificial sunlight was by the Danish physician Finsen who, in 1893, used the red region of the visible spectrum to treat smallpox. In 1895, he used ultraviolet radiation to treat *lupus vulgaris* successfully (Figure), a form of skin tuberculosis. The UV radiation was generated by using powerful carbon-arc discharges. Thus obtained ultraviolet radiation mostly contained UVA. The heat caused by infrared radiation was used for local treatment of sensitive face regions. Finsen's ultraviolet device became known as the Finsen lamp.



*Niels Ryberg Finsen*  
(1860–1904)

## Linearly Polarized Light in Medicine

We shall describe how linearly polarized light is created from diffuse light, and how devices based on linearly polarized light function.

When diffuse light reaches a surface under a certain angle, depending on the type of material (tissue), this surface performs light polarization (usually of the vertical, i.e., of the electric component). This angle is called the Brewster's angle. Since light is polychromatic, various wavelengths effect tissues and tissue processes. Due to the dominant presence of





Example of linearly polarized light effect on the neck region and the upper part of the spinal column (BIOPTRON).

the electric component in the reflected linearly polarized light (vertical polarization), the effect is primarily on the tissue's (specimen's) electronic states. Another method for linearly polarized light generation is via the specular reflection (the angle between the incident light and the reflected light is  $90^\circ$ ) using a mirror system.

MAIN HEALING EFFECTS

- Effect on ATP, intracellular energy boost
- Microcirculation and cell activity improvement
- Stimulates generation of fibroblasts (collagen and elastin)
- Edema and inflammation reduction
- Dermatological and skin problems
- Sports injuries
- SAD (Seasonal Affective Disorder)
- Ordering of (water, biomolecules) dipole moments

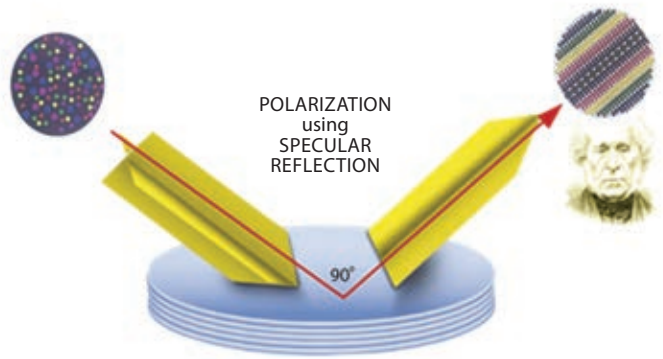


Figure 6.2 Transformation of diffuse white light into the linearly polarized light under the Brewster's angle (Bolleter, H., Int. Pat. App. PCTEP95/03221, 1995, Applicant BIOPTRON, Switzerland).

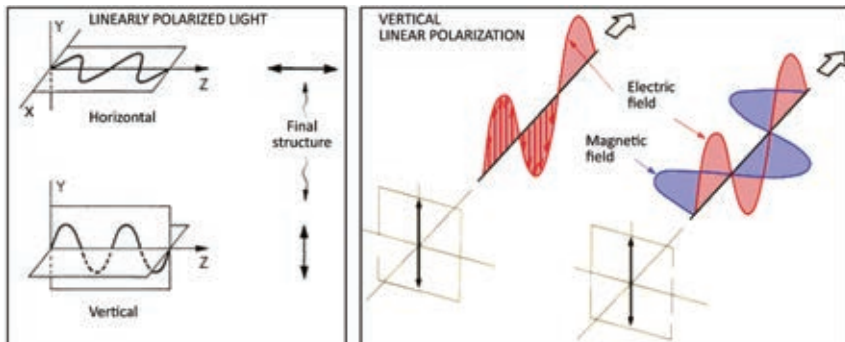


Figure 6.3 Vertical component of the photon wave is the electric field, and the horizontal component in this case is the magnetic photon field. Inverse system configuration is possible, while the electric and the magnetic field always remain orthogonal.

## Lasers in Medicine

Depending on the wavelength, laser light can be:

- Infra-red (IR),
- Ultra-violet (UV)
- X-ray laser light



**Table 6.1** Laser light applied in medicine.

Application	Wavelength (nm)							Power (W)
Photodynamic therapy (PDT)	630	635	652	660-690	753			1–15
Laser therapy low power	465	630	635	652	660-690			0,5–10
Stomatology	465						810-980	0,5–10
Surgery							800-1500	0,5–10
Cancer hyperthermia						940	980 1064	15–50

**Table 6.2** Advantages and shortcomings of light applied in therapeutic medicine.

Type of light	Advantages	Disadvantages	
		Primary	Secondary
<b>diffuse</b> (Sunlight or lamp)	<ul style="list-style-type: none"> <li>• Light of wavelength 450–780 nm is not harmful</li> <li>• UVA of wavelength 385–400 nm is beneficial in limited dosage for vitamin D2 synthesis. Beneficial for the treatment of lupus vulgaris, etc.</li> </ul>	<ul style="list-style-type: none"> <li>• Light of wavelength 320–385 nm harmful to skin and eyesight</li> <li>• Light 385–450 nm damages the cornea</li> <li>• Prolonged exposure to light is not recommended</li> </ul>	<ul style="list-style-type: none"> <li>• Uncontrolled prolonged exposure can cause genetic impairments in skin cells and eyes</li> <li>• Causes degradation of vitamin A and C in prolonged exposure to light</li> </ul>
<b>Linearly polarized</b> (Reflected polarized sunlight or lamp with Brewster's angle)	<ul style="list-style-type: none"> <li>• Positive effect on ATP synthesis</li> <li>• Positive effect on fibroblast synthesis</li> <li>• Decreases free radicals</li> <li>• Tissue becomes less paramagnetic, more diamagnetic</li> <li>• Favorable effect on membranes (lipids), the „comb“ effect</li> <li>• Adequate for diagnostics based on polarized light reflected from the tissue</li> </ul>	<ul style="list-style-type: none"> <li>• Exceeding 3 J/cm<sup>2</sup>, min is harmful</li> <li>• Polarized UVA has increased adverse effects compared to diffuse light of the same wavelength</li> <li>• At seaside, it can cause burns even in shade (indirect Sun effect)</li> </ul>	<ul style="list-style-type: none"> <li>• Main effect – local effect on tissue</li> </ul>
<b>Lasers</b>	<ul style="list-style-type: none"> <li>• Adequate for tissue ablation</li> <li>• Adequate for surgery</li> <li>• Adequate for treatment (low power)</li> <li>• Adequate for diagnostics (Raman and other spectroscopy methods)</li> </ul>	<ul style="list-style-type: none"> <li>• Harmful to the eyes</li> <li>• Restricted to professional medical application</li> <li>• Expensive</li> </ul>	<ul style="list-style-type: none"> <li>• Main effect – local effect on tissue</li> </ul>

### 6.3. Problem Identification and its Conceptual Solution

Table 6–2 displays the main advantages and disadvantages of different light types in medical practice today. The main reasons why biomedical engineering experts are seeking a new light type are:

1. Diffuse, linearly polarized and laser light are „wild“ energies, acting strictly energetically, without recognizing what stimulants are actually necessary to particular biomolecules, tissues and organs. They do not cover all energy states of biomolecules and tissues, but primarily the electronic energetic states (1.4–3.4 eV) of valence electrons, without acting on the basic energy, vibrational and rotational states (Figure 6.4). It is not easy to cover all energy states of biomolecules, cells and tissues, however, from the energetic aspect, we shall focus on the domain 0.012–1.6 eV (from fundamental vibrations and vibro-rotational energies to ground electronic states of biomolecular valence electrons). Present devices generate linearly polarized light, such as BIOPTRON (~40 mW/cm<sup>2</sup>). The new apparatus should generate ~28 mW/cm<sup>2</sup>, to have enough energy and spatial information to act upon basic electronic, vibrational and rotational states of biomolecules and tissues (30% energy is lost in photons ordering).

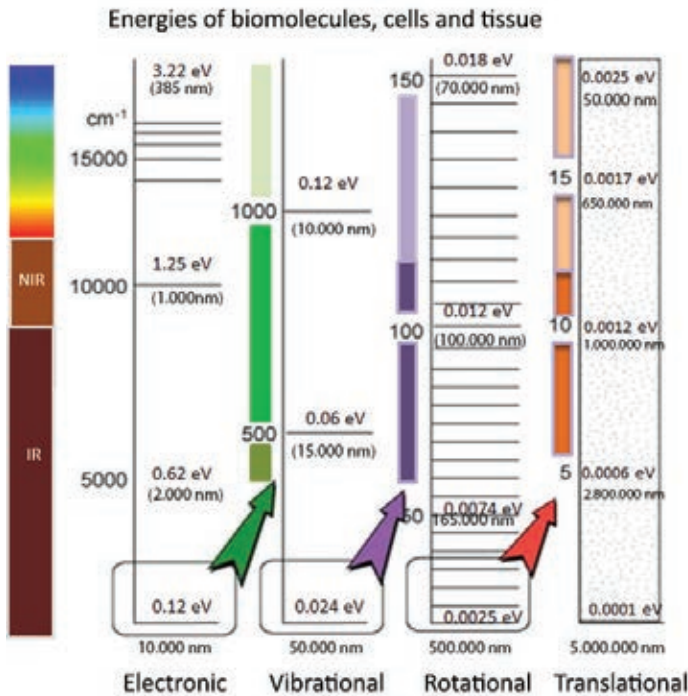


Figure 6.4 Electronic, vibrational, rotational, and translational energy values of biomolecules.

2. All three present light energy types (diffuse, linearly polarized and lasers) act primarily locally, although the linearly polarized light, due to the possibility to act on the organization of dipole moments of water molecules, can act regionally (via organized water).
3. Biomolecules and tissues are based on the union of structure, energy and information, not only on structure and energy.
4. Biological information processes are very important for the functioning, maintaining functionality, and healing biomolecules, tissues and organs.
5. Biomolecule symmetry defines electronic states (ground and excited) and vibrational-rotational energy, thus defining signal (information) propagation from one end of cell to another (principle of resonant biomolecular recognition at a distance through water).
6. Light (photons) for conservation and treatment of biological structures must be compatible with biostructures, that is, photons (spatial-temporal) organization must correspond to the symmetry of the biological structure, defining its electronic, vibrational, and rotational energy states.
7. Based on the above, the task is to generate light compatible with biomolecules, according to the principle:

**SYMMETRY of biomolecules = SYMMETRY of photon organization**

Analogous conclusion is made in the paper by Natalie Litchinitser „Structured Light Meets Structured Matter“ (*Science*, 337 pp 1054-1055, 2012) „It can be expected that by synergy of complex materials and complex light a new breakthrough in the science on light and its application will be made“. The paper, however, did not recognize that for biological systems icosahedral and dodecahedral symmetry is the basis for this recognition.

8. By establishing synergy of light and matter based on the icosahedral and dodecahedral symmetry, a resonant recognition is established between organization patterns, including, beside their energy states, the entropy states as well, and consequently the information states.
9. In Chapter V, we observed that the icosahedral symmetry is found in clathrin, collagen, microtubules, cilia, centrioles, and water (in water clusters dodecahedral symmetry is present as well). The technological solutions will be sought accordingly providing photons' organization according to the icosahedral symmetry, before they interact with tissue.

Therefore, it is necessary to reexamine the process of signal generation and propagation in biological systems, because information has an essential role in the functioning of biological systems from embryogenesis to the conservation of the organism in a healthy state.

It should be emphasized that symmetry plays an important role in science (Icke, 1995), especially in the physics of structure and space-time (Elliott, 1990), i.e., in the quantum dynamics of field theory (Miransky, 1993). In this Chapter, emphasis is on the symmetries determining the electronic, vibrational and rotational energies (Harris and Bertolucci, 1978). For example, crystals are organized according to point symmetry, DNA as aperiodic, clathrin, microtubule, etc. as molecular crystals. Different symmetry types describe various phenomena, starting with elementary particles, up to complex space-time structures.

## 6.4. Light in Medicine

### *Analysis of Action Strength*

First of all, it is necessary to determine the type of symmetry dominant in biological structures and processes responsible for signal (information) generation and transfer. On the other hand, it is necessary to observe the relationship between the electric and the magnetic component in biological structures. The previous Chapter emphasized the importance of *water* for the human organism (70% of the human organism; water is prevalent in all body parts), *collagen* (40% of all protein, one of the most important extracellular structures), *microtubule* („brain of the cell“, dominant cytoplasmic protein structure responsible for the matter transportation within the cell, determines cell shape, together with actin and intramedial protofilaments determines the cell bias voltage state, provides signalization between the cell membrane –nucleus membrane and, through interaction with clathrin and water, generates preprocess activity in the brain, in neurons responsible for memory, learning and probably for the consciousness phenomenon), *cilia* (very important function of epithelial tissue surface), *flagella* (important in male reproductive cells- spermatozoids), and *centrioles* (microtubular structure that, together with DNA, represents the central enigma of molecular biology; responsible for cell division, cytoskeleton organization, and regulative functions in the cytoplasm).

In Chapter V (light) we demonstrated that the ratio of the magnetic to the electric component of valence electrons is  $F_M/F_E \approx 10^{-4}$ , consequently it is necessary to investigate light–matter interaction as action  $A_E = F_E \times d \times t$  for the electric component, and  $A_M = F_M \times d \times t$  for the magnetic component. The electric force in biomolecules equals 0.01–1.0 nN, displacement 0.01–0.5 nm, and action time is  $10^{-8}$ – $10^{-10}$  s. The average electric action ( $A_E$ ) is:

$$A_E = 10^{-10} \times 10^{-10} \times 10^{-10} = 10^{-30} \text{ Js}$$

For the magnetic component, action ( $A_M$ ) is:

$$A_M = 10^{-30} \times 10^{-4} = 10^{-34} \text{ Js}$$

which is very close to the quantum action, consequently it can be stated that the electric component is primarily responsible for the classic action, and the magnetic component for quantum action ( $h = 6.626 \times 10^{-34}$  Js).

As the conformation states of biomolecules are primarily quantum-mechanical phenomena, correction of biomolecular functionality is established primarily using the convector of light energy into magnetic energy, at the nano and pico Tesla level, because the magnetic component of biomolecules is by 4 orders of magnitude closer to quantum phenomena than the electric component.

Therefore, the new light type should act on the basic energetic, vibrational and rotational states of biomolecules, tissues and processes in the organism (above all on the generation of Gibbs free energy) and should satisfy the following conditions:

1. The energy level should be within the interval 0.012–1.6 eV, meaning that a part of light (approximately 62%) coming from the light source should pass through (0.6–1.6 eV), to act on basic electronic states and processes.

2. The other part (about 38%) should be transformed, by the „nanophotonic transformer“, into energies 0.012–0.6 eV (to act on vibrational and rotational states of biomolecules and processes).

3. Photons transmitted through the „nanophotonic generator“, and the newly transformed electromagnetic energy in the light–nanomatter interaction, should be organized according to the icosahedral symmetry („structured light meets structured matter“).

### *Nanophotonic Generator of Hyperpolarized Light*

The nanophotonic generator (NPG) of hyperpolarized light should transform diffuse light or linearly polarized light into a new light form characterized by icosahedral symmetry, harmonized with the organization of biomolecules or bioprocesses (the Fibonacci law  $\phi$  and  $\Phi$ , i.e., values in the table relating symmetry and energy eigenvalues). The first task of the NPG is to generate photon organization as displayed in Table 5.3 (Chapter V), and the second to generate photon energies through the light–matter interaction, based on the overall orbital momentum, that are not within the visible electromagnetic spectrum, but within the far infrared domain.

In diffuse light, the position of the electromagnetic component of each photon is arbitrary in space and variable in time; „crosses“ in Figure 6.5 rotate randomly.

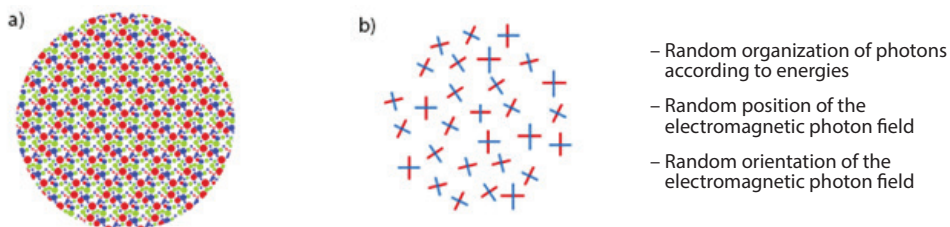


**Figure 6.5** *a) Polychromatic diffuse light as a random set of photons with respect to energies, and b) random position of the electromagnetic photon rotating field (blue– electric photon field, red– magnetic photon field); photons have random orientation along the light propagation direction (rays are not parallel, they can intersect).*

In linearly polarized light, two main phenomena can occur: vertical polarization and horizontal polarization. Polarization is defined with respect to the electric photon field (Figure 6. 6).

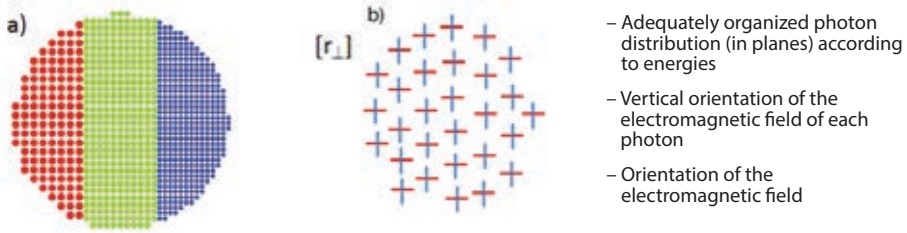


**Figure 6.6** a) Polychromatic vertically polarized light as an ordered set of photons with respect to energies, and b) fixed position of the electromagnetic photon field (blue– electric photon field, red– magnetic photon field), and complete orientation of the electromagnetic photon field along the light propagation direction (rays are parallel). As the electrical field (blue) is vertical, this type of polarization is called the vertical linearly polarized light.

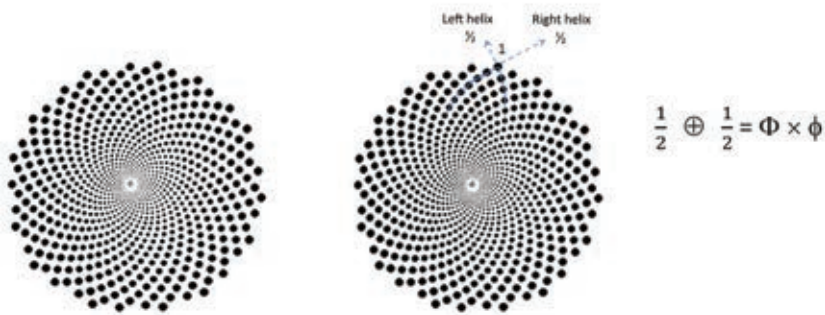


**Figure 6.7** Biological structures (clathrin, collagen, microtubule, cilia, centrioles, water, etc.) with icosahedral symmetry necessitate that photon energetic organization, interacting with them, be ordered as in Figure (left). However, in this case the photon is „quantized“ in a very strange way (it seems it has half of its action), but since photons „overlap“ at every point, their quantization is preserved at each moment because  $(\frac{1}{2})^L + (\frac{1}{2})^D = 1$ . This unity is established through  $\phi \times \Phi = 1$ . The process that had „split“ the photon has at the same time also „joined“ the photon (spatial-temporal unity). How is this possible? The total angular momentum of the photon is composed of the angular orbital momentum of the photon and of the photon spin (in space-time they form a double helix, resembling DNA). Chapter III described the latest electron model where two light packets (Salhofer model, Table 3.1) form a helix in space-time.

A new type of photon organization is necessary that would correspond to the organization of electronic, vibrational and rotational energies of biological structures. Translational biomolecular energies are not considered, because they are at the level of 0.0001 eV –0.0025 eV, i.e., 50 000–5 000 000 nm, implicating not only photons but also quantum gravitation in the technological solution of the nanophotonic generator, which is not possible at this stage of technological development, at least for commercial

usage. However, the existence of gravitational waves experimentally confirmed (measuring accuracy is  $4 \times 10^{-18}$  m, the measuring equipment is about 4 km) clearly points to the „duality“, similarly to the turtle travelling the quantum path (Chapter II, Figure 2.4). The left spiral is shorter (smaller), and the right spiral is longer (bigger), but they always meet at one point. If each point represents a photon, the orientation of the electric and the magnetic field is the same for the „left“ and for the „right“ photon. In other words, photon's *state* is a *superposition* of the vertical and of the horizontal polarization.

The increment of the angular photon momentum during the realization of the pair  $(r_n, \theta_n)$ , defining the evolution of the hyperpolarized light, gives a realistic view of the relationship between the electric and the magnetic photon field remaining mutually orthogonal, but as tangents to the evolution curve (surface), where  $\theta = 360^\circ \times \phi = 360^\circ \times 0.61803 = 222.5^\circ$  ( $r$  is the distance to the evolution center) is the Fibonacci angle defining the *input* position of the electric and magnetic photon field (orbital and spin) and their *output* position as the superposition of the vertical and horizontal polarization:

$$(r_n, \theta_n) = [(1/\sqrt{5}) r_{n-1}, \theta_{n-1} + \Delta\theta]$$

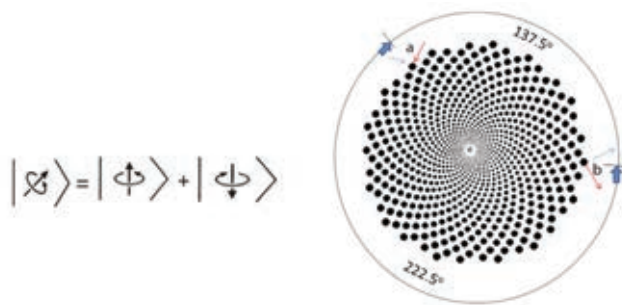


**Figure 6.8** Hyperpolarized photon is a Fibonacci superposition of its vertical ( $|\updown\rangle$ ) and horizontal ( $|\leftrightarrow\rangle$ ) polarization. Defining polarization position of the photon under the angle of  $222.5^\circ$ , which starts from the middle with two „half quantized“ states ( $E_0 = \frac{1}{2} h\nu$ ), where one evolves along the left spiral (L), and the other one along the right (D) spiral. However, at each point, the energy of the photon is  $E = h\nu$ , because  $(\frac{1}{2} h\nu)^L + (\frac{1}{2} h\nu)^D = h\nu$  (due to  $\phi \times \Phi = 1$ ).

In this case (Figure 6.8), the electric and the magnetic photon field position is defined by  $222.5^\circ$  for each point. We call this phenomenon of photon organization *hyperpolarization*. Electric and magnetic photon fields maintain their orthogonality via tangents to the evolution spiral, the photon is vertically and horizontally polarized at the same time, that is, photon is neither vertically nor horizontally polarized (it has novel polarization - hyperpolarization). It is useful to recall the far-reaching ancient Greek thought „Only one thing is wise, to be and not to be called by the name of Zeus“, because we have a similar situation in quantum mechanics today - the superposition of two states ( $\uparrow, \downarrow$ , as in Figure 6.8, left) - the new state includes both previous states, but in a transcendent form. Similarly, in *hyperpolarized* light, vertical and horizontal polarizations are transcended, but at the same time preserved. Namely, photon hyperpolarization (light) is



a simultaneous relative phase displacement of the vertical polarization and a relative amplitude displacement of the horizontal polarization according to the Fibonacci law on the Poincaré sphere.

During the spatial-temporal photon evolution „half quantization“ occurs, giving the energy value  $\frac{1}{2} h\nu$ , because the quantum number  $n = 0$  defines the ground energy state of the quantum oscillator [ $E = (n + \frac{1}{2})h\nu$ ]. Figure 6.9 demonstrates that the vertical ( $r_{\perp}$ ) and the horizontal ( $r_{\parallel}$ ) linear polarization are in the Fibonacci superposed state producing hyperpolarization ( $\langle r_{\perp}, r_{\parallel} \rangle = r_{\diamond} = r_{\text{IE}}$  for simpler notation, meaning the „centered 5“ ).

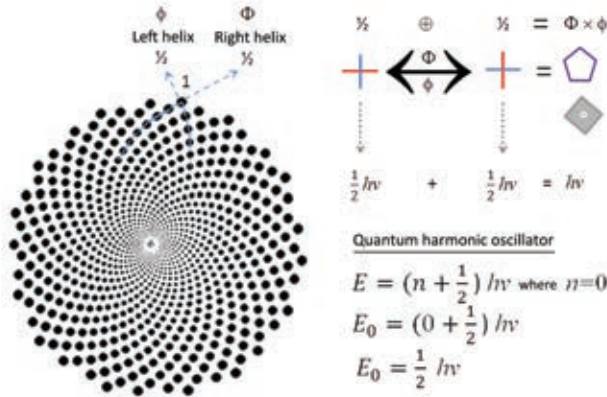


Figure 6.9 The quantum harmonic oscillator provides the possibility that photon energy is  $\frac{1}{2}h\nu$  and that, in Fibonacci structured photons, the horizontal and vertical polarization in the superposed state become hyperpolarized.

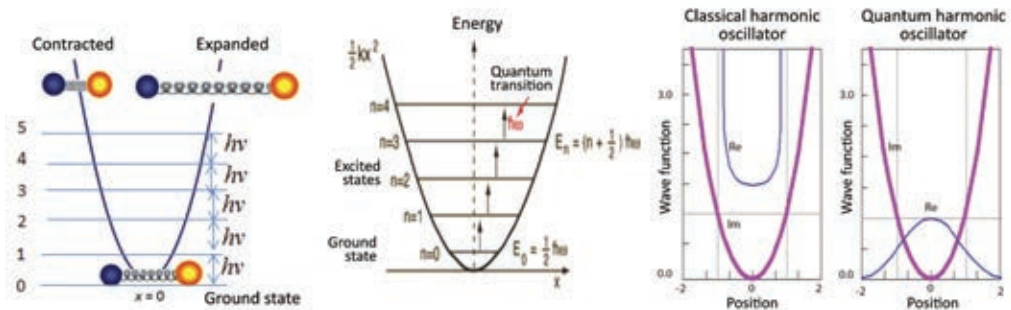
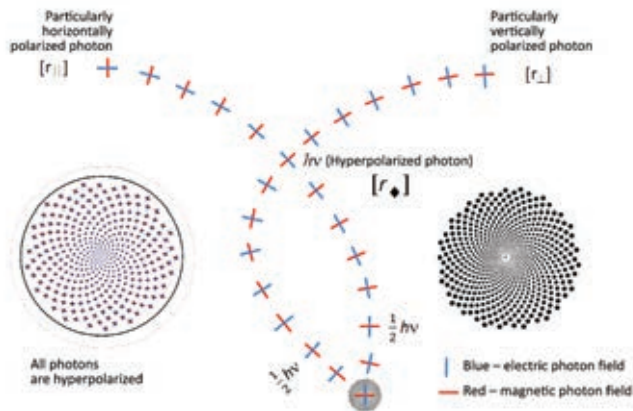


Figure 6.10 Comparative presentation of the Re (real) and the Im (imaginary) solution of the wave function of the classical and of the quantum harmonic oscillator. Quantum transition is  $h\nu$ , where the energy of the ground state ( $n = 0$ ) for the classical oscillator is  $E_0=0$ , and for the quantum oscillator it is  $E_0= \frac{1}{2}h\nu$  (Adapted from Alonso, 1992 and Zettili, 2009)

The relationship between the vertically and horizontally polarized photon is given in Figure 6.11 in detail. It can be said that the photon is particularly (in the local state) vertically and horizontally polarized, while it is actually hyperpolarized. We accept the dogma

that photon can be „either one or the other“, but do not accept „one and the other, neither one nor the other“. An obvious example of dogmatic approach can be noted in everyday life when we say „...the Sun rises in the East at 5:32 A.M., and sets in the West at 20:47 P.M. ...“, we actually pronounce a particular (local) truth of the observer. The Sun neither *rises* nor *sets*; the Earth *rotates* about its axis. This approach seems logical to us, not only „logical“ but practical for everyday life on Earth. However, if we wish to travel to cosmos (to the Moon and back) this dogma is automatically discarded. The same goes for the vertically and horizontally polarized light: everything is alright while we use them in „everyday“ approach, but if we want the approach „structured light meet structural matter“ (the *tally* principle – two coded halves that are joined into a whole), i.e., to improve the application of light in medicine, a metamorphosis occurs – enters *hyperpolarized* light ( $\langle r_{\perp}, r_{\parallel} \rangle = r_{\diamond} = r_{\text{E}}$ ).



**Figure 6.11** Relationship between the horizontal and the vertical polarization of photons, their organization and generation of hyperpolarized light as a Fibonacci structure (Koruga, Dj., Int. Pat. App. PCT/EP2016/063174, 2016, and WO 2017/211420A1, 14. december 2017. Applicant Fieldpoint, ZEPTEK GROUP).

The basic similarities and differences between the vertically and horizontally polarized light and the hyperpolarized light were presented above. The hyperpolarized state of photons is the ground energy state of photons ( $E_0$ ) due to its structure based on the quantized *orbital angular momentum* (OAM) and *spin* (producing *halfquantization* of the ground energy state of the photon  $E_0 = \frac{1}{2} hv$ ). Diffuse, vertically polarized, horizontally polarized, circular, etc., states are only possible particular solutions at higher energy levels  $E_1 = 3/2 hv, E_2 = 5/2 hv, E_3 = 7/2 hv, \dots$ , (consequently, the difference between energy states is *one quant*,  $hv$ ), therefore the basic principles of quantum mechanics are not violated.

Comparing Figures 6.5, 6.6 and 6.11 we observe basic similarities and differences. Diffuse light is, figuratively speaking, „wild“ regarding photon orientation, rotation of the electromagnetic photon field, and organization, while according to the overall effect it is very complex. In linearly polarized light „wild“ photons are ordered („militarization“), they are organized according to energies, oriented along a direction, no rotation of the electromagnetic photon field is present (it is fixed; when the electric component is vertical, light is *vertically polarized*, and when the electric photon component is horizontal, light is

*horizontally polarized*). In hyperpolarized light (as in the linearly polarized light) photon organization is strict, although the electromagnetic photon field is neither horizontally nor vertically polarized, but organized (one photon with respect to another photon) under a strictly defined angle (the Fibonacci angle:  $222.5^\circ$ ), while the internal organization of photons corresponds to the expression  $360^\circ - 222.5^\circ = 137.5^\circ$ . Value  $\phi_\alpha = 137.4908$ , defines the internal organization of the photon structure. As the *fine matter structure*,  $\alpha^{-1} = 137.035$ , is defined according to the electric charge ( $e$ ), light velocity ( $c$ ) and Planck's constant ( $h$ ), so the *fine structure of photon organization* is defined according to the „half quantization“ ( $\frac{1}{2}hv$ ) of the ground photon's energy state, the total orbital angular photon momentum (total OAM) and the Fibonacci structural light organization ( $\Phi$ ) of a set of photons and of each individual photon ( $\phi$ ), because  $\Phi \times \phi = 1$ . This testifies that principle „structured light meets structured matter“ does not refer only to forms of organization and energy, but to a deeper physical level as well, i.e., to the unification of all interactions. In other words, *hyperpolarized light* is the *tally* of matter, that is, a „codogenic“ interaction providing light- matter recognition ( $\alpha^{-1}/\phi_\alpha = 137.035/137.4908 = 0.9966 \approx 1$ ). Everything points to the conclusion that there is a strong connection between *light* and *matter* in nature (in this case *light* and *electric charge*), which we still do not understand well enough.

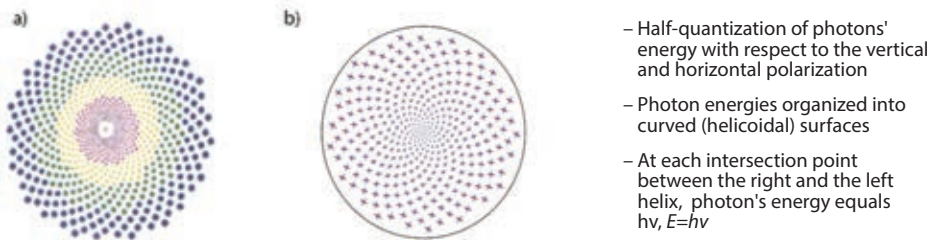


**Figure 6.12** Hyperpolarized light, as an organized photon structure according to the Fibonacci law with angular structural organization  $\phi_\alpha = 137.4908$  (Koruga, Dj., *Int. Pat. App. PCT/EP2016/063174*, WO 2017/211420A1, 14. december 2017. 2016, Applicant Fieldpoint, ZEPTEK GROUP).

## 6.5. Fibonacci Light Structures vs. Fibonacci Biological Structures

### *Material for the Fibonacci Light Structure*

In order to establish the interaction between Fibonacci light structures and biological Fibonacci material structures we need technical devices to generate the Fibonacci light (photonic) structure. The first technical realization of a Fibonacci structure, associated with light transportation, was performed by the Italian-Dutch research team headed by Dal Negro in 2005 (Dal Negro, 2003).

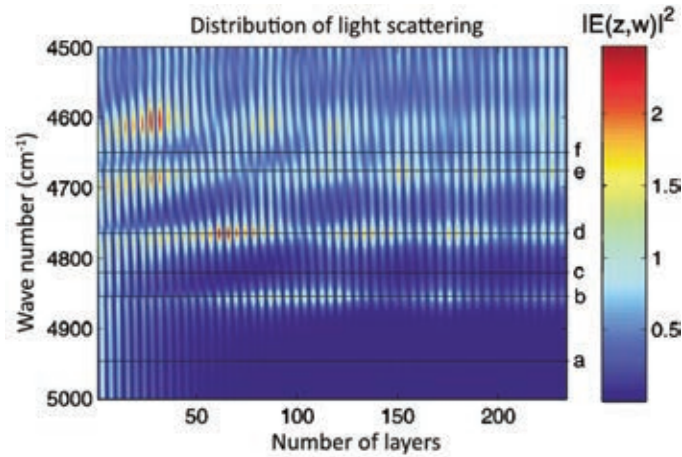


**Figure 6.13** Fibonacci photonic structure based on quasicrystalline icosahedral organization of 250 layers of silicon. Energy distribution and signal propagation correspond to the Fibonacci laws (Dal Negro, 2003).

In order to better understand advantages and problems of usage of nanomaterial with real icosahedral symmetry (instead of quasicrystals as in Figure 6.13), let us remind that the  $C_{60}$  molecule is one of the most serious candidates for building nanophotonic devices. This material was discovered in 1985, and this discovery was awarded the Nobel Prize for chemistry in 1996 (Kroto, 1985). Actually,  $C_{60}$  is a molecular crystal of diameter 0.71 nm (at the level of the carbon atom position), i.e., 1.02 nm (on the external position of the  $\pi$  electron ( $1.02 - 0.71 = 0.31$  nm), consequently  $\pi$  is an electronic cloud  $\delta_\pi = 0.155$  nm thick). The  $\pi$  electrons are located on the internal side of the carbon atom, thus, there is empty space within the  $C_{60}$  (vacuum) of  $0.71 - 0.31 = 0.4$  nm. Therefore, atoms can be encapsulated in the  $C_{60}$ , even a water molecule (endohedral fullerenes) (Matija, 1999).

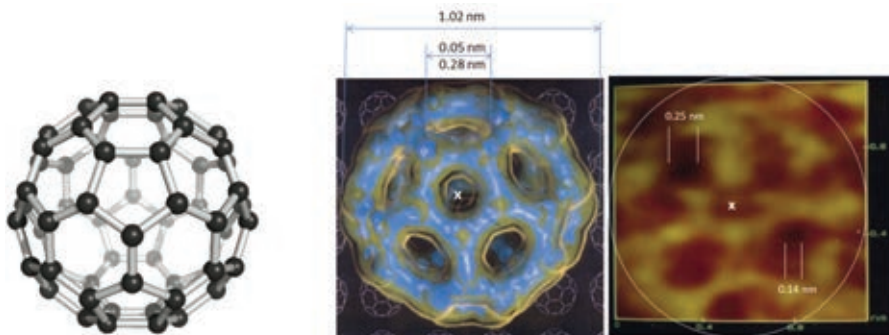


**Figure 6.14** The 3D view of the  $C_{60}$  molecule (left) (Kroto, 1985) and its shape based on quantum-mechanical calculations (published in 1991 on the cover of *Science* in December, as the molecule of the year) (middle). The STM image of the  $C_{60}$  molecule experimentally confirms the quantum-mechanical calculations, including punctures in hexagons (right) (Koruga, 1993).

The  $C_{60}$  molecule is a very dynamic vibrational-rotational structure built from sixty carbon atoms, which are arranged in 12 pentagons and 20 hexagons, a truncated icosahedron. Its dual structure is the dodecahedron, resulting from Euler's formula on polyhedra. Pentagons are energetically closed, while hexagons „breathe“, they can have holes up to 0.28 nm, so that in the interior, under certain conditions, smaller atoms can be encapsulated. However, from the aspect of hyperpolarized light, these punctures in hexagons are interesting regarding photon's transition, that is, collision between a photon and an electron of  $C_{60}$ . We established experimentally the existence of punctures in hexagons using the STM (Figure 6.14).

The  $C_{60}$  molecule rotates fast, about  $10^{-10} \text{ s}^{-1}$ , while photons travel much faster,  $3 \times 10^8 \text{ m/s}$ , and when the size of the  $C_{60}$  molecule is considered, interspaces between  $C_{60}$  molecules, and punctures in hexagons, photons can easily penetrate the  $C_{60}$  molecule, it is highly porous. In order to establish the interaction between photons and the  $C_{60}$  molecule, a large number of layers of this molecule is needed. Its rotation is not oriented in one direction, it is random in all directions (twisting, the „bang-bang“ concept).

Even more,  $C_{60}$  represents a quantum pirouette because according to the laws of classical physics a particle (body) can spin either to the left or to the right. However, a quantum entity could exist in a superposition of both possibilities. This sounds fantastic, but for  $C_{60}$  and other quantum particles, this is reality confirmed by experiment (Markus, 1999).

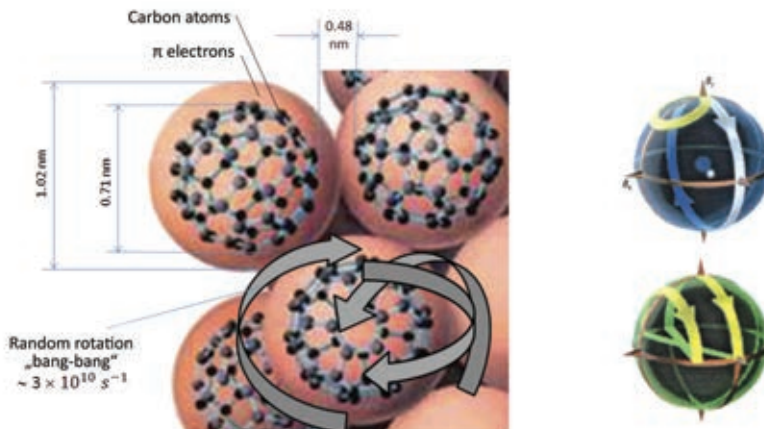


**Figure 6.15** Basic elements and parameters of the  $C_{60}$  molecule (Hayden, 1987) (left) and illustration of the „bang-bang“ rotation principle of the  $C_{60}$  molecule with an encapsulated nitrogen atom  $N@C_{60}$  (Morton, 2005) (right).

Another interesting feature of the  $C_{60}$  molecule, of its pentagons and hexagons: it is one of the rare molecules simultaneously exhibiting *paramagnetic* (hexagon) and *diamagnetic* (pentagon) features. Vertical linearly polarized light is sequentially changed into horizontal linearly polarized light according to the Fibonacci order – „sunflower“ – because 20 hexagons (*paramagnetics*) generate the Faraday effect, which rotates the plane of polarization of the electromagnetic wave proportionally to the thickness of the material through which the light passes, while 12 pentagons (*diamagnetics*) are changed

by rotation, step-by-step, sequentially according to the Fibonacci law. If it were not rotating randomly, if its rotation were directed, it would be an ideal nano motor (a self-propelled vehicle on „four wheels“ could be built).

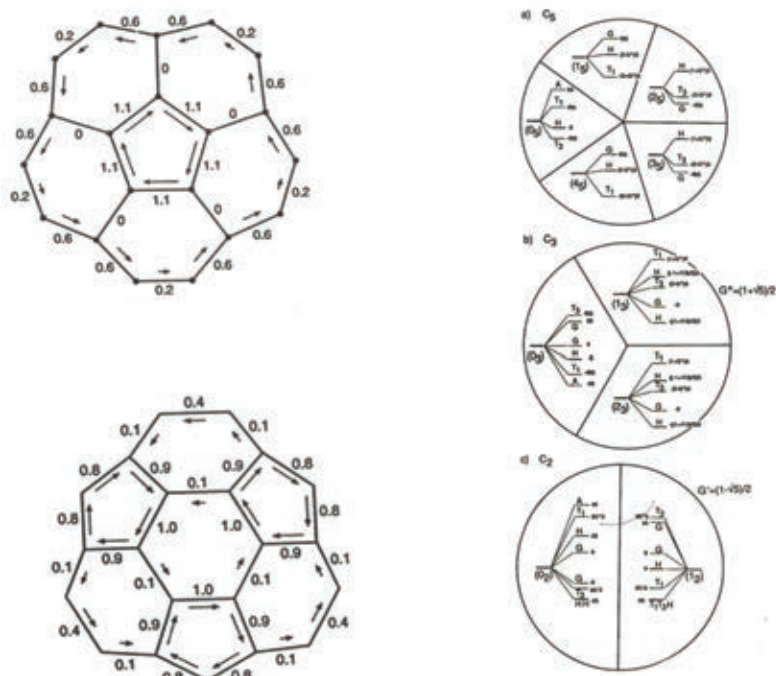


**Figure 6.16** Normalized values of the electric charge flow in pentagons (*above left*), electric charge flow in hexagons (*below left*), and symmetric clusters  $C_5$ ,  $C_3$ ,  $C_2$  (*right*) (center of inversion  $E$  is not displayed) (Harter, 1989).

Beside the quantum-mechanical appearance of the  $C_{60}$  molecule recorded using the STM, its surface energy that corresponds very well with its vibrational properties (Figure 6.17) was determined. Although the  $C_{60}$  molecule includes hexagones, it does not have symmetry axes of the *sixth* order (as would seem likely at first sight), the axis is of the *third* order (symmetry element  $3:6 = \frac{1}{2}$ ). This reminds us of the electron spin  $\frac{1}{2}$ : it has to perform *two revolutions* to coincide with itself. The  $C_{60}$  molecule is the most perfect symmetry structure of point symmetry in nature (more perfect than the diamond that has 48 symmetry transformations), having 60 symmetry transformations (it could have 120,  $60 \times i$  symmetry transformations:  $E$  (inversion center), 12  $C_5$ , 12  $C_2^5$ , 20  $C_3$ , 15  $C_2$ , and, 12  $S_{10}$ , 12  $S_{10}^3$ , 20  $S_6$ , 15  $\sigma$  (symmetry planes)). The total number of (energy) eigenvalues is 46 (there is a small discrepancy of 5% to 10% between theory and experiment).

The  $C_{60}$ , molecule, as a molecular crystal, has the role of an atom in classical crystallography, thus we have a crystal within a crystal (because of its distribution into the crystal lattice  $T_h$  as the *fcc* lattice). The first crystal structures of the  $C_{60}$  molecule were experimentally detected by (Huffman, 1991).

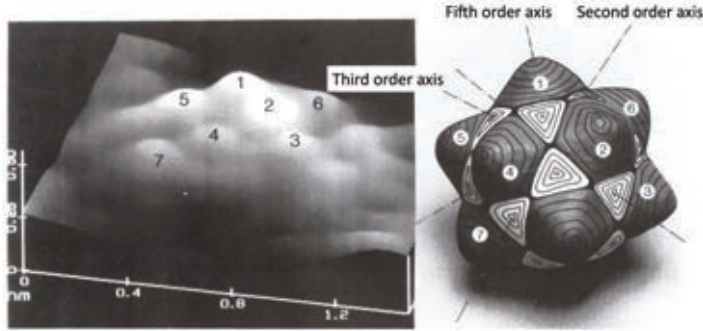


**Figure 6.17** The STM image of the surface energy of the  $C_{60}$  molecule taken at the NanoLab, at the Faculty of Mechanical Engineering in Belgrade (**left**), and the theoretical prediction of the surface energy of the molecule. The STM image displays that molecule energy is concentrated in pentagons and that it actually is the Fibonacci molecular energy (Koruga, 1993).

When the vibrational-rotational energies of the  $C_{60}$  molecule are observed temporally, a series of states is obtained as displayed in Figure 6.18. Calculations of the Hamiltonian via the total angular momentum  $J$ , tensors  $T^{[6]}$  and  $T^{[10]}$  depending on the angle  $\vartheta$ , and constant  $B$ , are given by the expression (Harter, 1991):

$$H(\vartheta) = B|J|^2 + (\cos\vartheta)T^{[6]} + (\sin\vartheta)T^{[10]}$$

This powerful mathematical-physical tool produces very good results, as seen in Figure 6.17 that correspond very well with experiments. These vibrational-rotational energy values (there are 46 modes) are within the interval 0.20 eV - 0.012 eV. These are the output values of photon's energy resulting from the interaction between the photon and the electron of the  $C_{60}$  molecule. However, this is only about 31% of photons that have been transformed, while about 54% of photons remain energetically unchanged, but structurally reorganized into a Fibonacci form, and about 15% remain unchanged (as emitted from the source– vertical linear polarization). From the aspect of specific energy density, about 69% photons are within the 400–3.000 nm range, and 31% in the range 3000–50 000 nm (with 46 frequency modes).

Temporally dependent wave packets  $\psi(x, t)$  of the  $C_{60}$  molecule represent not only a De Broglie wave with an adequately defined frequency and wavelength ( $\lambda = h/\sqrt{2m_e E}$ ), but a larger number of wavelengths (Jex, 2000). There are 46 main vibrational-rotational modes of the  $C_{60}$  molecule, and the function is:

$$\psi(x, t) = \frac{1}{\sqrt{2\pi}} e^{ik_0(x-v_{ph}t)} \int_{-\infty}^{+\infty} g(k - k_0) e^{i(k-k_0)(x-v_g t)} e^{-i(k-k_0)^2 a t + \dots} dk$$

where:  $\vartheta_g$  – group velocity of the wave packet,  $\vartheta_{ph}$  – velocities of individual waves,  $k$  and  $k_0$ – values defining amplitudes  $\phi(k) = g(k-k_0)$ , so that the frequency  $\omega$  is a function of  $k$ ,  $\omega = \omega(k)$ .

$$v_g = \frac{d\omega(k)}{dk}, \quad v_{ph} = \frac{\omega(k)}{k}.$$

Light type	Reorganized according to Fibonacci, energetically unchanged	Energetically transformed in interaction with $C_{60}$ and organized according to Fibonacci	Light remains the same, as emitted by the source	Loss in photon emission (scattering and heating)
Photons	54%	28%	12%	6%
Hyperpolarized (HP)	+++	+++	+ (LP)	+, -
Source: specific energy density 40mW/cm <sup>2</sup> (for HP)	21.6 [mW/cm <sup>2</sup> ]	11.2 [mW/cm <sup>2</sup> ]	4.8 [mW/cm <sup>2</sup> ]	2.4 [mW/cm <sup>2</sup> ]

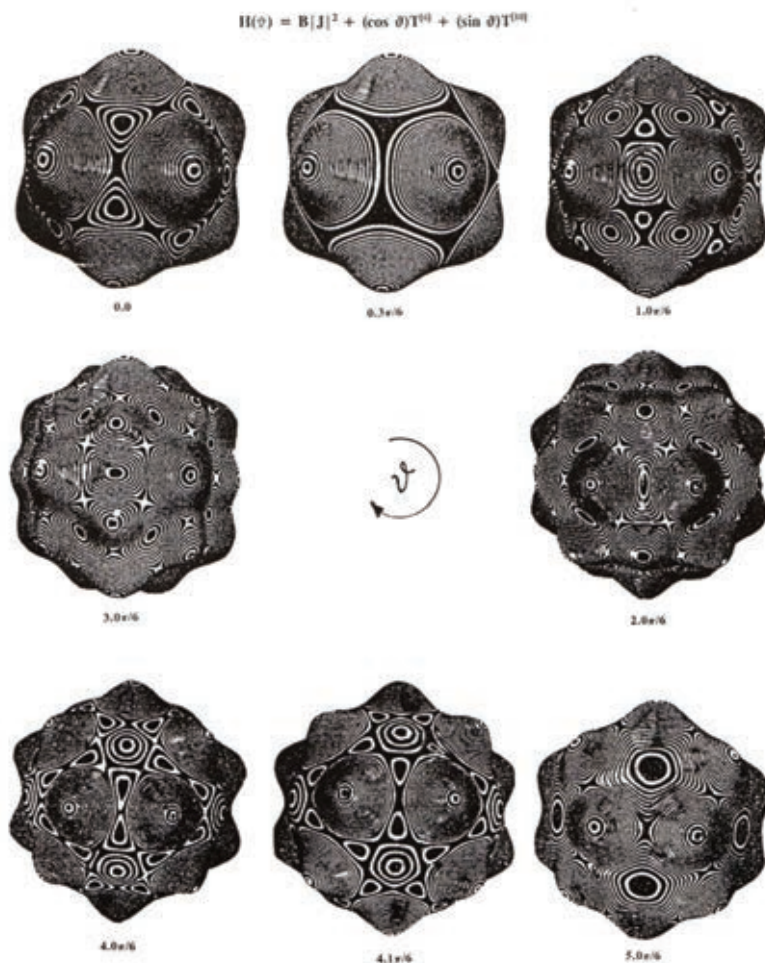


**Figure 6.18** Fibonacci vibrational forms of the  $C_{60}$  molecule, obtained by the Hamiltonian and the tensor (of the sixth and tenth order) of the total angular momentum (Harter, 1991).



**Table 6.3** Table of 46 energy eigenvalues in the range  $274 \text{ cm}^{-1} - 2085 \text{ cm}^{-1}$  ( $3000 \text{ nm} - 50\,000 \text{ nm}$ ) of the  $C_{60}$  molecule, based on icosahedral symmetry that can interact resonantly with light and reemit light (Koruga, 1993).

$C_{60}$ energy eigenvalues Even parity		$C_{60}$ energy eigenvalues Odd parity	
$I_h$ group	Wave number ( $\text{cm}^{-1}$ )	$I_h$ group	Wave number ( $\text{cm}^{-1}$ )
$A_g$	1830	$A_u$	1243
	510		
$T_{1g}$	1662	$T_{1u}$	1868
	1045		1462
	513		618
			478
$T_{2g}$	1900	$T_{2u}$	1954
	951		1543
	724		1122
	615		526
			358
$G_g$	2006	$G_u$	2004
	1813		1845
	1327		1086
	657		876
	593		663
	433		360
$H_g$	2085	$H_u$	2086
	1910		1797
	1575		1464
	1292		849
	828		569
	526		470
	413		405
	274		

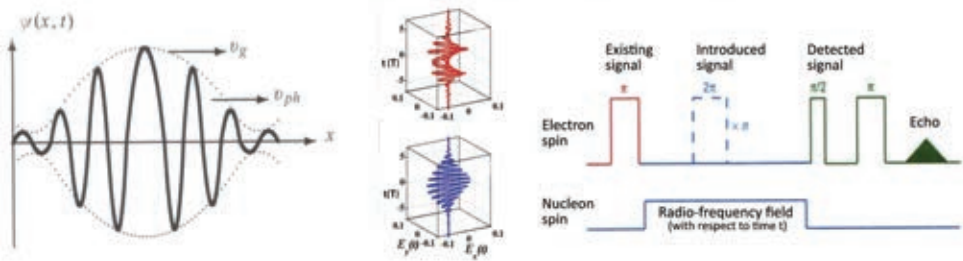


**Figure 6.19 a)** Localized wave function of the  $C_{60}$  molecule as a wave packet, travelling by group velocity  $v_g$ , while individual waves travel by different phase velocities  $v_{ph}$  (left). This mode unites a large number of different waves (46 in case of  $C_{60}$ ); each individual wave does not lose its individuality. Polarization harmonics for two simultaneous pulsations (middle). Heisenberg's uncertainty principle holds for quantum wave packets ( $\Delta x \Delta p = \hbar/2$  where  $\hbar = h/2\pi$  is the Dirac's constant) - we cannot determine simultaneously the position ( $x$ ) and the momentum ( $p$ ) (Jex, 2000, Fleisher, 2017). Experimental confirmation that the  $C_{60}$  molecule transforms the input signal (existing signal  $\pi$ ) under the effect of the applied signal ( $2\pi$ ,  $n$  times applied) into a new signal ( $\pi/2$ ,  $\pi$ , and echo) (right) (Morton, 2005).

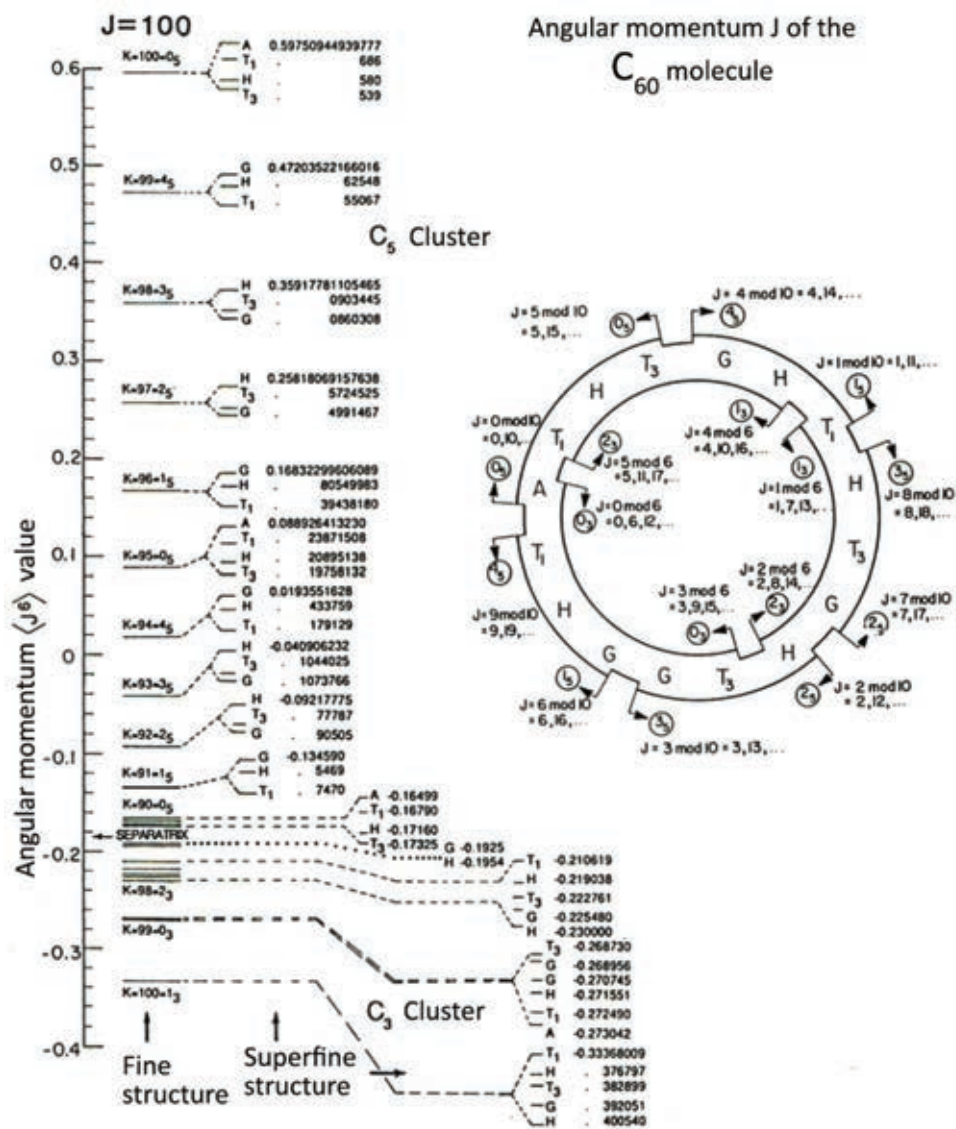
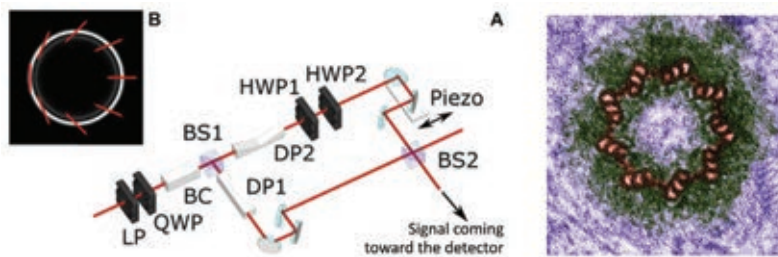


Figure 6.19.b Fine and superfine vibrational-rotational energy structure of the  $C_{60}$  molecule based on the total angular momentum  $J$  and symmetry clusters  $C_5$ ,  $C_3$  of the  $C_{60}$  molecule (Harter, 1991).

However, the total number of active modes of the  $C_{60}$  molecule is  $3N-6 = (3 \times 60) - 6 = 174$ , because  $A_g$  has 2 energy modes of dimensionality 1 ( $2 \times 1 = 2$ ),  $T_{1g}$  has 3 modes with dimensionality 3 ( $3 \times 3 = 9$ ),  $T_{2g}$  has 4 modes of dimensionality 3 ( $4 \times 3 = 12$ ),  $H_g$  has 8 modes of dimensionality 5 ( $8 \times 5 = 40$ ), etc.

## Characteristics of Light with $\frac{1}{2}$ -Quantization („half-quantization“) of the Total Angular Momentum

Regarding the electron, there is the phenomenon of the Russell-Saunders coupling of the orbital momentum of the electron and its spin (Russell, 1925). The explanation was that electrons in orbitals are not mutually independent, because, via the magnetic field generated by their motion, they influence each other. Therefore, their *orbital momenta* (motion about the atom nucleus) and their *spin* are coupled by the electric and the magnetic field. As these are vector values, coupling is established via their vector values. However, in lighter atoms, up to the periodic number 30 (zinc), spin vectors are more strongly coupled than orbital vectors, and in heavier atoms coupling is established between the spin of an individual electron and its orbital momentum. However, this is not an absolute rule, because it is not effected completely.



**Figure 6.20** Experimental setup of the apparatus for determining photon's total angular momentum  $J_{1/2}$ ; (1) light source generating photons according to the Gaussian distribution, (2) linear polarizer (LP), (3) quarter-wave plate (QWP), (4) bi-axial crystal (BC) (left A). The value of the angular momentum is measured with the interferometer whose optical unit rotates and is coupled with the light source generating photons with adequate angular momentum. Measurement of  $J_{1/2}$  is performed by the rotation of the digital record forming the image and establishing polarization under different angles. This is accomplished with two prisms (DP1 and DP2) rotating the obtained image by  $180^\circ$  and transmitting it through two half-wave plates (HWP1 and HWP2) that rotate the polarization by  $90^\circ$ . Light beam splitters (BS1 and BS2) divide and recombine the light beam. DP1 and DP2 are orthogonal, while HWP1 and HWP2 are under the angle of  $45^\circ$ . A signal coming into the detector produces red lines representing polarization „angulations“ of photons with  $|j| = \frac{1}{2}$ , coming from a randomized light source (Ballantine, 2015) (left B). Fibonacci biomolecular structure (centriole) with curved position of microtubules organized according to the rule  $E_0 = \frac{1}{2}h\nu$  (right).

Regarding photons, coupling between the orbital angular momentum and spin was not taken into account until recently; there were attempts 30 years ago, although experimental confirmation was obtained only recently (Ballantine, 2016). The research team from Dublin started with the hypothesis that quantum numbers of spin *eigenvalues* and the photon orbital angular momenta are relevant for the explanation. They performed the experiment described in Figure 6.20 (left, A and B). When rotation was introduced

into the experiment, the rotational Doppler shift emerged curving polarization planes (Figure 6.20, *left B*). This is a simplified technical realization (basic principle) of what nature accomplishes with biomolecules having Fibonacci organization (Figure 6.20, *right*).

Figure 6.20 (*right B*), demonstrates that similar spatial *curvature* of the polarization plane occurs when  $|j = 1/2\rangle$  as in biomolecular Fibonacci structures (centriole, *right*). This experimental setup is actually „stone age“ compared to what nature accomplishes in biomolecules. Nevertheless, this experiment is the first „tool“ enabling better understanding of the mechanism, „structured light meets structured matter“. It should be noted that Niels Bohr did not quantize the electron state according to its *energy* (as is usually believed), but according to *momentum*, determined by electron's orbital motion about the nucleus and by its spin. In other words, the light-matter interaction („meeting“) should be realized through action or/and *momenta* (angular and momentum) within their *synergy*.

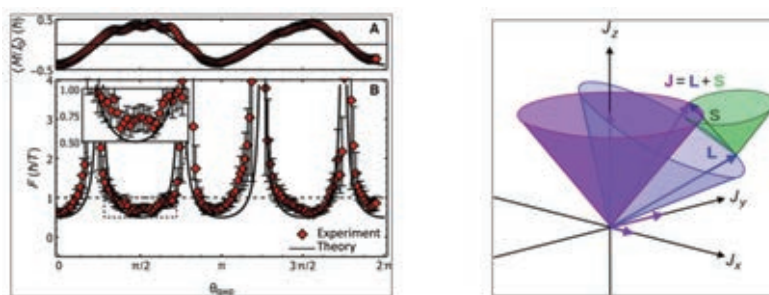


**Figure 6.21** Experiment results - the average photon's total angular momentum is  $|j = 1/2\rangle$  and  $|j = -1/2\rangle$ , implicating that „half quantization“ is established, thus  $E_0 = 1/2h\nu$  (left A). Value  $E_{\text{ij}} = \pm 1/2h\nu$  signifies simultaneous left and right orientation in the  $2\pi$  system. Theory conforms very well to the experiment based on the total angular momentum  $J = L+S$  (left B). Principle of vector addition between the orbital angular momentum (L) of the photon and photon's spin (S) ( $J = L+S$ ) (right) (Ballantine, 2015).

The apparatus from Figure 6.20 is not practical and precise for what we need, for the „meeting“ of light and matter according to the *moment of momentum*, *orbital angular momentum*, *spin* and *action*, and their application in medicine. Chapters on the electron and the light-matter interaction demonstrated that  $C_{60}$  molecule has certain properties that could be useful (its shape is sphere, very fast rotation, the size of only 1 nm, so that a large number of molecules must be used, which is adequate for randomization, etc.). The  $C_{60}$  molecule is a sphere, therefore, from the mathematical viewpoint (useful for physical, and later for engineering solutions) connection with other structures should be examined, because interaction between light and matter is a dynamical process. This resembles chemical reactions; for example, when we observe structure 1 and structure 2, as in Figure 6. 22, both structures are composed of the same atoms, although they are different. However, under certain conditions (volume, pressure, temperature, free Gibbs energy, etc.) a transition can occur from one into the other. We say that there is an adequate connection given by a mapping (which connects atoms of one structure with the atoms of the other structure). When a connection exists between atoms, we inscribe 1 into

a matrix field, and when this connection does not exist, 0 is written. Thus, two matrices are obtained composed of 1 and 0, which seem different at first sight, but are essentially (from the aspect of a possible chemical reaction) the same. We still need two structures A and B associated via the wave function. One is a „model“ (HΨ), and the other is effective (EΨ). However, this association cannot be arbitrary, it has to be via the Fibonacci numbers ( $\phi, \Phi$ ), i.e., their structures. The Euler-Descartes connectedness surface characteristic of two body surfaces is a natural number  $h$ . A polyhedron is  $h$ -connected if  $h-1$  broken lines can be drawn on its surface, whose segments are polyhedron's edges that do not cut the polyhedron. However,  $h$  broken lines cut the polyhedron in two parts; the first of these broken lines must be closed, while others connect two points of previous lines.

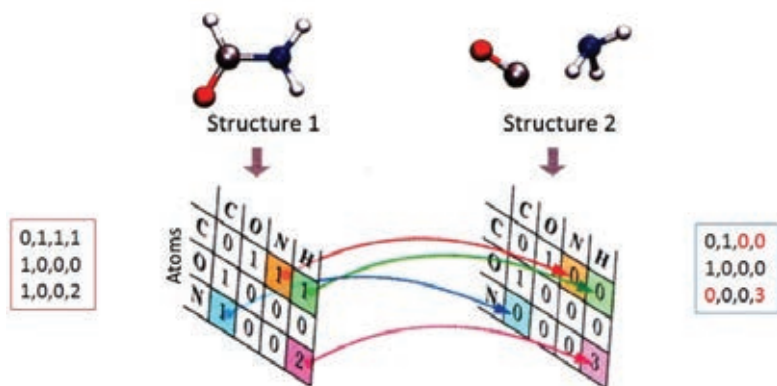


**Figure 6.22** Schematic representation of the connection between two structures based on participation and connectivity of atoms in both structures.

As seen in Figure 6.23, connectedness of the sphere surface is  $h = 1$ , while for the torus surface  $h = 3$ . Another property that the sphere and the torus should fulfill is the relation of their volume with their surface via the first derivative. Just as in physics, the first derivative of *distance* with respect to time defines *velocity*, and the derivative of velocity with respect to time defines *acceleration*, thus the first derivative of the sphere volume with respect to the sphere radius defines its surface. The same holds for the torus. Why is this important? Chapter II, about dimensions and unit spheres (which are the basis of coding and information) of various dimensions, presented the unit sphere of dimension  $N = 5$  with the largest capacitance. The same Chapter demonstrated that gravitation and electromagnetism are coupled via Planck's length as a 5D phenomenon, which will be useful for technical solutions that should act upon weak rotational and still weaker translational energies in biological systems.

As the magnetic photon component is by nine orders of magnitude closer to the quantum action than the electric component ( $M/E = 3.3 \times 10^{-9}$  s/m, because light velocity is  $\sim 3 \times 10^8$  m/s, which is at the same time the ratio of the electric to the magnetic field in vacuum where light propagates with this velocity), and in valence electrons by 4 orders of magnitude (because electrons orbit about the nucleus with the speed  $\sim 10^6$  m/s, and light velocity is  $\sim 10^8$  m/s), therefore, the interaction between light and  $C_{60}$ , as

well as the light effect on biological systems, will be treated and investigated primarily from the magnetic aspect.

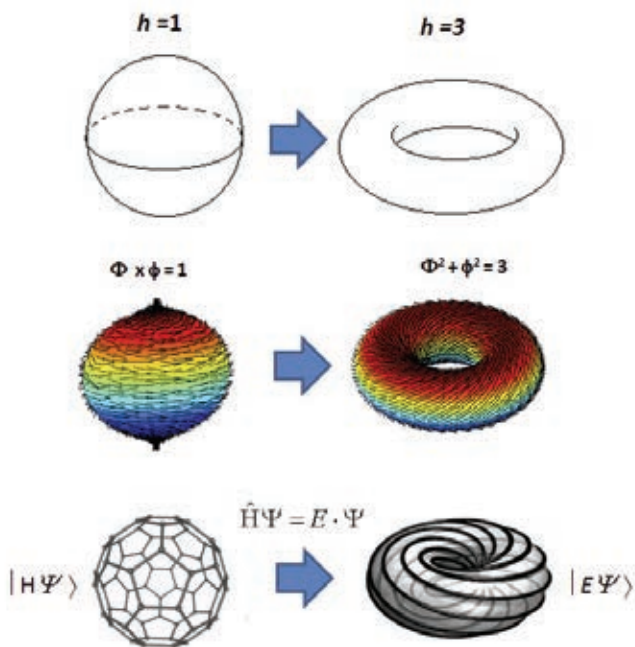


**Figure 6.23** Topological similarity between the sphere ( $h = 1$  connected) and torus ( $h = 3$  connected) via the Fibonacci numbers  $\phi$  and  $\Phi$ . This correspondence enables the photon energy to be coupled with the  $C_{60}$  molecule based on the total angular momentum.

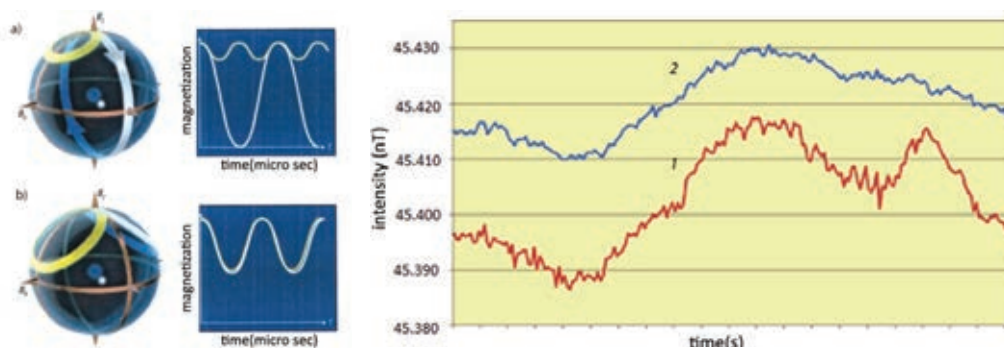


**Figure 6.24** Two different instances of „bang-bang“ motion of  $C_{60}$  and its magnetization under the influence of microwave radiation (100kHz) (left). This demonstrates two phenomena: (1) that  $C_{60}$  rotates randomly, and (2) that it can be controlled by microwave radiation (Morton, 2005). The difference of intensities of the  $C_{60}$  magnetic flux in the Earth's magnetic field before (1 – red line) and after (2 – blue line) the effect of the linearly polarized light (right). Average difference is  $9.9 \pm 0.4$  nT for a layer of 100  $C_{60}$  molecules (Koruga, 2005).

Rotational energy of the  $C_{60}$  molecule is within 5 meV –9 meV, however, the main values are between 6 meV –8 meV, when from a *qubit* quantum state  $|10\rangle$  or  $|1\pm 1\rangle$  it transits into  $|00\rangle$ . However, a very interesting and important phenomenon occurs when the rotation of  $C_{60}$  is acted upon (its rotation is oriented, directed). The resulting distribution  $V(\theta, \phi)$  of rotational energy is not uniform, while in random rotation („bang-bang“), without external influence, the  $V(\theta, \phi)$  distribution is uniform. Consequently, the  $C_{60}$  molecule behaves as a „perfect“ natural randomized Gauss classifier, which we need to transform the vertical linearly polarized light into hyperpolarized light.

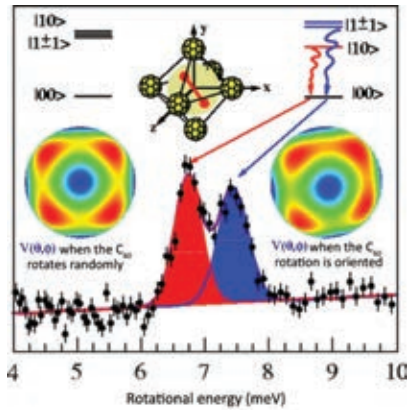


**Figure 6.25** Rotational energies of the  $C_{60}$  molecule when the quantum transition from  $|10\rangle$  or  $|1\pm 1\rangle$  into  $|00\rangle$  occurs. Energy of 6 meV –8 meV corresponds to the average wavelength of about  $170 \mu\text{m}$  (Jex, 2000).

Chapters II and III demonstrated that the photon can be described by the Poincaré sphere (regarding polarization), and the quantum electron characteristics using the Bloch sphere. However, this interaction is not static (like an incident light beam on a static plate) but dynamic ( $C_{60}$  rotates randomly, „bang-bang“). A portion of light transits through the molecule unchanged (about 12%), another portion of the photons is organized according to the Fibonacci law  $\Phi$  in the interaction (about 54%) regarding energies of total angular momenta, while the remaining photons (about 28%) are transformed and organized according to the  $\phi$  Fibonacci law. Their angular momenta are summed, and newly obtained (transformed) photons are *mapped* from  $\phi$  into  $\Phi$ , and vice versa by interactions. Both processes are randomized by the  $C_{60}$  („deterministic chaos“) and, therefore, their behavior in the phase space resembles an attractor (Schuster, 2005).

The main processes are correspondences of type  $x_{n+1} = f(n)$ , thus the Lyapunov’s exponent will be the measure of separation of two proximal points during iteration (for example:  $\Phi$  [13/8] and  $\phi$  [8/13]). When the initial distance  $\epsilon$  is modified according to the formula  $\epsilon^{(N)}$ , where  $N$  is the number of applied iterations (for example: for  $\Phi$  [13/8] and  $\phi$  [89/144], there are 4 iterations: 55/89, 34/55, 21/34, 13/21, in order to arrive at 8/13, which is the complementary pair in the mapping), then:

$$\lambda_0 = \lim_{N \rightarrow \infty} \lim_{\epsilon \rightarrow 0} \frac{1}{N} \ln \left| \frac{f^N(x_0 + \epsilon) - f^N(x_0)}{\epsilon} \right|$$

which is directly related to the first derivative, consequently surfaces of the sphere and the torus must be first derivatives of their volumes.

Mappings are associated with information. If we relate Shannon's expression for the calculation of classical information (Shannon, 1963)

$$I = -\sum_i p_i \log_2 p_i$$

with Lyapunov's exponents in simpler mappings of type  $f(x_n) = ax_n$ , we can determine the average information loss during one iteration. To this effect, let us divide the interval of allowed  $x$  values into  $N$  segments and assume that the initial point  $x_0$  can be located in any of the segments with equal probability  $1/N$ . By finding out in which segment point  $x_0$  is located we obtain the information:

$$\Delta I = -\lim_{N \rightarrow \infty} \frac{1}{N} \sum_{i=0}^N \ln |f'(x_i)|$$

which is Lyapunov's exponent exactly. Therefore,  $\Delta I = \lambda$  (Lyapunov's exponent) is the measure of information loss in the system during iteration. This is directly related to system entropy elucidated by Kolmogorov (K-entropy), which gives the measure of system chaos, i.e., disorder. According to Shannon's interpretation, disorder is closely associated with the quantity of information in the system at a given level of resolution. Let  $I(\varepsilon, T)$  represent the quantity of information obtained by observing a trajectory within the time interval  $T$  with resolution  $\varepsilon$ . When the phase space is divided into cells of volume  $\varepsilon^m$ , which are observed in intervals  $n\tau$ , so that  $t = N\tau = T$ , Kolmogorov's entropy can be expressed as:

$$K \equiv \lim_{T \rightarrow 0} \lim_{\varepsilon \rightarrow 0} \lim_{N \rightarrow \infty} \frac{1}{NT} \sum_{n=0}^{N-1} (K_{n+1} - K_n)$$

Thus, it represents a limit value of the information contents being mapped. It precisely determines a trajectory in the phase space and establishes a one-to-one correspondence of photons according to the Fibonacci series. As this dynamic system oscillates in two (coupled) group frequencies  $f_{1(\Phi)}$  (photons that are not transformed energetically, but are through the interaction with  $C_{60}$  organized according to the Fibonacci law) and  $f_{2(\phi)}$  (photons energetically transformed through the interaction with  $C_{60}$  and organized according to the Fibonacci law), its quasiperiodic motion can be described by a torus (Figure 6. 26). When  $k$  mutually independent frequencies are found in the system spectrum (for instance,  $f_{3(\Phi)}$  and  $f_{4(\phi)}$ ), it is said that the system performs quasiperiodic motion on a  $k$ -dimensional torus ( $T^k$ ).

The phenomenon of manipulation of polarization waves by twisting structures (Liu, 2014) is known. The interaction of photons with twisting structures, such as the  $C_{60}$  molecule, represents a phenomenon with a rotational Doppler shift (Ballantine, 2016). Photons behave according to the rules of the Poincaré sphere, and electrons according to the rules of the Bloch sphere. We should keep in view that electrons constitute the  $C_{60}$  molecule which is an icosahedral structure with the „bang-bang“ phenomenon of approximate frequency  $10^{10}$  per second. Its complex motion produces two main photonic effects: processes  $f_{1(\Phi)}$  and  $f_{2(\phi)}$  (coupled frequencies of photons organized according to  $\Phi$  and  $\phi$ ).



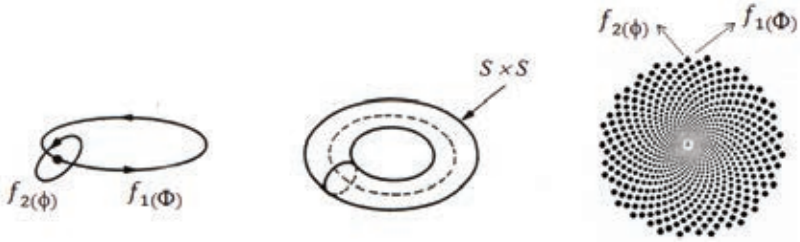


**Figure 6.26** The dynamics of a system with two independent frequencies  $f_{1(\Phi)}$  and  $f_{2(\phi)}$  is described as quasiperiodic motion on the torus. However, when the process is observed in a plane, the „sunflower seed“ shape is obtained where frequencies  $f_{1(\Phi)}$  and  $f_{2(\phi)}$  are coupled (Strogatz, 1994).

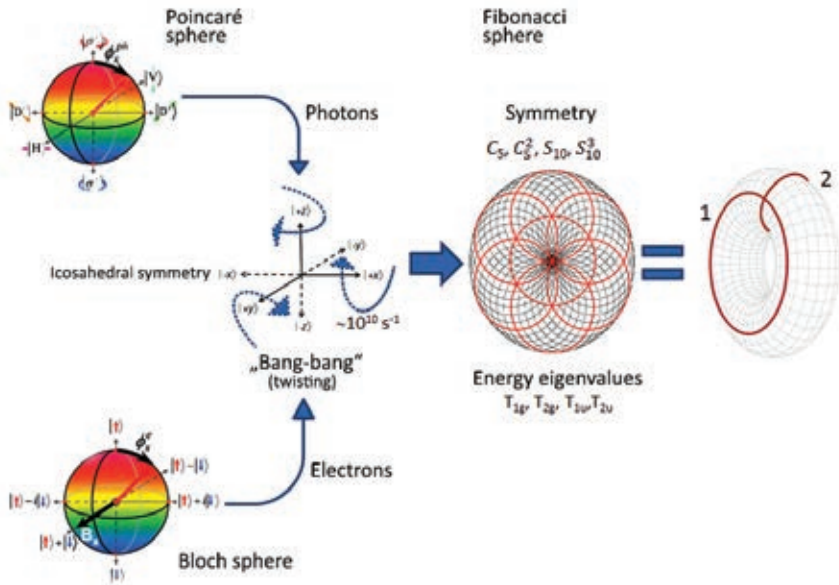


**Figure 6.27** Schematic representation of hyperpolarized light generation : **a)** linearly polarized photons coming to interact with electrons **b)** which belong to the icosahedral structure performing the „bang-bang“ motion **c)** spatial  $(x,y,z)$  and temporal  $(t)$  dynamics with velocity  $10^{10}$  per second. This generates „deterministic chaos“ providing coupling of the orbital angular momenta of photons and electrons, and forming a 2-D  $(\Phi, \phi)$  „pattern“ **d)** which is actually a 3D twisting torus with  $f_{1(\Phi)}$  and  $f_{2(\phi)}$  group frequencies.

A research team from Oxford and Princeton experimentally demonstrated dynamics of the  $C_{60}$  molecule encapsulating a nitrogen atom within the  $C_{60}$  - the so called endohedral fullerene,  $N@C_{60}$  (Morton, 2005). This was effected by coupling nuclear and electronic spins through the influence of a resonant radio-field (of the coupled Rabi oscillator) in order to generate electronic quantum qubits ( $M_s = +3/2$  and  $-3/2$ ) and the nuclear qubit ( $M_I = +1,0$ ). These experiments point strongly to the conclusion that the  $C_{60}$  molecule is one of the serious candidates for future quantum computers.

Experimental visualization (Figure 6.29) of photon's orbital angular momenta (with left and right orientation) obtained by the USA-Israel-China research team in order to improve capacitance in communication systems (Wang, 2012). Two years later, the USA-Canada research team succeeded in recording orbital angular momenta of photons of visible light (Karimi, 2014).

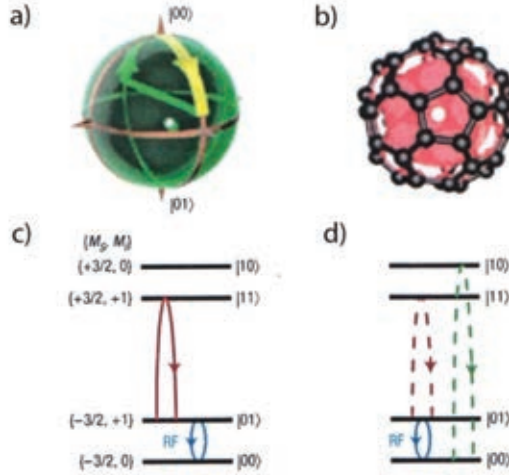


**Figure 6.28** The  $C_{60}$  molecule as the basic element for the generation of qubits based on the influence of radio-waves (RF) under the control of the Rabi oscillator (Morton, 2005).



**Figure 6.29** Photon's orbital angular momenta with left and right orientation (Wang, 2012). When the first two images are „overlapped“, their intersecting points result in a Fibonacci  $[\Phi, \phi]$  system (right).

In order to grasp more easily the differences between the diffuse, linearly polarized and hyperpolarized light, it is necessary to examine the organization of the electromagnetic field. This has been represented in Figures 6.5, 6.6 and 6.12, but when all three images are put together in one place, similarities and differences between these three light types (Figure 6.30) can easily be grasped at a glance.

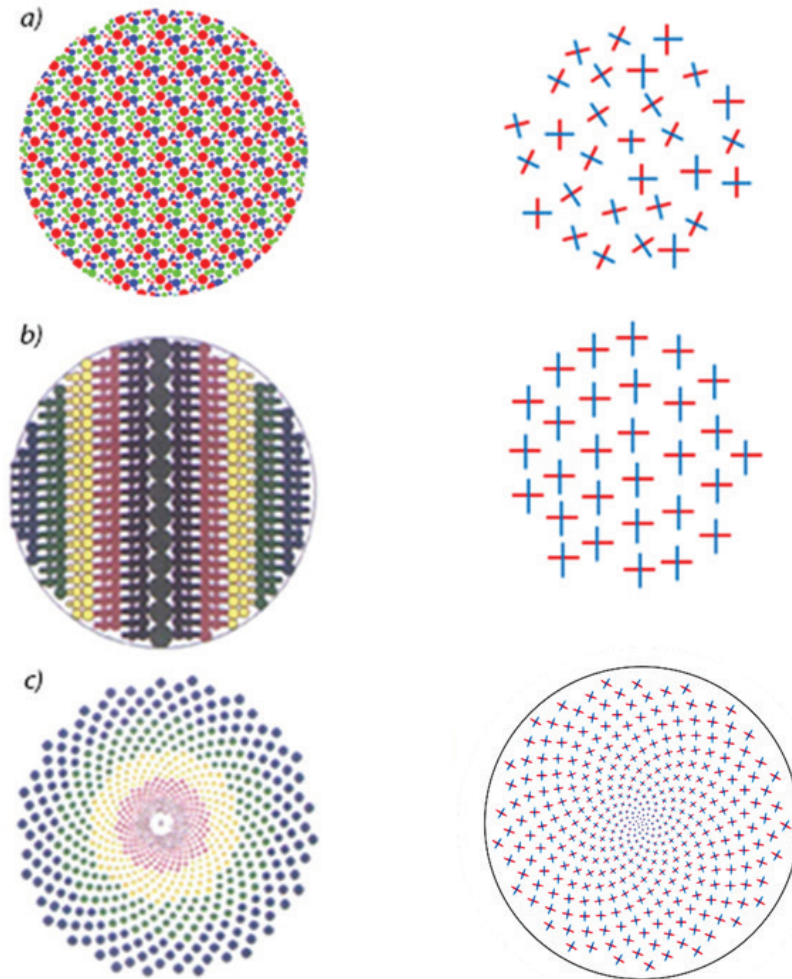


**Figure 6.30** Comparative illustration of diffuse (a), vertical linearly polarized (b) and hyperpolarized light (c). The major difference is in the orientation and organization of electromagnetic photon fields. In all three cases, the electric (blue) and magnetic (red) field are mutually orthogonal. In diffuse light, the EM field of each individual photon is „twisting“, alternatively one moment to the left, one moment to the right; viewed in entirety, the EM photon fields are randomly oriented. In the vertical linearly polarized light, the EM fields are oriented strictly vertically, and photons are organized into planes according to energy levels (wavelength/frequency/wave numbers). In the hyperpolarized light, the EM photon fields are organized into curved planes according to the Fibonacci laws, photons are organized according to energies, so that the „half quantization“ principle holds for the total orbital angular momentum, consequently also for energy, based on Planck’s constant and frequency.

## 6.6. Engineering Hyperpolarized Light Based on the $C_{60}$ Molecule

The  $C_{60}$  molecule was discovered accidentally or, better yet „when the time was right“. The three most deserving scientists for this discovery are Eiji Osawa, Harold Kroto and Donald Huffman. Osawa predicted its existence in 1973, but since his paper was published in Japanese, it went unnoticed until 1985 when the  $C_{60}$  was experimentally produced. This is primarily due to the effort of Kroto from UK, who spent his sabbatical year of a university professor at the Rice University in the USA. He worked with two colleagues: Richard Smalley and Robert Curl, and two Ph.D. candidates - Jim Heath and Sean O'Brien. The three professors set up an experiment to observe what would be produced in the collision between laser light of high power and graphite. They charged the candidates to vary the parameters of the experiment, while they „had coffee“ (at the University café) and tended administrative tasks at the University (a much harder job than experimenting). From time to time, they would look up to check the experiment progress. Until one day the students rushed in and exclaimed excitedly: „...we obtained something very unusual, what is it, we don't know ... there is only one mass peak at 720...“ The shock was complete, carbon structure with 720 mass units means that it includes 60 carbon atoms ( $720:12 = 60$ ). State of shock turned into a headache, and later into a nightmare. The riddle of the structure with 60 carbon atoms had to be solved. No easy task for chemists, because they kept thinking within the „given framework“ of chemistry, and this was something out of the cliché. They were aware that due to the existence of only one peak, all atoms are equal with respect to the center of mass. First, they concluded that the structure is not two-dimensional but three-dimensional, and equality of atoms can provide the solution only if the atoms are distributed on the surface of a sphere. Although from today's aspect this seems simple (students today grasp this in 10 seconds), it was a big breakthrough then. When they thought that they had solved the problem, they realized that they have not „crossed the river“, only a river branch. They tried to cover a sphere with hexagons with no success. Kroto recalled his children's homework of many years ago, and Smalley called in mathematicians from the University to help. Approximately at the same moment, after about ten days of deliberation, they arrived at the solution. Kroto remembered that the children, beside hexagons, used also pentagons to construct from paper the geodesic dome of the pavilion from the 1967 world fair in Montreal, and mathematicians told Smalley the solution in 30 seconds: it is based on Euler's characteristic of a polyhedron, therefore, beside hexagons, 12 pentagons must also be used. Attention, number of pentagons must always be 12, while the number of hexagons can vary. A strange rule, but this is *mathematica naturalis*! Everybody was excited waiting to see how the cut pentagons and hexagons would cover the sphere surface. When the task was completed, the headache turned into enthusiasm, Kroto proposed that the newly obtained structure be called Bakministerfuler (Buckminster Fuller, or popularly *Bucky*), after the American architect who constructed the geodesic dome of the USA pavilion in Montreal at the 1967 world fair. They wrote a paper published on November 14, 1985 in *Nature* (Figure 6.31). Besides scientific results, they enclosed a

picture of a soccer ball, to make clear the structure of the  $C_{60}$  molecule to everyone at a glance, and as a warning to researchers not to „cocoon“ within existing knowledge and accustomed ways of reasoning. Many solutions are right before our eyes, we see them, but are unable to grasp them in the right way with our „mind’s eye“. Kroto, Smalley and Curl were awarded the Nobel Prize for chemistry in 1996 for this discovery.

From the scientific aspect, it is good to know that a new structure was created, a molecular crystal that by its point symmetry is the most beautiful solid in nature, but what about the practical aspect? A single molecule of the size of only 1 nm cannot be utilized. Milligram or gram quantities of the  $C_{60}$  molecule had to be produced in order to explore its physical and chemical characteristics. Different synthesis methods were tried, using chemical methods, to produce gram-quantities of the  $C_{60}$  molecule. However, with no success for several years, although in this period, 1985–1991, theoretical physicists were also exploring this problem. They conducted research and investigated the new structure from the aspect of classical and quantum mechanics. It was calculated that this new structure should have the absorption spectra at  $528\text{ cm}^{-1}$ ,  $577\text{ cm}^{-1}$ ,  $1163\text{ cm}^{-1}$ , and at  $1429\text{ cm}^{-1}$ . Based on obtained calculations, they arrived at the approximate shape of the structure (cover illustration of *Science*, 1991, Figure 3.10, *middle*).



**Figure 6.31** Mass spectrum from the experiment with one mass peak at 720 (left) and a soccer ball (right), published in *Nature* 1985. Sir Harold Kroto symbolically presents a new structure to the world - the  $C_{60}$  molecule.

Research is full of uncertainty and unforeseeable situations as in the example of the Exxon research team, from the USA. They had the same laser system as Kroto, Smalley and Curl at the Rice University. Moreover, the lasers were constructed at the Rice University at the request of the Exxon company for their research project „alternative energy sources“. Experiments were started at Exxon with carbon, while at the Rice University silicon was used until Kroto came to Rice University and proposed experiments with graphite (carbon). The Exxon research team obtained the results and published in 1984 (Rohlfing, 1984) a year before the team from the Rice University. They obtained the  $C_{60}$  molecule, but were unaware of this. Their mass spectrum was similar to the first spectrum (under *c*, Figure 6.31) of the Rice University team. However, they could not escape the „framework“ of stereotypical reasoning, therefore, they did not adequately interpret their own result. Fortune was not on their side and they missed the Nobel Prize, although, they published a paper demonstrating that they had synthesized the  $C_{60}$  molecule first.

Completely independent from these investigations, synthesis of small carbon particles was conducted at the University of Arizona in Tucson by Prof. Donald Huffman. He was investigating the phenomenon of light scattering about giant stars, whose nuclear reactions are based on the „carbon chain“, therefore, he assumed that, in the neighborhood of „red giants“, the interstellar dust is composed of carbon particles. In order to simulate this process in laboratory conditions, he devised a chamber filled with helium gas under (varying) pressure and introduced two electrodes, a metal electrode and a graphite electrode. With adequate current intensity and voltage, he created spark discharges, which transformed graphite into a dust cloud, minute carbon particles. Because of this black dust his laboratory was not well looked upon at the University, it was considered that it polluted the environment. He started experiments already in 1974 and produced gram quantities of the  $C_{60}$  molecule (although with slight efficiency 1%–2%). Only when the theoretical physicists, in 1990, calculated the absorption spectra of the  $C_{60}$  molecule, did he decide to investigate the „carbon dust“ in this spectrum range. When he performed dust spectroscopy obtained under pressure in a reactor of 10 tor, nothing could be distinguished. However, the dust, created in the helium atmosphere under the pressure of 100 tor, contained all four absorption peaks of the  $C_{60}$  molecule. When the dust was purified by liquid chromatography, he obtained milligram carbon quantities of 95% saturation. This was a revolutionary breakthrough for the production of gram quantities, and later of much larger quantities of the  $C_{60}$  molecule.

Circumstances were such that the author of this monograph spent a year at the University of Arizona, the 1984/1985 school year, working in the field of nanotechnology (at the time this field was called molecular electronics), and in 1990, came again to the same University, occasionally traveling between Tucson and Belgrade, and stayed there until 1998. When the news of the production of milligram quantities of the  $C_{60}$  molecule circulated the University toward the end of 1991, I was present in the laboratory of Prof. Huffman. I told him that we have the Center for Molecular Machines in Belgrade with the STM/AFM device and that I wish to examine the  $C_{60}$  molecule at the nano level. I was given a few milligrams of  $C_{60}$ , and for the New-Year holidays took the plane to Belgrade. Beside competence, we also had luck and the shape of the  $C_{60}$  molecule was for the first time experimentally obtained (Figure 3.11, *right*). It must be said that the theoretical model and experimental image (produced by the Scanning Tunneling Microscope with atomic resolution) conformed very well. The paper was published in a journal (Koruga, et al., 1992), and a few weeks later, an invitation arrived from the Elsevier publishing house to write the first book on the  $C_{60}$  molecule (Koruga, et al., 1993).

However, the reader should be aware that, already in 1992,  $C_{60}$  molecule was discovered in rocky structures of north Russia, and afterwards in Colorado (USA). Moreover, it was discovered in a meteorite older than the Solar system that hit Canada many years ago. This caused a mild „disappointment“ in the originality of human endeavor within the scientific community enlightened in this problem. It had been thought that something completely new, unique, was discovered – however, it turned out that we were „knocking on nature’s open door“. A complete shock came from the MIT laboratories regarding geological fullerenes: „...gentlemen,  $C_{60}$  is found in candle’s flame ...“. Therefore, the  $C_{60}$  molecule is not exceptional in nature – it is an omnipresent form. This transition, from

the perception that  $C_{60}$  was *unique* to the realization that it is *omnipresent*, actually gave priceless value to this molecule and the icosahedral symmetry (omnipresence of the Fibonacci laws in nature).

### *Manufacturing the $C_{60}$ Molecule*

Producing the molecule  $C_{60}$  in gram quantities using the electric arc in helium atmosphere under the pressure of 100 tor, in 1990, encouraged many entrepreneurial researchers and businessmen to start manufacturing fullerene. Overnight, several smaller companies were founded, but the best known one is MER Corporation, Tucson, USA. Of course, we joined these research-development endeavors and at the end of 1997 built our first reactor for the production of gram quantities of the  $C_{60}$  molecule (Figure 6.32). Due to sanctions, the work was conducted in the USA and transferred to Serbia in 1998.

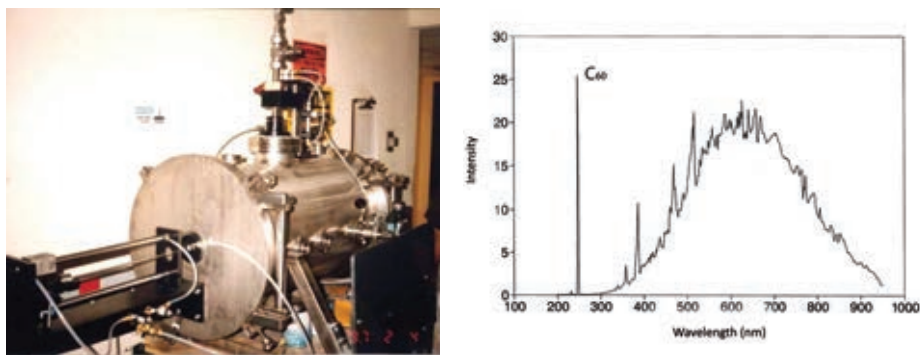


**Figure 6.32** Backy-SER reactor for the production of the  $C_{60}$  molecules (*left*) built according to the American reactor, in cooperation with researchers from the USA, financially supported by the „GOŠA“ Holding company (above all by its manager Branislav – Raf Milanović). Spectrum demonstrating that the carbon dust contains  $C_{60}$  molecules (*right*) (Matija, et al., 2011).

Using the electric arc (and other methods), „carbon dust“ was formed, it contained (in the beginning of process development) only about 2% –3% of  $C_{60}$  molecules. Later, as the technology developed, up to 24% concentration of  $C_{60}$  was obtained. The dust is purified by chemical methods to obtain 95–99.95% saturation. There is also concentration of 99.99%, but it is very expensive.

### *Thin Films Based on the $C_{60}$ Molecule*

Thin  $C_{60}$  films are produced either by the CVD method (chemical deposition of  $C_{60}$  molecules on a scaffold) or by sputtering (physical method). In the first case, the  $C_{60}$  molecules are in the form of powder, and in the second case in solid state (usually powder pressed into tablets).

The energetic HOMO-LUMO gap in the  $C_{60}$  molecule varies depending on how the  $C_{60}$  molecules are distributed in the thin film. When the organization is adequate, *black* powder color is transformed into *yellow* color of the thin film with transparency up to 95%. Thickness of the thin film can vary; thickness of 30 nm to 250 nm is usually produced for various usages (presently for protection from the UV radiation and for the modification of the EEG signal under the influence of light on the CNS via eyesight).



**Figure 6.33** Thin film of  $C_{60}$  molecules 60 nm – 100 nm thick on a glass scaffold. Distribution of  $C_{60}$  molecules in the film. Due to  $\pi$  electrons present in each  $C_{60}$  molecule, repulsive forces are generated and the molecule rotates freely about  $3 \times 10^{10} \text{ s}^{-1}$  (Koruga, Dj, PCT Patent US2008/0286453 A1, Applicant DVB Global USA).

### Nanophotonic Material $C_{60}$ @ PMMA



**Figure 6.34** Possible organization of  $C_{60}$  into a polymer material PMMA, HEMA, etc. (left). Ambient photographed by a camera with and without the nanophotonic filter. The maximum peak of hyperpolarized light with reorganized photons equals 728 nm. To achieve this, the filter thickness should be about 20 nm. The second part of light energetically transformed is in the domain of far infrared light (Koruga, Dj, Int. Pat. App. PCT/EP2016/063174, 2016, WO 2017/211420 A1, Publication date December 14<sup>th</sup> 2017, Applicant Fieldpoint, Cyprus/ ZEPTEP GROUP).

The second method for the production of the photonic material based on  $C_{60}$  is by incorporating  $C_{60}$  molecules into a transparent polymer material. Why does the basic material have to be a monomer? The answer is that the base material should enable the  $C_{60}$  molecule to be physically placed between monomers. It should not bind chemically,



thus working temperatures must not exceed 289°C which would sever the double C=C bonds in hexagons (one liberated bond later binds the C<sub>60</sub> molecule to the polymer and thus prevents rotation of the C<sub>60</sub> molecule). Figure 6.34 displays a possible distribution of C<sub>60</sub> molecules in the polymer PMMA material. Materials obtained in this way are denoted as C<sub>60</sub>@PMMA, indicating that the C<sub>60</sub> molecule is incorporated into the polymer.

When Figures 6.33 and 6.34 are compared, it can be seen that the transparency of C<sub>60</sub>@PMMA and thin film of C<sub>60</sub> is the same, indicating that C<sub>60</sub> molecules are regularly distributed in the basic (PMMA) material. Surfaces of 15 mm in diameter are obtained according to the principle of contact lens material production, technology is being developed and very high quality nanophotonic materials are obtained. However, in producing material of larger diameters problems arise that have to be managed „during work“, because a new production technology has to be established. Presently, plates of 350 mm have been produced, which is adequate for the production of nanophotonic devices of various diameters.

### System for the Generation of Hyperpolarized Light

The system for the generation of hyperpolarized light has three main elements: (1) diffuse light source, (2) polarizer transforming diffuse light into the vertical linearly polarized light, (3) nanophotonic polarizer transforming vertically polarized light into hyperpolarized light.

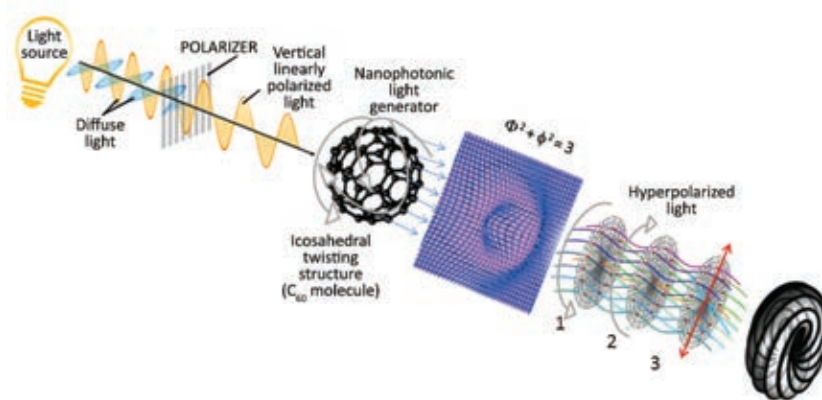


**Figure 6.35** Schematic representation of the nanophotonic light generation. The key element is the icosahedral twisting structure (C<sub>60</sub> molecules incorporated into the polymer material) generating photon distribution by creating a 2D energy membrane [ $\Phi^2 + \phi^2 = 3$ ] which „filters“ propagating photons according to the Fibonacci law [ $\Phi, \phi$ ]. The final output is a Fibonacci twisting torus resulting from the dynamics of three (1, 2, 3) energy forms (left helix  $\phi$ , right helix  $\Phi$ , and attractive-repulsive interactions determining the value at each intersection of the left and the right helix). (Koruga, Dj., Int. Pat. App. PCT/EP2016/063174, 2016, WO 2017/211420 A1, Publication data December 14<sup>th</sup> 2017, Applicant FIELDPOINT, Cyprus/ZEPTEK GROUP).

Diffuse light can produce different spectra. When the UV radiation is present, it will be partly absorbed (by the  $C_{60}$  molecule), and partly transformed into light of a different wavelength (one part toward the red spectrum, and the other part in the domain of vibrational-rotational frequency modes). Blue light (wavelength up to 475 nm) is absorbed and reemitted in a similar way. There is minimum radiation transformation into thermal energy, so that the nanophotonic filter is heated only slightly. The existing radiation source of 350 to 1070 nm has two main spectral intervals: from 470 nm to 1050 nm, with the maximum peak at 728 nm (red), and another interval, from 5000 nm to 35000 nm, with 64 peaks, the vibrational-rotational spectrum interval (Table 6.3). The first spectral interval is used to influence the electronic states of tissue, and the second for the vibration and rotation modes of biomolecules.

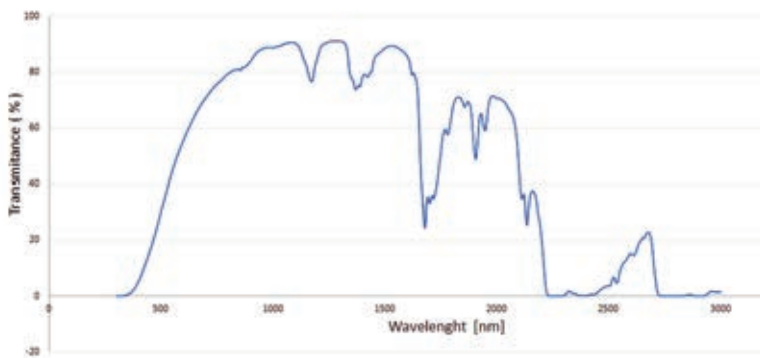


**Figure 6.36** Transmittance by the nano photonic filter of 0.034 percentage of  $C_{60}$  molecules into PMMA. UV and high blue (up to 415 nm) energies are absorbed. Transmittance with different percentage exists until 2200 nm. Between 2200 nm and 3000 nm, there is a peak at 2688 nm with transmittance 20.68%.

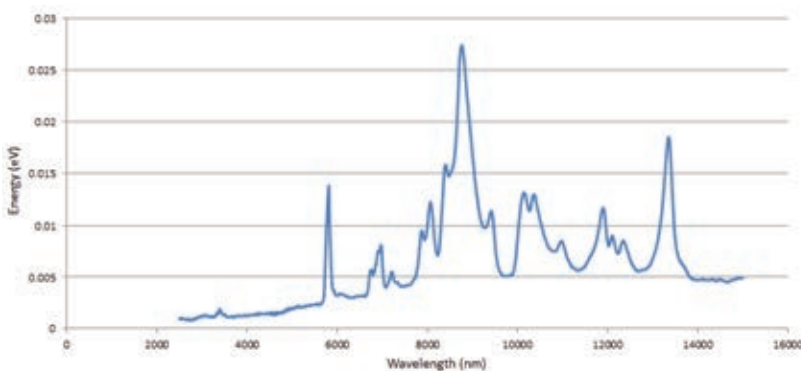


**Figure 6.37** Rotation-vibration energy of nano photonic material with 16 peaks in the range of 3000 nm to 15000 nm. There are three characteristic peaks: 5811 nm (0.0133 eV), 8732 nm (0.0268 eV) and 13300nm (0.0181 eV)

## References

1. Alonso, M., Finn, E.J., Physics. Addison-Wesley, Harlow, 1992.
2. Ballantine K. E., Donegan, J. F., Eastham. P. R., There are many ways to spin a photon: Half-quantization of a total optical angular momentum. *Science Advances* Vol. 2, no. 4, pp. 1-7, 2016.
3. Dal Negro, L., Oton, C. J., Gaburro, Z., Pavesi, L., Johnson, P., Lagendijk, A., Righini, R., Colocci, M., Wiersma, D. S., Light Transport through the Band-Edge States of Fibonacci Quasicrystals. *Physical Review Letters*, VOL. 90, No. 5, pp. 055501-1-4, 2003.
4. Elliott, J.P., Dawber, P.G., Symmetry in Physics. Vol. 1 and Vol. 2, Oxford University Press, New York 1990.
5. Fleisher, A., Bordo, E., Kfir, O., Siderenko, P., Cohen. O., Polarization-fan high order harmonics. *J. Phys.B: At Mol Opt Phys*, 50, 034001, 2017.
6. Feynman, R.P., QED: The strange theory of light and matter. Princeton University Press, Princeton and Oxford, 1985.
7. Harris, D.C., Bertolucci, D.M., Symmetry and Spectroscopy: An introduction to Vibrational and Electronic Spectroscopy. Dover Publications, New York, 1978.
8. Harter, W.G., Weeks, D.E., Rotation-vibration spectra of icosahedral molecules Icosahedral symmetry analysis and fine structure. *J. Chem. Physics*, 90 (9): 4724-4743, 1989.
9. Harter, W.G., Reimer, T., Rotation-vibration spectra of icosahedral molecules III. *J. Chem. Physics*, 94 (8): 5426-5434, 1991.
10. Hargittai, I., (ed) Fivefold symmetry. World Scientific, Singapore, 1992.
11. Hayden, G.W., Mele, E.J.,  $\pi$  bonding in the icosahedral  $C_{60}$  cluster. *Phys. Rev. B.*,36(9): 5010-5015, 1987.
12. Huffman, D.R, Solid  $C_{60}$ . *Physics Today*, 44: 22-29, 1991.
13. Icke, V., *The force of symmetry*.Cambridge University Press, Cambridge 1995.
14. Jex, I., Alber, G., Rotational wavepacket dynamics of the  $C_{60}$  molecule. *J. Phys.B: At Mol Opt Phys*, 33,1663-1674, 2000.
15. Karimi, E., Schulz, S.A., De Leon, I., Qassim, H., Upham, J., Boyd, R., Generating optical orbital angular momentum at visible wavelengths using a plasmonic metasurface. *Light: Science and Application*, 3,e167;doi10.1038/Isa.2014.48, published 9 May 2014.
16. Koruga, Dj., Hameroff, S., Withers, J., Loutfy, R., Sundereshan, M., Fullerene  $C_{60}$ : History, Physics, Nanobiology, Nanotechnology. North-Holland, Amsterdam, 1993a.
17. Koruga, D., Simic-Krstic, J., Trifunovic, M., Jankovic, S., Hameroff, S., Withers, J.C., Loutfy R.O., Imaging Fullerene  $C_{60}$  with atomic resolution using Scanning Tunneling Microscope. *Fullerene Science and Technology*, 1, 93-100,1993b.

18. Koruga, Dj., Nikolić, A., Mihajlović, S., Matija, L., Nanomagnetic Behaviour of Fullerene Thin Films in the Earth Magnetic Field in Dark and Under Light Polarization Influence. *Journal Nanoscience Nanotechnology*, Vol.5: 1660-1664, 2005.
19. Koruga, Dj., Apparatures for Harmonized Light. PCT Patent US2008/0286453 A1, owned by DVB Global USA, date of publishing 20. November 2008.
20. Koruga, Dj., Optical filter and Method of manufacturing an optical filter. Int. Pat. App. PCT/EP2016/063174, 2016, owner ZEPTER-BIOPTRON, Switzerland, patent application by Fieldpoint, Cyprus.
21. Kratsschmer, W.M., Lamb, L.D., Fostropoulos, K., Huffman, D., Solid  $C_{60}$ : a new form of carbon. *Nature*, 347:354-358, 1990.
22. Liu, X., Xu, Y., Zhu, Z., Yu, S., Guan, C., Shi, J., Manipulating wave polarization by twisted plasmonic metamaterials. *Optical Materials Express*, Vol.4, No.5:1003-1010, 2014.
23. Markus, A., Nairz, O., Vos-Andrea, J., Klier, C., van der Zouw, G., Zeilinger, A.: Wave-particle duality of  $C_{60}$  molecules, *Nature*, 401:680-680, 1999.
24. Matija, L., Enohedralni fulereni, Zadužbina Andrejević, Beograd, 1999.
25. Matija, L., Kojić, D., Vasić, A., Bojović, B., Jovanović, T., Koruga, Đ., Uvod u nanotehnologije. Nauka, Beograd, 2011.
26. Miransky, V.A., *Dynamical Symmetry Breaking in Quantum Field Theory*. World Scientific, Singapore, 1993.
27. Morton, J.J.L., Tyryshkin, A.M., Adavan, A., Benjamin, S.C., Porfirakis, K., Lyon, S.A., Briggs, A.G.D., Bang-bang control of fullerene qubits using ultrafast phase gates. *Nature Physics*, 2005, doi:10.1038/nphys192.
28. Rohlfing, E.A., Cox, D.M., Kaklor, A., Production and characterization of supersonic carbon cluster beams. *J.Chem. Phys.* 81(7):3322-3326, 1984.
29. Russell, H. N., Saunders, F.A., New Regularities in the Spectra of the Alkaline Earths. *Astrophysical Journal*, vol. 61, p. 38, 1925.
30. Schuster, H.G. Just, W., *Deterministic Chaos: An Introduction*. Wiley-VCH, Weinheim, 2005.
31. Shannon, C.E., Weaver, W., *The Mathematical Theory of Communication*. Illini Books, 1963.
32. Strogatz, S.H., *Nonlinear dynamics and chaos: With Application to Physics, Biology, Chemistry, and Engineering*. Westview/Perseus Books, Cambridge, 1994.
33. Wang, J., Yang, J-Y., Fazal, I.M., Ahmed, N.Y., Huang, H., Ren, Y., Yue, Y., Dolinar, S., Tur, M., Willner, A. E., Terabit free-space data transmission employing orbital angular momentum multiplexing. *Nature Photonics* 6, 488-496, 2012, doi:10.1038/nphoton.2012.138
34. Zettili, N., *Quantum Mechanics: Concept and Applications*. John Wiley and Sons, Chichester, 2009.

# 7

## APPLICATION OF HYPERPOLARIZED LIGHT IN MEDICINE



*Engineering without medicine is blind,  
medicine without engineering is feeble*

This chapter presents two studies and nine case studies of hyperpolarized light implemented in medicine. The first study was conducted on a sample of 32 research subjects (7 males and 25 females, aged between 26 and 63 years) whose biophysical skin status and skin modifications under the influence of hyperpolarized light were determined. The first study was conducted at the BIOPTRON center in Belgrade.

Medical cases treated by doctors of the general medical practice ZEPTEK MEDICAL in Belgrade are also described. The following cases were treated: burns, skin lichenization (pruritus), burn wounds, psoriasis, acne, bronchial asthma, spondylolisthesis, lumbar syndrome, and chronic venous insufficiency. A short introduction to each problem is given, case described, treatment protocol presented, mechanism of hyperpolarized light action explained, treatment results displayed, and a conclusion is given.

The second study investigates effects of daylight acting via eyesight on the brain and EEG signals. Twelve research subjects participated in the study; light effect on the brain was implemented using glasses made of fullerene thin film. The study was conducted at the Medical Faculty of the Belgrade University and at the Military-Medical Academy in Belgrade.

## ***7.1 Effects of Hyperpolarized Light on Biophysical Skin Status***

*Duro Koruga, Laboratory for Biomedical Engineering, NanoWorld AG, Belgrade*

The biophysical skin status depends primarily on the adequate relationship between water and lipids in the epidermis, collagen and elastin in dermis, and on the status of the basement membrane. This study examines the biophysical skin status based on the water status and the interaction between water and lipids. The method of opto-magnetic imaging spectroscopy (OMIS) was used for the identification of the biophysical skin status.

## Introduction

Epidermis, the outermost skin layer, does not contain blood vessels and represents the main barrier preventing fast water evaporation and heat loss on the one side, and excess penetration of radiation, minute particles and pathological microorganisms on the other. Dermis, the inner skin layer, is characterized by good vascularization and abundant presence of collagen and elastin. They are bonded, and at the same time separated, by the undulated dermo-epidermal membrane of very complex structure. The hypodermis is located below dermis, separated from the muscular tissue by fiber structures. Human skin contains 65% -70% of water, depending on age and sex.

Collagen, the protein most frequently found in the skin, was discussed in Chapter V. Collagen of type I is prevalent in the skin, followed by type III collagen, and types IV, VI and VII. Collagen is found throughout dermis. It is considered that mutations of type VI collagen are linked with the development of myasthenia and wasting of muscular tissue.

Elastin fibers display good flexibility, i.e., attractive-repulsive capabilities: ability to be easily deformed, and yet to return to original state after skin distortion. The anisotropic nature of skin structure is complex, so we cannot attribute specific mechanic features to any particular component. However, the system of elastin fibers is the basis for tissue elasticity. Elastin fibers can be formed from several components, such as cross-linked elastin fibers, microfibrils rich with fibrillin, glycoproteins bonded by microfibrils (MAGPs), fibulins, proteins for bonding the latent TGF $\beta$  (LTBPs).

Skin aging occurs with time (the so called „internal“ or „chronological“ aging) or due to the cumulative effect of external factors („external“ aging). UV radiation is the most important external factor, thus this type of aging is often called „photoaging“. Regardless of the dominant aging cause, skin becomes wrinkled, rigid, less capable of following movement without consequence, etc. Both aging processes are associated with phenotype modifications within skin cells, although crucial functional manifestation of aging results from structural and composition remodeling of otherwise long-living proteins of the extracellular matrix (ECM) within dermis.

In chronologically aged skin, fine wrinkles are formed, elasticity is reduced (impaired coordination of skin with face/body movement and capability of skin to contract after dilatation). The same changes, although much more pronounced, occur in the photodegraded skin, probably as a result of excess exposure to UV radiation. The most significant modifications in both aging types are found in the ECM, on fibrillar proteins – collagen, elastin and proteoglycans that provide flexibility, elasticity, i.e., hydration. These molecules have very long life compared with proteins within the cell making them susceptible to the accumulation of impairments, which, in turn, reflects on their ability to provide adequate mechanical features and maintain tissue homeostasis. Half-life of the internal cell proteins is measured by hours, at most days, yet many ECM proteins live for years; collagens of type I and II in the skin connecting tissue have a half-life of 15-95 years, while elastin fibers age matches the age of the organism. Elastin synthesis occurs in the fetal period, or in the early postnatal period, through post-translation mechanisms, which control the decay of the mRNA elastin in adults. Therefore, human elastin fibers last many years and accumulation of impairments occurs often by cross-linking via glucose, by accumulation



of calcium or lipids, or by the modification of aspartic acid remains with time. All this affects mechanical characteristics of tissues rich with elastin, decreasing the ability of aged arteries, lungs and skin to deform and adapt to the performance of the organism.

With age, approximately 20% of the dermis layer is reduced, it disappears. The number of cells and blood vessels in aged skin dermis is decreased. Collagen creation is reduced and fragmented elastin fibers are formed. Collagen and elastin, as insoluble proteins of the dermis matrix, naturally have numerous intra-molecular and inter-molecular bonds. Collagen is the protein most frequently found in humans; it is the primary structural component of dermis, representing 70% of the skin dry mass. In aged skin, collagen has thickened fibrils, organized in bundles, resembling cords, haphazardly oriented within dermis. Less collagen is synthesized in aged fibroblasts. In chronologically aged skin, atrophy is present in epidermis and dermis with the loss of the undulating structure of the basement membrane (Gawkrodger, 2002). In young skin, collagen of type I constitutes 80% of the skin mass, while collagen of type III makes approximately 15% of the overall skin collagen. In older skin, this relationship is changed: there is a sizeable reduction in type I collagen, and type III collagen becomes prevalent. With aging, the overall collagen quantity per area unit is reduced by approximately 1% per annum. In skin exposed to radiation, level of type I collagen is reduced by 60%. This reduction is explained by increased photodegradation. Aging effects in dermis are present not only in type I collagen, but in other collagen types as well.

Collagen of type IV is the basic component of the dermo-epidermal membrane. It forms a structural lattice for other molecules, and plays the main role in maintaining mechanical stability. No significant differences were found in the type IV collagen quantities between the photoexposed and normal skin, although a considerably reduced quantity was found in the wrinkle base compared to lateral surfaces of the wrinkle. Mechanical stability, created by the dermo-epidermal membrane, can be additionally compromised by the loss of collagen of type IV aiding to wrinkle formation. Collagen of type VII is the main component of fibrils, which connect the zone of the basement membrane to the papillary dermis situated immediately below it. A significantly reduced number of fibrils was found in patients with chronically photo-exposed skin with respect to the normal, unexposed skin (Gawkrodger, 2002). It is possible that wrinkles are formed as a result of the weakened bond between dermis and epidermis, due to the degradation of fibrils connecting them. Loss of type VII collagen is much more pronounced at the wrinkle base, than in the lateral wrinkle surfaces.

## *Material*

The research objective is the investigation of the biophysical skin status of epidermis (without the horny layer) and dermis (up to the hypodermis- the adipose tissue) (Figure 7. 1-1). Research was conducted on the left and right forearm (Figure 7.1-7).

As noted, biophysical skin's status depends primarily on the adequate relationship between water and lipids within epidermis, collagen and elastin in dermis, and on the basement membrane status. Water in the epidermis is found mostly within the stratum

granulosum (Figure 7.1-2), between cells and the lipid layer. When the lipid layer is adequately organized (adequate lipid layer thickness), water needs more time to perfuse the epidermis to the outer skin layer (horny layer). In case of thinner lipid layers, water is detained shorter in the skin and evaporates faster. In this case, we say that the loss of water through epidermis is accelerated and that biophysical skin status is inadequate.

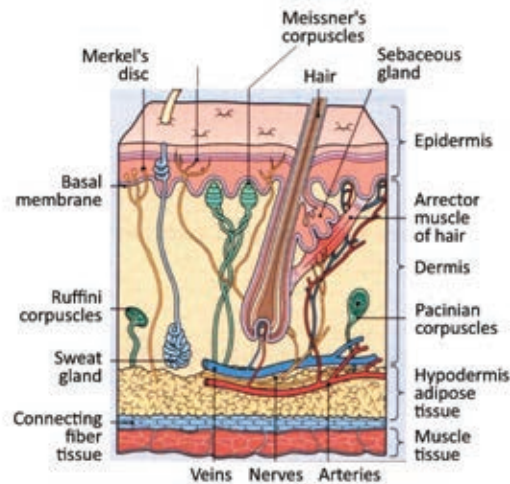


Figure 7.1-1 Schematic representation of skin cross section and its basic structural elements (Adapted from: Graham-Brown, 1998).

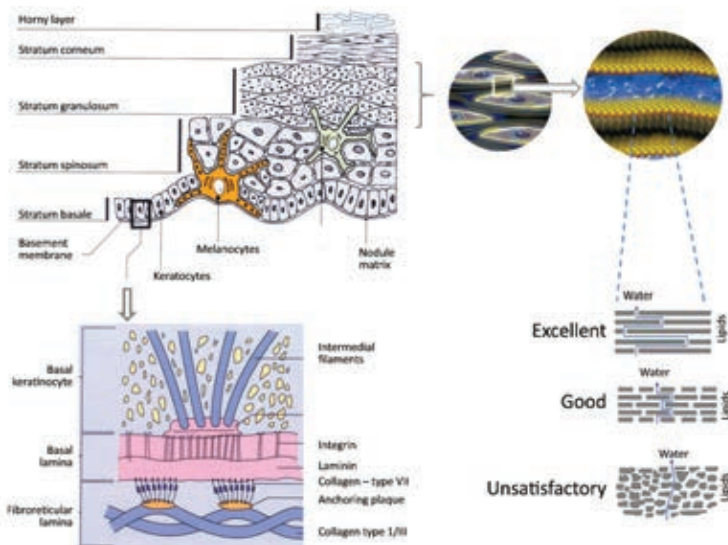


Figure 7.1-2 Schematic representation of main skin layers (strata), basement membrane, the relationship between lipids and water in epidermis and TEWL (trans-epidermal-water-loss) (Adapted from: Gawkrödger, 2002; Fluhr, 2005).

The basement membrane status also affects significantly the biophysical skin properties. If it is regularly undulated, with small prominences and depressions it has an adequate biophysical status. However, when collagen fibers, forming the reticular lamina of the basement membrane (Figure 7.1-2 and Figure 7.1-3), disintegrate or their number is reduced, depressions are formed resulting in wrinkles, skin becomes less elastic. Collagen of type I is reduced, collagen of type III expands, consequently the skin biophysics is impaired due to their different mechanical characteristics.

Skin biophysics is a complex phenomenon; it is established that inadequate organization of water (for example, in lipid layers) and collagen (in the basement membrane and dermis), especially its loss, leads to drastic modifications of biophysical skin characteristics.

This research will focus especially on the role of water in the skin; the method for the biophysical skin characterization will be adapted to this objective.

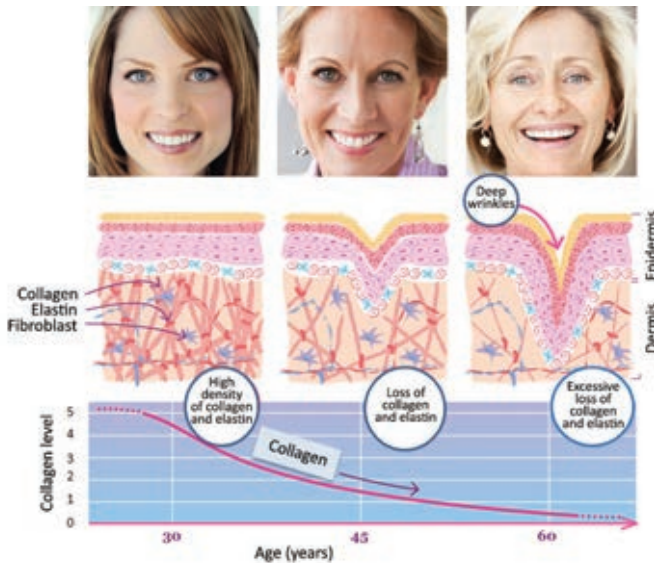
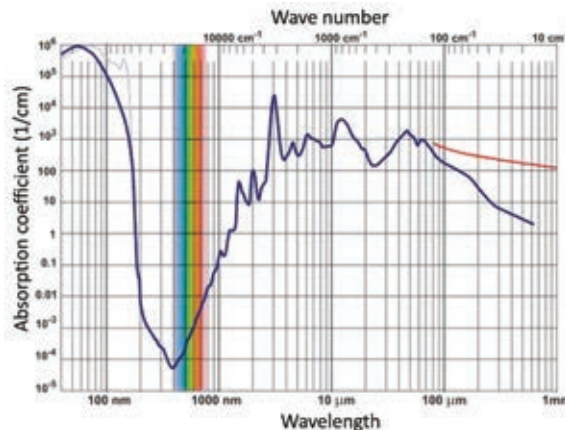


Figure 7.1-3 Age-related reduction of collagen and elastin (Adapted from: [www.gold-collagen.com](http://www.gold-collagen.com)).

## Methods

### Characterization of the Biophysical Skin Status

Characterization of the biophysical skin status will be based on the light-matter interaction. Therefore, understanding of absorptive, reflexive, and pulverization water features for different wavelengths is necessary. Figure 7.1-4 shows that the absorption (reflection) coefficients for the blue and red light differ by 100 times. This water feature will be used to obtain adequate information on skin biophysics and the influence of water on its status.



**Figure 7.1-4** A diagram of absorption (reflection) coefficient of water for different wavelengths. For blue light, the coefficient is of the order  $10^{-4} \text{ cm}^{-1}$ , while for the red light  $10^{-2} \text{ cm}^{-1}$ . The difference of absorption/reflection coefficients between the blue and the red light is 100 times (Chaplin, 2008).

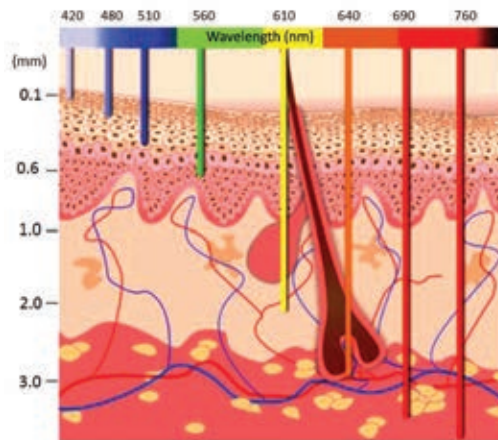


**Figure 7.1-5** Skin penetration depth of visible light of wavelengths 400nm -800nm. Blue light penetrates through the horny layer and a part of the stratum corneum, while the red light penetrates up to the hypodermis (Adapted from: Jacques, 2013).

In order to obtain actual information on the biophysical skin status based on the presence of water, it is necessary to apply a method to eliminate information on the horny layer (because water coming from dermis is not present here, only water coming externally can be present, which is not relevant for skin humidity), and the first part of the stratum corneum (which is about to start scaling).

Opto-magnetic imaging spectroscopy (OMIS) was chosen from the available methods for skin characterization. This method exhibited good results in the characterization of skin and its layers (Koruga, et al., 2010, Koruga, et. al., 2012), and in the characteri-

zation of healthy/morbid tissue (Matija, et al., 2014; Papić-Obradović, et al., 2010) and contact lenses (Stamenković, et al., 2010). The method is based on the interaction of white diffuse light (W) and reflected white polarized (P) light; the blue channel (B) is subtracted from the red channel (R) obtaining (R-B)(W-P) as shown in Figure 7.1-6 (Koruga, Tomić, Patent US No. 14/695,990.2009 *Published after filing*).

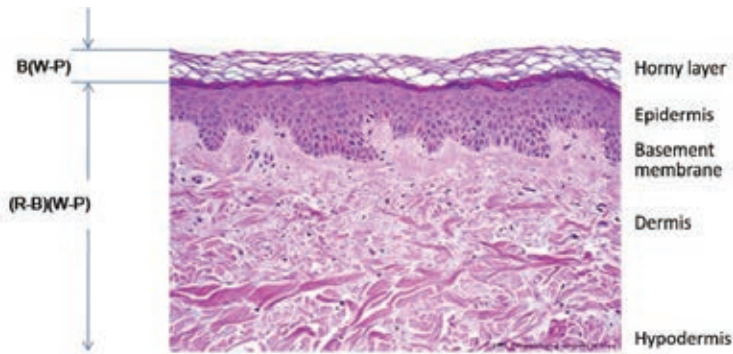


**Figure 7.1-6** Principle of opto-magnetic imaging spectroscopy applied to determine the skin biophysical status (Koruga, 2009).

The protocol of the biophysical skin status imaging before and after the treatment, and the treatment itself, is as follows: at temperature 22°C, humidity 45%, in a day-light ambient, research subjects were seated, arm relaxed on a pillow on the table in front of them (Figure 7.1-7). Before treatment, the selected location on the left and the right forearm was recorded (contralaterally, the inner side, hairless location) with white light (W) and with the same light under Brewster's angle for water-air of 53° (light, after being reflected from the skin, is linearly polarized). Because of water dynamics (Figure 5.22) the tissue image was taken ten times; data were memorized, and processed later according to the given algorithm. Immediately after the imaging was completed, tissue treatment started of the right arm only (at the same location that was recorded) with hyperpolarized light. The clearance from the tissue was 10 cm, treatment duration 10 min,  $\lambda = 450-900$  nm, light source power 20W, specific energy density 40 mW/cm<sup>2</sup>, light energy per minute 2.4 J/cm<sup>2</sup>, opto-magnetic field 10 nT. After the treatment had been completed, the same location was characterized by the device for opto-magnetic spectroscopy. Results of the same location before and after treatment are displayed on diagrams, where the  $x$ -axis displays the difference of wavelengths (nm), and the  $y$ -axis the dynamics of intensity change of tissue paramagnetism/diamagnetism (water, its status and its interaction with other biomolecules is the main cause of these modifications).

The recorded results of the left and right arm (contralateral position) enabled insight into similarities and differences of the biophysical skin status of the left and the right body part (it is a well established fact of science that in some people this difference is more and in some people less pronounced, depending on gene expression, hormone status, and sex).

### Skin Treatment

As outlined in the section referring to the protocol, the subject's right arm (forearm) was treated with hyperpolarized light; the patients volunteered to be examined. In order to compare the results of the study, the subject's left arm was treated with linearly polarized light after imaging. The power spectrum of corresponding wavelengths in the visible spectrum of the hyperpolarized light (*blue* curve) and the vertical linearly polarized (*red* curve) light is represented in Figure 7.1-7 *left* – for wavelengths of 400 nm -1000 nm and *right* – for wavelengths of 1000 nm –50000 nm. The wavelength of approximately 680 nm is crucial regarding the number of photons in the linearly polarized and hyperpolarized light. In the first spectrum region, wavelengths are redistributed, giving the specific energy density by approximately 40% less for the hyperpolarized (HP) light than for the linearly polarized (LP) light, although the areas below spectral lines are approximately the same ( $[LP-HP]_{400-680\text{ nm}} \approx [HP-LP]_{680-1000\text{ nm}}$ ). As a rough estimate, we can assume that the average wavelength is  $\lambda_I = 540\text{ nm}$  within the 400 nm -680 nm interval, and  $\lambda_{II} = 840\text{ nm}$ , so the ratio of the specific energy densities is  $E_{II}/E_I = 64\%$ . For wavelengths greater than 1000 nm, the LP light acts up to 3000 nm, while the HP light has effect up to 38000 nm; these energies act on vibrational and rotational biomolecular modes.

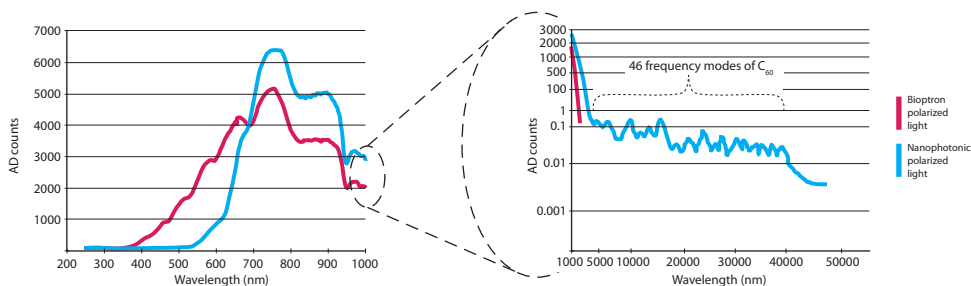


**Figure 7.1-7** The spectrum of hyperpolarized (HP) and linearly polarized (LP) light across the 400 nm -40 000 nm interval. The LP light acts within the interval 400 nm -1100 nm, while the HP light acts in the interval 470 nm-38000 nm. However, the LP light contains photons of higher energy in the interval 400 nm -680 nm compared to HP light (having more photons of low energy), so that the difference in the specific energy density is 36%. Therefore, the LP light acts mostly on electron states of valence electrons (80%) and vibration modes (20%), while the HP light acts 30% on electron states of valence electrons and 70% on vibrational and rotational biomolecular modes.

As shown in Figure 7.1-7 and Figure 7.1-8 (*left*), light source of the LP and HP light has an adequate spectrum (same lamp), because the optimal peak necessary to effect the *water-lipid* interaction is in the interval 720 nm -760nm (Jacques, 2013). Therefore, the critical light energy necessary to rebuild the destructed *lipid-water* layers is within the 720 nm -760nm wavelength interval. Because the HP light has greater number of photons in this interval ( $\sim 6400/5050 = 1.27$ ) than the LP light, the HP light is approximately 27% more efficient than LP light for this process. This is due not only to the energy input

into tissue, but also regards photons (their wavelength) taking part in the treatment. In order to activate something, or if functionality is impaired, it is necessary to provide a certain energy amount per unit of time. However, this is a necessary condition (energy threshold), although not a sufficient condition. The necessary and sufficient conditions must be satisfied: the adequate amount of energy per unit of time should be applied to reach the *action threshold* (necessary condition), however, this amount of energy should be composed of photons whose quanta interact resonantly with the structure in order to be absorbed by it.

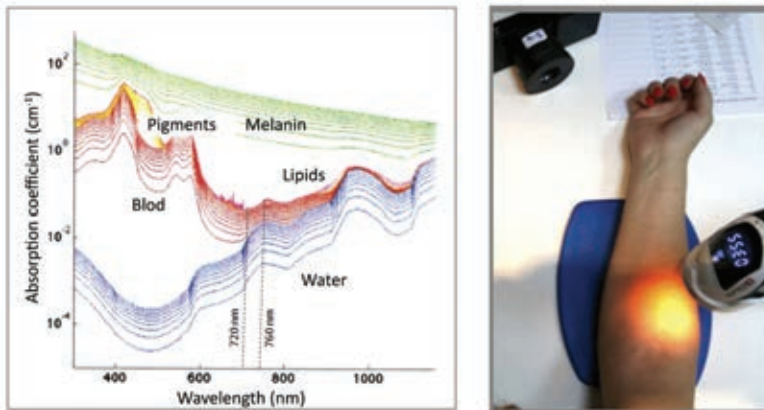


**Figure 7.1-8** Optical characteristics of some biological structures such as water, lipids, melanin, etc., in the interval 400 nm -1000nm (left). It can be observed that the critical wavelength for the lipid-water complex in the epidermis is between 720nm -760nm (Jacques, 2013). Application example of hyperpolarized light (right) used in the study (BIOPTRON HP was fixed at a distance of 10 cm from the arm, which was motionless about 10 minutes during treatment).

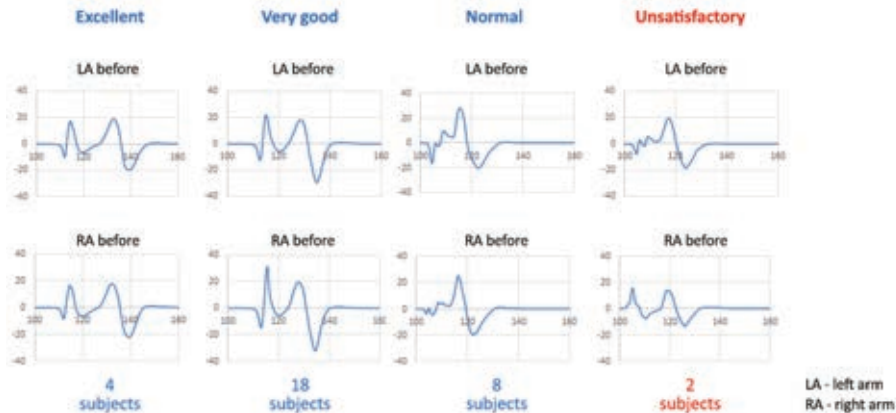
## Results

Results of 32 research subjects were grouped into four categories according to the biophysical skin status: *excellent*, *very good*, *normal* and *unusual*. Four research subjects had excellent biophysical skin status, eighteen very good, eight normal (good, i.e., average) and two subjects had unusual skin status.

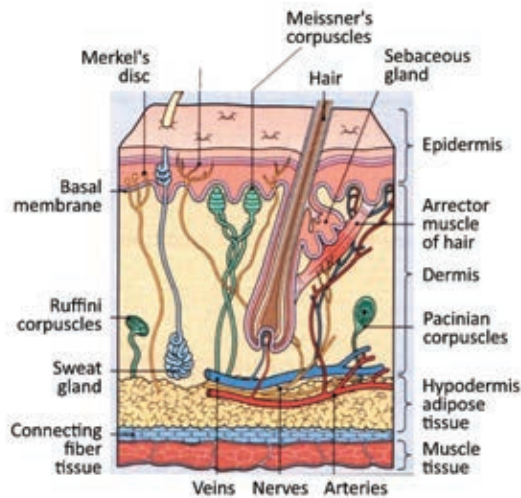
Under the influence of hyperpolarized light, the skin's biophysical status was modified. In four research subjects, having excellent biophysical skin status, no change in the skin status occurred, while in research subjects with very good skin status slight modifications, about 3% -5%, occurred. Since the accuracy of repeatability of the opto-magnetic spectroscopy is 99.2% for rigid bodies, while for biological samples it is 98.5%, and for *in vivo* imaging 97.4%, it can be said that up to 4.5% modifications of the biophysical skin status occurred. In research subjects with normal skin status, modification was at most 15%, while in research subjects with unusual biophysical skin status up to 50%.

Figure 7.1-10 displays two cases of modified biophysical skin status. The first case is from the category *unsatisfactory*, and the second is from the category *normal*. In both

cases, the biophysical skin status, according to the diagram shape, was in the category *excellent*, although by the intensities of peaks in the category *very good*. Therefore, under the influence of hyperpolarized light initial improvement of the biophysical skin status occurred, from the aspect of water status in lipids (primarily), and regarding the interaction between water and collagen (secondly).



**Figure 7.1-9** Summary results of biophysical skin status investigation in 32 research subjects grouped into IV categories: (I) excellent biophysical skin status had 4 research subjects, (II) very-good -18 subjects, (III) normal -8 subjects and (IV) unsatisfactory- 2 subjects.



**Figure 7.1-10** „Case 1“ – in the subject that had unsatisfactory biophysical skin status before treatment, after treatment with hyperpolarized light an improvement was registered. Local skin region (Figure 7.1-8) after treatment reestablished excellent local biophysical status. „Case 2“ was from the category normal, yet after being treated with hyperpolarized light the subject was classified into the category „very good/excellent“.



## Discussion

Interaction Type	Covalent (molecules)	Non-covalent (intermolecular)
Bond type	Chemical	Physical (Van der Waals, hydrogen, ionic, dipole, etc.)
Energy (kJ/mol)	4-60	0.02-4.5
Stability	Stable	Open to change
Contribution to free energy $\Delta G$	Primary $\Delta H$	Both $\Delta H$ and $\Delta S$
Nature	Chemical reaction	Physical interaction
Solvent influence	Secondary	Primary
Establishment of cooperative bonds	Little importance	Very important

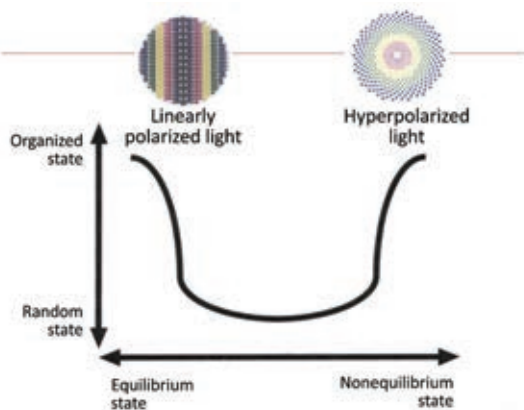


**Figure 7.1-11.** Table of interaction categories (covalent interactions) needing photons of higher energies (in the domain of visible spectrum) (*left*), and categories needing photons of lower energies (non-covalent interactions) (*right*).

While treating research subjects with hyperpolarized light (right forearm), the left arm was treated (contralaterally) at the same time with vertical linearly polarized light. It was already mentioned that results in this case are better with hyperpolarized light by approximately 27%. We presented the cause for this and described the reason for satisfying necessary and sufficient conditions. However, we need to clarify the nature of influence from the aspect of covalent and noncovalent bonds, of stability, Gibbs free energy, the nature of reaction (chemical reaction or physical interaction), influence of the solvent and the establishment of cooperative bonds. Explanation of these effects is systematically displayed in the table of Figure 7.1-11 (*left*). The same Figure (*right*) shows primarily successful effects of linearly polarized and of hyperpolarized light. Linearly

polarized light has a better effect due to the photon emission of higher energies in equilibrium states, in covalent bonds, where there is a primary effect of enthalpy ( $\Delta H$ ), in chemical reactions, when there is the secondary effect of the solvent (water), and where there is a slight effect of cooperative bonds. However, in nonequilibrium states, where establishing of cooperative bonds is very important, where the solvent (water) plays an important role, and physical (intermolecular) interactions are significant, where beside enthalpy, entropy ( $\Delta S$ ) is significant, which is via the state probability associated with information, hyperpolarized light exhibits better therapeutic results. Hyperpolarized light, in case of the *water-lipid layers* system, has a better effect on water, which is one of Fibonacci structures with pronounced dependence on entropy and significance of cooperative bonds (non-covalent hydrogen bonds), while linearly polarized light has a positive effect, via dipole moments, on lipids (it acts as a „comb“).

## Conclusion

Initial study of the biophysical skin status and skin modifications took place at the BI-OPTRON center (ZEPTER MEDICAL General Practice) including 32 research subjects. It is demonstrated that under the influence of hyperpolarized light the biophysical skin status is modified. In four research subjects, having excellent biophysical skin status, no change occurred. In research subjects having average or inadequate biophysical skin status, changes (initial improvement) were recorded. Hyperpolarized light exhibited 27% better effects in improving biophysical skin status than linearly polarized light. A study on a larger number of research subjects should be performed (about 1000), taking into consideration age (5 groups of 40 subjects each), sex (two groups) and skin type (we investigated three skin types), based on these variables adequate conclusions would be made.

**Acknowledgment:** I express my gratitude foremost to ZEPTER International for the organization of the study realization, then to volunteers for taking part in the study, and to my associates Aleksandra Dragičević, M.Sc., and Andrea Stylet, M.D. for their assistance in recording and processing results.

## References

1. Baldock, C., Sherratt, M.J., Shuttleworth, C.A., Kielty, C.M., The supramolecular organization of collagen VI microfibrils. *J Mol Biol.* 330(2):297-307;2003.
2. Baumann L. Skin aging and its treatment. *J Pathol.* 211:241-251;2007.
3. Chaplin, M.F., Water structure science. <http://www.lsbu.ac.uk/water/>
4. Gawkrödger, D.J., Dermatology. Churchill Livingstone, Edinburgh, 2002.
5. Graham-Brown, R., Bourke, J.F., Dermatology. Mosby, Edinburgh, 1998.

6. Jacques, S.L., Optical properties of biological tissues: a review. *Phys. Med. Biol.* 58:R37R-61R; 2013.
7. Fluhr, J., Elsner, P., Berardesca, E., Maibach, I.H, Bioengineering of the Skin: Water and the Stratum Corneum. CRC Press, Boca Rton, 2005.
8. Koruga, Dj., miljković S., Ribar, s., Matija, L., Kojić, D. Water Hydrogen Bonds Study by Opto-Magnetic Fingerprint. *Acta Physica Polonica A.* Vol.117, No.5, pp. 777-781, 2010.
9. Koruga, Dj., Bandić, J., Janjić, G., Lalović, Č., Munćan, J., Dobrosavljević Vukojević, D. Epidermal Layers Characterisation by Opto-Magnetic Spectroscopy Based on Digital Image of Skin. *Acta Physica Polonica A.* vol. 121, issue 3, pp. 606-610, 2012.
10. Koruga, Dj.,Tomic, A. System and method for analysis of light – mater interaction based on spectral convolution: PCT US 2009/030347. Granted in: Japan: Patent No.10-1150184, Singapore: Patent No.163043, China: Patent NoCN200980108822.9, Russia: Patent No.2440603, Mexico: Patent No.308206, Australia: Patent No.2009204227. *Under Examination:* EU, Brazil, Canada, Indonesia, India. *Published after filing:* US No. 14/695,990.2009.
11. Langton, A.K., Sherratt, M.J., Griffiths, C.E.M., Watson, R.E.B., Review article: a new wrinkle on old skin: the role of elastic fibres in skin aging. *Int J Cosmet Sci.* 32(5):330-339;2010.
12. Martires, K.J., Fu, K., Polster, A.M., Cooper, K.D., Baron, E.D., Factors that affect skin aging. *Arch Dermatol.* 145(2):1375-1379;2009.
13. Matija, L., Jeftić, B., Nikolić, G., Dragičević, A., Mileusnić, I., Munćan, J., Koruga, D., Nanophysical approach to diagnosis of epithelial tissue using Opto-magnetic imaging spectroscopy, Nanomedicine, One Central Press, 2014, ISBN (E-book) 978-1-910086-01-8.
14. Naylor EC., Watson REB., Sherratt MJ., Molecular aspects of skin aging. *Maturitas.* 69:249-256;2011.
15. Papić-Obradović, M., Kojić, D., Matija, L., Opto-Magnetic Method for Epstein – Barr Virus and Cytomegalovirus Detection in Blood Plasma Samples. *Acta Physica Polonica A.* Vol.117, No.5, pp. 782-784, 2010.
16. Rittie, L., Fisher, G.J., UV-light-induced signal cascades and skin aging. *Ageing Res Rev.* 1(4):705-720;2002.
17. Rock, M.J, Cain, S.A., Freeman, L.J., Molecular basis of elastic fiber formation – critical interactions and a tropoelastin-fibrillin-1 cross-link. *J Biol Chem.* 279(22):23748-58;2004.
18. Stamenković, D., Kojić, D., Matija, L., Miljković, Z., Babić, B., Physical Properties of Contact Lenses Characterized by Scanning Probe Microscopy and Opto-Magnetic Fingerprint. *International Journal of Modern Physics B.* Vol. 24(6-7), pp.825-834;2010.
19. Waller, JM., Maibach. HI., Age and skin structure and function, a quantitative approach (II): protein, glycosaminoglycan, water and lipid content and structure. *Skin Res Technol.* 12(3):145-154;2006.

## 7.2 Medical Cases

### 7.3.1 Hyperpolarized Light Applied to Burns

*Dr Biljana Lučić, ZEPTER MEDICAL General practice, Belgrade*

#### **Introduction**

Skin is composed of three layers: epidermis, dermis and hypodermis. Between epidermis and dermis there is the basement membrane connecting the epithelium layer of epidermis with the connecting tissue of dermis. The basement membrane is made of basal lamina built of collagen fibers and epithelium cells, and the reticular lamina, where reticular fibers are prevalent. In healthy skin, epidermis and dermis represent a barrier against various impairments. When this barrier is damaged, cascade of biochemical modifications occur in order to repair the damage. This process includes chemostasis, inflammation, proliferation, i.e., new tissue formation and maturation, and tissue remodeling. Various blood elements, growth factors, collagen, fibroblast cells, and other elements take part in these processes.

#### **Case Description**

Burns are skin lesions resulting from impact of heat, chemical agents, electricity, friction, or radiation on the body surface. Various thermal agents can cause high temperature burns: hot gas, open flame, liquid metal and rigid bodies. When the burn is caused by steam or boiling liquids it is called a vapor burn. Burns are accompanied by chemodynamic changes - the initial, short lasting, vasoconstriction, followed by vasodilatation of capillaries and venules of increased permeability. Dilated blood vessels provide for better alimentation and supply of oxygen to injured tissue. In mild thermal burns, histamine is released from mastocytes, while in more severe burns necrosis of endothelial cells of small blood vessels is present, with transudation and thrombosis. Morphologically, the burn lesion has three zones: central zone of coagulation necrosis, zone of inflammation, and hyperemia zone on periphery. Based on the depth of damaged tissue and regeneration capacity, burns are classified as: I degree burns (*combustio erythematosa*), surface burns, where only epidermis is compromised accompanied with erythema and mild skin edema, II degree burns (*combustio bullosa*) are characterized by redness, edema and bullae. In the II A degree, there is coagulation necrosis of epidermis, and formation of blisters filled with serous liquid between the necrotic epidermis and dermis. They are accompanied with redness, moist bullae, and are very painful. In the II B degree, beside the epidermis necrosis, there is also dermis necrosis up to the reticular layer, with preserved skin adnexa. They are usually yellow or white, sometimes accompanied with bul-

lae, causing pressure sensation and uneasiness. In both cases, the tissue can regenerate completely. The III degree burns (*combustio escharotica seu crustosa*) result in necrosis of epidermis and corium with skin adnexa, and blood vessel thrombosis. Necrosis can extend to subcutaneous adipose tissue, and deeper structures: fasciae, skeletal muscles, bones and joints. The lesion is stiff, of white-brown color, resembles prepared leather. The healing process is finalized by forming a keloid scar. In IV degree burns (*carbonisatio*), the tissue is charred; they end with amputation, and can even be lethal. Based on the tissue regeneration capability, burns can be classified as partial (I and II) and total (III and IV). Burns can be accompanied with shock, infection, electrolyte disbalance, and respiration impairment. In the assessment of the burns severity, depending on the body area affected, „rule of nines” is observed, which divides the body surface into segments, each measuring 9% of the total body surface.

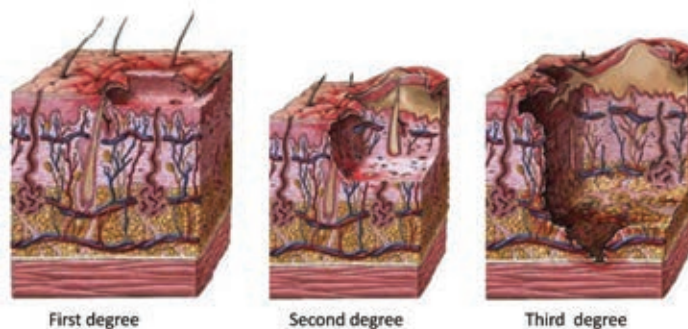


Figure 7.2.1-1. Three degrees of burns (Obtained from: MedlinePlus Medical Encyclopedia).

### Case Description

Patient, 53 years old, accidentally spilled boiling water over clothes on the front femur region, a day later a big blister appeared that burst after two days, mild hemorrhage occurred from the wound, intense pain was felt all the time. Local antiseptic was used in the lesion area.

At the admission, a morbid change was observed - lesion in the front region of the femur having 2x1.5 cm diameter, separated wound edges in the central zone, zone of inflammation and neighboring hyperemia, corresponding to the II degree burn.

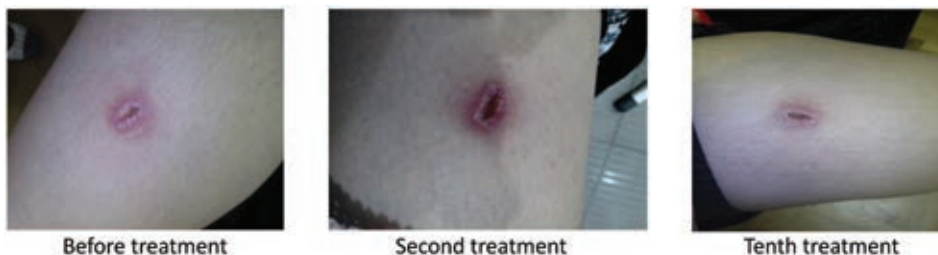


Figure 7.2.1-2 Lesion status: before treatment, the second day of treatment, and the tenth treatment with BIOPTRON.

On the fifth day since the morbid change occurred, hyperpolarized light application was started according to protocol, using the BIOPTRON MedAll apparatus at a distance of 5 cm. Twenty eight treatments were administered, OXsy Sterile spray was used. After the second treatment, the hyperemia intensified and subsided after the fourth treatment. Noticeable closing of the wound edges was registered after 10 treatments, and significant decrease of lesion depth with reduced hyperemia was observed after the 15<sup>th</sup> application of hyperpolarized light. After 28 treatments, complete healing of the wound edges occurred. Subjectively, the pain sensation was relieved considerably after the third treatment. Patient was advised to continue treatment in order to achieve a complete esthetic result.

### ***Action Mechanism***

In the II degree burns, the basement membrane is compromised and bullae filled with serous liquid are formed between the necrotic epidermis and dermis. Under the influence of hyperpolarized light, collagen I and III is activated, followed by collagen of type VII and IV in the basal lamina, and transferred into the stratum spinosum. At the same time, lipids are organized into nano layers, assisting the formation of water channels, which by their thermal capacity aid local tissue cooling. In an impaired membrane, the healing process lasts up to 7 weeks. By the application of hyperpolarized light this time was reduced to 4 four weeks, the painful impulse transfer was quickly diminished as well.

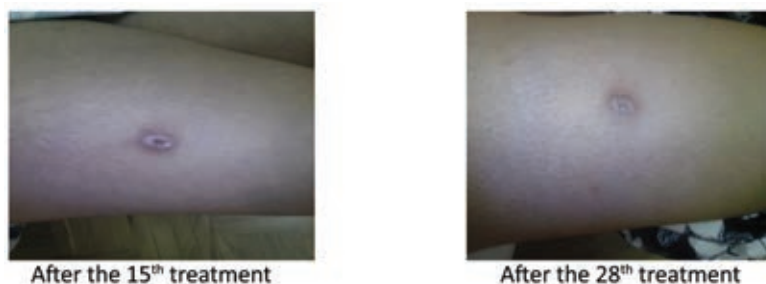


Figure 7.2.1-3 Lesion after the 15<sup>th</sup> and the 28<sup>th</sup> treatment with BIOPTRON.

### ***Conclusion***

Application of the hyperpolarized light to the burns of the II degree resulted in the initial intensified hyperemia, followed by gradual lesion depth reduction, wound edges closing, reduced hyperemia and complete healing during 28 treatments. Subjectively, patient described the treatments as very agreeable and efficient in relieving the pain sensation.

### ***References***

1. Atanacković M, Bacetić D, Basta-Jovanović G, Begić-Janeva A, Boričić I, Brašanac D. i sar., Patologija. Medicinski fakultet, Beograd, 2013.
2. William D. James, Timothy G. Berger, Dirk M. Elston, Andrew's: Diseases of the Skin: Clinical Dermatology. 12 edition, 2015.

### 7.2.2 Hyperpolarized Light Applied In the Treatment of Lichenification

**Dr. Danijela Mitrović, ZEPTER MEDICAL General practice, Belgrade**

Skin is the largest organ of the human body, of complex structure with multiple functions:

1. creates a barrier toward the external environment,
2. participates in thermoregulation,
3. participates in the immune system response.
4. has an esthetic and cosmetic role.

Skin is made of three layers:

1. Epidermis, of ectodermal origin, formed of cells with sweat and sebaceous glands.
2. Dermis, of mesodermal origin, is mostly a connecting tissue structure.
3. Hypodermis, of mesodermal origin, built mainly of adipose tissue.

#### ***Lichen Simplex Chronicus Vidal***

The basic skin change in *lichenification* results from repeated scratching, followed by the release of mediators causing pruritus.

It can manifest due to clothes friction or in the intertriginose regions of obese persons. Occurs also after a banal incident such as an insect bite, irritation, sweating.

It was observed that individuals are not equally prone to lichenification. It occurs more frequently in persons with psychic anxiety, or with low tolerance for pruritus. The disorder occurs mostly between the ages of 30 and 50, seldom in children; in females more often than in males.

Changes are localized on the front and lateral side of the neck, capillicium, inguino-crural flexures, vulva, scrotum, extensory regions of elbows, crura, and around ankles.

The basic clinical manifestation is *lichenification* (exaggerated skin lines). At the beginning, there is edema and erythema, which later subside.

A typical morbid change is thus formed, vaguely circumscribed, the size of a coin up to the size of palm.

At the center of lamina, skin is thickened with squamae and pigmented, surrounded by a zone of lichenification. In periphery, there are dispersed singular lichenoid papulae between exaggerated skin lines.

Pruritus is intense and disproportional to the objective finding.

Sometimes, the thickenings are considerable and lead to the formation of nodules. Complications are super infections.

Diagnosis is established based on clinical findings.

Histologically, there is hyperkeratosis in the epidermis, in dermis there is chronic inflammatory infiltrate.

Therapy: locally, corticosteroids, ointment or cream, emollient creams.

General therapy includes administration of sedating H1 antihistaminics, anxiolytics, and, if necessary, tricyclic antidepressants.

Patient, in the case study, is 60 years old, of poor general health (HTA, hyperthyroid disorder, bad alimentary habits, cigarette smoker).

On the external region of the left ankle a morbid change can be seen corresponding to the clinical manifestation of LSC (*Lichen simplex chronicus*).

According to patient's statement, this change appeared two years ago in the form of erythema and edema accompanied by pruritus, which, according to the patient, were caused by an insect bite.

After local therapy was applied with corticosteroids and general antihistaminics, no improvement occurred. During two years, on the contrary, the change aggravated, with constant pruritus causing patient's psychic agitation.

Hyperpolarized light treatment of skin impairment was started, using the following protocol:

Lesion was treated with hyperpolarized light at a distance of 7 cm from the skin surface. Each treatment lasted 8 minutes and 30 seconds, during four weeks discontinuously.

The patient felt improvement already after the first treatment - reduction of pruritus, accompanied by an objective finding on the lesion. Epithelization and healing of minute rhagades started.

Reduced pruritus was the sign of skin cells regeneration, because secretion of active proteolytic enzymes and mediators causing pruritus was considerably decreased.

The first Figure displays damage to the epidermal layers, while on the second image the epithelization has already started. The last two Figures show forming of new epithelium at lesion edges, progressing toward the center, gradually decreasing the wound and closing it.

At the bottom of the wound red eminences occur - this is granular tissue filling the lesion from bottom up.

### **Action Mechanism**

Neurodermatitis treatment with hyperpolarized light (HPL) consists of the following: under the effect of HPL epithelization starts on the surface layer and healing of minute rhagades, with subjectively reduced pruritus because cell regeneration started (based on the regulation of Gibbs free energy, better organization of water, ion channels, etc.) leading to decreased secretion of mediators, causing reduced pruritus sensation.

The HPL affects the regulation mechanisms, the cell is closed, histamin is not released, and thus there is no impulse for scratching toward the skin surface. As the mechanism of HPL action is through water, in this case the tissue regeneration occurs in depth.

### **Conclusion**

Since no previous therapy was sufficiently successful, and since the patient's general health was poor, which additionally hampered the wound healing process, condition deteriorated with time.



Based on the above, it can be concluded that hyperpolarized light application in this study resulted in fast wound healing, which not only objectively, but also subjectively improved subject's quality of life.



### ***7.2.3 Hyperpolarized Light Applied in the Therapy of Burn Wounds***

***Dr. Milica Komnenić, ZEPTER MEDICAL General practice, Belgrade***

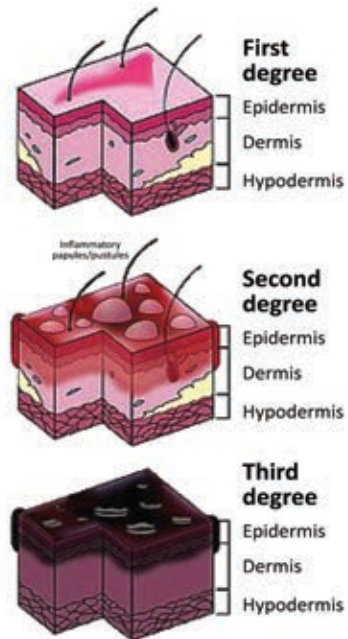
Burns are tissue lesions caused by the effect of dry or humid heat.

They occur instantaneously, however consequences remain forever.

Burns are classified according to the size of compromised area and the depth of the burn.

Table 7.2.3–1

Burns severity classification (American Burns Association)		
Mild burns	Moderate burns	Severe burns
I degree	II degree 10% –20% TBSA in adults	II degree > 20% TBSA in adults
II degree < 10% TBSA in adults	II degree 5% –10% TBSA in children and the aged	II degree > 10% TBSA in children and the aged
II degree < 5% TBSA in children and the aged	III degree 2% –5% TBSA	III degree > 5% TBSA Burns of functional regions, electric burns, chemical burns, radiation burns, in- halation injuries, combined injuries, burns in persons under increased risk (chro- nic disease)
III degree < 2% TBSA	-	-



Contact with viscous materials	<ul style="list-style-type: none"> <li>• Burns caused by contact with hot lipids, oils, viscous inflammable materials (plastics, resins, tar or asphalt, cosmetic wax).</li> <li>• Burns are usually in the shape of maculae in a smaller region (these materials, due to their viscosity, do not diffuse on the skin surface and are not absorbed through skin),</li> <li>• These materials adhere strongly to the burned skin and are hard to remove, thus affecting tissue depth of the II and the III degree, up to the IV degree.</li> </ul> <p style="text-align: center;">THEY OCCUR IN 10% OF ALL BURNS</p>
--------------------------------	---

Children = younger than 10 years; adults = 10 to 50 years; elderly = older than 50 years, TBSA = total body surface area.

*COMBUSTIO - Skin change affected by hot viscose mater.*

Under the influence of heat the following occurs:

1. Protein coagulation, not only in the skin, but in the tissue as well;
2. Blood vessel thrombosis resulting from blood clotting accompanied by insufficient blood perfusion and occurrence of hypoxia;
3. Cell necrosis – cell death deep in the tissue, affecting a progressively widening area.

### Case Description

The research subject is a female, 52 years old.

The burn was caused by hot cosmetic wax. Burn is located in the region of the left hand thumb, 2 cm long, 1cm wide, II degree.

Immediately after injury and later on, other therapy was not used.

Injury was accompanied with intense pain in the hand region and decreased motility.

### ***Conservative Therapy***

Standard conservative therapy of such injuries includes:

Protection and processing of burnt surface;

Prevention of infection, because necrotic tissue is an excellent basis for infection development;

Surgical processing of an injury affecting more than 1% of body surface.

This type of burns often heals with scared tissue and changed pigmentation at the site of injury. Time necessary for healing is up to 40 days.



**Figure 7.2.3-2** *Wound healing followed during seven days.*

### ***Protocol***

#### ***Application of BIOPTRON Hyperpolarized Light***

BIOPTRON light is applied locally at the injury site, once a day, during 8 minutes, at a distance of 10 cm, 7 days continuously.

### ***Action Mechanism***

Second-degree burns affect the epidermis and the deep dermis layer, the sweat and the sebaceous glands and the hair base. In pathogenesis, the key factor is the diffusion of plasma – liquid and proteins, and their buildup in the interstitium. The hyperpolarized light accelerates the process of lipid organization into nano layers, between which are located H<sub>2</sub>O molecules as the main protective factor.

Histamin receptors of type 1 are also blocked, thus preventing edema formation. Hyperpolarized light activates natural defense mechanisms of the organism preventing infection development in the necrotic tissue.

Retarded healing, sometimes longer than 40 days, accompanied by the formation of scars, is now accelerated by HPL activating collagen of type VII and II, thus the wound heals two, even three times faster; in 14-21 days.

### **Conclusion**

1. Edema in the vicinity of the wound receded already on the third day of therapy.
2. Secretion from the lesion is reduced and the wound dries and heals faster.
3. Antibacterial effects of the light spectrum prevent the development of infection.
4. Wound healed after 7 days.
5. According to the patient, the pain was relieved and motility improved – „skin is not rigid“ - after the first treatment.
6. My opinion, as the physician following the case : lesion healed without scarring and pigmentation change in an extremely short time, in spite of the fact that the lesion was deep, of the II B degree, and that tissue was additionally damaged during wax removal.
7. By applying hyperpolarized light, we stimulate organism's immune system to resist the threat and to activate the regenerative processes already existing in the body.

### **References**

1. A case review of patients presenting to Royal North Shore Hospital, with hair removal wax burns between January and November 2006
2. Zoumaras, J., Kwei, JS., Vandervord, J., Pathologic Basis of Disease .7 th edition, Kumar, Abbas, Fausto.

## **7.2.4 Hyperpolarized Light Applied in Psoriasis**

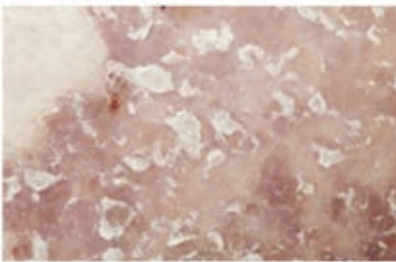
*Dr. Miloš Mladenović, Dr. Jelena Simić, ZEPTER MEDICAL General practice, Belgrade*

Psoriasis, (Lat. *psoriasis*; Greek *psora*- itch) is a chronic, presently incurable, noninfectious, multifactor, inflammatory disease characterized by hyperproliferation of keratinocytes in the skin epidermis and increased proliferation of epidermal cells. It is estimated that approximately 2% of world population have psoriasis. The illness can manifest at any age, from birth to old age, although it is mostly manifested in the period of sexual maturity (between the ages of 15 and 25), equally in males and in females. Psoriasis is not an infectious disease; it is not transmitted from person to person. This chronic skin state is not life threatening; however, patients with psoriasis are more prone to diabetes, psoriatic arthritis, heart disease, and depression.

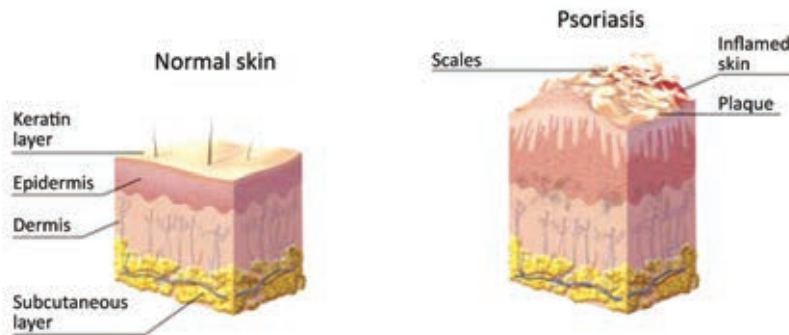
Psoriasis is a systemic, immunologically mediated inflammatory disease, primarily of the skin, with inflammatory, sometimes painful manifestations, often accompanied with pruritus and burning sensation, lasting for years. Morbid changes are found mostly on knees, elbows, head and torso, although they can be found on any other location, including nails, palms, soles, face, genitals, and even joints. Lesions are usually symmetrical, on the same location of the left and the right body side. This skin disorder is characterized by periods of remission and relapse.

Psoriatic lesions biologically differ from classical dry skin, known as xerosis; they are classified as erythrosquamous, meaning that blood vessels and deeper layers of the epidermis are affected as well. Reduced cell regeneration results in the so-called scales. Multiple factors are the cause of this illness:

- inflammatory reactions in deeper dermis and the upper epidermis,
- increased production of keratinocytes (dominant cell type in the epidermis),
- shorter cell growth cycle, and
- impaired desquamation process (desquamation is the natural process where the surface skin layer peels off).



Psoriasis is, therefore, manifested by erythematous-infiltrated patches covered with silvery squamae. These specific changes can be expressed in the form of pink patches, covered with white scale, characteristically slightly elevated, symmetrical, and clearly circumscribed, of irregular or oval shape, of different dimension– from a few centimeters in diameter up to patches covering large skin surfaces.



The cause of psoriasis is still unknown, however everything points to the conclusion that genes are responsible for its origin. Research shows that psoriasis genesis can be initiated by infection, micro trauma, drugs or stress. Most scientists consider psoriasis to be an autoimmune disease. Normal skin cells mature after 28-30 days and are unnoticeably peeled off -skin continuously regenerates itself in this way. In psoriasis, skin cells need only three to four days to mature, so they accumulate and form red lesions on the skin. Thus, cells are reproduced much faster than they can produce keratin, the enzyme responsible for the hard skin surface.

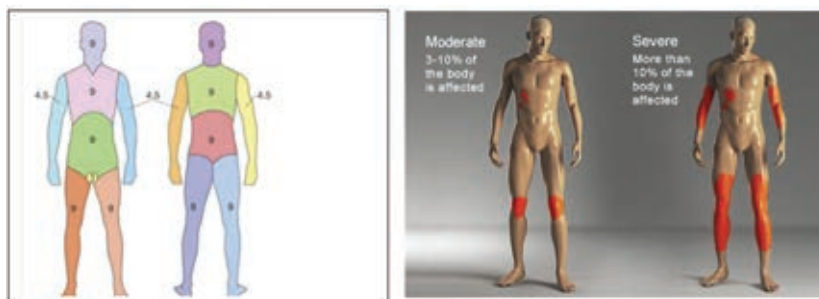
Depending on the shape and magnitude of the morbid changes, we differentiate:

- \* *Psoriasis punctata* (2-3 mm) in the form of points,
- \* *Psoriasis guttata* (0.5-1 cm) in the form of drops,
- \* *Psoriasis nummularis* (3-4 cm) in the form of coins,
- \* *Psoriasis in placibus* (*en plaques* -plaques of several centimeters),
- \* *Psoriasis geographica* (several blending plaques).

Depending on the localization of the psoriatic change, we differentiate:

- \* *Psoriasis capitis*,
- \* *Psoriasis unguius*,
- \* *Psoriasis palmaris, plantaris, palmoplantaris*,
- \* *Psoriasis inversa*

Severity of the plaque psoriasis clinical manifestations is defined based on the size of the skin surface under change, taking into account the characteristics of lesions themselves. Tools for assessing the clinical manifestations are numerous; however, the so-called PASI score is mostly used. The PASI score (Psoriasis Area and Severity Index) was developed in 1978 with the aim to assess the effect of therapy on psoriatic lesions. Numerical representation of the affected area and characteristics of changes are input into a formula, and the final score is obtained within the 0 -72 interval. This is accepted today as the standard for the assessment of the efficiency of the applied antipsoriatic therapy. A faster and more easily applied tool for everyday use, the so-called BSA (Body Surface Area) score is used, where the surface under psoriasis is expressed in percentage, using the known “rule of nines”.



Depending on the body surface under lesions, psoriasis is classified as mild, where body surface affected is up to 3%, moderate, where body surface affected is from 3% up to 10%, and severe psoriasis, where over 10% of body surface is affected.

### **Case Description**

The patient is male, 32 years old. During the past 6 years suffers from *Psoriasis vulgaris* L40.0 (MKB10). Dominant changes on crura. Treated both locally and systemically, without effect. Currently, he is not undergoing neither systemic, nor topical therapy. Occasionally sunbathes, uses regenerative cream.

***Protocol***

Application of BIOPTRON hyperpolarized light in the area of both crura, once a day. Light is applied during 8 minutes and 30 seconds at a distance of 7-10 cm. Cycle of 10 weeks, i.e., 50 treatments overall.

***Patient Status before Treatment***



Diffuse psoriatic changes in the area of crura accompanied by pruritus, bilaterally; minor changes in the elbow region. Positive phenomenon of hemorrhagic rose.

***Patient Status after 50 Treatments***



After two months of therapy and intensive treatment, significant improvement is registered in psoriatic changes on the skin of lower extremities in the patient with prolonged problems.

During treatment, initial inflammation occurred with exacerbation within the first two weeks in the surface skin layer, followed by the redness receding, and even improvement in skin changes. The initial inflammatory reaction receded after the third week, and

changes receded gradually, concentrating on smaller formations. After the fiftieth treatment, changes have almost completely receded, in contrast to the initial diffuse state.

Patient also observed and enthusiastically confirmed considerable improvement and absence of pruritus. Redness subsided; skin is no longer dry and splitting.

### **Action Mechanism**

Psoriatic lesions differ biologically from the normal and classical dry scaling skin. The inflammatory reaction in deeper dermis and upper epidermis, proliferation of keratinocytes and the impaired cell cycle cause skin desquamation. This results in excess water loss.

Due to the hyperpolarized light effect at the lesion site (on lipids, collagen, basement membrane and the regulation of water perfusion from dermis into epidermis), instead of the accelerated formation of squamiae in the *stratum corneum* resulting from the *stratum granulosum* dysfunction, conformation changes occur, nano layers of water in *stratum granulosum* are regularly formed leading to a regular cell cycle. The basement membrane is regenerated and collagens are adequately organized, which restores the physiological skin cycle.

### **Conclusion**

Case description demonstrates that hyperpolarized light application resulted in improvement and skin change decrease in a form of psoriasis. Hyperpolarized light used as monotherapy resulted in skin regeneration and receding of psoriatic changes in the cura area, with decreased inflammatory skin reaction. Pruritus was eliminated as well.

### **References**

3. Lalević Vasić, B. M., Medenica LJ. M., Nikolić, M.M., Dermatovenerologija sa propedevtikom. Savremena administracija, Beograd, 2002.
4. Jankovic S, Raznatovic M, Marinkovic J, Jankovic J, Kocev N, Tomic-Spiric V, et al. Health-Related Quality of Life in Patients with Psoriasis. *J Cutan Med Surg*. 2011;15,1:29-36.
5. Langley RGB, Krueger GG, Griffiths CEM. Psoriasis: epidemiology, clinical features, and quality of life. *Ann Rheum Dis*. 2005;(Suppl II):ii18-ii23.doi.
6. Raychaudhuri SP, Farber EM. The prevalence of psoriasis in the world. *J Eur Acad Dermatol Venereol*. 2001;15:16-17.
7. Farber EM. Epidemiology: natural history and genetics. In: *Psoriasis* (2nd ed). Roenigk HH, Maibach HI (Eds). Marcel Dekker, Inc, Ny, USA, 1991, pp. 209-258.
8. Krueger GG, Eyre RW. Trigger factors in psoriasis. In: *Dermatologic Clinics*. Weinstein GD, Voorhees JJ, eds. WB Saunders Co., PA, USA, 1984, pp. 373-381.



### 7.2.5 Hyperpolarized Light Applied in Acne Treatment

*Dr. Biljana Lučić, ZEPTER MEDICAL General practice, Belgrade*

#### **Introduction**

Skin is the largest organ of the human body, total skin area is approximately 1.5-2m<sup>2</sup>, and it weighs approximately 15% of body mass. It has three layers: epidermis, dermis and hypodermis. Epidermis is the outermost skin layer where keratinocytes prevail, cells that create keratin-the protective protein. Four layers constitute the epidermis: basal, spinose, granulose, and the horny layer. From the basal layer toward the horny layer, continuous keratinization occurs. Keratinocytes are regenerated normally within 28 to 56 days. The non-keratinous components of epidermis are melanocytes (cells responsible for the creation of melanin and its transport to keratinocytes), Langerhans' cells (play a role in the immune response), and Merkel's cells (mechanoreceptors).

The sweat glands, sebaceous glands, hair and nails represent the epidermis adnexa. Sebaceous glands of acinous structure are present in the skin of the entire body, except palms, soles and interdigital areas. They are connected to the upper part of the hair follicle and include a secretory duct (the pilosebaceous unit). Hair is a solid, fibrous, keratinous structure, created in the follicle. Nail, i.e., the nail plate, is a solid keratinous structure, formed by accelerated division of epidermal cells.

Dermis is located between epidermis and hypodermis. It is made of collagen, elastin and fibrin fibers (the fibrinous component), immersed into the amorphous dermis mass.

Hypodermis is made of adipose cells, lipocytes, forming primary microtubules, circumscribed by connective walls transversed by blood vessels, lymph vessels and nerves.

Skin has a three-dimensional network of blood vessels, organized in two levels: deep vascular plexus, in the border area between the hypodermis and dermis, and the surface subpapillary vascular plexus. Somatic sensory and autonomous sympathetic nerve fibers are located in the skin.

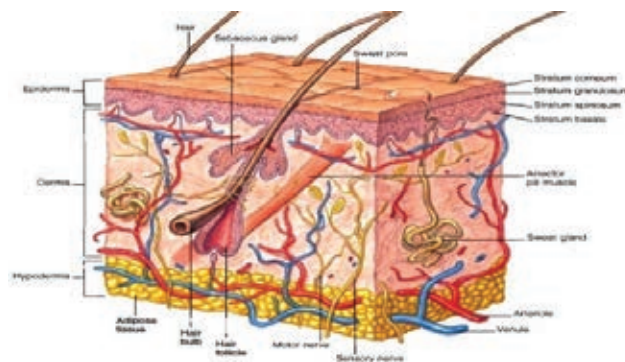


Figure 7.2.5-1 Skin cross section.

Skin performs several important functions: protects from external physical, chemical and biological agents, prevents excess water loss, participates in thermoregulation, absorption of UV light, metabolism of vitamin D, the immune system, is a neuroreceptive organ, has an esthetic and cosmetic role. The chemical reaction of skin surface is acid,  $\text{pH} = 5-5.5$ .

Skin is susceptible to various pathological changes: hereditary, inflammatory, neoplastic (benign and malignant tumors), endocrine, traumatic and degenerative.

### Case

Acne is the inflammation of the pilosebaceous unit of the skin. Several factors participate in acne genesis. Sebum proliferation leads to hyperplasia of sebaceous glands. Hyperkeratinization of the horny layer prevents the draining of sebum to the skin surface resulting in its agglutination in sebaceous glands. They become dilated, leading to the formation of microcomedones. This noninflammatory lesion can be opened under pressure, leaving an „open comedo” on the skin surface, a black draining spot. Progress of this change can lead to the formation of a „closed comedo” without draining, where sebum is accumulated, it is progressively enlarged. Colonization of *Propionibacterium acne* occurs in the comedo, a bacterium permanently present in the skin, which under these circumstances reproduces rapidly. Increased permeability of the follicle wall leads to the penetration of leukocytes and the formation of an inflammatory lesion. Further progress can lead to follicle rupture. There is a genetic predisposition for an intensified skin reaction to the regular production of the androgen hormone.

Acne manifests most frequently in puberty, more frequent and severe forms occur in males. They are localized on the central face regions (cheeks, forehead, nose, chin), on the chest, between scapulae, and can spread on the entire face.

There are several acne types: comedo form that can lead to the papulo-pustuleous form and cystic nodules form, usually of larger diameter often leaving keloid scars. Acne is a considerable psychological problem of the young.

Acne lasts a couple of years, and disappears spontaneously after all predisposed follicles are seriously impaired by the prolonged inflammation process.

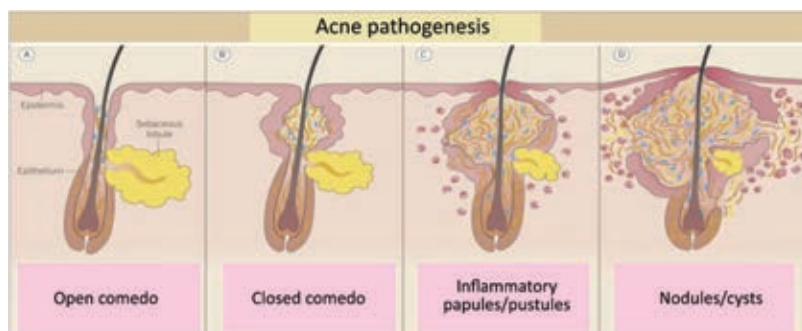


Figure 7.2.5 -1 Acne pathogenesis.

**Case Description**

The patient is a female, 21 years old, diagnosed with *acne vulgaris*, on both cheeks, lasting about four years.

The treatment: hyperpolarized BIOPTRON light was applied locally on both cheeks (clearance 5 cm), each treatment lasting 8.5 minutes at the treated zone. Fifteen treatments were performed, every second day. The BIOPTRON Pro 1 apparatus was used and the *Oxy Sterile Spray*.

Objective finding at the beginning of the treatment: adipose, glossy skin with pronounced papulo-pustulose form of acne on both cheeks. Subjectively, patient describes occasional stinging and pruritus of the skin, and dissatisfaction with her esthetic appearance.

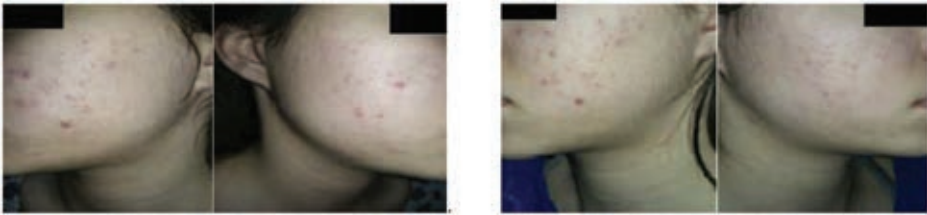


**Figure 7.2.5-2** Case presentation: the first day of therapy (first two images left), and after five days of therapy (two images on the right).

The effect of therapy led, at first, to intensified inflammation, followed by gradual inflammation reduction, decreased number of papules and pustules, and healing of changes.

After 10 treatments, no pustules could be discerned on the skin. After 15 treatments, esthetic improvement in the skin appearance is noticeable, only scarce papules can be observed.



**Figure 7.2.5-3** Case presentation after 15 treatments.

The patient described the treatments as very agreeable, the stinging and itch are reduced and she is exceptionally satisfied with her esthetic appearance.

The patient was recommended to continue treatment due to the positive effect of polarized light on the stimulation of collagen fibers production, and the effect on the regulation of scared tissue.

### **Action Mechanism**

Hyperpolarized light activates phagocytosis and prevents excessive *Propionibacterium acne* reproduction, decreases the exaggerated sebum secretion and acts anti-inflammatory via cytokine. In the healing process, collagen of type I and III is activated, followed by type VII collagen, and through the laminin and integrin, migration of keratinocytes, the healing of the surface skin layer occurs.

### **Conclusion**

Application of BIOPTRON hyperpolarized light on the papulo-pustulose acne vulgaris form led to an increased inflammatory reaction at first, followed by a gradual decrease in the number of pustules and papules, and tissue healing. Objectively, significant esthetic improvement can be observed.

### **References**

1. Lalević-Vasić B, Medenica Lj, Nikolić M. Dermatovenerologija sa propedevtikom – udžbenik za studente medicine, 6. izdanje, Beograd 2010.
2. Jakac M. Dermatologija i venerologija, udžbenik za studente medicine, 3. izdanje, Medicinska knjiga, Beograd - Zagreb 1989.
3. Bumbaširević V i sar. Histologija, Medicinski fakultet, Beograd, 2009.
4. Trpinac D, Obradović M. Repetitorijum histologije i embriologije, Medicinski fakultet, Beograd, 2013.
5. Fitzpatric T, et al. Dermatology in general medicine, McGraw-Hill, New York, 1987.
6. Atanacković M i sar. Patologija, Medicinski fakultet, Beograd, 2013.
7. Freedberg IM, Eisen AZ, Wolff K, et al, eds. Fitzpatrick's Dermatology in General Medicine, 5th edition, New York; McGraw Hill, 1999.

## **7.2.6 BIOPTRON Hyperpolarized Light Applied in the Therapy of Bronchial Asthma**

*Dr. Aleksandra Ignjatović, ZEPTER MEDICAL General practice, Belgrade*

### **Introduction**

Bronchial asthma is a respiratory syndrome caused by a functional pulmonary disorder manifested as the reversible obstructive hyperinflation of the lung. The disease is clinically manifested by paroxysmal episodes of dyspnea, difficult respiration and cough, with prolonged expirium and chest wheezing. This syndrome is manifested due to a specific or nonspecific irritation, followed by a spasm of smooth musculature of bronchi and bronchioles, mucosal edema of respiratory paths, and hypersecretion of mucosal glands.

The disease is characterized by periods of stable status interchanging with periods of exacerbation, which are mostly caused by provocative factors such as viral respiratory infections, exposure to a large quantity of allergen, psychophysical stress.

During asthmatic attacks, simultaneously with the spasm of smooth musculature and the edema of bronchioles mucosa, increased secretion occurs of bronchial glands that discharge a viscous, fibrous, adhesive secretion. This secretion forms a covering of the mucosa, paralyzing the normal function of the ciliate epithelium, decreasing cilia motility, resulting in secretion stagnation. Cough that occurs under these circumstances is not a defensive action any more, but leads to an even closer contact between the secretion, the antigen and the bronchial mucosa.

During asthmatic attacks, a triad of symptoms is manifested: spasm of the smooth musculature of bronchioles leading to difficult respiration, i.e., dyspnea, edema of bronchial mucosa causing cough and accumulation of a viscous, adhesive secretion caused by intensified secretion of mucosal glands, thus significantly impairing air transit in lower respiratory paths, especially during expiration, causing chest wheezing.

Basic asthma classification is into atopic (allergic), and nonallergic (intrinsic) asthma. The basis of atopic asthma is allergy to various allergens. Sensitization is established to certain substances entering the organism, usually via the respiratory system: house dust, bedding (wool, cotton, feathers), molds, workplace dust, pollens, etc. Among nutritive allergens provoking bronchial asthma are: eggs, fish, crustacea, flour, milk, pork meat, medication - aspirin, penicillin, streptomycin, etc.

Nonallergic asthma is usually manifested in older persons, with no previous record of allergic disorders in the personal and family anamnesis. Skin tests on inhalation allergens are negative and the level of the IgE in the serum is normal.

### ***Case Description***

Research subject is S. Đ., 78 years old, suffering from bronchial asthma during the past 5 years. Standard tests determined that she is not allergic to known allergens and the diagnosis was established of nonallergic bronchial asthma. She is taking therapy regularly, prescribed by her pulmonologist – inhalatory corticosteroids (formoterol) and inhibitors of leukotriene receptors (montelukast), drugs reducing the local inflammation in the bronchial mucosa, combined with agonists of the  $\beta$ -2 adrenoreceptors with prolonged action (budesonide) resulting in the relaxation of bronchial muscles. When needed, fast-acting agonist of  $\beta$ -2 adrenoreceptors (fenoterol) is used for fast bronhodilatation and respiration facilitation. Protocol: hyperpolarized light (BIOPTRON Pro 1 apparatus) was applied on the chest (sternum) each day, lasting 8.5 minutes, at a distance of 7 cm, 19 days continuously.

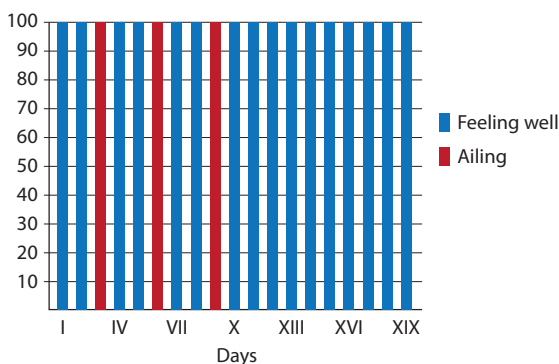
Before the beginning of light therapy, the subject observes that, in spite of the prescribed therapy she is taking regularly, during longer walking or when ascending her breathing is difficult.

During the first two weeks of treatment, subject's general illness status remarkably improved, problems occurred on a few occasions, on the third, sixth and on the ninth day of the study. Problems were difficult morning respiration, dyspnea and cough. During the treatment sequel, from the tenth to the nineteenth day, the subject did not experience the above problems; subjectively she is feeling much better. On the eleventh day,

the subject underwent a control examination at her pulmonologist, and the diagnostic spirometry test showed significantly better result than the previous test six months ago.

### **Action Mechanism**

The effect of the hyperpolarized light – photons structurally organized according to Fibonacci laws, in the treatment of bronchial asthma is explained by the fact that cilia of the respiratory ciliate epithelium are built of microtubules, which are organized and oscillate according to Fibonacci laws. The HP light activates microtubules and the creation of GTP, so that cilia have better motility in order to excrete the thick secretion from bronchi and facilitate respiration.



### **Conclusion**

The goal of asthma treatment is the elimination of symptoms and the establishment of a normal, or as normal as possible lung function, and decreased risk of severe attacks. In addition, the treatment should reduce the number and the severity of attacks and enable normal life style of the patient, including sports activities.

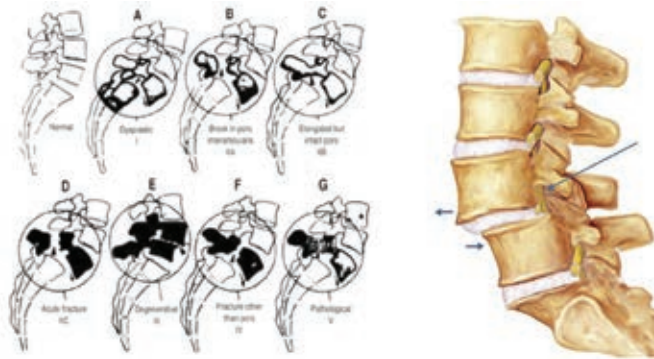
According to the subject, she experienced a significant improvement in her illness status since the beginning of the hyperpolarized light therapy. Occasional problems were provoked by sudden weather changes and considerable air humidity, which do not agree with her.

It can be objectively concluded that the treatment with hyperpolarized light resulted in improved life quality, and it is prescribed as an adjunct therapy to maintain the disease in a stable state in patients suffering from bronchial asthma.

## **7.2.7 Hyperpolarized Light Applied to Spondylolisthesis**

*Dr. Aleksandar Nešković, ZEPTER MEDICAL General practice, Belgrade*

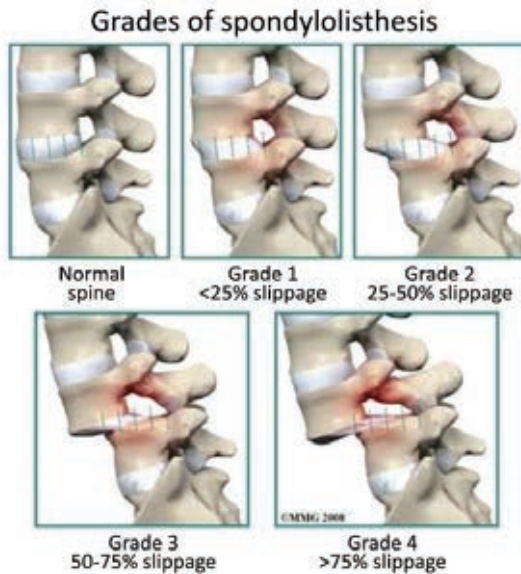
Spondylolisthesis is a pathological entity where one vertebra is displaced over another, often localized in the L5/S1 and L4/L5 regions. In most patients, it occurs asymptotically, so that the radiological finding of spondylolisthesis is discovered only when processing another illness. The illness is mostly of isthmic or degenerative etiology.



The most frequent clinical manifestation, in symptomatic patients, is pain in the lower back, while sometimes radiculopathic pain and neurogenic claudication occur as well.

Clinical practice is still employing the etiological classification according to Wiltse from 1969.

The first type, according to the spondylolisthesis classification is the dysplastic type; dysplasia is found in the form of the L5 trapezoid shape, rounded sacral arch, of elongated or separated pars, missing L5 segment or S1 laminae, and the tropism of lumbosacral facets. The second type is the isthmic type where the defect is located in the interarticular part of the vertebra. Subtypes of the second Wiltse classification type are the following: 2A spondylolithical, stress fracture of the pars interarticularis, 2B -elongation of pars, and 2C -acute traumatic fracture of pars. The third type is the degenerative type, resulting from prolonged intersegmental instability. The fourth type is a posttraumatic disorder where the defect is located within elements located posteriorly from pars. The last type in Wiltse classification is the pathological destruction of posterior elements caused by a generalized or localized bone disease (Wiltse et al. 1993).



There are four degrees of spondylolisthesis. In the first degree, less than 25% of the vertebra body is displaced, in the second degree 25% to 50%, in the third- between 50% and 75%, and in the fourth degree, more than 75% of the surface has been displaced. Depending on the degree, the intensity of symptoms (i.e., pain) increases.

### ***Case Description***

The patient A.I. is 26 years old. For the past four years has a problem with the lumbar spine. She was diagnosed with (MKB 10)-M43.1 spondylolisthesis L5-S1 gr. II with developed bilateral foraminal stenosis in 2014.

She was treated for 20 days by standard physical therapy in the Spinal Center of the Institute for Orthopedic Surgery „Banjica“.

### ***Protocol***

- Application of the BIOPTRON hyperpolarized light on the lumbar spine
- Once per day, 8.30 minutes
- At a distance of 5 cm -7 cm
- 10 days in continuo

### ***Status Description***

Before therapy:

- Dull pain in the lumbar region, classified as 5/10,
- Morning stiffness,
- Strain after prolonged sitting.

After the first treatment:

- Subjectively, minimum reduced pain intensity,
- „Less stiffness in the morning“
- There was no prolonged sitting.

After the third treatment:

- Subjectively, relieved pain; sensation 2/10,
- Unchanged status in the morning,
- After prolonged sitting, still feels strain.

After the fifth treatment:

- Reaction to the weather change, pain before the sixth treatment- about 4-5/10,
- Less stiffness the morning before,
- She is linking the strain feeling with the weather.

After the seventh treatment has been completed:

- Subjectively, pain is almost gone,
- Minimum stiffness at awakening,
- Prolonged sitting is still a problem.

\*A day pause between the seventh and the eight treatment.



After the tenth treatment:

- Reduced pain of varying intensity,
- Maximum improvement regarding stiffness,
- Strain after sitting.

### ***Action Mechanism***

After the application of the hyperpolarized light on the dendrites of nerve cells, conformation changes in microtubules occur, similarly to the action of *taxol* (microtubules with 13 protofilaments in organization 13 (8.5), which are informationally very active, reorganize themselves under the influence of water dipole moments into 13 (10.3) which are less informationally active), resulting in reduced/slower transfer of painful impulses (sensation) toward the nerve cell and further toward the brain.

### ***Conclusion***

Subjective (patient):

- Reduced symptoms and improvement of the general health status,
- Patient wishes to continue light therapy.

Objective finding:

- Too short period to draw conclusions, although positive effects definitively exist, thus continuation of this research is justified,
- Ability to function normally without medication would be, by itself, a significant step forward.

## ***7.2.8 Hyperpolarized BIOPTRON Light Applied in the Lumbar Painful Syndrome***

*Dr. Zlatica Kecić, ZEPTER MEDICAL General practice, Belgrade*

### ***Introduction***

The lumbar painful syndrome is one of the most frequent health problems today, and the most frequent cause for leave of absence. It is estimated that 80% of the population, at least once in a lifetime, experience pain in the region of the lower, lumbar spine, relapsing in at least 50% of these patients. The “painful back” problem is frequently manifested in the most productive period of human life, between the ages of thirty and fifty, equally in both sexes. In most patients, it is accompanied by reduced working ability and the need for adequate medical treatment. The positive aspect is that most patients with the lumbar syndrome complete adequate medical treatment and recover completely, while only in 5% of these patients the pain enters the chronic disease stadium (1, 4, 5).

Lumbar painful syndrome is a set of symptoms of various etiologies, manifested as pain in the lumbar region, at the transition of the lumbar into the sacral spine, between the very dynamic and stressed posterior lumbar vertebra and the scarcely motile sacral bone (Figure 1).



Figure 7.2.8.1 Localization of the lumbar syndrome.

The most frequent spinal changes causing lumbar pain are the degenerative changes of discs and joints of the spinal column.

Other changes causing lumbar pain are the piriformis syndrome, structural disorders (scoliosis, kyphosis and lordosis), trauma of the skeletal, muscular and ligamentous system of the lumbar region – trauma, inflammatory rheumatic diseases, infective diseases and tumors (2, 3).

### **Case Description**

Patient (76 years old) is followed since the occurrence of changes in the lumbar spine, with degenerative changes of disc and joints of the spinal column. Degenerative spinal column changes include:

- *Spondylosis* – ossification of two or more neighboring vertebrae, resulting from degenerative changes,
- *Spondylolisthesis* – displacement of the vertebra forward with respect to surrounding vertebrae, resulting from trauma,
- *Stenosis spinalis* – stenosis of the spinal channel, resulting from degenerative and inflammatory processes on one or more discs,
- *Discus hernia* – rupture of the external fibrose covering of the discus and the prolapse of soft pulpy discus contents into the neighboring space, resulting in compression of surrounding structures, most frequently *n. Ishiaticus* and accompanying symptomatology (2, 3, 5).

Patient's problems began five years ago, with a sudden exacerbation in the past six months, when she experienced severe pain in the lumbar region, especially in the morning. There is no pain propagation along the leg, there never was. Pain is localized in the lumbar region with mild lateralization toward the left hip.

Documentation: native magnetic resonance image from 2014 showing: spondylitic changes periodically along the entire spine, discarthrosis in *L4*, *L5*, protrusion of the intervertebral discus in *L3*, in *L4* moderate, and in *L4*, *L5* mild, and stenosis of the spinal channel *L2*, *L3* with critical stenosis located at the level of *L3*.

BIOPTON hyperpolarized light was applied with a filter of 11 cm diameter according to protocol, once a day, in the painful region at two locations of the lumbar spine L4 and L5, also laterally, left of the spinal column, during 8 minutes and 30 seconds at a distance of 7 cm, 11 days in continuo in the first phase. After achieving positive results, the treatment was continued for another 10 days.

#### Patient Follow Up and Reaction to the Therapy with Hyperpolarized Light

In the first week, patient subjectively had a feeling of improvement; she did not need to take diclofenac, an analgetic, which she used previously.

In the second week, due to weather change, pain is still present in the lumbar spine, especially in the morning, without pain intensification with respect to the status before the beginning of therapy with the BIOPTON hyperpolarized light.

In the next phase lasting another two weeks, the patient, besides being treated with the BIOPTON hyperpolarized light, underwent physical therapy prescribed by the physician at the local medical facility.

After the third week, she felt considerable improvement subjectively, easier getting up from bed. Objective finding – it was observed that she gets up much easier from the chair, without pausing.

After the fourth week of therapy, patient states that the pain is relieved, which was most intense in the morning, there is no pain lateralization toward the left hip, felt before the treatment.

After treatment, beside the general physical examination, which confirmed improved motility, no additional diagnostics were performed in order to gain a complete insight whether an improvement in lumbar spine structures was achieved.

### **Conclusion**

Application of BIOPTON hyperpolarized light in case of the patient with the lumbar painful syndrome and discopathy resulted in improvement. There were no relapses, nor side effects in combination with additional physical therapy that was performed in the last two weeks.

Based on this individual case, I consider that further application of the BIOPTON hyperpolarized light in the lumbar syndrome and discopathy could lead in the direction of a controlled study. This study should certainly be on a relevant number of research subjects, in order to obtain a picture of the real achievement and gain data that would be used as a representative sample for further research.

### **References**

1. Radojčić B. Klinička neurologija. XVI izdanje, Elit Medica, Beograd 2006.
2. Lević Z. Osnovi savremene neurologije. Dečje novine, Gornji Milanovac 1989.
3. Lević Z., Nikolić M. Neurologija. Praxis Medica, Beograd 1982.
4. zdravlje.gov
5. Grupa autora, katedra za neurologiju. Neurologija za studente. Beograd, 2007.

## ***7.2.9 Hyperpolarized Light Applied in the Treatment of Chronic Venous Insufficiency***

*Dr. Đuja Lazić, ZEPTER MEDICAL General practice, Belgrade*

Skin is the largest organ of the human body. If flattened on a surface, skin of the adult has an area of approximately 2 square meters, almost the size of a bed sheet. It weighs 3 kg, which is about 20% of the overall body mass.

Skin thickness varies from 0.5 mm up to over 5 mm. It is thinner in locations where no friction or pressure occurs, such as the interior of the forearm, while thicker on exposed surfaces, such as soles. About somatic apertures, skin is transformed into mucosa.

### ***Skin Functions***

Skin is a body covering in direct contact with the external environment. In invertebrates and primitive chordates (tunicates, amphioxus) skin has one layer, while in vertebrates it has several layers. The main skin functions are:

- Protective – it protects the body from mechanical injury, pathogenic organisms (skin is impenetrable for viruses and bacteria when undamaged), and from damaging UV Sun radiation. Therefore, skin is the first line of defense of the organism from bacteria, viruses and other microorganisms.

- Maintaining constant composition of the internal body environment (homeostasis), preventing water and salt loss in terrestrial vertebrates, while in marine vertebrates excess penetration of water into the body.

- Participates in the matter and gas exchange process, which is extremely significant for the respiration of water organisms.

- Participates in excretion of skin glands,

- Reception of external stimuli via numerous sensory organs in the skin. Receptors for heat and cold, touch, pressure and pain are located in the skin.

- Participates in thermoregulation of homeothermic organisms (organisms having constant somatic temperature, such as birds and mammals) regulating heat released from the body (sweating).

### ***Skin Structure***

It can be seen under the microscope that skin in vertebrates has two layers:

- The outer layer –epidermis;

- The inner layer – dermis. These two layers differ in structure, function and origin.

### ***Epidermis***

The epidermis is composed of several layers of epithelial cells closely packed together to form a compact layer. The number of layers (20 to 30) is different in different body regions, for example, in humans the number of layers is larger on palms and soles. Surface layers are made of completely flattened cells, gradually dying out and being replaced with new ones. These cells overlap like tiles on the roof enabling skin to extend during

movement. Each day thousands of dead cells fall off, yet the skin is not abraded because the cells are constantly being regenerated.

The lower layers of epidermis, next to dermis, are active throughout life and form upper cell layers by division. They represent the so called germinative layer. In the cells of upper layers cornification occurs— cells are gradually filled with keratin, leading to cell death. Thus, a layer of dead cells is formed on the body surface – the horny layer. Between the horny layer and the germinative layer, transitive layers are located where cornification is not yet completed. The horny layer has a protective role and is especially developed in typical terrestrial vertebrates, reptiles, birds and mammals, while in amphibians it is relatively thin. Surface horny layers are constantly shed completely or partially (desquamation), or periodically - complete change (molting in serpents— viper shed skin). During lifetime, a person loses approximately 18 kg of dead skin.

The melanocytes are located in the lower layer of epidermis. They create the pigment melanin, protecting the skin from excess ultraviolet radiation -melanin becomes darker as it absorbs light energy. This induces suntan when skin is exposed to sunlight. Melanin is transferred to the surface and is shed together with dead cells, causing the suntan to disappear gradually. Persons with darker complexion have more melanin. The melanocytes can be berry-shaped forming freckles.

During evolution, various protective structures have developed from the horny layer, such as horny scales (covering the body of lizards and vipers), horny plates (turtles and crocodiles), feathers, hair, claws, nails, hoofs, horns, etc. Feathers (by ecdysis) and hair (shedding) are also periodically cast off.

### ***Dermis***

The *dermis* is formed of airy connecting tissue where collagen fibers are dominant, submersed in a matrix containing fibroblasts, macrophages, lymphocytes, and adipose cells.

Intertwined fibers of a special protein called collagen and elastin make the skin elastic. Terminations of blood and lymph vessels, nerve terminations, various sensory organs, muscle fibers, derivatives of epidermis and dermis are located in the dermis.

Dermis surface forms multiple protrusions entering into epidermis, resulting in close connection between these two layers. Blood and lymph vessels, smooth muscle fiber braids (connected to the hair and feathers), free nerve endings, and sensory organs are located in dermis. Various exocrine glands that discharge secretion to the skin surface via ducts are also located in dermis.

When it is too hot, thousands of minute blood vessels in dermis dilate, allowing more blood to flow. This surplus blood near the skin surface enables the heat to leave the body and to cool off. This is why we blush when we are hot. When we are cold, blood vessels contract preserving heat, resulting in a pale complexion.

Blood in these blood vessels transports aliments to both skin layers, and takes away the by-products. When we cut or hurt ourselves, a blood clot is formed closing the wound, serving as protection against germs, at the same time preserving essential body fluids.

Dermis contains various nerve terminations, connected to the brain, enabling us to experience the world via the sense of touch. Nerve terminations, or receptors, branch-

ing toward the epidermis, react to pain. Meissner's corpuscles are located in the upper dermis - touch receptors detecting slight pressure. Ruffini corpuscles - heat receptors, and Krause corpuscles - cold receptors are located deeper in dermis. Near the dermis root, Pacinian corpuscles are situated, reacting to intense pressure. When these nerve terminations detect any kind of pain, pressure, or temperature change, they send a message to the brain. The brain then commands muscles to act - this is how we retract the hand from a hot cup.

### ***Skin Glands***

Sweat glands are deeply rooted in dermis. Liquid secretion of sweat glands eliminates matter exchange products, and plays a vital role in thermoregulation (reducing body temperature). They are shaped as tubules whose lower termination is curled into a bulb and situated in dermis, while the upper ending leads to the skin surface. These glands produce sweat, watery, slightly saline liquid, coming from sweat pores onto the skin surface when we feel too hot. It evaporates helping us to cool down.

Sebaceous glands produce a thick, viscous, fatty secretion or sebum, which is discharged near the hair root and serves for hair lubrication, prevention of skin drying and desquamation. Without this protection, the skin would dry and split and could not withstand everyday wear. They are missing from hairless regions, except the eyelids and lips. Sebaceous glands in some people cause inflammation, especially in teenagers, because they produce too much sebum. This blocks hair follicles that can be infected by bacteria and thus transformed into acne.

To each hair follicle, an arrector muscle is attached. When we are cold or scared, these muscles shrink and raise the hair. Skin around the hair is also lifted – forming goose bumps. This reaction is from the time when the human body was covered with thick hair. When it was cold, hair would rise to capture more air and provide better isolation. When a cat is scared; its fur rises, the cat appears bigger and fierce. This is the same reason human hair rises when humans feel fear.

Adipose tissue is located below the dermis, acting as an insulator and covering, protecting the body from cold by preventing heat loss. This is also an energy source in emergency situations. When excess calories are consumed, this is the location where they are stored. Internal organs are located below the fat, including muscles, glands and main nerves and blood vessels. Their safety depends on this live barrier - the skin.

Mammary glands are well developed only in female mammals and their secretion serves to feed the young. Mammals have also glands with scented secretion serving for mutual recognition or as a defense tool.

### ***Skin Color***

Skin color depends on three factors: on the yellowish shade of epidermis cells, transparency of epidermis cells permitting the reflection of blood vessels located below giving purple tones to the skin, and on the type and quantity of pigment. Pigment carrying cells are mostly located within dermis, although they can be found in epidermis. Beneath the skin, there is the subcutaneous layer, which is fluffier, compared to dermis. This layer connects the skin with muscles. Adipose reserves are often accumulated in this layer.

**Chronic Venous Insufficiency**

Chronic venous insufficiency (CVI) can be defined as a dysfunction of the venous system caused by valvular inadequacy, isolated or combined with vein obstruction. This term includes all primary and secondary venous disorders except the mentioned acute states. It can be caused either by impairments of the perforating system or of the deep venous system, and its basic characteristic is raised blood pressure in veins of lower extremities (venous hypertension). CVI can be combined with visible varicosities. The disorder is manifested as a progressive chronic vein stasis, edema and changes on the skin, such as pigmentation and thickenings (lipodermatosclerosis). In the terminal stadium of CVI, ulcerations appear. *Ulcus cruris* is defined as "a lesion – defect of skin and subcutaneous tissue on crus that does not heal during 6 weeks". In 95% cases *ulcus cruris* is of venous etiology, but it can also be the result of arterial (20%- 25%) or mixed, arterial-venous disorders, only rarely the result of hematologic, lymphatic, neoplastic or other disorders.

Residual proximal thrombotic occlusion of veins of lower extremities; (i.e., insufficient lumen recanalization) leads to progressive distal valvular incompetence, vein reflux, vein stasis and hypertension, manifested by leg edema, occurrence of secondary varicosities, „venous claudications“ and, in the end, by the appearance of venous ulcerations on the crus. Stasis in the deep veins leads to progressive impairment of valvulae of perforating veins, causing the development of a pathological reflux of blood from deep veins into the surface system, resulting in a progressive stasis in the surface system as well, impaired microcirculation of the skin and the subcutaneous tissue.

The latest classification of CVI, beside the clinical manifestations, takes into account the etiology, anatomic distribution and patophysiological mechanisms. This classification is called the CEAP classification (C-clinical manifestation, E-etiology, A -anatomic distribution, P -patophysiological finding). The CVI diagnosis is established based on anamnesis, clinical manifestations, noninvasive and invasive diagnostic procedures.

Therapy: compression, sclerotherapy, medicamentous therapy, surgical procedures.

**Case Description**

Patient is 62 years old. Problems started 5 years ago. First an edema occurred, followed by pain in crura, more to the right. Followed by skin scaling; the skin is red, thinned and dry.

**Protocol**

Application of the BIOPTRON hyperpolarized light:

- once a day,
- during of 8.30 min,
- clearance -7cm, lasting 20 days.

**Patient Status before Treatment**

The patient had not been treated with medicaments, neither systemically or locally before the beginning of the treatment. The patient experienced fatigue, heaviness sensation in lower extremities, pain, edema, redness, trophical skin changes, blue-green network of dilated capillaries and veins.

### **Patient Status after Treatment**

In mid treatment, after 10 days, a reduction of edema and inflammation is visible. At the end of treatment, after 20 days, reduction of accompanying symptoms is visible.

### **HPL Action Mechanism**

When the surface skin layer is impaired, the epidermis is damaged. If the basement membrane is not impaired, the natural healing process of lesions without scarring lasts from 28 to 45 days, depending on patient's age, sex, and biophysical skin status. However, when we want to accelerate the healing process of a skin surface impairment with hyperpolarized light (HPL), we activate: (1) collagen fibers of type VII, which, via the laminin and integrin, stimulate the reproduction of keratocytes in the basement membrane, (2) we accelerate their transition from the *stratum basale* into *stratum spinosum*, (3) and then into *stratum granulosum*. As soon as the forming of new cells in *stratum granulosum* starts, the HPL (4) organizes lipids into nano layers, between which water is located as the main protective factor against the external environment influence. With the forming of *stratum granulosum*, the process of skin repairment is completed. Owing to the HPL effect, this process takes from 10 to 24 days.

### **Patient's Opinion**

At the beginning of treatment patient felt slight pain and heaviness in the legs, while at the end of the treatment, pruritus and skin strain are rarely felt.



### **Conclusion**

Hyperpolarized light applied to cutaneous manifestations of the chronic venous insufficiency produced excellent results; all symptoms were reduced almost completely. Conclusion is that this method is more efficient with respect to expected results than other methods.

### **References**

1. Šorić, V. Morfologija i sistematika hordata. Kragujevac: Univerzitet, Prirodno-matematički fakultet, 2002.
2. Kalezić, M. Osnovi morfologije kičmenjaka. ZUNS, Beograd, 2001.
3. Maksimović, Ž. Klasifikacija i klinička slika akutnih i hroničnih vaskularnih oboljenja. U: Osnove vaskularne hirurgije i angiologije (Ž. Maksimović i sar.), CIBID, Medicinski fakultet, Beograd, 117-123, 2004.
4. Dijagnostika i lečenje venskih oboljenja. Medicinski fakultet Beograd, Medicinski fakultet Niš, Udruženje flebologa Srbije i Crne gore, Gamzigradska Banja, 2005.



### 7.3 Effect of Hyperharmonized Light on the Modification of EEG Signals

*Duro Koruga, Laboratory for Biomedical Engineering, NanoWorld AG, Belgrade*

#### Introduction

The aim of biomedical photonics is to aid the prevention and maintaining of the functional status of tissues, organs and the human organism. However, when a dysfunction occurs, it should be eliminated, that is, the impaired function of the biomolecule, tissue, organ or the organism should be restored.

Three basic light types are used today in biology and medicine: diffuse, polarized (linearly or circularly) and laser light. Chapter VI described basic characteristics and applications of diffuse, linearly polarized and laser light in medicine. Circularly polarized light is applied mostly for the determination of optically active chromophores and secondary protein structures ( $\alpha$ -helix,  $\beta$ -plate, and R-„random structure“) (Campbell, 1984).

This monograph investigates light and its influence on biological systems, in case when *diffuse* light interacts with the  $C_{60}$  molecule forming a thin film ( $C_{60}$  can also be incorporated into polymer material or some other material having transparency greater than 92%). We named this kind of light *hyperharmonized*, because the electromagnetic photon fields are organized according to the degree of curvature, and not as „aligned soldiers“ (as in the case when the linearly polarized light is transformed into hyperpolarized light); they are distributed randomly regarding energy but *hyperharmonized* as an active (information) pattern (Koruga, 2008). We have already seen how the linearly polarized light effects the „shift“ of wavelengths (left and right of 680 nm, Figure 7.1-7), this being very significant for the protection of the human eye from the intense blue light. This study examined the effect of *hyperharmonized light* on the human brain, primarily the modification of EEG signals.

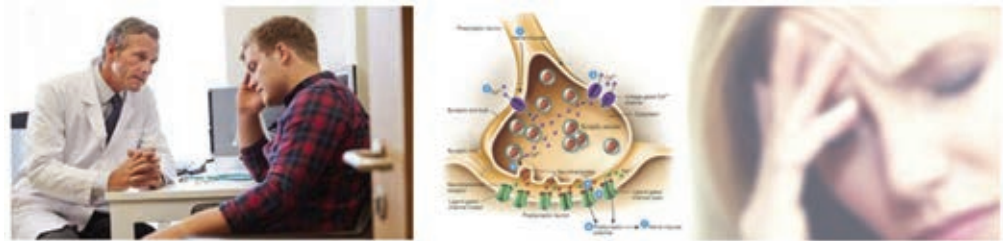


**Figure 7.3-1** Most disorders of brain functioning, such as headache (left), depression (right) etc., are caused by inadequate neurotransmitter discharge at the synapses ([www.headache.com](http://www.headache.com)).

Similarities and differences between hyperharmonized and hyperpolarized light are displayed in Figure 7.3-2. In diffuse light, the direction, orientation of the electromag-

netic photon field (EM) and photon intensity are arbitrary. When photons of different energies (wavelengths/frequencies) interact with the  $C_{60}$  molecule, the orbital angular momenta are oriented according to the Fibonacci laws [ $\phi$ ,  $\Phi$ ], however, the energy intensities remain diffusely distributed. Regarding the hyperpolarized light originating in the interaction with the  $C_{60}$  molecule, orbital angular momenta ( $J = L + S$ ) and energies are organized according to intensities (in the hyperpolarized light; the organization of energies according to intensities was “prepared” by the linearly polarized light, because photons of the same wavelength are already „packed” in a plane).

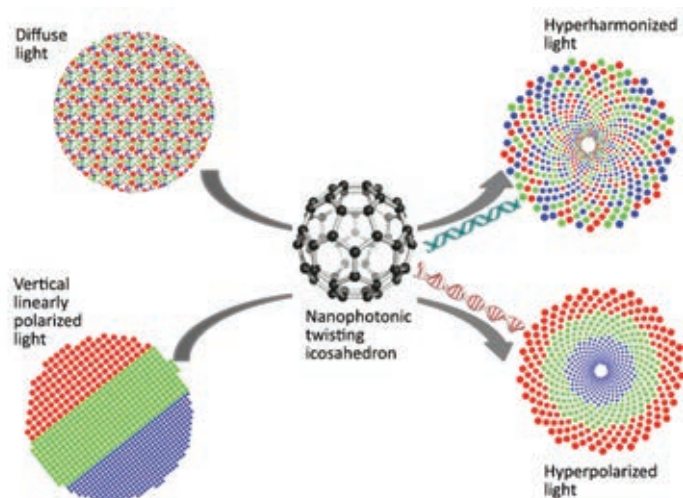


**Figure 7.3-2** Similarities and differences between hyperharmonized and hyperpolarized light: the first originates in the interaction between the diffuse light and  $C_{60}$  molecules, twistingly rotating at  $\sim 10^{10} s^{-1}$ , and the HPL is formed in the interaction between the linearly polarized light and  $C_{60}$  molecules.

The study examined twelve research subjects (volunteers); three subjects were recorded at the Military Medical Academy in Belgrade, and nine research subjects at the Medical Faculty in Belgrade. Recorded data were processed at the „Siniša Stanković” Biological Institute, at the Department for Multidisciplinary Research.

It is known that the EEG (electrical) and MEG (magnetic) brain signals are modified under the influence of daylight, signals are different when eyes are open and when eyes are closed (Figure 7.3-4).

The dynamics of neurotransmitters discharge at synapses is one of the main mechanisms of EEG and MEG signal generation (Figure 7.3-5). The character of electrical and magnetic dynamics established depends mainly on the carrier of neurotransmitters to the presynaptic part of the neuron. This is the role of the clathrin structure (Fibonacci biomolecular structure; refer to Chapter VI). As the hyperharmonized light is, regarding the orbital angular momenta (OAM) organized according to Fibonacci laws [ $\phi/\Phi$ ], the study’s aim was to determine whether hyperharmonized light via clathrin affects the EEG signals and how.

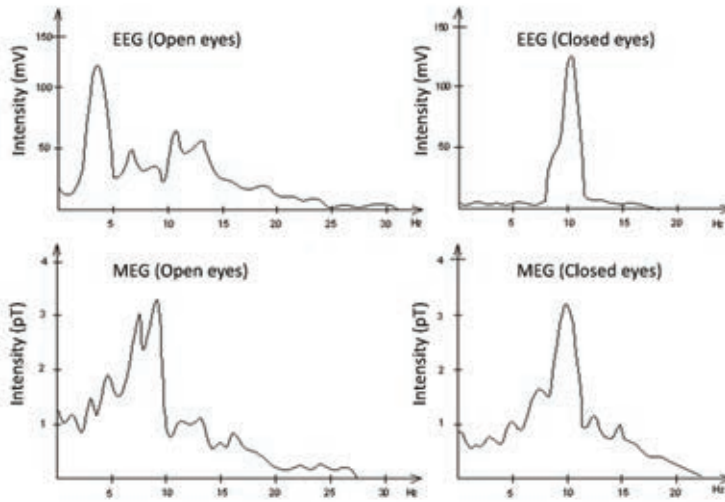


**Figure 7.3-4** Light influence on the functioning of the CNS: when eyes are open and when eyelids are closed. Electrical (EEG) and magnetic (MEG) brain signals operate at approximately the same frequencies when eyelids are closed (the main magnetic peak is at 9 Hz, and the electrical peak is at 10 Hz), while they are different when eyes are open: the main magnetic peak is at 9 Hz, and the electrical peak at 3 Hz. (Adapted from: Kato, 2006)

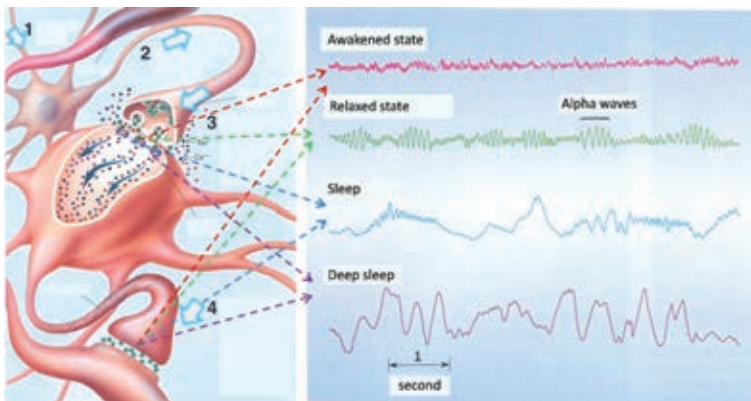


**Figure 7.3-5** Different forms of EEG signals when awake, during sleep, etc., resulting from the discharge of neurotransmitters at synapses. The process is very complex and takes place in the system of neuronal networks. Many dysfunctionalities of the brain can be observed through the regularity/irregularity of EEG signals: (Adapted from: Kato, 2006; Basar, 1990, Torotora, 1981).

## Material

Eight males and four females volunteered in this initial study investigating the influence of harmonized light on the EEG signals. Subjects' ages were between 26 and 54 years.

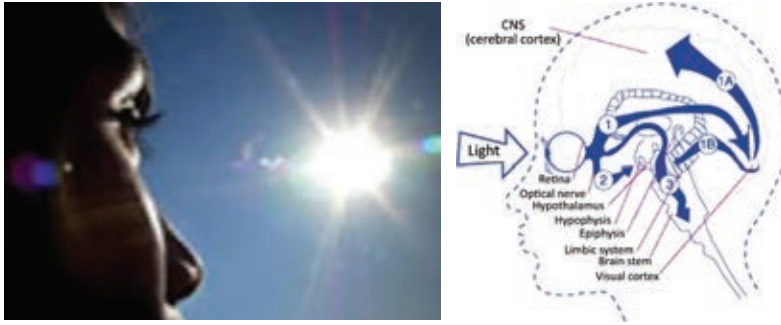


**Figure 7.3-3** Light via the eyesight affects the hypothalamus, the visual cortex, the cerebral cortex, and other CNS structures. Since the regulation system is the integral neuro-endocrine-immune system, the influence of light through the CNS on the endocrine and immune system is possible.

## Method

Nanophotonic glasses were constructed for this study by applying a thin film of 100 nm  $C_{60}$  molecules on a glass 1.5 mm thick. Above the thin film, a covering glass was mounted, 1 mm thick, and edges of these two glass surfaces were connected with adhesive tape, so that air could not infiltrate the space where thin film was applied for a time (Figure 7.3-6).



**Figure 7.3-6** Volunteers with glasses (left and right) that in the interaction with daylight generate hyperharmonized light. A differential EEG system (middle) was used for measuring the electrical brain activity).

Four positions were used (Fp1, Fp2, F3, F4) for the recording of EEG signals, which were, via the EEG headpiece (Figure 7. 3-6, *middle*), connected to the apparatus and the analyzer. At these four points, intensity of EEG signals under good functional conditions of the brain is approximately the same. Before the glasses were put on, the EEG signals were recorded during 10 minutes, and diagrams determined giving the average value in this period. Under the same ambient conditions, research subjects put on the nanophotonic glasses and the recording of EEG signals was continued during next 10 minutes. Average values were calculated based on the recorded data for all four positions during this period.

## Results

All research subjects experienced changes in EEG signals. Figures 7.3-7 and 7.3-8 show two characteristic cases. In the first case, signal Fp1 was not of adequate intensity with respect to other three signals. Ten minutes later, the intensity of the Fp1 signal reached an adequate value. Other three signals were improved as well (Fp2, F3, F4), especially signal Fp2.

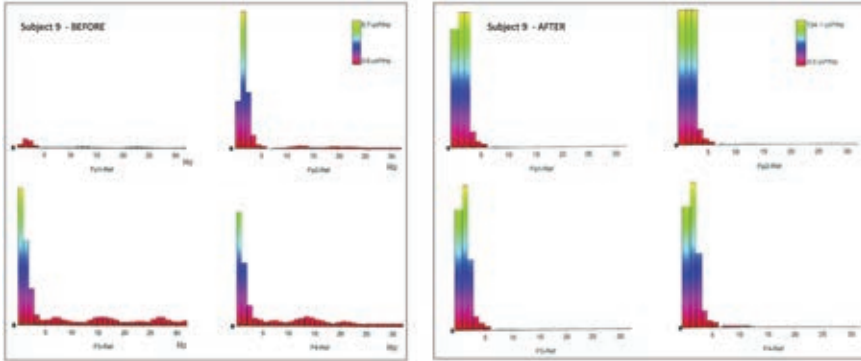


**Figure 7.3-7** Example of EEG signals in one of the 9 research subjects when electrodes were positioned at locations Fp1, Fp2, F3, F4 of the “brain cap”; (left) before the treatment; and (right) 10 minutes after exposure to daylight.

The second case is more characteristic: at first, three signals were not adequate (Fp1, F3 and F4). They were improved after the treatment, that is, a more functional performance of brain structures was obtained.

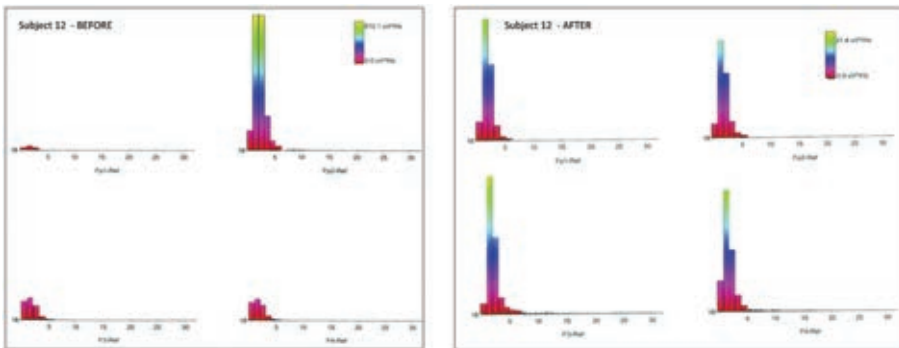


**Figure 7.3-8** Example of EEG signals in one of the 9 research subjects when electrodes were positioned at locations Fp1, Fp2, F3, F4 of the “brain cap”; (left) before the treatment, and (right) 10 minutes after exposure to daylight.

Mechanism of the hyperharmonized light action on the modification of EEG signals is explained by the effect, via the visual cortex, on clathrin having the same structural (icosahedral) matrix as the harmonized light.

Research conducted in the USA by the leading psychiatrists also points to the conclusion that the entire human brain functions according to the principle of the Fibonacci law  $\Phi$  (Tononi, 2012). Giulio Tononi is a professor at the University of Wisconsin (USA), one of the leading researchers of the consciousness phenomenon. He cooperated with Gerald Edelman, the Nobel Prize winner for physiology and medicine in 1972, in the field of the immune system research.

## Discussion

Acquired, preliminary results point strongly to the conclusion that we can influence brain functioning by hyperharmonized light to regulate the normal discharge of neurotransmitters at synapses. Since good results were achieved in the treatment of psoriasis by hyperpolarized light, it would be necessary to organize a study, where, by applying hyperpolarized light through eyesight, with eyes closed, we would act on the brain (Figure 7.3-9) simultaneously with another device treating the region with psoriasis. This is justified reasoning, because psoriasis is, besides being of organic origin, caused by psychosomatic factors as well. Gerald Edelman believes that not only the brain functions according to the „ $\Phi$ ” law, but the entire human organism. His attitude is based primarily on the information viewpoint, because information is central for the investigations of the consciousness phenomenon.



**Figure 7.3.9.** *Volunteers in the ZEPTEr Medical and ZEPTEr International center testing the subjective feeling of hyperpolarized light action through eyesight, with eyes closed.*

One more paper points to the conclusion that brain is functioning according to Fibonacci laws (Weiss, 2002). This paper proposes that the principle of information coding within the brain is based on the Fibonacci law  $\Phi$ , that this is the missing link between the psychometric intelligence measurement and comprehension. Metrics of brain waves, according to the authors, can always be represented as a superposition of  $n$  harmonics multiplied by  $2\Phi$ , where half of the basic state is represented precisely by  $\Phi$  ( $= 1.618$ ) and has the meaning of a resonant point. Such wave series represent bifurcation processes occurring in the brain functioning as “deterministic chaos” (Basar, 1990) because  $2\Phi = 3 + \phi^3$ . Having in mind that  $\Phi^2 + \phi^2 = 3$  (basis of the twisting torus of  $C_{60}$ ), functioning of the brain, as a system operating in the domain of “deterministic chaos”, can be corrected

(brought to a functional state by the influence of hyperharmonized and hyperpolarized light:  $2\Phi = \Phi^2 + \phi^2 + \phi^3$ ).

## **Conclusion**

Results of the initial study of hyperharmonized light effect (synchronized spatial-temporal effect of diffuse light on the  $C_{60}$  molecule) on the EEG signals, in twelve research subjects, clearly point to the modification of signals. Everything points to the fact that the action mechanism is established through Fibonacci structures: orbital angular momenta of the photon and of clathrin in the brain have the same symmetry. This is a classical example how the principle „structured light meets structured matter”, which researchers have predicted several years ago (Lichinister, 2012), is realized.

**Acknowledgement:** I am grateful to Prof. Dr Nikola Ilanković and his associates at the Medical Faculty in Belgrade and the Military Medical Academy for assistance in the measurement of EEG signals. My gratitude goes also to the associates of the „Siniša Stanković” Biological Institute for the assistance in processing EEG signals. Ljubomir Latinović provided important support to the study, and took part in the study (as a research subject). I owe special gratitude to volunteers - students of master, specialist, and doctoral studies at the Belgrade University. Contribution to this study of Željko Ratkaj is especially valuable and outstanding.

## **References**

1. Basar, E., Chaos in Brain Function. Springer-Verlag, Berlin, 1990.
2. Berne, M.R., Levy, N.M., Physiology. Mosby, St.Louis, 1998.
3. Campbell, I.D., Biological Spectroscopy. The Benjamin, Menlo Park, 1984.
4. Edelman, G., and Tononi, G.: A Universe of consciousness, Basic Books, 2000.
5. Kato, M. (ed), Electromagnetics in Biology. Springer, Tokyo, 2006.
6. Koruga, Dj., Apparatus for Harmonizing Light. Patent US 2008/0286453 A1, Published Nov. 20, 2008.
7. Lichinister, M.N., Structured Light Meets Structured Matter. *Science*, Vol. 337, pp. 1054-1055, 2012.
8. Tononi, G., PHI: A Voyage from the Brain to the Soul. Pantheon Books, New York, 2012.
9. Tortora, G.J., Anagnostakos, Principles of Anatomy and Physiology. Harper&Row, New York, 1981.
10. Weiss, H., Weiss, V., The golden mean as a clock cycle of brain waves. *Chaos, Solitons and Fractals*, vol. 18, issue 4, pp. 643-652, 2003.





# 8

## EPILOGUE



*There is nothing worth thinking  
that has not been thought before  
We must only try to think it again*  
GOETHE

## **8.1. Time Phenomenon and Biological Time**

It seems like scientists are going where poets and artists have already been. This fundamental thought of Goethe, directs science to deal with nature, its laws, and technology created by man in the interaction with nature.

The tool of science is the language of mathematics, and the tool we use to investigate nature and create technology is the world of numbers and number systems. There is a consensus among philosophers that *technology* seriously puts forward the question *what is man* (Burger, 1979). It is hard not to agree with scholars contemplating reality and concluding that modern civilization has embarked into „space and time, and got carried away by motion“, whereby „time denaturation“ occurred- time became separated from man’s organic and natural requirements, such as awareness and sleep, or, in nature, the rising and setting of the Sun, and transformed into a machinery created by the *clock*. It is believed that the first modern clock was constructed in 1370 in Paris, and that since „eternity ceased to be the *measure* and *focus* of human existence“ that is reflected above all in creation. Consequently, many philosophers consider the *clock*, and not the *steam engine*, the main driving force of the modern industrial era.

We are „walking a tightrope“ toward this awareness – followed by the thought of St. Augustine (Christian saint and philosopher from the 4 century) „we do not live in time, we are the time“. In both cases (space–time and time denaturation) there is a *scenario* and harmonization of factors that constitute it in reality: *mass, energy, information, organization, and control*. According to the approach presented in Chapter II, *space* and *time* are unit spheres ( $C_{space}^{C_0} = 0!$ ,  $C_{time}^{C_1} = 2$ ) (see Table 2.2, values of unit sphere  $C_0$  and volume  $V_0 = C_0 r^0$  for  $N = 0$ ), whose packing generates code (information, meaningful content) built into all five mentioned reality attributes. In other words, our approach to the examination of the Universe (and man) as a 3D space where events take place in time, results from „denatured time“ that evolves in our being. Due to the experience of time as a „denatured“ entity, we perceive events according to the „arrow of time“ (successive events taking place one after another – a process in this time is irreversible). Science does not define time clearly; it does not define time nor does it explain time’s properties, i.e., „it is most frequently used as an intuitively clear concept“ (Gruyitch, 2006).

To explain the phenomenon of „denatured time“ let us examine an example from biology. Let us observe any protein, for instance  $\alpha$ -tubulin containing 450 amino acids. This is a structure (4 x 3 nm) resembling a football ball (or, at the nano level, the  $C_{70}$  molecule). Another, perhaps more obvious example, is clathrin, the biological analogue of the  $C_{60}$  molecule. In both cases, when the S-S covalent bond and the intramolecular noncovalent bonds are severed, a linear amino acid structure results (more precisely a linear sequence of peptide planes and lateral amino acid groups); we say that the protein is in a denatured state. However, it should be noted that generation of each protein is actually DNA denaturation (the double helix is deconstructed, generating mRNA from one DNA thread, from mRNA the rRNA originates, which, in synergy with tRNA, transforms the amino acid into a ribosome and a protein chain). If the DNA contains the „code“ of the biological being (proteins are only a segment of the „other side“ of the DNA, as in heads/tails), it would be interesting to analyze the DNA from the aspect of its denaturation into mRNA and light. In the denaturation of the double DNA helix into a single mRNA thread, one of the significant events is the addition of water to the newly formed, denatured DNA thread. Note that DNA and mRNA exist in a water environment, therefore, it is necessary to analyze the structure and dynamics of DNA, mRNA and water.

## 8.2. Biological Systems as Light Beings

If we examine the DNA from this aspect, we observe that „denaturation“ means disentanglement of the chromosome from the complex 3D form (Figure 8.1, pos. 6) seen under the microscope (size  $6 \times 1.5 \mu\text{m}$ ), into a double helix, as a quasi 1D form (Figure 8.1, pos. 1). The double helix is about 1 m ( $10^9$  nm) long, its diameter is only 2 nm (a structure where one dimension is million/billion times greater than the other dimension in  $N$  space, is called a *quasi-N-dimensional object*).

Light velocity, defined in vacuum via the electric permittivity  $\epsilon_0 = 8.85418 \times 10^{-12} (F \cdot m^{-1})$  and magnetic permeability  $\mu_0 = 4\pi \times 10^{-7} \text{ N} / \text{A}^2 \approx 1.25663 \times 10^{-6} (H/m)$  is expressed as

$$c_0 = \frac{1}{\sqrt{\epsilon_0 \mu_0}} \quad \text{pa je} \quad c_0 \times \sqrt{\epsilon_0 \mu_0} = 1 \quad (8.1)$$

where

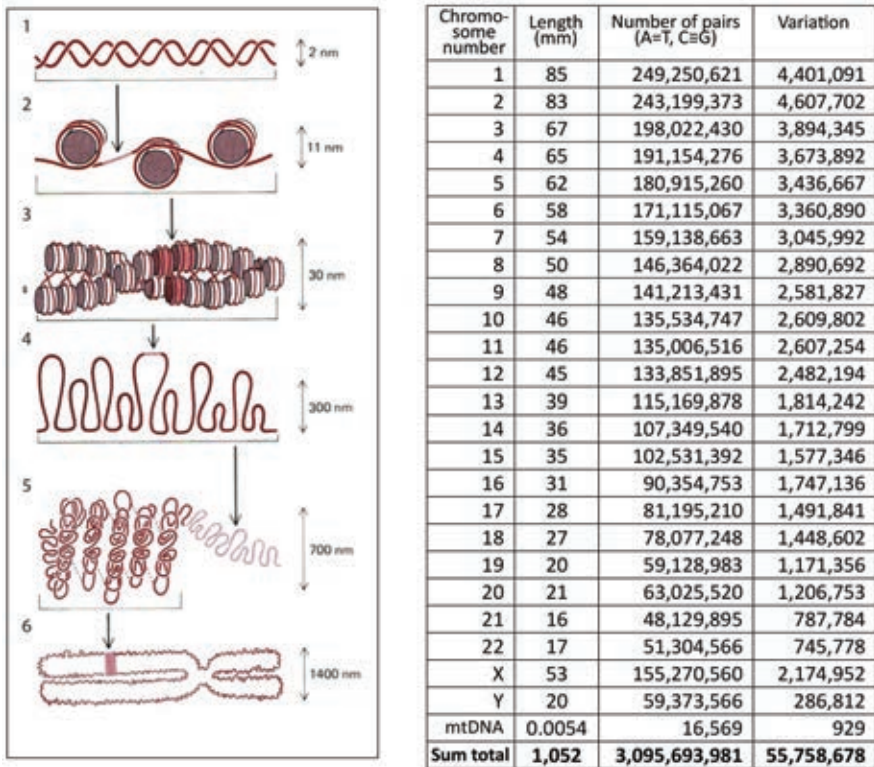
$$\sqrt{\epsilon_0 \mu_0} = \sqrt{8,854 \times 10^{-12} \times 1,257 \times 10^{-6}} = \sqrt{11,22 \times 10^{-18}} = 3,35 \times 10^{-9} \text{ (s/m)} \quad (8.2)$$

giving

$$c_0 \times \sqrt{\epsilon_0 \mu_0} = (2,99 \times 10^8) \times (3,35 \times 10^{-9}) = 1 \quad (m/s \times s/m = 1). \quad (8.3)$$

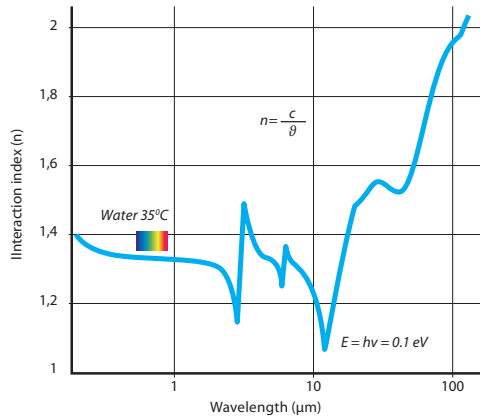
As *velocity* (m/s) implies a spatial change of *position* of the mass point in time, likewise in the (s/m) *scenario* we have a temporal change of *scene* in space. If (and only if) the carriers of information processes in biological systems are a direct unity of electromagnetism

and matter, the basic elements of codogenic structures (DNA – nucleotides, proteins – peptide planes, and biological water – the water molecule) will become protagonists of the *scene* in the biophysical *scenario*. Each nucleotide in the DNA will be a protagonist of the scene. Therefore, the number of scenes in the scenario equals the number of nucleotides. If the *light biological being* were to exist in a vacuum, it would have  $3.35 \times 10^9$  nucleotides. However, this is not the case, because the light biological being (man) exists in a water environment (man is 65–70% water), therefore, it is necessary to correct light propagation in biological water (temperature 37 °C). Chapter VI demonstrated that water at temperature of 37 °C and water in a „water bridge“ at 25 °C have the same spectroscopic characteristics across the 10–14  $\mu\text{m}$  domain (Fuchs, 2012). We observe that the refraction index for the 12  $\mu\text{m}$  wavelength is ( $n = c/\vartheta$ ) 1.08, and not 1.33, as in ordinary water at 25 °C (Figure 8.2).



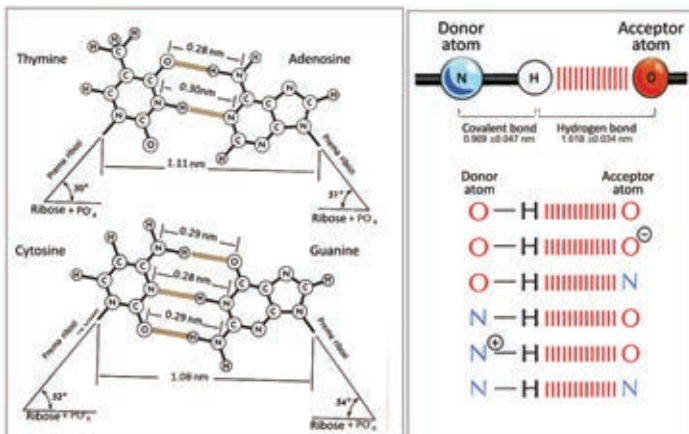
**Figure 8.1.** Hierarchical organization of the DNA structure (from the double helix „1“ to chromosome „6“ (left), and chromosome length, pair number, and variation in the chromosome within the human genome (right) (Adapted from: Alberts, 2002, and the Human Genome Landmarks, 2009).

Transiting from „vacuum electromagnetism“ to „aqueous electromagnetism“, i.e., correcting the refraction index, we obtain  $(3.35 \times 10^9)/1.08 = 3.10 \times 10^9$  for the number of nucleotides, which corresponds 99.83% with the number of nucleotides within the human genome (male sex).



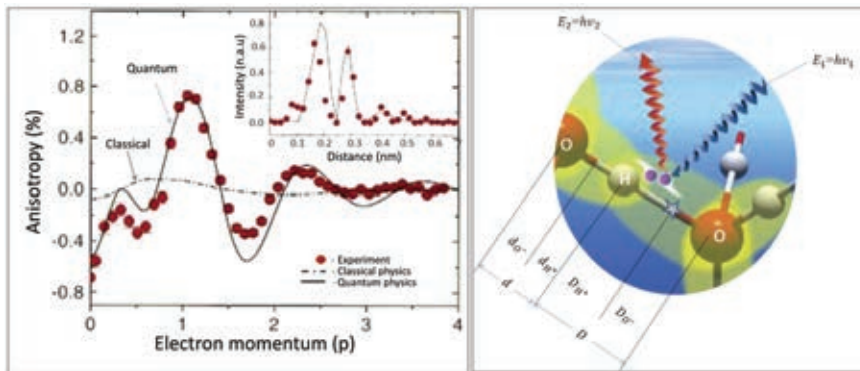
**Figure 8.2.** Water refraction index at 37 °C has characteristic peaks at 2.85  $\mu\text{m}$ , 3.3  $\mu\text{m}$ , 5.8  $\mu\text{m}$ , 6.2  $\mu\text{m}$  and 12  $\mu\text{m}$ . Peaks 2.80/3.30 are significant for the hydrogen bonds of water molecules, while peak 12  $\mu\text{m}$  is important for bonding nucleotides  $A = T$  and  $C \equiv G$ . For the water-DNA interaction (between the phosphorous group and ions), the external side of the interaction is at 110  $\mu\text{m}$ , giving the refraction index  $n = 2$ . Light travels two times slower through the external DNA (phosphorus, ribose), than through the DNA axis (central symmetry axis), which intersects, under a right angle, the double ( $A = T$ ) and triple ( $G \equiv T$ ) hydrogen bonds.

Table (Figure 8.1, right) displays the number of nucleotides 3 095 693 981 in males, for 22 chromosomes, plus the X and the Y chromosome. Since the female sex has two X (XX) chromosomes, this gives 3 191 590 975 nucleotides, resulting in 97.2% conformation to the calculated value. Photon energy for the best light-DNA interaction (in water, at temperature of 37 °C) is 0.1 eV ( $\lambda = 12 \mu\text{m}$ ), which is about 10 times smaller than the visible light energy.



**Figure 8.3.** Nucleotides  $A = T$  connected by two hydrogen bonds (left) and  $C \equiv G$  connection having three hydrogen bonds, which oscillate between the donor and the acceptor (right), varying distance within given limits. There are 6 basic types of hydrogen bonds linking the donor and the acceptor within DNA (modified from: Alberts, 2002).

The DNA nucleotides (A, T, C, G), in the form of triplets (ATT, GAC, etc.), code 20 amino acids that enter the protein structure, therefore, the code system is given by  $4^3 = 64$  codons. However, it is less known that the above code is in a one-to-one correspondence with the genetic code  $2^6 = 64$ , which was discovered later (Doolittle, 1981, Swanson, 1984, Rakočević, 1998).



**Figure 8.4.** Comparing the classical and the quantum approach to hydrogen bonds with experimental results (left). Experiments and quantum physics correspond very well. The experiment demonstrates that, from the aspect of quantum mechanics, there can be several hydrogen bond lengths, although two values are dominant: 0.16 nm and 0.28 nm (Isaacs, 1999) (right). The ratios between distances (oscillations) of a noncovalent hydrogen bond ( $D_{H+}$ ) to the distances between donor and acceptor atoms (compare to Figure 8.3, right).

Considering the classical binary DNA code, six types of hydrogen bonds, and that the hydrogen bond is quantum-classical (not just classical, as it used to be believed), the synergetic DNA code can be expressed as  $2^6(2^{6+1} - 1) = 8112$  (Koruga, 2012). This result points to the conclusion that the DNA does not code only amino acids, but also codes what used to be called „junk“ in molecular biology (93%); actually it codes regulation processes within the organism. This coding is based on the synergy between the *classical* chemical-physical code ( $4^3 = 64 = 2^6$ ) and the *quantum* code ( $2^{6+1} - 1 = 127$ ).

Consequently, the DNA is a codogenic entity having a codogenic electromagnetic field based on noncovalent hydrogen bonds. The structure of this field is defined by *triple* and *double* hydrogen bonds ( $3/2 : [≡]/[=]$ ). There are indications that this structural organization is related to the structural organization of the  $N = 0$  dimension, whose dimensionality is  $3/2$  (Chapter II, Table 2.2). This points strongly to the conclusion that dimension  $N = 0$ , from the information aspect, is realized in biological systems through DNA, proteins and water, as entities which are, although of material nature, in a direct relationship with light under certain circumstances- „structured light meets structured matter“.

The above findings about DNA establish priority of *information* over mass, energy, and other conventional concepts of the classical and quantum physics. The maxim by Victor Hugo „nothing is stronger than the idea whose time has come“ leads us to the *codogenic spacetime* within us. From the aspect of science, it seems that the time has come, because as we presented in Chapter III, one of today’s leading mathematical

physicists Roger Penrose demonstrated, using universal physical constants ( $G, h, c$ ), that a *science* is missing from the contemporary system of sciences, which would unite and transcend *classical* and *quantum* physics.

The first herald of *information physics* is undoubtedly Schrödinger, because, already in 1943, in his book *What is Life? Mind and Matter*, he characterized chromosomes (DNA) as aperiodic crystals. In other words, he anticipated the „codogenic mass“ containing information, as opposed to the ordinary mass not containing codogenic information (Schrödinger, 1943). Even after 50 years, at the meeting of eight eminent scientists from this research domain much progress was not made, but consensus was reached that *a new science is necessary* in order to understand the life phenomenon (Murphy, M.P. and O'Neill, 1995). This new science is precisely the science that Penrose perceived, and one of the three supports of this science is Schrödinger's cat, leading us along the path of quantum matter states, based not only on energy, but on something missing from the official physics.

Vlatko Vedral anticipates this new science in the form of *information physics*, relying on Schrödinger and Shannon. In his book *Decoding Reality: The Universe as Quantum Information*, 2010, he postulated information (*quantum* information) as one of the basic physical entities. He approaches *information physics* via Shannon's information theory and entropy. In the epilogue of this book, the author remarks: „...everything in our reality is composed of information... information can be created from a void... viewing reality as information leads us to recognize two opposed trends ... *natural laws* are *information* about *information* and beyond them there is only darkness...“ (Vedral, 2010).

### 8.3. Full Moon Phenomenon

What is darkness in nature with respect to information and light? What is the fundamental feature of nature? According to contemporary scientific findings, this could only be gravitation (related to dark matter and dark energy). However, until now gravitation was only „to blame“ if we were awkward, fell and sprained an ankle or sustained some other injury. „We blame“ gravitation when full Moon shows in the skies, because some individuals become irritable and disrupt the „harmony“ of living, they stage a performance. The full Moon phenomenon and its effect on some people (not on everyone) actually exist, but it has not been adequately explained yet. This phenomenon is, from the scientific aspect, usually dismissed as „nonscientific“, based on the standpoint that gravitation is its cause, while the Moon's mass remains the same whether it is full or new, thus any discussion on the subject is pointless. However, those living daily with persons sensitive to full Moon know that this phenomenon exists.

Since science has not explained this phenomenon, people attribute mystic characteristics to the full Moon. The key question is: why does the Moon affect only some people, and not everyone? The answer could not be found because the problem was investigated within the classical gravitational effects of the Moon on the human organism. However,



the nature of this influence is more complex; this effect is based on natural *physical* information-quantum phenomena and *biophysical* quantum-information properties of the human organism.

According to physics, the full Moon phenomenon is not only of gravitational nature, but of light nature as well, because physical effects caused by the full Moon action imply that it is illuminated by the Sun, that is, maximum reflected and scattered light reaches the Earth's surface. If we assume that the early dawn has illumination of 1 *lux*, then daylight on a clear day on Earth has about  $10^4$  *lux*, and a cloudy day about  $10^2$  *lux*. However, a clear night with full Moon has  $10^{-1}$  *lux*, and a cloudy night with full Moon about  $10^{-2}$  *lux*. We should have in mind that the greatest influence on humans has Moon's scattered and reflected near infrared radiation of wavelengths 770–1000 nm penetrating well the eyelids even when eyes are closed.

The biophysical phenomenon in hypersensitive persons is caused by the degree of sensitivity to electric and magnetic influence. Light, as an electromagnetic wave, has an electric and a magnetic component. The electric force of valence electrons is generally greater than the magnetic force  $10^4$  times, this holds also for retinal eye structures and brain structures responsible for the reception and processing of light signals. If the reception of the light signal is *primarily* in the eye and its processing in the brain is electromagnetic, which is mostly the case, light reflected from the Moon has no significant influence. However, if the reception and processing of the light signal is primarily magnetoelectric (inverse), the sensitivity is increased by  $10^4$ , therefore additional illumination with moonlight during cloudy nights with full Moon affects serotonin secretion (i.e., the serotonin/melatonin regulation mechanism) as on a cloudy day (difference in illumination between them,  $10^2$  and  $10^{-2}$ , is  $10^4$ , as the ratio of the values of the electric and magnetic component of valence electrons). In a nutshell, hypersensitivity is the result of the inverse solution in the reception and processing of the electric and the magnetic light component in biological structures, which can be explained by oscillatory processes in the lattice of biomolecular (crystal) structures such as clathrin (responsible for the secretion of neurotransmitters at synapses). This phenomenon is known as the principle of the Möbius strip. The strip that had two surfaces now has only one!? By investigating the full Moon phenomenon we intended only to hunt the „fox“, when to our surprise, a „bear“ appeared from the woods. Light and gravitation (photon and graviton) can be coupled through the Möbius strip „walked“ by the Schrödinger's and Fibonacci's cat. In order to clarify and explain this (appearance of the „bear“, instead of the „fox“) we have to go back to the time phenomenon (built into our biological structure under the influence of the gravitation effect of the environment).

Earth's revolution is divided into 24 segments (why?), and the  $1/24$  unit contains a smaller unit, 60 times smaller, equal to  $1/1440$  of one revolution, Earth's spin (why?). This new unit is again divided into 60 smaller units -into  $1/86400$  of Earth's revolution (why?). Based on present knowledge, we can say that Earth's *spin* is divided into *two segments*, the *darkness-light* pair, i.e., *night-day*, as the  $12 + 12 = 24$  units we call *hours*. Now comes the key point: if the laws of symmetry are the fundament of nature, then the symmetry structure of the icosahedral clathrin, which is responsible for information processes within the brain (discharge of neurotransmitters at synapses), and its dual

– the dodecahedron (according to which biological water clusters are formed), makes sense, because both polyhedrons have 12 pentagons each, hence beside the spatial, we have a *temporal icosahedral system* within ourselves as well. A still smaller unit is 60 times smaller than the hour, it is called *minute*, and 60 times smaller than the minute is the *second*. Why does 60 appear twice!?

History tells us that we inherited the system of *time* calculation from the ancient Sumer civilization. How did the ancient Sumerians come by such a system (which we have not tried to modify although in history we attempt to change everything)? One possible answer, and the most probable, is that this system is *built* into us by nature, by its physical rhythms, which became biological rhythms, and that the Sumerians, at the time, expressed a system on the basis of which we are all fashioned. The state of human consciousness is not the same today as it was then. Today, man is *homo technicus* (we are disunited from nature, we create machines, technical devices), while the ancient civilizations were much closer to nature (*homo naturalis*). This resembles the mother-child relationship: during the first six months, the child is completely dependent on its mother, and becomes independent only gradually. It can be said that ancient civilizations were much closer to nature than we can even imagine today.

Which are the natural phenomena (rhythms) that can produce the „60“ phenomenon? The closest explanation is provided by the Earth–Moon gravitational synergy.

The Moon does not orbit around the Earth, as is usually thought (and said in everyday life), rather the Earth–Moon system, as a binary entity, orbits a common center – the barycenter. When the Moon is at zenith, the barycenter is at a distance from Earth's center of  $4467 \pm 460$  km, and from Earth's surface  $1904 \pm 460$  km toward Earth's center. Earth's radius equals 6378 km, mass  $5.972 \times 10^{24}$  kg, Moon's radius is 1738 km, mass  $7.34 \times 10^{22}$  kg, and the average distance between the Moon and the Earth is 384 400 km.

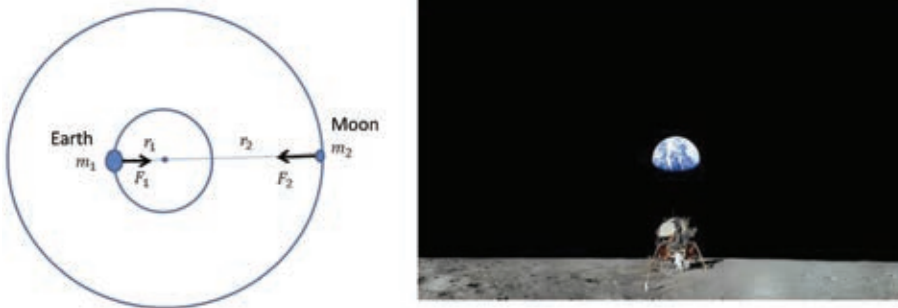


**Figure 8.5.** *The Earth-Moon duo and basic elements of the gravitation interaction (left). The Earth viewed from the Moon (right) recorded during the Apollo 11 space mission, on July 20, 1969 (NASA:www.nasa.gov/mission\_pages/apollo/apollo11.htm).*

Since the centripetal forces  $F_1$  (Earth),  $F_2$  (Moon) equal the gravitation forces between the Earth and the Moon ( $F$ ), the relation holds  $F_1 + F_2 = F$ , i.e.,  $m_1 r_1 \omega^2 = m_1 r_1 \omega^2 = F$ . Knowing that the centripetal Moon's acceleration causes Moon's gravitation force, this gives  $F = m_2 g_2$ , finally resulting in the solution:

$$g_2 = \frac{1}{60^2} g, \quad (8.4)$$

where  $g$  is the gravity acceleration at Earth's surface. This results from the fact that the average distance between the Earth and the Moon is 60 times larger than the Earth's radius (on the average  $384400 : 6378 = 60.2$ ). In other words, nature's rhythm built its „time scale“ and its time rhythm into humans with average precision of 99.66%.

Experiments have confirmed that Earth's gravitation field is quantized, which opens completely new possibilities for the investigation of numerous phenomena, including biological life on Earth. The experiment with cold neutrons was conducted at Grenoble, and it was demonstrated that the first quantum gravitation state of neutrons equals 110 pg, which corresponds to the energy of  $E_1 = 1.4$  peV, the second quantum state equals  $E_2 = 2.5$  peV, the third  $E_3 = 3.3$  peV and  $E_4 = 4.1$  peV (Figure 8. 6) (Nesvizhevsky et al., 2002).

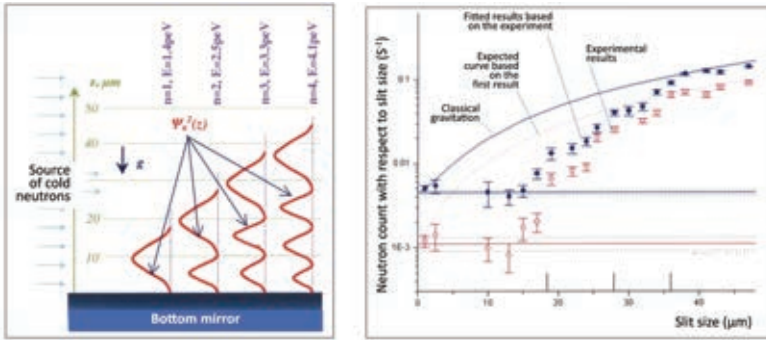


**Figure 8.6.** Grenoble experiment: experiment results demonstrate that the Earth's gravitation field is quantized (Nesvizhevsky et al., 2002).

At the same time, independently from the Grenoble team, the Belgrade team was at work (Koruga, Tomić, Ratkaj) investigating the gravitation phenomenon at Earth's surface and its effect on biological systems (Koruga, et al., 2003). Astronomy calculates the effect of body's gravitation respective to its center and with respect to a time interval of several minutes. We calculated the gravitation effect of the Sun, the Moon and of all planets at each position on Earth, including altitude differences (mountains and valleys). Only when we changed units from *minutes* to *seconds* in calculating the gravitation effects did we obtain a *gravitational wave* of 110 pg amplitude (Figure 8.7). This *nanogravitation* of 0.110 ng corresponds to the first quantum state of the Earth's gravitation field of 1.4 peV.

As there are several quantum levels of Earth's gravitation field, there are also several levels (*micro*, *nano*, *pico*) of gravitation effects of the Solar system bodies at Earth's surface with respect to Earth's gravity  $g = 9.81$  m/s<sup>2</sup> (Figure 8.8). At the 110 pg level, coupling of quantum and classical gravitation actions occurs at Earth's surface. These gravitation effects can influence intermolecular interactions (weak noncovalent hydrogen bonds, weak ion-ion, ion-dipole, dipole-dipole, dipole-induced dipole). Using the example of microtubules, we shall demonstrate various reorganizations that can be effected by the dynamic action of gravitation forces of the Sun, the Moon, and the planets.

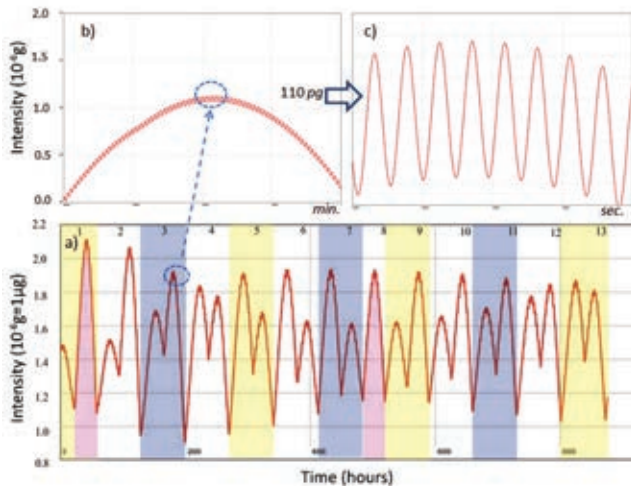


**Figure 8.7.** Three levels of gravitation effects of the Solar system bodies on Earth's surface: a) in the annual cycle there are 13 gravitation peaks, meaning that Moon's gravitation dominates at Earth's surface, b) the annual –monthly cycle includes the day-hour cycle, and within the latter the minute-second cycle is included. Only the secondary cycle enables the coupling of the classical (nano) gravitation and the quantum state of Earth's gravitation field (Koruga, et al., 2003). The second, as the time unit, is crucial for Earth.

Peak type	Number of peaks	Maximum peak amplitude	Minimum peak amplitude	Difference
Annual	13 (8/5; 7/6)	2.10 mg	1.84 mg	0.26 mg
Monthly	60	195 ng	118 ng	77 ng
Daily	2 peaks	138 ng	130 ng	8 ng
Constant Nano/quantum	Wave every 7.272 min	110 pg	110 pg	0 pg

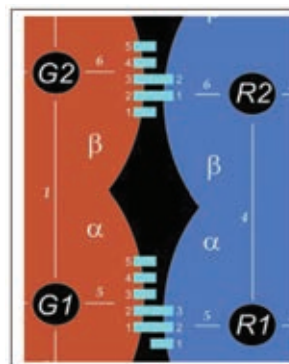


**Figure 8.8.** Table -various levels of gravitational actions of Solar system bodies on Earth's surface (left). Intramolecular interactions between two protofilaments of the microtubule, established via the lateral surface weak interactions of the  $\alpha$  and  $\beta$  tubulin (right). The total number of bonds that can be established between two protofilaments is 81. The strength of lateral bonds, between the  $\alpha$  and  $\beta$  dimers in two different protofilaments, in various combinations, equals 4.2 N/m, and 4.0 N/m between two dimers within the same protofilament.

The dynamical *micro/nano/pico* gravitation ( $g_{mnp}$ ) can, through weak intramolecular interaction between two protofilaments ( $\alpha$  and  $\beta$  dimers: bond intensity 4.2 N/m) and within one protofilament ( $\alpha$  and  $\beta$  dimer: bond intensity 4.0 N/m), reorganize microtubules (microtubule packing 8/5 is transformed into 7/6 or 6/7 or 5/8, etc.). Although,

it cannot effect reorganization or deconstruction of existing microtubules, because the intensity of bonds within the dimer is 12.6 N/m (monomer „head-to-head“) and 20 N/m within the monomer („head-to-tail“), and the maximum *mnp action* is  $g_{mnp}^{max} = 10 \text{ N/m}$ , the minimum being  $g_{mnp}^{min} = 5 \text{ N/m}$ . Consequently, biomolecules with covalent bonds are stabile, because the covalent bond values are within 400–1600 N/m. In other words, modification of gravitational conditions affects polymerization of microtubules (Papaseit, et al., 2000, Himmelspach, et al., 1999).

Earth’s gravity  $g$  is calculated by the expression

$$ma = G \frac{m_G m'_G}{d^2} \text{ giving } g = G \frac{m_z}{r^2} = 9,81 \text{ m/s}^2$$

where  $m$  – mass (kg),  $a$  – acceleration ( $\text{m/s}^2$ ),  $G$  – universal gravitational constant ( $G = 6.6742 \times 10^{-11} \text{ Nm}^2/\text{kg}^2$ ),  $m_G, m'_G$  – interacting masses,  $d$  – distance between masses,  $m_z$  – Earth’s mass ( $5.972 \times 10^{24} \text{ kg}$ ),  $r$  – Earth’s radius ( $r = 6\,371\,302 \text{ m}$ ).

With respect to the Earth’s *static* (constant) gravity  $g = 9.81 \text{ m/s}$  (at sea level) particular bodies of the Solar system have a *dynamic* (changing, because they are moving bodies) effect on Earth’s surface with the following order of magnitude: Sun  $10^{-7}g$ , Moon  $10^{-6}g$ , Mercury  $10^{-10}g$ , Venus  $10^{-9}g$ , Jupiter  $10^{-7}g$ , Saturn  $10^{-8}g$ , Uranus  $10^{-10}g$ , Neptune  $10^{-11}g$ , Pluto  $10^{-12}g$ , asteroids  $10^{-10}g$ .

If Earth’s motion around the Sun is observed, we conclude that the Earth needs 7.272 time units (minutes) to change its position in space by one *spatial unit* (Earth’s diameter), which are 60 times smaller than the unit of the *icosahedral temporal system* (hour). When the base of the natural logarithm is raised to the power by this value, we obtain:

$$e^{7,272} = 1.440 \tag{8.5}$$

representing the number of minutes needed by the Earth for one revolution (spin), for the day-night alteration. Very strange, but also challenging for further investigation.

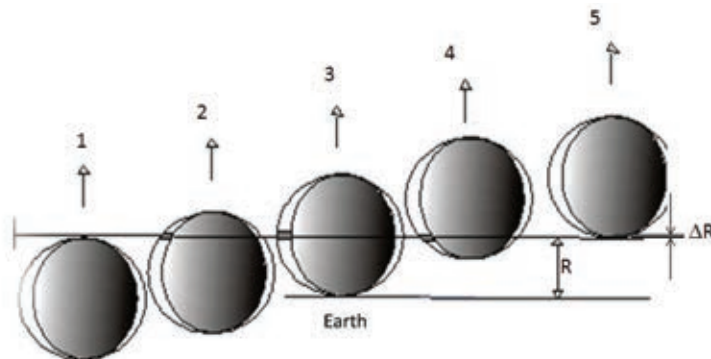


**Figure 8.9.** Average Earth’s „quantum“ unit displacement (by one Earth’s diameter) during Earth’s orbiting about the Sun equals 7.272 minutes. When we raise the base  $e$  to this power we obtain 1440 minutes, which is the time of Earth’s rotation about its axis. Earth’s motion about the Sun and Earth’s rotation about its axis are related by the number  $e$ .

Why is it significant that Earth's *space-time* (*spacetime*) is determined by the number  $e$ ? In order to explain this, let us examine which is the most advantageous basis for information coding. We are accustomed to base 2 (*binary* system: 0 and 1) in computers, and in genetics to base 3 (*ternary* systems: ATT, GTA, etc.). Nature chose the ternary code for biochemical information processes, and for biophysical information - the binary code (however, these are two sides of the same coin:  $4^3 = 64 = 2^6$ ). The binary system was chosen for computers because it is the simplest for technical solutions („on“/„off“ - current, magnetism, etc.). We are looking for a number system where a minimum of symbols and class intervals are used for number representation, i.e., to optimize this ratio. It is established that the size of the information apparatus  $K$  can be written as  $K = anR$ , where  $n$  is the number of class intervals,  $R$  number of symbols in the given number system, and  $a$  is the coefficient of proportionality, meaning that the number of symbols used in a given number system is equal to the base of the system  $R$  (Hill, 1986, Jafarkhani, 2005). The maximum number  $N_{max}$  which can be written in the  $n$  system's class interval is:  $N_{max} = R^n - 1$ . If  $n$  is large enough:  $N_{max} \approx R^n$ , we obtain:

$$n = \frac{\ln N_{max}}{\ln R}$$

If we substitute  $n$  into the equation  $K = anR$ , we obtain:

$$K = \frac{a \ln N_{max}}{\ln R}$$

$$\frac{\partial K}{\partial R} = 0 \Rightarrow \ln R = 1$$

giving the optimal number of symbols  $R = e$ .

We have reached a new conclusion; Earth's *space-time* is coded with base  $e$ , i.e., information physics of *space-time*, of the „spaceship“ called Earth, is determined with the optimal *information* base  $e$ . Considering that the Earth's gravitation field is quantized (experiment with cold neutrons), everything points to the conclusion that we exist not just within the Earth's gravitational and electromagnetic field, but also within its *information field*! This field is directly related to *quantum information*, because the wave function has the form:



$$|\psi\rangle = e^{i\gamma} \left( \cos \frac{\theta}{2} |0\rangle + e^{i\varphi} \sin \frac{\theta}{2} |1\rangle \right) \quad (8.7)$$

The base of the natural logarithm  $e$  occurs in the above expression, as in many other physical laws and processes in nature; therefore, it is realistic and appropriate to say that „*The laws of nature are information about information and beyond them there is only darkness... This is the gateway to understanding reality.*“ (Vedral, 2010).

The above findings bring us back to the investigation of the full Moon phenomenon as the synergy of the *reflected Sun's photons* off the Moon's surface and the *Moon's gravitons* which *originate* and *propagate* from a single point on Moon's surface with the same velocity, arrive at the same time (in just 1.28 seconds) on Earth and act upon the

biological (*information*) structure which exerts the full Moon effect (anxiety, irritability, etc.). Therefore, we are interested in a biological (energetic-informational) „sensor“ that detects photons and gravitons and couples their actions. Thus *coupled action* will be called *geefton* (from: *g*, graviton, as *ge*, *f* from **photon**, as *ef*, and they have *ton* in common - graviton and photon), it is pronounced *gifton*. The Symbol is  $\ddot{e}$  (from  $\ddot{e}$ , because in the word *geefton* *e* appears twice, two *ton-s* become one and since they originate from the same base as *e*, thus *ton-ton* =  $\dot{e}$ , giving:  $\ddot{e} + \dot{e} = \ddot{e}$ ).

Figure 8.10. Schematic representation of the full Moon phenomenon and cou-



pling between the Sun's photon reflected off the Moon's surface and the Moon's graviton (left); the looking glass is used to search for a biological structure that could unite the graviton and the photon and create the  $\ddot{e}$  (geefton) phenomenon (right).

Spin's *action* is a promising solution. We know that photon's *spin* equals 1, and graviton's *spin* equals 2 (Tomonaga, 1997, Cartan, 1996, Levitt, 2008). In case of *coupling actions* of the photon and the graviton, what would be the resulting *geefton's* „*spin*“ (graviton's and photon's *spin* is the input information causing formation of the *geefton* within a structure)? Can the action of a single photon and a single graviton be paired, or do several actions of the photon and several actions of the graviton have to be coupled to produce the *geefton*?

Generally speaking, the unity of gravitation and electromagnetism is a difficult question, and from the aspect of physics and the unification of interactions (gravitational, electromagnetic, weak and strong) it is almost unsolvable at present. However, a moment has to come to leave the accustomed paths of thinking (the given framework preventing us to see things from a different perspective), and to implement the saying „the shortcut is closer, a detour is faster“ or „the longest way around is the shortest way home“ in order to gain new insights, such as the *geefton* (unification of actions). This will be possible when we stop thinking „one-dimensionally“ (observing only space—i.e., what is closer), and turn to thinking „two-dimensionally“ (including both space and time, i.e., *spacetime*, because the point you have to reach will be closer when you arrive earlier, although the distance travelled is longer). In order to better understand the principle „the shortcut is closer, a detour is faster“ we shall recall two actual situations. The first: imagine a 500 m race with sand, water, grass, and asphalt on the track. If you were to take the shortest

path toward the finish line, you would encounter sand and shallow water (60% : 40%), but when you take the side path and zigzag you encounter sand, grass, and asphalt (10% : 60% : 30%). The „second“ path is longer, but you arrive at the finish in a shorter time, because you can run faster on grass and asphalt than on sand and shallow water. The second example concerns light propagating through mediums with different refraction indexes  $n$ . Light chooses the path with the smallest refraction index. The lightning is an obvious example; it zigzags, because electricity chooses the atmosphere area with the least resistance, reaching the goal in the shortest time.

Specifically, we are investigating the relationship between gravitation and electromagnetism, i.e., coupling actions of the graviton and the photon in biosystems. We can choose the path of the classical physics and run through „sand and water“, spend increased effort and arrive at the goal eventually (which will actually happen one day). Or, we can choose a detour and run „faster on sand, grass and asphalt“ and arrive at the goal earlier. We have to cross some sand, because we have to take into account all presently known findings on graviton and photon, grass and asphalt are „new paths“ unused by classical physicists, such as *biophysics* (grass) and *information* (asphalt). These are our choice topics, because they can improve human health (presently we are not interested in the photon and graviton *in themselves* and *for themselves* but in their effect on biosystems).

Chapter II demonstrated that gravitation is the representation of dimension  $N = 0$  in  $N = 3$  (mass is organized as a ball-like structure about a point), while the photon is the reduction of 5D into 3D (5D originated from  $N = 0$ ), therefore,  $N=0$  is common to both the graviton and the photon. This is Ariadne's thread that will guide us through „wilderness“ from start to finish.

Since all bodies are sphere-like due to gravitation, the sphere form of the biological structure (pseudo 0D) that will detect gravitons as a sensor is necessary. However, the nature of biomolecules is primarily electromagnetic, meaning that, in order to obtain a 0D structure (pseudo 0D in 3D) complying to gravitational and electromagnetic constraints, *information* must be included (because the electromagnetic force is energetically  $10^{36}$  times stronger than gravitation). This information is contained within DNA (DNA  $\rightarrow$  iRNA  $\rightarrow$  rRNA  $\rightarrow$  protein) and by establishing an adequate sequence of amino acids, it creates the basic constructive element providing physical conditions for the curvature of the new structure, and finally by their union forms a sphere-like structure coupling the relationships of the electron charge to the total electrical charge of the structure, and Earth's gravitation to the nanogravitation (or to the first quantum level of the Earth's gravitation field). In both cases the ratio equals  $\sim 1 : 10^9$  (*nano*).

The most serious candidates for the structure - sensor of graviton action, and the synergy of graviton, photon and electron in biological systems are clathrin, microtubules and centrioles (generally, Fibonacci structures). Clathrin has been discussed in Chapter V; we shall reiterate significant points relevant for the investigation of coupling actions (autocorrelation action, „superposition action“) of graviton and photon by electrons (codogenic electrons), i.e., relevant for the forming of *geeftons*.

The coupling of graviton's (g) and photon's (p) actions  $\langle g | p \rangle$  can be established via the Fibonacci electronic biological structures, by summing their spins (that generate actions), while the spin sum remains constant:



$$g_{\text{spin}} + p_{\text{spin}} = \Phi^2 + \phi^2 = 3. \quad (8.8)$$

If we illustrated this with playing cards, as in Chapter II, *ace* and *queen* would be paired, giving a new card, *triskelion* (this „new card“ is the symbol found on the flags of Sicily and the island-state -Isle of Man located between the United Kingdom and Ireland):

$$\text{ace} + \text{queen} = \text{triskelion}$$

However, it is not probable that we would use a single *ace* and a single *queen* in a new game of cards based on pairs. We must have a „game“ that is meaningful and that has a practical value. Therefore, the *triskelion* is only the starting point, initial elements like the spins of graviton and photon are only the initial, input information in coupling; their value and *form* is preserved, *their action effects* a modification in the Fibonacci structure, in its *contents*. This modification preserves their values in a modified form, in the sense of „Aufgehoben“ - to *abolish* and *transcend-preserve*, used by Hegel to explain Heraclitus' thought *Only one thing is wise, to be and not to be called by the name of Zeus*, or in modern terms: nuclein acid code (DNA) transfers the information contents to amino acids (proteins); code form is abolished, but the information content is preserved, although the 0D structure is not. Three gravitons are needed for the triskelion (*spin* : 2<sub>3</sub>) and three photons (*spin* : 1<sub>3</sub>) which are activated alternatively to generate code providing their *pseudospin-spin* coupling  $(s_g + s_p)/3 = (\Phi^2 + \phi^2)/(\phi^2 + \Phi^2) = 1$ , because three gravitons and three photons in Fibonacci structures result in their action  $\langle S_g | 3 | S_p \rangle = 1$ . However, these triskelions are only nodes of a more complex structure, their pseudospins have to be complementary with the molecular spin of this system based on spins of all atoms and electrons in this molecule. For more complex structures (biomolecules), it is calculated via the Hamiltonian  $H = H^0 + H_{RF}$ , where  $H_{RF}$  is the interaction with the reference field, while  $H^0$  is defined with the expression  $H^0 = \sum_j \omega_j^0 I_{jz} + \sum_{j < k} 2\pi J_{jk} I_j I_k$ , where  $\omega_j^0$  - Larmor's frequency,  $I_{jz}$  - angular momentum spin along the *z axis*,  $J_{jk}$  - J tensor of coupling between spins  $I_j$  and  $I_k$ ,  $I_j$  - vector operator for the spin of the angular momentum *j* and  $I_k$  - vector operator for the spin of the angular momentum *k* (Levitt, 2008).

It is established that 36 triskelions are necessary (Figure 5. 2) to create an electromagnetic structure resembling by its „shape“ gravitation bodies  $\|36 \langle s_g | 3 | s_p \rangle\|$ . Therefore, clathrin, as the sensor of photons and gravitons (coupling their action) in the form of *geeftons*, is realized via 6 triskelions (18 photons and 18 gravitons are coupled), forming the code GIF  $6^2 = 36$  (of 36 *geeftons*). When 6 triskelions are excited with 2 different triggers (*photon* and *graviton*), we obtain 36 different clathrin states (an example: open 3 triskelions and release (slightly) neurotransmitters, open 6 and release (more), open 12 and discharge (still more)... close... etc., there are 36 combinations in all).

The GIF code  $6^2$ , by its base and exponent, is the inverse to the biophysical DNA code  $2^6 = 64$  based on hydrogen bonds (where there is donor-acceptor position exchange). Note that number 6 (as the first perfect number) has a strange characteristic; the sum and the product of its factors are the same number 6 ( $1+2+3 = 1 \times 2 \times 3 = 6$ ), thus in the  $2^6$  code (DNA) we have  $2^{(1 \times 2 \times 3)} = 2^1 \times 2^2 \times 2^3 = 2 \times 4 \times 8 = 64$ , and in code  $6^2$  (*geefton*) we have  $(1+2+3)^2 = (1+2+3)(1+2+3) = 1+2+3+2+4+6+3+6+9 = 36$ . At the same time  $(1 \times 2 \times 3)^2$  is possible

when the base and exponent are replaced, which is  $1^2 \times 2^2 \times 2^3 = 1 \times 4 \times 8 = 2^5$ , which is half of 64, resulting in – the *half* equals the *whole*! This is a strange feature of the first perfect number. Since clathrin is a DNA product, the full Moon sensitivity is the result of a genetic variation in clathrin, thus, when synergy between the photon and graviton is established, clathrin activates more often the command „open“ -release serotonin at synapses (compared to when there is only a photon present directly from the Sun). Excess secretion of serotonin (and other neurotransmitters) „inopportune time“ causes irritability, because it conflicts with the biorhythm of biological substances secretion (Figure 8.11).

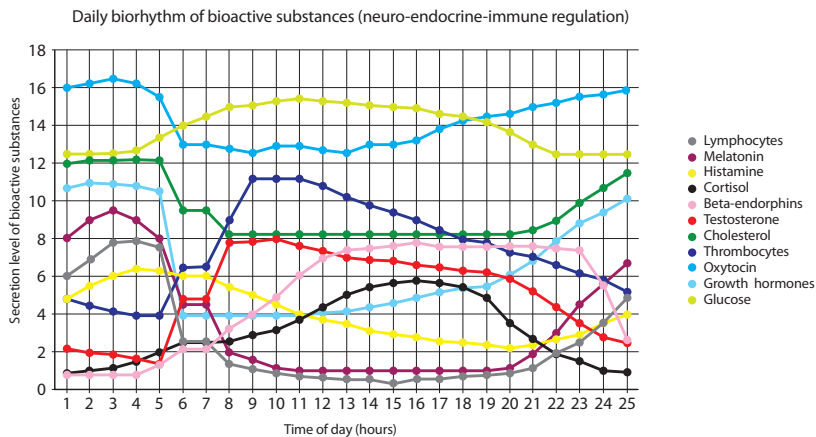


**Figure 8.11.** Secretion levels of bioactive substances during 24 hours (circadian biochemical rhythm) are defined by the neuro-endocrine-immunological regulation. Melatonin secretion starts in the evening, about 21 P.M., and reaches maximum during the night at 3 P.M., afterwards falling to a minimum between 8 and 10 A.M. Serotonin secretion has inverse dynamics (melatonin/serotonin are a „seesaw“ pair, according to the Yin/ Yang principle). From the biochemical aspect, we are not the same person in the morning, during the day, in the evening, and during the night. Inbuilt natural rhythms are responsible for our biochemical states.

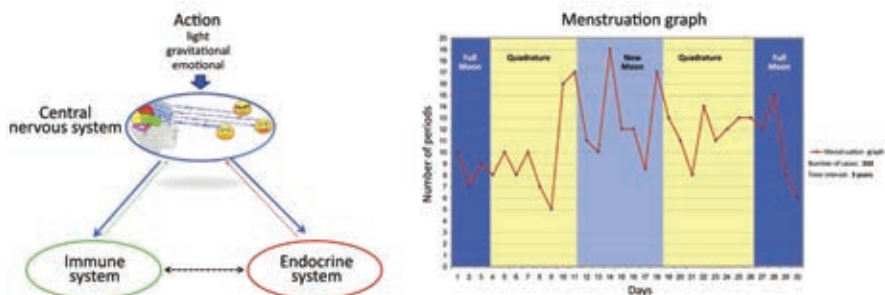


**Figure 8.12.** Light, gravitation, emotion, driving, etc., expose us to various effects. When the actions are within normal limits, we feel agreeable. When actions are slightly above the allowed threshold, we feel slightly uneasy (something is bothering us, but not to the point where we react violently), however, when the action significantly exceeds the threshold limit, we feel uncomfortable (as in the full Moon phenomenon).

Beside the full Moon phenomenon, there is the phenomenon of somnambulism. This is a drastic example of the GIF code occurring when *mirror symmetry* expressions (planar symmetry axis) of the DNA code and the GIF code coincide, caused by the DNA, proteins and water. Males are more prone to this phenomenon because in the Y chromosome, the genetic sequence is a *palindrome* („*radar, level, rotor*“, from the information aspect  $\frac{1}{2} = 1$ , because it reads the same backward and forward -only „half“ of the sequence is necessary in order to know the „whole“ information), as in the case  $6^2 = (1 \times 2 \times 3)^2 = 32$  (half of 64), consequently there is a one-to-one correspondence GIF code  $\leftrightarrow$  DNA code.

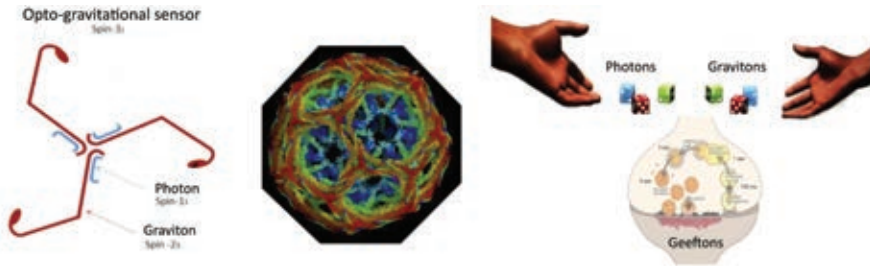


**Figure 8.13.** Schematic representation of the triskelion as an optogravitation sensor; it is activated by three photons and three gravitons (gift) (left). 36 gifts (middle) create a codogenic structure  $6^2 = 36$ , which regulates the neurotransmitter secretion at synapses and determines information states (biophysical states) of the brain. One of these states is the full Moon phenomenon (right).

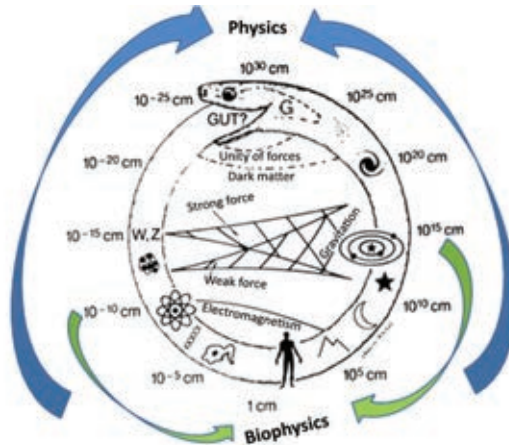


**Figure 8.14.** Physics is the most general science about nature, including man as constituent of nature. Since man is a contemplative being, he is, from the aspect of physics, more oriented toward the „infinitesimally small“ and „infinitesimally large“ within nature, then toward himself. This is why we have biophysics, investigating man via physical laws, at the same time expanding the limits of physics by thoroughly investigating man and the influence of gravitational and electromagnetic natural phenomena on humans. It can be stated that the range of biophysics is from  $10^{-15}m$  to  $10^{15}m$  (from the size of the electron, proton and neutron to the size of the Solar system) (Adapted from: Salam, 1990, who obtained permission from Sheldon Glashow).

Although this has not solved the problem of the physical unification of gravitation and electromagnetism from the aspect of classical physics- this resolves the problem of their synergy (coupling, autocorrelation, superposition) in biomolecules. The difference between physics and biophysics is in the direction and domain of research, as shown in Figure 8.14.

The greatest human enigma is consciousness, especially existential awareness. This is a complex problem, however, we are interested, from the practical aspect, to have a healthy and adequate life quality. The „corner stone of health“ is better understanding of the origin of a living being (embryogenesis: interdependence, connection, synergy of cells, tissues and organs), prevention and personal medicine. Hyperpolarized light is one of the best methods for prevention, it can also aid in case of dysfunction in tissues, cells or biomolecules, which are Fibonacci structures (constituting about 75% of the human organism).

## 8.4. Light model of Embryogenesis

Human embryology is a science dealing with the investigation of the first phase of the embryonal development (Greek *embryon* – embryo, *logos* – science). In a wider sense, this period of human development is known as the *embryonal development period*, in this phase the germ is called *embryo*. The embryonal phase is considered a critical development period, because the embryo is then most sensitive to the influence of various factors that can lead to developmental impairments (*teratogenic factors*). The embryonal period of child's development begins in the third week after ovulation. The *fetal development period* starts from the time when *the embryo*, according to morphological and functional features, thus according to its appearance, can be classified as a biological species. From this moment, the embryo is called the *fetus*. The period of *fetal development* ranges from the eight week to childbirth.

Everything starts with the union of the male and female reproductive cells. The spermatozoid (the male reproductive cell) is from 45 to 60 microns long and is made of a *head* (acrosome), DNA, *neck* (centriole), middle (microtubule), ATP, and membrane. Spermatozooids travel with the speed of about 3 mm per minute, carry 22 chromosomes plus the X and the Y chromosome. The ovum has a diameter between 150 and 200 microns – one of the largest cells in the human body. It carries the XX chromosome. Both reproductive cells have a haploid number of chromosomes ( $n = 23$ ).

Ovum fertilization creates a new cell called the *zygote*, this is the zero starting event, where  $2^0 = 1$  (one cells is formed from two). Mature ovum is located within the female organism after ovulation and is capable of fertilization only 24 to 48 hours after separation from the ovaries. The minimum requirements for male fertility are: 20 million spermatozooids/ml, maximum with good motility, normal size and shape.

Two main types of cell division are: *mitosis* (somatic division) and *meiosis* (reduction division). By the union of reproductive cells, a new organism is formed with a diploid number of chromosomes, equal to the parents' number.

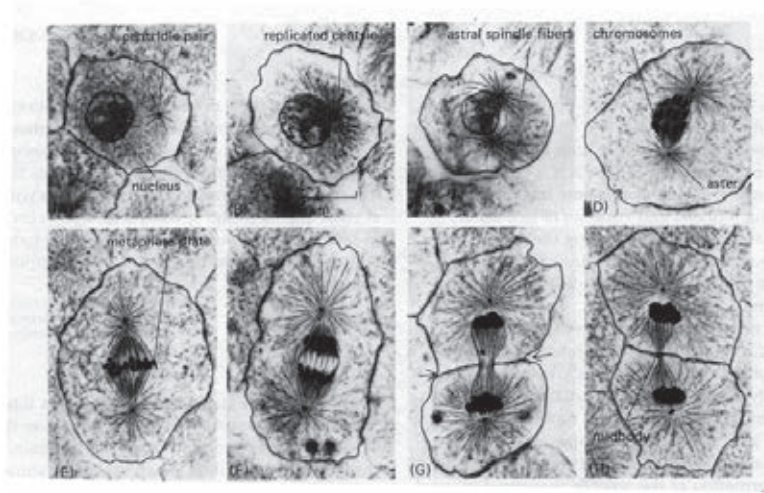


Figure 8.15. Cell division phases with visible poles (centriole), the mitotic spindle (microtubule) separating chromosomes (e, f) by forming a new cell (g, h) (Alberts, 2002).

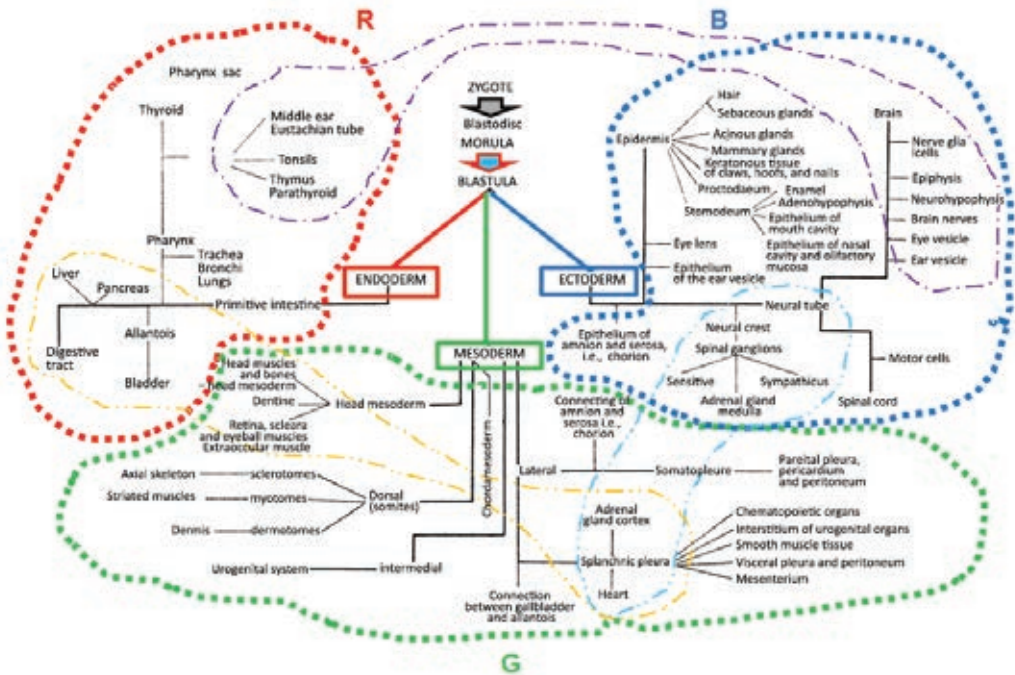


Figure 8.16. Schematic representation of the human organism development phases from zygote, blastula to the embryo and fetus with tissues and organs developed from the endoderm, ectoderm and mesoderm (Adapted from: Pantić, 1973).

It was presented that the *classical* biophysical code system of the DNA is  $2^6$  (biochemically  $4^3$ ), however, there exists also a *quantum* biophysical DNA code system  $2^{6+1-1}$

(based on hydrogen bonds within DNA and coding of peptide planes within proteins), giving in synergy  $2^6 (2^{6+1}-1)$ , belonging to a general formula of the type:

$$2^n(2^{n+1}-1) \quad (8.9)$$

which is used to calculate perfect numbers. The unity between the *classical* and the *quantum informational* code system of DNA is established via perfect numbers. Therefore, biological systems are the most beautiful and sublime natural entities.

Since the DNA code is responsible for embryogenesis, the formula of the *classical-quantum-informational* code will be used to determine the development phases from the zygote (fertilized ovum), embryo, and fetus to the newborn.

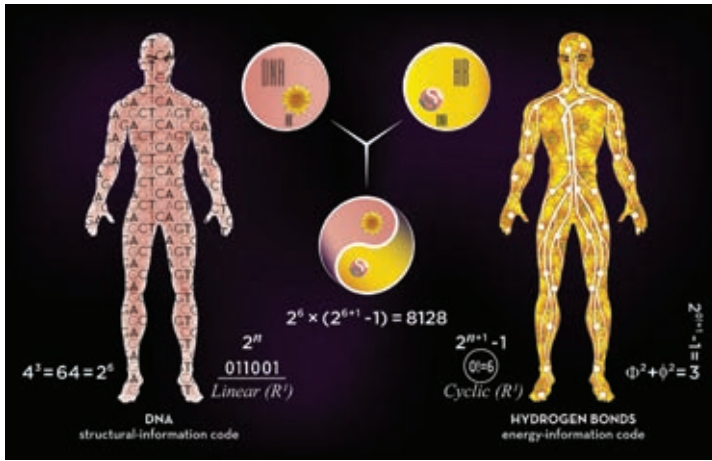


**Figure 8.17.** Our entity (mind-body) is composed of four basic codes:  $4^3$ ,  $2^6$ ,  $\Phi^2 + \phi^2$  and  $2^{6+1}-1$ , which are generating perfect synergic code (classical/quantum code with 8128 code elements – equal to the value of the fourth perfect number). The first two codes are structural-energy codes (linear on  $R^1$ ), while the third and the fourth are energy information codes (cyclic and orthogonal). Since any type of code is rooted in information, this means that information is the major building component of our entity. Biological systems are primarily information beings.

The *first phase* (the most important, without which there would not be other phases) is the union of the spermatozoid and the ovum (two become one), giving  $2^0(2^{0+1}-1) = 1$ , the *second phase* - zygote formation  $2^0(2^{0+1}-1) = 6$ , where cells divide by bifurcation  $2^n$  into six phases, gives  $n = 1-6$ . The *third phase*  $2^2(2^{2+1}-1) = 28$  is performed in 28 information steps. Therefore, the first phase is realized with the zero-th perfect number 1, the second phase with the first perfect number 6, and the third phase with the second perfect number 28.

Embryogenesis is established through perfect numbers; since the sum of reciprocal perfect number and its reciprocal factors equals 2, our organism must be composed of two symmetric parts. This symmetry is not absolute, a minor asymmetry exists, because the factors of perfect numbers (except  $SB_1 = 6$ ) are asymmetric at one point ( $SB_2$ : 4 and

7,  $SB_3$ : 16 and 31, etc., Table 8.1). This is why humans are slightly asymmetric in their physical appearance (left and right face side) and with respect to organs (the heart).

Number 496 is very important in string theory (superstring theory), because Michael Green and John H. Schwarz showed in 1984 that it is one of the necessary conditions for the local symmetry group  $SO(32)$ . A year later, it became clear that this also holds for the  $E_8 \times E_8$  group, whereby the shortcomings of previous string theories were resolved (Green/Schwarz, 1984, Green, 1985).

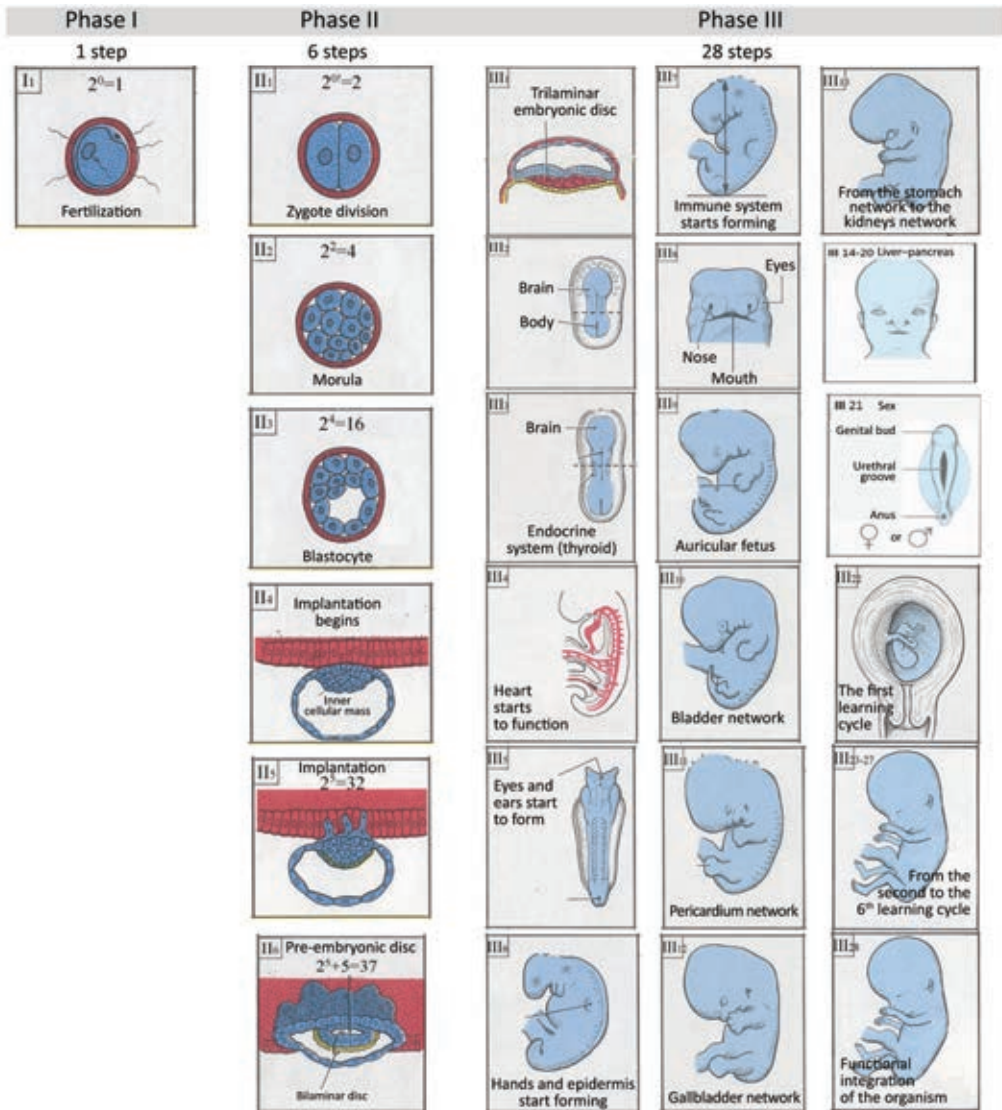


Figure 8.18. Three basic phases and 34 steps of embryogenesis from the zygote to the newborn (Adapted from: Moore, 1988).

Table 8.1. Embryogenesis based on perfect and Fibonacci numbers.

No. bif.	Number of cells	Lunar month	Development phase	Perfect number				Division law	Number of information nodes
				Zero 1	First 6	Second 28	Third 496		
1	2	3	4	5	6	7	8	9	10
2 <sup>0</sup>	1	1	1	1			1	(Φ+φ <sup>2</sup> ) <sup>0</sup> = 1	1
2 <sup>1</sup>	2		2		1 <sup>1</sup>		3	(Φ+φ <sup>2</sup> ) <sup>1</sup> = 2	2
2 <sup>2</sup>	4				2 <sup>2</sup>		7	(Φ+φ <sup>2</sup> ) <sup>2</sup> = 4	4
2 <sup>3</sup>	8				3 <sup>3</sup>		15	(Φ+φ <sup>2</sup> ) <sup>3</sup> = 8	8
2 <sup>4</sup>	16				4 <sup>3</sup>		31	(Φ+φ <sup>2</sup> ) <sup>4</sup> = 16	16
2 <sup>5</sup>	32				5 <sup>3</sup>		63	(Φ+φ <sup>2</sup> ) <sup>5</sup> = 32	32
2 <sup>6</sup>	64				6 <sup>3</sup>		100	(Φ+φ <sup>2</sup> ) <sup>5</sup> + 5 <sup>1</sup> = 37	37
2 <sup>7</sup>	128		3			1 <sup>1</sup>	127	(Φ+φ <sup>2</sup> ) <sup>5</sup> - 5 <sup>1</sup> = 27	27
2 <sup>8</sup>	256					2 <sup>2</sup>	154	(Φ+Φ <sup>-2</sup> ) <sup>3</sup> = 27	27
2 <sup>9</sup>	512					3 <sup>2</sup>	181	(Φ+Φ <sup>-2</sup> ) <sup>3</sup> = 27	27
2 <sup>10</sup>	1024					4 <sup>4</sup>	208	(Φ+Φ <sup>-2</sup> ) <sup>3</sup> = 27	27
2 <sup>11</sup>	2048					5 <sup>4</sup>	235	(Φ+Φ <sup>-2</sup> ) <sup>3</sup> = 27	27
2 <sup>12</sup>	4096					6 <sup>6</sup>	262	(Φ+Φ <sup>-2</sup> ) <sup>3</sup> = 27	27
2 <sup>13</sup>	8192					7 <sup>7</sup>	289	(Φ+Φ <sup>-2</sup> ) <sup>3</sup> = 27	27
2 <sup>14</sup>	16384					8 <sup>8</sup>	316	(Φ+Φ <sup>-2</sup> ) <sup>3</sup> = 27	27
2 <sup>15</sup>	32768					9 <sup>9</sup>	343	(Φ+Φ <sup>-2</sup> ) <sup>3</sup> = 27	27
2 <sup>16</sup>	65536					10 <sup>10</sup>	353	2 (Φ+Φ <sup>-1</sup> ) <sup>2</sup> = 10	10
2 <sup>17</sup>	131072					11 <sup>11</sup>	363	2 (Φ+Φ <sup>-1</sup> ) <sup>2</sup> = 10	10
2 <sup>18</sup>	262144					12 <sup>12</sup>	373	2 (Φ+Φ <sup>-1</sup> ) <sup>2</sup> = 10	10
2 <sup>19</sup>	524288					13 <sup>13</sup>	383	2 (Φ+Φ <sup>-1</sup> ) <sup>2</sup> = 10	10
2 <sup>20</sup>	1048576					14 <sup>14</sup>	388	(Φ+Φ <sup>-1</sup> ) <sup>2</sup> = 5	5
2 <sup>21</sup>	2097152					15 <sup>14</sup>	393	(Φ+Φ <sup>-1</sup> ) <sup>2</sup> = 5	5
2 <sup>22</sup>	4194304					16 <sup>14</sup>	398	(Φ+Φ <sup>-1</sup> ) <sup>2</sup> = 5	5
2 <sup>23</sup>	8388608					17 <sup>14</sup>	403	(Φ+Φ <sup>-1</sup> ) <sup>2</sup> = 5	5
2 <sup>24</sup>	16777216	2				18 <sup>14</sup>	408	(Φ+Φ <sup>-1</sup> ) <sup>2</sup> = 5	5
2 <sup>25</sup>	33554432					19 <sup>14</sup>	413	(Φ+Φ <sup>-1</sup> ) <sup>2</sup> = 5	5
2 <sup>26</sup>	67108864					20 <sup>14</sup>	418	(Φ+Φ <sup>-1</sup> ) <sup>2</sup> = 5	5
2 <sup>27</sup>	134217728	3				21 <sup>14</sup>	423	(Φ+Φ <sup>-1</sup> ) <sup>2</sup> = 5	5
2 <sup>28</sup>	268435456					22 <sup>14</sup>	429	2 (Φ+Φ <sup>-2</sup> ) = 6	6
2 <sup>29</sup>	536870912	4				23 <sup>14</sup>	435	2 (Φ+Φ <sup>-2</sup> ) = 6	6
2 <sup>30</sup>	1073741824					24 <sup>14</sup>	441	2 (Φ+Φ <sup>-2</sup> ) = 6	6
2 <sup>31</sup>	2147483648					25 <sup>14</sup>	447	2 (Φ+Φ <sup>-2</sup> ) = 6	6
2 <sup>32</sup>	4294967296	5				26 <sup>14</sup>	453	2 (Φ+Φ <sup>-2</sup> ) = 6	6
2 <sup>33</sup>	8589934952	6,7				27 <sup>14</sup>	459	2 (Φ+Φ <sup>-2</sup> ) = 6	6
2 <sup>34</sup>	17179869184	8,9				28 <sup>14</sup>	496	(Φ+φ <sup>2</sup> ) <sup>5</sup> + 5 <sup>1</sup> = 37	37
2 <sup>35</sup>	34359738368	10A							
2 <sup>36</sup>	68719476736								
2 <sup>37</sup>	137438953472	B							
2 <sup>38</sup>	274877906944								
2 <sup>39</sup>	549755813888	C							
2 <sup>40</sup>	1099511627766								
2 <sup>41</sup>	2199023255552								
2 <sup>42</sup>	4398046511104	D							
2 <sup>43</sup>	8796093022208	E							

Φ - Fibonacci number: ~ 1.61803  
 φ - Fibonacci number: ~ 0.61803  
<sub>0</sub>SB - Zero-th perfect number: 1  
<sub>1</sub>SB - The first perfect number: 6 = 1+2+3  
<sub>2</sub>SB - The second perfect number: 28 = 1+2+4+7+14  
<sub>3</sub>SB - The third perfect number: 496 = 1+2+4+8 + 16+31+62+124+248  
 Perfect number is a natural number equal to the sum of its divisors.  
 The reciprocal value of SB plus the sum of its factors is 2.  
 $\frac{1}{1} + \frac{1}{2} + \frac{1}{3} + \frac{1}{6} = 2$      $\frac{1}{1} + \frac{1}{2} + \frac{1}{4} + \frac{1}{7} + \frac{1}{14} + \frac{1}{28} = 2$



Table 8.2 Perfect and imperfect numbers in embryogenesis.

N number	Calculation according to the formula $2^{n-1}(2^n-1)$	Number	Calculation according to the formula $2^n(2^{n+1}-1)$	Number	Connected via N
0	$2^{0-1}(2^0-1)=\frac{1}{2}\times 0=0$	No Cardinality of the set N	$2^0(2^{0+1}-1)=1\times 1=1$	$2^{No}$ Numerical line $R_1$	No $2^{No}$
1	$2^{1-1}(2^1-1)=1\times 1=1$	1 1	$2^1(2^{1+1}-1)=2\times 3=6$	6	1 6
2	$2^{2-1}(2^2-1)=2\times 3=6$	6	$2^2(2^{2+1}-1)=4\times 7=28$	28	6 28
3	$2^{3-1}(2^3-1)=4\times 7=28$	28	$2^3(2^{3+1}-1)=8\times 15=120$	120	28 120
4	$2^{4-1}(2^4-1)=8\times 15=120$	120	$2^4(2^{4+1}-1)=16\times 31=496$	496	120 496
5	$2^{5-1}(2^5-1)=16\times 31=496$	496	$2^5(2^{5+1}-1)=32\times 63=2016$	2.016	496 2016
6	$2^{6-1}(2^6-1)=32\times 63=2016$	2016	$2^6(2^{6+1}-1)=64\times 127=8128$	8.128	2016 8128
7	$2^{7-1}(2^7-1)=64\times 127=8128$	8128	$2^7(2^{7+1}-1)=127\times 256=32512$	32.512	8128 32512

Euclid (IV century B. C.) was aware of the first four perfect numbers (6, 28, 496, and 8128). Today, the largest known perfect number, 49-th in sequence, was discovered on September 2, 2016, it has 44 677 235 digits (hundreds of pages are needed to write this number). However, it is significant that the fourth perfect number is the product of the *classical* binary code  $2^6 = 64$  and the *quantum* code  $(2^{6+1}-1) = 127$ , because  $64\times 127 = 8128$  representing the DNA genetic code (Koruga, 2012).

Table 8.2 demonstrates that only for the natural number  $N \{0,1,2\}$  there is correspondence between two perfect numbers (without „defect“); However, in  $N \geq \{3\}$  mapping for  $N$  is established via 120, 2016, 35512, etc., called the *imperfect* numbers. As an example, the perfect number 496 (according to which embryogenesis is performed) can be realized, for  $N = \{4\}$ , perfectly according to the formula  $2^n(2^{n+1}-1)$ . If for some reason, a process were to originate according to the formula  $2^{n-1}(2^n-1)$ , the embryogenesis would be irregular. A similar case as in 496, but inverse, occurs for  $N = \{5\}$ . Consequently, two main defects can occur in embryogenesis: one seriously hampering further fetal development; but if defect progression is promptly arrested, gene expression is interrupted leaving the fetus without a body part, or another anomaly. The other defect causes functional „weak points“ during embryogenesis (they can remain unexpressed, but are usually activated under stress).

The table demonstrates that fertilization has only one „node“ (the most important event and the most important „node“ is denoted as 1 in Figure 8.19, *left*). The preembryonal period has 99 interactive „nodes“ (when zygote is *informationally* transformed into blastula, transiting the evolution of the biological world). Follow 396 „nodes“ constituting a network of information flow based on centrioles, giving  $1 \rightarrow (496-99) = 397$

# Human embryogenesis

## The third perfect number 496

I	<b>Fertilization</b> ( $2^n (2^{n+1} - 1)$ the first step for $n=0$ ): <i>the 0th perfect number 1</i>	
	1. Chromosomes unite: <i>interaction</i> $2^0 = 1$	1
II	<b>Pre-embryo</b> ( $2^n (2^{n+1} - 1)$ 6 steps for $n=1$ ): <i>the first perfect number 6</i>	
	1. Division of the zygote into 2 blastomeres: <i>connection</i> $2^1$	2
	2. From the zygote to morula : <i>connection</i> $2^2$	4
	3. From the early to the mature blastocyte: <i>connection</i> $2^3$	8
	4. Implantation : <i>connection</i> $2^4$	16
	5. Amnioblast: <i>connection</i> $2^5$	32
	6. <b>Bilaminar pre-embryonic disc</b> : 37 <i>connection</i> $2^5 + 5$	37 99
III	<b>Embryo and fetus</b> ( $2^n (2^{n+1} - 1)$ 28 steps for $n=2$ ): <i>the second perfect number 28</i>	
	<b>Integrating structure, organism functioning</b>	
	1. <b>Trilaminar embryonic disc</b> : the first functional step $2^5 - 5$ <i>node points</i>	27
	2. <b>Embryo</b> -the second functional step: <i>brain-body</i> ( $3 \times 9 = 27$ )	27
	3. <b>Embryo</b> -the third functional step: <i>the endocrine system</i> (thyroid) ( $3 \times 9 = 27$ )	27
	4. <b>Embryo</b> -the 4th functional step: <i>the heart</i> ( $3 \times 9 = 27$ )	27
	5. <b>Embryo</b> -the 5th functional step: <i>the eyes and ears</i> ( $3 \times 9 = 27$ )	27
	6. <b>Embryo</b> -the 6th functional step: <i>epidermis</i> ( $3 \times 9 = 27$ )	27
	7. <b>Embryo</b> -the 7th functional step: <i>lymphatic system</i> (thymus) ( $3 \times 9 = 27$ )	27
	8. <b>Embryo</b> -the 8th functional step: <i>lips</i> ( $3 \times 9 = 27$ )	27
	9. <b>Embryo</b> -the 9th functional step: <i>auricula</i> ( $3 \times 9 = 27$ )	27 243
	10. <b>Embryo – MT network 1</b> : of the digestive system	10
	11. <b>Embryo – MT network 2</b> : of the cardiovascular system (periph.)	10
	12. <b>Embryo – MT network 3</b> : of the urinary system (bladder)	10
	13. <b>Embryo – MT network 4</b> : of the gallbladder	10 40
	14. <b>Embryo – MT network 5</b> : of the liver	5
	15. <b>Embryo – MT network 6</b> : of the respiratory system (lungs)	5
	16. <b>Embryo – MT network 7</b> : of the colon	5
	17. <b>Embryo – MT network 8</b> : of the cardiovascular system (heart)	5
	18. <b>Embryo – MT network 9</b> : of the spleen	5
	19. <b>Embryo – MT network 10</b> : of the small intestine	5
	20. <b>Embryo – MT network 11</b> : of the kidneys	5
	21. <b>Embryo – MT network 12</b> : of the pancreas	5 40
	22. <b>Fetus</b> -1st cycle of the MT learning network for organism functioning	6
	23. <b>Fetus</b> -2nd cycle of the MT learning network for organism functioning	6
	24. <b>Fetus</b> -3rd cycle of the MT learning network for organism functioning	6
	25. <b>Fetus</b> -4th cycle of the MT learning network for organism functioning	6
	26. <b>Fetus</b> -5th cycle of the MT learning network for organism functioning	6
	27. <b>Fetus</b> -6th cycle of the MT learning network for organism functioning	6 36
	28. <b>MT network</b> : 13 and 14 ( $27+10$ : functional integration of the organism)	37 37
		496

regulation nodes (the preembryonal nodes are not included in the network, only the nodes relating to the human species).

The system of extra-bioactive loci („information nodes“) is obtained in the following way: fertilization point „1“ is the *central* point, resulting in 360 nodes on the main circle circumference (each degree represents a „node“). In order to connect point „1“ with other 360 loci, another 6 circles are formed, each having 6 „nodes“, resulting in the number  $1+360+(6\times 6) = 397$ . This completely conforms to the Chinese system of acupunctural points (system of 361 regular points and 36 extraordinary points) (The Academy of Traditional Chinese Medicine, 1975).

### INDEX OF THE ACUPUNCTURE POINTS

(361 Regular Points and 36  
Extraordinary Points)

Abdomen-Tonggu (腹通谷, K. 20), 60,  
160  
Abdomen-Yinjiao (阴交, Ren 7), 200  
Abdomen-Zhongzhu (中注, K. 15), 60,  
159

Chengshan (承山, U.B. 57), 152, 220,  
222, 239, 246, 263  
Chest-Zigong (胸紫宫, Ren 19), 203  
Chize (尺泽, Lu. 5), 22, 86, 95, 97, 227,  
250

Note that the expression „acupuncture point“ is widely used in the West and in China (when English is used), although the phenomenon is not represented by „points“ rather by *xie* („cave“, biological „black-hole“, as  $-1_4$ ) leading from body surface into adequate tissue depth (2–50 mm), where a „node“ connected via „channels“ (the main *quantum information highways* developed during embryogenesis) is located. When the needle reaches adequate depth, the feeling of *de qi* (slight numbness) is sensed.

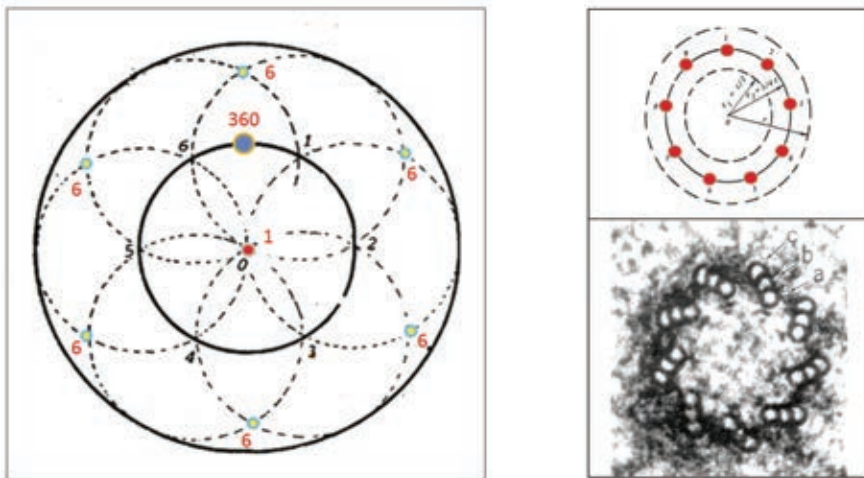


**Figure 8.19.** The system of extra-bioactive loci of the human body numbering  $1+360+(6\times 6) = 397$ , generated by the Fibonacci structure of 9 triplets (27 microtubules) (left). This structure is found in each cell, it is the main molecular machine of the mitotic spindle.

We began investigating extra-bioactive body points (information „nodes“) based on hydrogen bonds of biomolecules like collagen, microtubules, centrioles, and water in 1976 (Koruga, 1984). A significant encouragement came that year from the University in Toronto, Canada, where I had an opportunity to discuss this subject with Prof. Brus Pomeranz. He was just then beginning research of this topic, and 12 years later, published the book *Scientific Bases of Acupuncture* (Pomeranz and Stux, 1988 Eds.). After returning from Canada, I continued research in this domain with Prof. Antonije Škokljević, our doyen in the application of Chinese medicine (Škokljević, 1976), at the Military-Medical Academy in Belgrade.

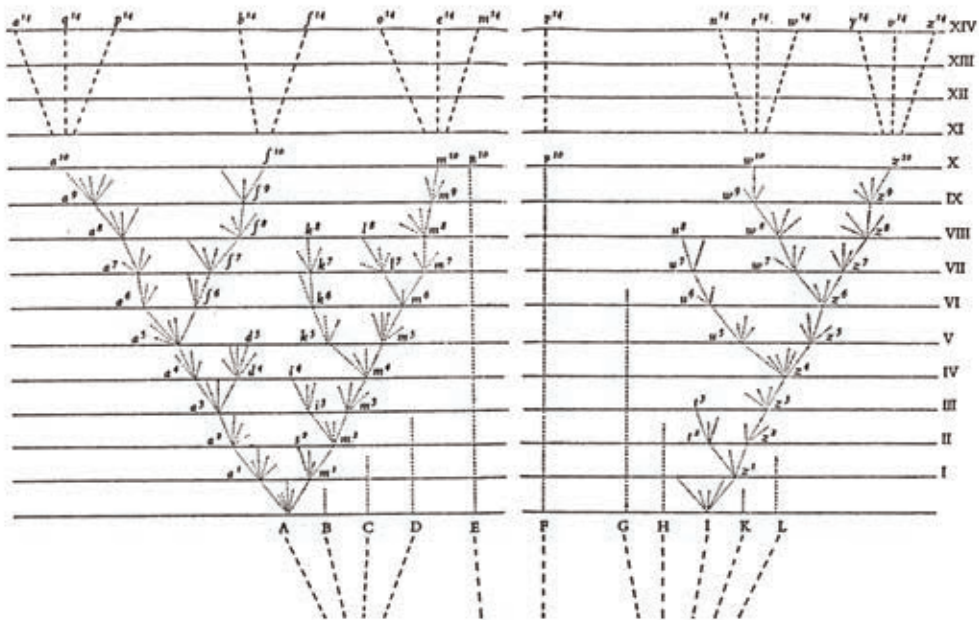


**Figure 8.20.** Darwin's diagram of evolution in 14 steps (according to the second perfect number 28, via the Y chromosome with palindrome information content: the half is equal to the whole  $\langle 28 \mid = \mid 14 \rangle$ ). The diagram demonstrates that everything begins from a three-layered „germ“ (ABCD, EF, and GHJK), the middle part is excluded (everything except the F as the „symmetry axis“ of evolution (break at the X level), A and I remain branching (principle of Cantor's random triadic set). Various branches have different evolution lengths, some die off, some continue evolution (Darwin, 1989). Darwin „saw“ what was in front of him, which is, according to Goethe, the hardest thing to see: the evolution of the biological world. Today, we watch every day the Sun and the Moon, however, our mind still does not „see“ them, because, due to dogmas, they are viewed in a „distorted mirror“.

### 8.5. Energies ${}^{i\perp}E_3$ and ${}^{i\perp}E_4$

Let us go back to the general law of energy (Chapter II, expressions 2.17, 2.19, and 2.20) where we observed that according to the classical approach (expression 2.17) the first term is  $E_1 = mc^2$ , the second  $E_2 = 1/2 mv^2$ , while the third and the fourth are

$${}^{i\perp}E_3 = \frac{3}{8} m \frac{\vartheta^4}{c^2} \quad \text{and} \quad {}^{i\perp}E_4 = \frac{15}{48} m \frac{v^6}{c^4}. \tag{8.10}$$

Let us observe now the case of Earth’s motion around the Sun, as displayed in Figure 8.21. To simplify, we are going to assume that photon’s velocity, coming from Sun’s surface (not from Sun’s interior, that would take at least 10 000 years) is  $c = 3 \times 10^8$  m/s, and the average speed of Earth’s rotation about the Sun is  $\vartheta = 30000$  m/s. Vectors of photon’s velocity ( $\vec{c}$ ) and of Earth’s velocity ( $\vec{\vartheta}$ ) are always mutually orthogonal.

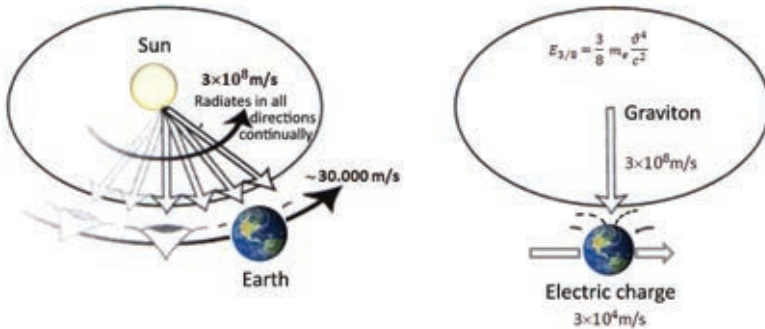


**Figure 8.21.** Schematic representation of the orthogonal Sun–Earth system ( $i^2 \perp i^4 = \perp_1 \perp^1$ ) with the graviton and photon acting on the electric charge; system energy  ${}^{i\perp}E_3$  induces information effects in biological structures, which originated during evolution under the influence of this system energy.

If we substitute velocities of the photon ( $c$ ) and of the Earth ( $\vartheta$ ), observing the orthogonality constraint ( $i^2 \perp i^4 = \perp_1 \perp^1$ ), into the expression for  $E_3$ , we obtain:

$${}^{i\perp}E_3 = \frac{3}{8} m \frac{\vartheta^4}{c^2} = \frac{3}{8} m \frac{(3 \times 10^4)^4}{(3 \times 10^8)^2} = \frac{3}{8} m \frac{81}{9} = \frac{3}{8} m \parallel 9 \parallel^{i\perp} \tag{8.11}$$

We observe that the orthogonal relationship between velocities is a congruence modulo 9, and that the biological sensor detecting the  ${}^{i\perp}E_3$  action should be orthogonal and composed of 9 units. This condition is satisfied by a pair of centrioles, mutually orthogonal, composed of 9 microtubule triplets (known sensors of electromagnetic and gravitation actions) as displayed in Figure 8.21.

Centrioles oscillate in several modes, as electronic, vibrational, and rotational structures. We are interested here in the oscillation phenomenon via twisting (torsion) (Figure 8.24, right). The centriole is opening at one endpoint (extending) and closing at the other end (contracting). Consequently, each centriole triplet can move, with respect to the zero angle, by an angle of  $300^\circ$  to  $420^\circ$  in both directions (*up* or *down*, i.e., *left* or *right*)

and make a turn. If centrioles are a *geefton* sensor, then *geeftons* can perform 6–12 twists (turns) in a second, however, 9 is the average and the most frequent value (Figure 8.22). This is because the *second* is not an arbitrary unit, but 86400-th segment of the spatial/temporal icosahedron of Earth's spin and of Earth's rotation about the Sun.

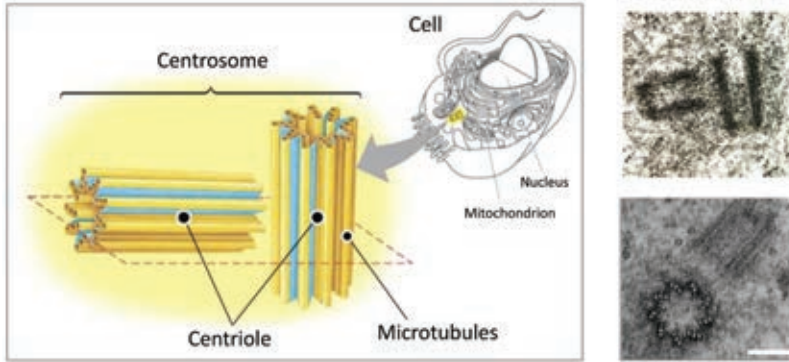


**Figure 8.21.** Schematic representation of the centrosome (centrosome =  $2^{\perp}$  centriole + associative structure) located in every cell (**left**). Centrioles are always mutually orthogonal (if this orthogonality is disturbed, functional cell impairments occur). Experimental proof of the centriole pair orthogonality obtained by an electron microscope from two different angles (**right**) (Glover, 1993, Alberts, 2002)

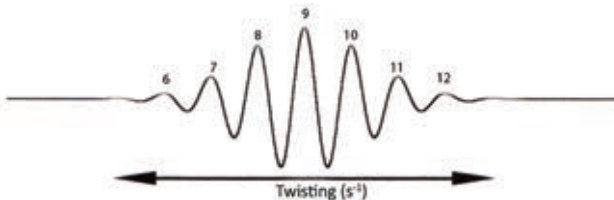


**Figure 8.22.** Centriole twisting with frequencies between 6 Hz and 12 Hz (9 Hz being the most frequent).

In living systems, from the aspect of information physics, two main processes are selfreproduction and learning. These two phenomena are mutually connected, because *selfreproduction* is the basis of a new entity having inborn adaptation to variation and natural selection (*phylogenetic learning*). *Learning* is also the basis for adaptation to the environment by experience (*ontogenetic learning*).

Let us observe autocorrelation  $\langle p, g \rangle$  as a „superposition“ of a graviton and a photon on a *geefton sphere* (clathrin with 36 triskelions), where 3 photons and 3 gravitons take part per triskelion. Let the sphere have two poles: north, denoted  $\langle G_p^N \rangle$ , and the graviton position on the south pole denoted by  $\langle G_g^S \rangle$ , and let the (quantum) autocorrelation be performed at the equator (resembling the quantum state of the electron on the Bloch sphere and of the photon on the Poincaré sphere). Autocorrelation means here that a one-to-one correspondence exists between the graviton and the photon in the triskelions and *geeftons* space, while observing incidence  $\langle G_p \rangle_3 \in \langle G_g \rangle$  (via electrons of the triske-

lion, geefton couples actions of the photon and the graviton). Coupling is performed through the Sun–Earth orthogonal system ( ${}^{\perp}E_3$ ) with base  $e$  (optimal energy-informational codogenic basis). Thus, we obtain that the classical photon spin, equal to 1, becomes, by coupling, the geefton spin  $e^{1i\pi}$ , graviton with spin 2 becomes  $e^{2i\pi}$ , and electron’s spin  $\frac{1}{2}$  becomes  $e^{1/2i\pi}$ . The coupled Fibonacci geefton satisfies  $\langle GF \rangle = e^{1i\pi} \times e^{2i\pi} \times e^{(1/2)i\pi} = e^{i\pi(1+2+1/2)} = (e^{i\pi})^{3/2} = -1^{(3/2)}$ , because  $e^{i\pi} = \cos\pi + i\sin\pi = -1$ . The final result is  $\langle GF \rangle = (i^2)^{3/2}$ , demonstrating that the geefton is a fractal state of the photon, graviton, and electron within the interaction with Fibonacci structures (mass, energy, and information). While the contemporary concept of quantum mechanics is based on  $i$ ,  $h$ , and the 2D Hilbert space, the fractal mechanics is based on  $i^2=-1=g_{55}$ ,  $\Phi/\phi$  and  $N=0$  ( $D_3, -2_5$  D) Cantorial space-time (see Chapter II, Table 2.2 and Expressions 2.44 and 2.54).

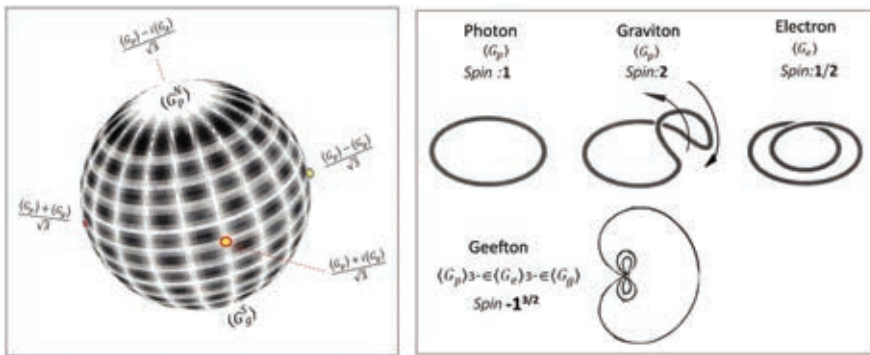


**Figure 8.23.** The geefton sphere with four basic autocorrelation („superposed“) states (left). Illustration of spins of the photon, graviton, electron and geefton (right). Geefton’s spin equals  $(-1)^{3/2} = (g_{55})^{3/2}$ , compatible and complementary value to the graviton’s spin (related to graviton) which is responsible, according to contemporary theories, for the dark matter (according to the standard cosmological model, the Universe is composed of 4.9% visible mass that we observe, 26.8% dark matter, and 68.3% of dark energy).

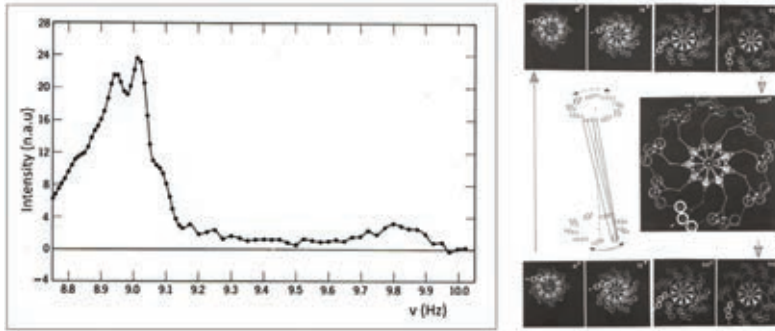
If two signals travel by the same velocity (as in the case of the photon and graviton) and act upon the same object, while there is a time difference between them (as in the case of the actions of the Sun and the Moon), then autocorrelation of two signals can be implemented – Moon’s  $f_M(t)$  and Sun’s  $(t+\tau)$ . In the Earth–Sun–Moon system, there are several situations, which in most cases act integrally, but there are also disturbances. The centriole accepts these signals and heterodynes them (superposes the MT oscillations, which are gravitation sensors, with fundamental oscillations of the centriole).

Figure 8.23 (left) displays that there are 4 autocorrelation („superposed“) locations, resulting in

$$4 \langle G_M | G_S \rangle = (G_M + G_S)^2 - (G_M - G_S)^2 \tag{8.12}$$

Since the microtubules (centrioles) carry electric charge, by twisting, under the influence of gravitation, they produce electromagnetic signals. Experimental measurements

and autocorrelation calculations of the EEG signals are displayed in Figure 8.20, *left* (Wiener, 1965). The diagram displays two proximal peaks, one at 9.05 Hz, and the other peak at 8.93 Hz. Peak width is 1 Hz (from 8.2 to 9.2 Hz), meaning that centriole twisting is within very narrow bounds about the average value of 9 Hz (there was a deviation in only one microtubule triplet).



**Figure 8.24.** EEG signal spectrum with the prominent peak 9.05 Hz (*left*). Measurement and data processing (by autocorrelation and heterodyne) were performed at MIT (Wiener, 1965). Schematic presentation (*right*) of centriole twisting and producing electromagnetic waves (due to „free“ electric charges on its surface and its dipole moments) under the influence of energy  $\pm E_3$  (that generates code information in Fibonacci structures).

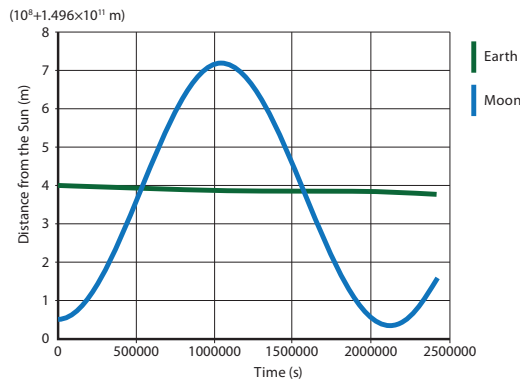


**Figure 8.25.** The green line indicates Earth's distance, and the blue curve indicates Moon's distance during 30 days. Distance is segmented into  $10^8$  m segments, which is approximately equal to a light-second, and a segment of  $1.496 \times 10^{11}$  m. Factor 1.496 is used in order for the Moon's curve to coincide with astronomical data. Number 1.496 can be written as  $1 + 496/1000$ , and developed into a series up to the 496-th member, which is the time photon and graviton travel between the Sun and the Earth in seconds.

Since centrioles and microtubules are responsible for extra-bioactive body loci (acupuncture points), we shall present the results of this experiment. Twelve volunteers took part in the experiment, and 1000 acupuncture loci were analyzed (about 28% of the total



number of acupuncture points in each subject). Obtained values are: 6.72 Hz, 8.90 Hz, and 11.50 Hz, having the standard deviations - 0.32 Hz, 0.40 Hz, and 0.002 Hz (Cohen, 1998, Ćosić, 1984). This means that centriole twisting was by two microtubule triplets to the left and to the right. However, the average value for all subjects is  $9.04 \pm 0.24$ . This means that centrioles are responsible for one type of EEG signals and for the acupuncture system. It is well known that impedance changes on acupuncture loci five times. Also, it has been presented that hyperpolarized light significantly reduces pain when acting onto acupuncture loci on mice. E-36 (Gulyar, 2017)

The time used by the photon and the graviton to arrive from the Sun to the Earth varies from 8 minute and 7 seconds to 8 minutes and 25 seconds, giving the average time of 8 minutes and 16 seconds, i.e., 496 seconds. In order that gravitons (traveling at the same velocity as the photons coming from the Sun and the Moon, and the reflected photons off the Moon on the rotating Earth's surface giving the correction factor  $\pm 12\ 600\ 000\ \text{m}$ ) be harmonized with photons and gravitons, fitting is performed by the Moon as displayed in Figure 8.21.

Centrioles, due to their own magnetic field, can be quantum „entangled“, resulting in a possibility of information „tunnels“ within our organism. Two centrioles are dynamically synchronized („coupled“), resembling ballet virtuosi performing complex choreography (Figure 8.26).

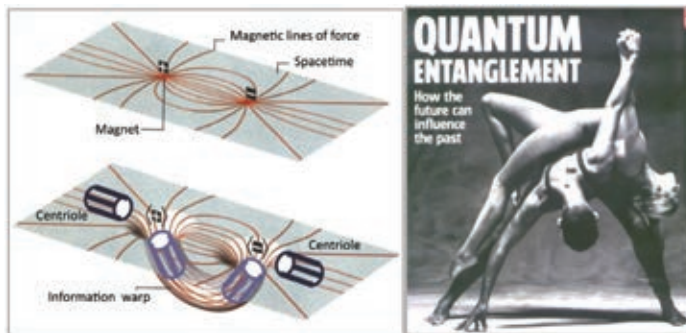


**Figure 8.26.** Centrioles and „bioinformation warps“ as a method to realize quantum information within the human organism via quantum fields. Therefore, in further investigations, we should use quantum field theory instead of quantum mechanics (Schrödinger's), build nanophysics (classical-quantum physics) and include the general theory of relativity (Koruga, 2012.).

## 8.6. Entropy Force and the Life Phenomenon

Investigations of gravitation, the second law of thermodynamics and of biological life foundations are presented in the paper by Linewearver and Egan (Linewearver, 2008). However, in a paper on the origin of gravitation in nature and on the Newton's law of

force and inertia, Verlinde (University in Amsterdam) presented a new interpretation of the gravitation force and the law of inertia (Verlinde, 2010). Newton defined force, within the classical mechanics, as the product of mass and acceleration

$$F = ma,$$

while Verlinde used the expression for energy and entropy: the product of force and distance equals the product of temperature and entropy (where distance and entropy are infinitesimal values, therefore, denoted as  $\Delta x$  and  $\Delta S$ ):

$$F \Delta x = T \Delta S. \quad (8.13)$$

The final expression defining force is, according to Verlinde

$$F = T \nabla S \quad (8.14)$$

as the product between temperature  $T$  and the entropy gradient  $\nabla S$  ( $\nabla$  is the *nabla* operator along all three coordinates).

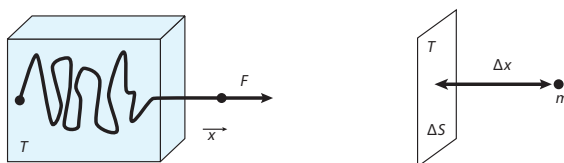


**Figure 8.27.** Free polymer under the effect of temperature leaves the equilibrium state and is displaced from the space it was in (by a distance  $x$ ) (left) generating a force that acts on other bodies in the most proximal vicinity (right) (Verlinde, 2010).

The *scenario* phenomenon presented from a different aspect of action (force, space, time) in this monograph is relevant for our investigations. A similar result is achieved according to Verlinde- space originates through a holographic scenario. Consequently, *gravitation* is nothing else save an *entropy force* related to *information* determining the location within the space of the mass point at each moment in time. According to this view, the *law of inertia* has also its origin in entropy.

From the aspect of biomedical engineering, the entropic approach to phenomena that we investigated as examples of classical mechanics opens new possibilities. One possibility is the example of a 5D (five-dimensional) *surgical knife* (similar to examples in Chapter II on 5D memory). In this case, the surgeon would obtain, via a holographic image formed outside the body (a 3D organ, tissue, i.e., location under operation), the possibility to follow his work in the organism through a „geefton energetic-information“ surgical „knife“, without the need to actually cut the tissue with a classical surgical knife. Beside many advantages of such a „geefton 5D surgical knife“, there would be no scars left after such an operation.

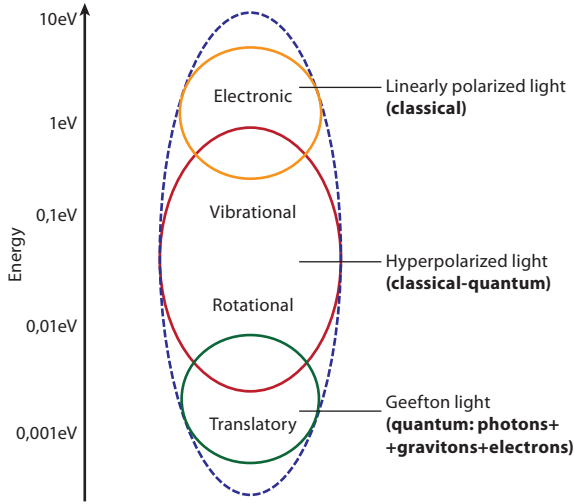


**Figure 8.28.** Four energy types (electronic, vibrational, rotational and translatory) determining human organism functioning from the energetic aspect.

In closing this Chapter we can conclude that there are three key sciences for the understanding of the life phenomenon and health: *quantum physics* (and quantum medicine symbolized by Schrödinger’s cat), *nanophysics* (and the integral classical-quantum medicine symbolized by Fibonacci’s cat) and finally *fractal mechanics* (based on light, gravitation and water, symbolized by a cat walking a „water thread“ toward the unity of photon, graviton, and electron within the „information black hole“, with tail as the symbol of this new unity).

Schrödinger’s cat is famous in science (although some believe that it is still missing), Fibonacci’s cat was introduced in Chapter V. However, there is a third cat we are going to meet – the fractal mechanics cat.

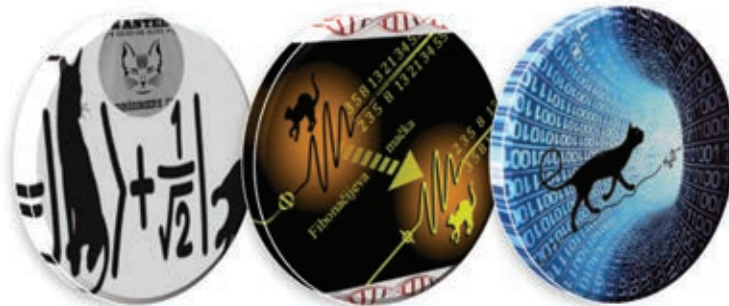


**Figure 8.29.** Symbols of three sciences: quantum physics (Schrödinger’s cat), nano physics (Fibonacci’s cat) and fractal mechanics (geefton cat). The cat was chosen as a symbol to represent these sciences because cats are, by their nature, headstrong (self-contained), like biological cats. What is on the other side of the above „tokens“? (See cover page III).

If we observe autocorrelation (superposition) from the aspect of spins 3 established in the triskelion (clathrin), the sum of input information on spins of the photon and the graviton equals 3 (they are coupled according to the law  $\Phi^2 + \phi^2 = 3$ ), and 6 electron spins (within an atom with 6 electrons) give also 3, because  $6 \times 1/2 = 3$ , they are coupled according to the law  $\Phi^2 + \Phi^{-2} = 3$ , resulting in the autocorrelation of this system:

$$4 \langle 3|3 \rangle = (3+3)^2 - (3-3)^2 = 36, \quad 8.15$$

which corresponds to the number of triskelions, i.e., to the condition of spin autocorrelation of photon, graviton, and six electrons within the clathrin hexagon  $||36 \langle s_g | 3 | s_p \rangle ||$ . These 6 electrons in clathrin hexagons must be in a resonant spin relationship with the 6 electrons of the atom included in this structure (hierarchical fractal connection). We know that this is the carbon atom with an electronic configuration of six electrons represented in the form:  $1s^2 2s^2 2p^2 [|\uparrow\downarrow\rangle, |\uparrow\downarrow\rangle, |\uparrow\uparrow\rangle]$ . Since clathrin is a hierarchically resonant structure with carbon, another curiosity results- clathrin and the carbon molecule of 60 atoms ( $C_{60}$ ) have the same number of nodes (common regions of pentagons and hexagons). Thus, we can say that clathrin is composed of 12 *pentagons* and *empty space* (on sphere's surface) or of 20 *hexagons* and *empty space* (on the surface of a sphere). In other words, clathrin with 12 pentagons and 20 hexagons on its surface gives a result  $5 = 6$ , because pentagons and hexagons, viewed independently (with empty space), produce the same structure. Why is the *empty space* important? The answer is simple, can you imagine a *house* without doors and windows (*empty space*), only with walls. Such an object would be useless, therefore *emptiness* (vacuum) is as important as *fullness* (matter).

We observe that the second term in the previous expression for autocorrelation equals zero, thus only the first member remains  $(3+3)^2$  that should observe orthogonality due to the orthogonality of the photon and graviton system coming from the Sun and the motion of electric charges (electrons within clathrin hexagons). This complex spin motion produces an orthogonal space ( ${}^i\perp = [0.61803 \ -0i^2] \oplus [0.61803 \ -i^2] = [\phi] \oplus [\Phi]$ ). Its *fractal information dimension* is calculated in the following way:

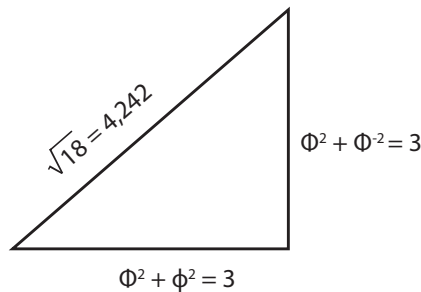


**Figure 8.30.** Spatial orthogonal dimension  $D = 4.242$  realized in biomolecules with the Fibonacci structure under the influence of  ${}^{i\perp}E_3$  (energy that generates information in synergy with Fibonacci structures), Sun's photons and gravitons, Moon's gravitons, and reflected sunlight off the Moon (Yang-yin-Yin-yang system).

Therefore, the dimension of the *space* where coupling of graviton's, photon's, and electron's actions takes place is not an integral number, it equals 4.242, i.e., it is a fractal dimension (Hausdorff's dimension). In other words, coupling of these three entities is not possible in an „ordinary“ 3D space, it is possible in the *fractal space* realizable between 4D and 5D. This space is formed in biomolecules, which are Fibonacci structures.

Coupling of gravitons, photons and electrons is established through *action*, which is a product of the force ( $F$ ), displacement ( $d$ ) and time ( $t$ ):  $A = F \times d \times t$ . However, this is equivalent to spin action,  $A_s = s(h/2\pi)$  of photon with spin  $s=1$ , graviton with spin  $s=2$  and electron with spin  $s=1/2$ . Thus, the autocorrelation process (coupling) is not entirely a spin and space phenomenon, but also a temporal phenomenon, hence the dimension of *spacetime* has to be determined, because beside coupling of photons, gravitons and electrons, *space* and *time* must be coupled to produce *spacetime*. The inclusion of time and its coupling with space results in a slight correction of the space dimension, at the same time observing the constraint of *orthogonality* and *Aufgehoben* in the *spacetime* system as well (Goldblatt, 1987, Callahan, 2000). What is the dimension difference and how should the *spacetime* of this *scenario* be defined (not *system* but *scenario*! Figure 8.31)? Care should be taken not to be led to believe, as most people do, that the *scenario* is strictly *deterministic*, because „dear God does *not gamble*“, but He *throws dice*. Since the spin action of photon and graviton is a major process in the interaction with the electron, this means that unity of spin's symmetry in clathrin and microtubules (Fibonacci structures), based on harmony  $\Phi^2 + \phi^2 = 3$ , is the root of biological information related to consciousness.

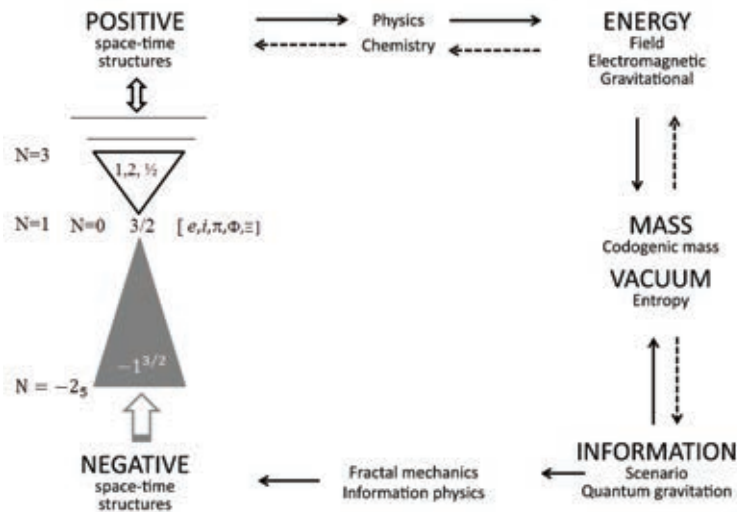
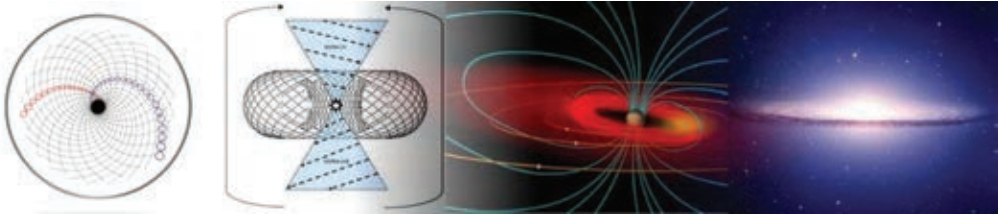


Figure 8.31. The relationship between positive and negative space-time structures (fractal mechanics as the missing science in the science system based on universal physical constants – see Figure 2.1, Chapter II and Table 2.2).

As is known, our 3D stars generate diffuse light and our main biological structures (DNA, proteins, water, etc., as entities of the 5D reduction into 3D space) generate electromagnetic energy (“biophotons”) as *hyperpolarized light*. Our goal is to generate hyperpolarized light on Earth locally (devices, rooms, houses, etc.) and one day globally by a new dust layer of  $C_{60}$  molecules in atmosphere (ionosphere), which will transform diffuse sunlight into hyperharmonized light.

$$|\psi_{12}\rangle = \frac{1}{2} (|\uparrow_1\rangle|\leftrightarrow_2\rangle + |\uparrow e^{-i\omega_1 t}\rangle|\uparrow e^{-i\omega_2 t}\rangle)$$



**Figure 8.32.** Photons with a combination of vertical and horizontal linear polarization may generate not only energy signals (on/off) but spatial-temporal information based on these signals. If the superposition of wave function follows 4D space (black hole, Figure 2.14) by the Fibonacci law, then quantum information processing of the twisting electromagnetic or/and gravity field is a torus with two simultaneous frequencies  $\omega_1(\Phi)$  and  $\omega_2(\Phi)$  as positive and negative spatial-temporal entities (situation similar to the cards game tablanet, when ace simultaneously has two values 1 and 11). The torus dust layer of  $C_{60}$  molecules in the Earth's atmosphere (ionosphere) under the influence of Sun's light will generate hyperpolarized light that will have both energy and information properties (the Earth as a communication device with 5D)

## References

1. Alberts, B., Bray, D., Lewis, J., Raff, M., Roberts, K., Watson, J.D., Molecular Biology of the Cell. Garland Publishing, 2002.
2. Albrecht-Buehler, G., Does the Geometric Design of Centrioles Imply Their Function? *Cell Motility*. 1:237-245;1981.
3. Ayres, R.U., Information, Entropy, and Progress: A New Evolutionary Paradigm, American Institute of Physics. New York, 1994.
4. Burger, H., Filozofija tehnike. Naprijed, Zagreb, 1979.
5. Callahan, J.J., The Geometry of Spacetime. Springer, New York, 2000.
6. Cohen, M., Behrenbruck, C, Ćosić, I., Shared frequency components between Schumann resonances, EEG spectra and acupuncture meridian transfer functions. *Acupuncture and Electrotherapeutic Research*, No.1: pp. 92-93, 1998.

7. Cartan, E., The theory of spinors. Dover Publications, New York, 1966.
8. Ćosić, I., Marinković, M., Veljković, V., Transfer Functions of Acupuncture Meridians. *Digital Signal Processing*, pp.673-675, 1984.
9. Darwin, Ch., The Origin of Species. Oxford University Press, Oxford, 1998.
10. Doolittle, R., Similar amino acids sequences: Chance or common ancestry. *Science*, 214:149-197, 1981.
11. Euklid, Euklidovi elementi: Preveo i komentare napisao Anton Bilimović. Srpska akademija nauka, Matematički institut, Beograd, 1957.
12. Feynman, R.P., QED: The strange theory of light and matter. Princeton University Press, Princeton and Oxford, 1985.
13. Glashow, S.H., The Charm of Physics. A Touchstone Book, New York, 1991.
14. Glover, D.M., Gonzalez, C., Raff, J.W., The Centrosome. *Scientific American*, No.6, pp.62-68, 1993.
15. Goldblatt, R., Orthogonality and Spacetime Geometry. Springer-Verlag, New York, 1987.
16. Green, M.B., Schwarz, J.H., Anomaly Cancellations in Supersymmetric D=10 Gauge Theory and Superstring Theory. *Physics Letters B*, 149: pp.117-122, 1984.
17. Green, M.B., Unification of forces and particles in superstring theories. *Nature*, 314: pp. 409-411, 1985.
18. Gruyitch, Ly., Time: Fields, Relativity and Systems. Lumina Press, 2006, ISBN-13 9781595266712.
19. Gulyar, S. and Tamarova, Z.A., Modification of Polychromatic linear polarized light by nano photonic fullerene and grapheme filter creates a new therapeutic opportunities, *Journal of US-China Medical Sciences*, Vol. 14, pp.173-191, 2017.
20. Hill, R., A First Course in Coding Theory. Clarendon Press, Oxford, 1986.
21. Human Genome Landmark, 2009: [www.ornl.gov/hgmis/posters/chromosome](http://www.ornl.gov/hgmis/posters/chromosome).
22. Isaacs, E.D., Covalency of the hydrogen bond in ice: A direct X-ray measurement. *Physical Review Letters*, 82, pp. 600-603, 1999.
23. Jafarkhani H., Space – Time Coding: Theory and Practice. Cambridge University Press, Cambridge, 2005.
24. Karafyllidi, I.G., Lagoudas, D.C., Microtubules as mechanical force sensor. *BioSystems*, vol. 88, pp. 137-146, 2007.
25. Koruga, Đ., Qi inženjering: Fenomen ekstara – bioaktivnih tačaka tela. Poslovna politika, Beograd, 1984.
26. Koruga, Đ., Neurocomputing and Consciousness. *International journal on Neural and Mass-Parallel Computing and Information Systems*, Vol.1, No 1: 32-38, 1991.
27. Koruga, Dj., Hameroff, S., Withers, J., Loutfy, R., Sundereshan, M., *Fullerene C<sub>60</sub>: History, Physics, Nanobiology, Nanotechnology*. North-Holland, Amsterdam, 1993.
28. Koruga, Dj., Informaciona fizika: U potrazi za naučnim osnovama svesti, st. 237-255, u knjizi SVEST: Naučni izazov 21. veka. ECPD, Beograd, urednici: Raković, D. i Koruga, Dj., Čigoja, Beograd, 1996.
29. Koruga, Đ., Tomić, A., Ratkaj, Ž., Gravity Potential Waves of Amplitude Nano-g on Earth's Surface. *Proceedings BPU-5: Fifth General Conference of the Balkan Physics Union*, August 25-29, 2003, Vrnjačka Banja, pp. 2199-2202, 2003.

30. Koruga, Dj., Classical and quantum information processing in DNA-protein coding, pp. 9-26, in book Ed. Obradović, B., Cell and Tissue Engineering. Springer, Berlin, 2012.
31. Levitt, H.M., Spin Dynamics: Basics of Nuclear Magnetic Resonance. John Wiley and Sons, Chichester, 2008.
32. Linewearver, C.H, Egan, A., Life, gravity and the second law of thermodynamics. *Physics of Life*, 5:225-242, 2008.
33. Mattick, S.J., Challenging the dogma: The hidden layer of non-protein-coding RNAs complex organisms. *BioEssays*, 25 (10) 930-939, 2003.
34. Moore, K.L., The Developing Human: Clinically Oriented Embryology. W.B. Saunders Company, Philadelphia, 1988.
35. Murphy, M.P. and O'Neill, What is Life? The Next Fifty Years: Speculations on the future of biology. Cambridge University Press, Cambridge 1995.
36. Nesvizhevsky, V.V., Borner, H.G., Petukhov, A.K., Abele, H., Baesier, S., Rueft, F.J., Stoferle, T., Westphal, A., Gagarski, A.M., Petrov, G.A., Strelkov, A.V., Quantum states of neutrons in the Earth's gravitational field. *Nature*, 415: pp.297-299, 2002.
37. Pantić, V., Embriologija. Zavod za udžbenike i nastavna sredstva Srbije, Beograd, 1973.
38. Penrose, R., Cycles of Time: An Extraordinary New View of the Universe. Alfred A. Knopf, New York, 2011.
39. Penrose, R., The Large, the Small and the Human Mind. Cambridge University Press, Cambridge, 1999.
40. Rakočević, M.M., The genetic code as a Golden mean determined system. *BioSystems*, 46: 283-291, 1998.
41. Salam, A., Unification of Fundamental Forces. Cambridge University Press, Cambridge, 1990.
42. Schrödinger, E., What is Life? Mind and Matter. Cambridge University Press, Cambridge 1967.
43. Swanson, A., A unifying concept for the amino acid code. *Bull. Math. Biology*, 46(2), 187-203, 1984.
44. Tomanaga, S-I., The story of spin. The University of Chicago Press, Chicago, 1997.
45. Škokljević, A., Akupunkturologija. ICS, Beograd, 1976.
46. The Academy of Traditional Chinese Medicine: An Outline of Chinese acupuncture, Foreign languages Press, Peking, 1975.
47. Vedral, V., Decoding Reality: The Universum as quantum information. Oxford University Press, 2010.
48. Verlinde, E., On the Origin of Gravity and the Laws of Newton. arXiv: 1001.0785v1 [hep-th], 6 Jan 2010.
49. Wiener, N., Cybernetics: or Control and Communication in the Animal and the Machine, The M.I.T. Press, Cambridge, 1965.



9

INDEX



## ***SUBJECT INDEX***

### ***A***

- adenine (A) • 10, 13
- acupuncture • 13, 14, 275, 276, 280, 281, 286, 287, 288, 304, 305
- acupuncture points • 13, 275, 280, 281, 304
- amniotic fluid • 106, 107, 110
- angular momentum • 60, 167, 168, 170, 171, 175, 176, 178, 179, 180, 182, 183, 185, 186, 187, 195, 196, 242, 247, 265, 307, 309
- asthma • 3, 199, 228, 229, 230
- Aufgehoben • 22, 44, 143, 265, 285,

### ***B***

- bang-bang • 3, 120, 121, 173, 182, 183, 184, 185, 196,
- Bioptron • 95, 101, 111, 161, 163, 196, 199, 206, 207, 210, 213, 214, 219, 223, 227, 228, 229, 232, 233, 235, 239, 302,
- biorhythm • 266
- Binnig, G. • 11, 61
- Bloch, F. • 2, 96, 97, 99, 183, 184, 278, 304,
- Bloch sphere • 2, 96, 97, 183, 184, 278, 304
- Bohr, N. • 27, 60, 61, 65, 66, 69, 70, 180,
- Brewster's angle • 93, 95, 160, 161, 205, 304
- burns • 162, 199, 212, 213, 214, 217, 218, 219, 220,

### ***C***

- $C_{60}$  • 2, 3, 4, 55, 83, 84, 85, 86, 87, 152, 172, 173, 174, 175, 176, 177, 178, 179, 180, 181, 182, 183, 184, 185, 186, 188, 189, 190, 191, 192, 193, 194, 195, 196, 206, 241-247, 252, 284, 286, 300, 304, 306, 309
  - $\pi$  electrons • 2, 84, 86, 172, 192
  - structure • 2, 10, 12, 14, 15, 22, 27, 43, 62, 65, 67, 68, 70, 71, 73, 83, 85, 96, 99,

- 100, 101, 102, 103, 104, 105, 106, 107, 110, 111, 117, 118, 120, 121, 122, 123, 125, 127, 130, 140, 145, 150, 151, 152, 157-159, 164, 165, 166, 167, 169, 170, 171, 173, 174, 178, 179, 180, 181, 184, 185, 188, 189, 190, 193, 195, 200, 201, 207, 210, 211, 213, 215, 225, 234-237, 241, 247, 252, 253, 255, 257, 263, 264, 265, 268, 274, 275, 277, 278, 279, 280, 284-286, 305, 306,  
rotations • 70, 93  
vibrations • 111, 134, 135, 163  
vibro-rotations • 163
- Cantor, G. • 48, 49, 50, 51, 52, 276, 279, 304, 305  
Cantor's set • 48, 49, 50, 51, 52, 276, 304, 305  
Casimir, H. • 24, 46, 47, 55, 309  
Casimir's force • 46, 47, 309  
cilia • 12, 111, 117, 119, 120, 121, 145, 152, 159, 164, 165, 167, 229, 230,  
cell • 2, 10, 106, 116, 117, 118, 119, 122, 124, 127, 130, 150, 151, 153, 154, 159, 163, 164, 165, 184, 200, 201, 202, 212, 215, 216, 218, 220, 221, 224, 225, 233, 236, 237, 238, 240, 268, 269, 270, 275, 278, 286, 288, 305, 306  
centriole • 12, 117, 119, 120, 122, 124, 145, 152, 159, 164, 165, 167, 179, 180, 264, 268, 269, 273, 276, 277, 278, 279, 280, 281, 286  
cycle • 124, 224  
division • 2, 10, 119, 124, 165, 237, 268, 269  
clathrin • 2, 12, 115, 116, 145, 152, 159, 164, 165, 167, 242, 245, 247, 252, 257, 264, 265, 266, 278, 284, 285  
code • 4, 42, 54, 147, 251, 252, 255, 262, 265, 267, 269, 270, 273, 280, 288  
classical • 255, 269, 270, 273  
quantum • 255, 269, 270, 273  
classical-quantum • 255, 270  
collagen • 99, 100, 124, 200, 305  
function • 34, 62, 64, 65, 67, 119, 144, 165, 175, 215, 225, 262, 304, 307, 308, 309, 310  
oscillations • 126  
organization • 101, 103, 115, 125, 126, 127, 128  
structure • 125  
fibers • 100, 101, 115, 127, 200, 201, 203, 212, 225, 238, 239  
coupling • 71, 86, 96, 179, 185, 259, 260, 263, 264, 265, 268, 279, 285, 305, 306, 308  
cytosine (C) • 10, 13

## D

- De Broglie, L. • 2, 11, 15, 27, 43, 61, 69, 175, 305, 310  
deterministic chaos • 9, 10, 15, 183, 185, 196, 246  
determinant • 75, 139  
system determinant • 139  
de qi • 275, 305  
DNA • 13, 42, 54, 127, 151, 165, 167, 252, 253, 254, 255, 256, 264, 265, 266, 267, 268, 269, 270, 273, 286, 288

**E**

- Einstein, A. • 1, 10, 11, 26, 27, 28, 29, 30, 33, 42, 43, 44, 48, 51, 54, 59, 61, 65, 98
- EEG • 192, 199, 241, 242, 243, 244, 245, 247
- electron • 69, 71, 73, 86, 98, 306
  - mass • 28, 29, 31, 42, 59, 60, 70, 73, 86, 116, 140, 251, 255, 256, 258, 261, 264
  - models • 70
  - charge • 20, 44, 60, 69, 82, 86, 99, 100, 277
  - spin • 19, 52, 69, 70, 71, 84, 86, 96, 97, 179, 194, 257, 261, 263, 264, 279, 287, 306, 307, 309
  - tunneling • 66, 67, 68
  - size • 19, 20, 69, 74, 92, 179, 262, 305
- embryogenesis • 13, 271
  - embryo • 268, 308
  - phases • 13, 93, 268, 270, 271
  - fetus • 106, 268, 309
  - light model • 2, 3, 13, 267, 270
- energy • 33, 277
  - radiation • 69, 134, 157, 158, 160, 257, 310
  - biomolecule • 14, 21, 73, 96, 100, 115, 132, 133, 150, 163, 164, 165, 167, 179, 180, 193, 206, 243, 257, 268
  - electron • 21, 96, 161, 163, 164, 166, 193, 206, 277, 282, 284
  - vibration • 133, 283
  - rotation • 84, 85, 163, 164, 166, 173, 183, 277, 282
  - translation • 69, 134, 157, 160, 257, 310
  - $E_3$  • 170, 259, 277, 279, 280, 284, 309
  - $E_4$  • 32, 259, 277, 309
- entropy • 132, 184, 209, 281
- extra-bioactive points • 274, 275

**F**

- factorial • 31, 34, 35, 50, 310
- Fibonacci, L. • 143, 144, 146
- Fibonacci's
  - biological structures • 150, 151, 170, 171, 176, 264, 268, 283, 284, 285, 306, 309
  - light structures • 171
- Fibonacci numbers ( $\Phi$ ,  $\phi$ ) • 144, 145, 147, 148, 306
- Fibonacci's cat • 256, 282
- five-dimension (5D) • 2, 34, 40, 42, 44, 181, 264, 283, 284, 295, 296, 304
- five-dimensionality ( $-2_5$ ) • 3, 38, 39, 44, 46, 48, 50, 51, 53, 86, 279, 307
- flagella • 120, 307
- fractal dimension • 51, 307
- fractal mechanics • 14, 284
- Freud, S. • 116
- Fresnel, J-A. • 23

fullerene • 83  
 full Moon phenomenon • 256, 257, 266, 267, 306

## G

Galilei, G. • 22, 23, 29  
 gamma function • 34, 35  
 geefton • 264, 265, 278, 279, 283, 285, 307  
   sphere • 1, 37, 38, 44, 51, 52, 90, 96, 118, 142, 180, 181, 278, 279, 306, 307, 309, 310  
   code • 41, 251, 255, 260, 265, 266, 269, 272  
 Gibbs, W. •  
 Gibbs free energy • 14, 99, 115, 130, 151, 159, 166, 180, 208, 215, 310  
 gravitation • 43, 53, 59, 73, 83, 172, 256, 259, 260, 261, 264, 282, 285, 307  
 gravitational constant • 28, 29, 44, 261, 292, 310  
 graviton • 3, 19, 43, 71, 257, 262, 263, 264, 265, 277, 278, 283, 307, 308, 309, 310  
 guanine (G) • 10, 13

## H

Hamilton, W.R. • 63  
 Hamiltonian • 2, 63, 64, 96, 175, 176, 265, 310  
 Hawking, S. • 70, 86  
 helix • 96, 100, 101, 105, 125, 128, 242, 252, 253, 307  
   double • 252  
 HOMO-LUMO • 190  
 hydrogen bonds • 74, 128, 150  
   covalent • 76, 77, 80, 101, 131, 136, 137, 138, 141, 252  
   noncovalent • 80, 131, 136, 138, 141, 143, 209, 252, 255, 260

## I

information • 9, 37, 91, 184, 204, 246, 252, 263, 264, 281, 283  
   classical • 255  
   quantum • 3, 28, 53, 65, 66  
   Shannon's • 184, 256  
 information warps • 281  
 information physics • 262, 286

## K

Kaluza, T. • 43, 54  
 Klein, O. • 44  
 Kroto, H. • 85, 172, 188, 189

## L

Lagrange, J.L. • 63  
 Lagrange equation • 64, 293  
 Larmor, J. • 97, 98

- Larmor's frequencies • 293
- laser • 11, 157, 158, 159, 160, 163, 294, 308
  - application in medicine • 162
  - power • 164, 188, 294
- levitation • 2, 46, 47, 294
- life • 2, 3, 4, 9, 10, 11, 12, 14, 24, 26, 32, 34, 42, 54, 59, 80, 83, 99, 115, 130, 131, 150, 158, 159, 169, 170, 200, 203, 215, 217, 220, 228, 230, 233, 237, 239, 251, 256, 258, 259, 267, 278, 281, 283
- light • 1, 9, 22, 23, 34, 91, 92, 159, 162, 164, 165, 176, 223, 243, 244, 254, 257, 263, 309
  - diffuse • 159, 160, 162, 163, 170, 193
  - harmonized • 242, 245
  - polarized • 162
    - circular • 11, 96, 170, 308
    - harmonics • 177
    - vertical linearly polarized • 94, 96, 100, 101, 103, 187, 193, 206
    - horizontal linearly polarized • 308
    - linearly polarized • 2, 24, 51, 95, 96, 99, 160, 164, 167, 206, 209, 242, 243, 308
    - hyperpolarized • 2, 3, 53, 170, 171, 206, 209, 224, 226, 229, 308
    - speed • 29, 30, 32, 48, 73, 181, 252, 309
- application • 1, 95, 162, 212, 214, 215, 217, 219, 220, 223, 225, 228, 230, 233, 234, 236, 240, 241, 302
  - acne • 199
  - asthma • 3, 228, 229, 230
  - lumbar pain syndrome • 199, 232, 234, 235
  - burns • 218, 219, 220, 221
  - psoriasis • 3, 199, 221, 222, 246
  - wounds • 53, 199, 213, 214, 216, 217, 219, 220, 259
  - vein insufficiency • 199, 237, 237
  - spondylolisthesis • 231, 232, 234, 235
- London interactions • 294
- LUMO • 191
- Lyapunov's exponents • 294

## M

- Maxwell, J.C. • 24
- Maxwell's equations • 25, 294
- mass • 42, 69, 101
  - dimension of mass  $3/2$  • 42
  - dimension of mass 1 • 42
- mass spectrum • 189
- microtubules • 3, 12, 99, 103, 117, 118, 119, 122, 123, 151, 158, 159, 165, 167, 229, 232, 260, 264, 268, 269, 279, 280, 306, 309
- Möbius strip •
- De Moivre's formula • 102

molecule  $C_{60}$  • 85, 86, 172, 173, 174, 183, 184, 185, 186, 188, 189, 190, 191, 192, 247, 284, 309  
 hexagones • 116, 173, 188  
 rotation • 70, 158, 173, 179, 261, 309  
 pentagons • 116, 188  
 thin film • 183, 192, 245, 246

## N

nano • 166, 286, 303, 304  
 biophysics • 264, 267  
 generator • 4, 167  
 filter • 95, 193, 195  
 nanotechnology • 1, 4, 190  
 5D • 34, 42, 44, 181, 264, 282, 283, 307  
 Nordstrom, G. • 43, 55

## O

OMIS • 106, 210  
 Optics •

## P

Pascal's triangle • 147, 148  
 patent • 111, 152, 192, 195, 205, 210, 248  
 Penrose, R. • 1, 28, 33, 37, 41, 127, 257  
 classification of sciences • 33, 286  
 perfect numbers • 272, 273, 274  
 the first perfect number • 272, 273, 274  
 the second perfect number • 272, 273, 275, 278  
 the third perfect number • 272, 273, 274  
 the fourth perfect number • 272, 273, 274  
 photon • 2, 11, 19, 20, 26, 27, 42, 52, 53, 71, 86, 167, 168, 169, 183, 257, 263, 264, 265, 305, 310  
 quantization • 15, 167, 169, 170, 171, 177, 180, 187, 195  
 spin • 263, 279  
 orbital angular momentum • 170, 171, 187, 242, 310  
 photoelectric effect • 11, 25, 27, 28  
 Planck, M • 1, 26, 32  
 Planck's constant • 20, 26, 28, 32, 305, 308, 310  
 Poincaré, J. H. • 91, 92, 99  
 Poincaré sphere • 2, 91, 186, 308  
 protein • 12, 13, 65, 96, 100, 101, 115, 116, 125, 129, 130, 132, 144, 165, 200, 201, 210, 218, 219, 225, 238, 242, 251, 252, 253, 255, 264, 265, 266, 267, 287, 305, 307  
 amino acids • 131



peptide planes • 2, 126, 127, 129, 253  
psoriasis • 220, 221

## Q

quantum bit (qubit) • 2, 96, 183, 185, 186, 294, 309  
quantum harmonic oscillator • 169, 294

## R

radiation • 157  
Sun's • 9, 32, 157, 158, 257, 260, 261, 265, 277, 278, 279, 281, 284, 309  
IR • 134, 135, 158, 162, 310  
lamp • 161, 163, 207  
UV • 27, 157, 158, 160, 162, 191, 193, 200, 211, 225, 237  
rotation • 190, 259, 278, 283

## S

skin • 12, 200, 212, 215, 225, 226, 235, 236, 239  
basement membrane • 212  
biophysical state • 3, 199, 202, 207, 208  
dermis • 201, 237, 238  
epidermis • 219, 224, 237, 238  
hypodermis • 200, 201, 204, 215  
layers • 100, 206, 209, 221, 224, 237  
treatment • 152, 159, 162, 205, 207, 208, 213, 216, 230, 233  
spin • 70, 279, 287, 309  
electron • 70, 97, 308  
graviton • 4, 19, 44, 71, 257, 262, 263, 264, 265, 266, 267, 277, 278, 279, 281, 283, 284, 285, 305, 308, 309  
photon • 1, 2, 3, 10, 11, 14, 19, 20, 26, 27, 28, 42, 43, 44, 45, 92, 93, 99, 161, 164, 166, 167, 168, 169, 170, 171, 173, 175, 176, 179, 180, 181, 182, 183, 184, 185, 186, 187, 193, 206, 209, 229, 242, 243, 247, 254, 262, 263, 264, 265, 267, 270, 277, 278, 279, 280, 281, 283, 284, 306, 307, 308, 309  
pseudo • 264, 265, 296, 308  
space • 41  
empty • 60, 172, 284  
3D • 19, 42, 44, 46, 51, 83, 86, 101, 151, 172, 185, 251, 252, 264, 283, 284  
5D • 2, 34  
 $-2_5$  • 3, 38, 39, 44, 46, 48, 50, 51, 53, 86, 279, 307  
 $-1_4$  • 14, 38, 275  
space-time • 41, 165, 167, 279  
spacetime • 41, 262, 263, 284, 285, 296  
sphere • 1, 37, 51, 52, 142, 181, 278  
Bloch • 96, 97, 186, 305

- geefton's • 279, 280
- Fibonacci's • 186, 306
- packing • 118, 260
- Poincaré • 2, 91, 186
- unit • 37, 118, 181, 309
- spectroscopy • 3, 83, 87, 128, 143, 154, 162, 190, 195, 199, 204, 205, 207, 211, 247, 301
- STM • 11, 66, 67, 68, 83, 84, 85, 172, 173, 174, 175, 190, 310
- Stonier, T. • 17
- structure • 12, 241, 254
  - atom • 11, 19, 20, 25, 27, 59, 60, 65, 68, 69, 70, 71, 72, 73, 76, 77, 78, 79, 81, 82, 83, 85, 101, 105, 129, 131, 136, 172, 174, 179, 180, 181, 188, 255, 265, 284, 309
  - molecule • 1, 2, 3, 4, 12, 25, 73, 75, 76, 77, 78, 79, 80, 81, 82, 83, 84, 85, 99, 101, 107, 125, 126, 127, 128, 131, 132, 133, 134, 135, 136, 137, 138, 139, 140, 141, 142, 144, 157, 158, 159, 164, 172, 173, 174, 175, 176, 177, 178, 180, 182, 183, 184, 185, 188, 188, 190, 191, 192, 193, 242, 244, 254, 265
- Schrödinger, E., • 2, 33, 61, 67, 69, 127, 256
- Schrödinger's equation • 61, 62
- Schrödinger's cat • 256, 283
- symmetry • 164, 165, 272
  - dodecahedral • 164, 306
  - icosahedral • 116, 164, 166, 184, 193, 306
  - point • 62, 84, 116, 124, 127, 165, 174

## T

- tally • 1, 2, 14, 170, 171, 296
- Tesla, N. • 25, 26, 32, 54, 55, 159
- Thomson, J.J. • 11, 15, 87
- thymine (T) • 10, 13
- time • 219, 281
  - arrow of time • 252
  - denatured time • 252, 253
  - biological time • 252, 253, 255
- topology • 93, 183
- topological similarity • 182
- torus • 181, 183, 185, 193
- translations • 117, 268, 284
- triadic set • 48, 49, 50, 51, 52, 276, 304, 305
- triskelion • 116, 265, 267, 278, 284
- tubuline • 118, 152, 260
- twisting • 174, 180, 186, 278, 281

## U

- unification of forces • 4, 43, 48, 171, 263, 267
- Universe • 13, 48, 51, 53, 130, 159, 251, 267, 270, 279

**V**

- Van der Waals, J.D • 75
  - interactions • 78, 80, 81, 82
- Vedral, V. • 256, 262, 287
- velocity of light •
- vibrations • 2, 4, 12, 21, 42, 62, 74, 76, 85, 111, 117, 127, 133, 158, 163, 164, 165, 166, 167, 173, 174, 175, 177, 193, 194, 206, 282

**W**

- wave • 23, 32, 61, 73, 75, 107, 175, 177, 257, 259, 260
  - acoustic • 107, 110
  - electromagnetic • 23, 73, 75, 92, 100, 257
- wave function • 62, 97, 262, 302, 309, 310
- wave number • 73, 92, 126
- water • 130, 131, 133, 134, 135, 201
  - loss • 184, 200, 201, 202, 203, 225, 236, 238, 310
  - clusters • 140, 142, 174
  - molecule • 12, 61, 83, 84, 99, 125, 129, 136, 137, 144, 172, 174, 177, 180, 182, 184, 185, 189, 190, 191, 192, 247, 252, 253, 284, 309
  - bridge • 101, 134, 135, 309
  - diamagnetism • 140, 141, 142
  - paramagnetism • 3, 141, 142
- Wiener, N. • 280, 281
- wounds • 214, 216, 217, 220, 257
  - burns • 213, 217, 218
  - healing • 216, 219

**Z**

- Zygote • 13, 268, 269, 270, 272, 274



### ***About the Author***

Djuro Koruga, Professor of biomedical engineering and nanotechnology at the Faculty of Mechanical Engineering of the University of Belgrade, obtained a doctoral degree jointly from the Faculty of Mechanical Engineering and from the Faculty of Medicine of the University of Belgrade in the field of biomolecular energy-informational processes in the human organism. He completed postdoctoral studies in the field of nanotechnologies and their application in medicine at the Medical Faculty of the University of Arizona in Tucson. In 1985, he founded the Center for Molecular Machines at the Faculty of Mechanical Engineering in Belgrade, which was, in 2002, transformed into NanoLab. In 2006, he founded the Biomedical Engineering Department at the Faculty of Mechanical Engineering of the Belgrade University. He was professor at the University of Arizona (USA) and at the University Chuo in Tokyo (Japan). As a visiting professor, he delivered lectures at universities in the USA, Japan, China and South Korea. During his stay in the USA, in 1990–1998, he was engaged in research besides teaching. He participated in projects of the NSF, NASA and DARPA, and in projects of private investors. With his research team, in 1992, he obtained the first image of the  $C_{60}$  molecule by using the STM with atom resolution. He discovered the opto-magnetic imaging spectroscopy method. Using this method, he developed, with his associates, a method for screening, monitoring and early diagnostics of the cervix cancer. Professor Koruga published about 125 scientific papers, 54 in journals with the impact factor and is the author of three monographs and coauthor of six books. He was awarded the „Nikola Tesla“ Golden medal for the discovery of the nano-harmonizing substance and its application in cosmetics. He is the author of three US patents, and four patent applications in the field of biomedical engineering and nanotechnologies. He participated in numerous domestic and international conferences and congresses, where he presented over 50 papers and chaired two international conferences on nanotechnology and nanomedicine. He was the principal investigator of five projects financed by the Ministry of Science and Technological Development of the Republic of Serbia and of eight projects in cooperation with industry. Presently, he is leading the R&D on the application of hyperpolarized light in medicine, at the ZEPTEK MEDICAL General practice Department in Belgrade.

## *Collaborating Authors in Chapter VII*

### *Application of Hyperpolarized Light in Medicine*

3



*Biljana Lučić, MD*

5



*Aleksandar Nešković, MD*

8



*Milica Komnenić, MD*

13



*Đuja Lazić, MD*

21



*Aleksandra Ignjatović, MD*

34



*Jelena Simić, MD*

55



*Daniela Mitrović, MD*

89



*Miloš Mladenović, MD*

144



*Zlatica Kecić, MD*

**Dr. Biljana Lučić:** doctor of medicine, graduated from the Medical Faculty of the University of Belgrade in 1993. She attended specialist studies in psychiatry during 1996–2000 specializing in the domain of family therapy. During 1995–2004, she worked in health care, as the founder of a private medical practice and as a practicing physician. From 2009 to 2016, she was employed at the Zepter International, as a medical consultant, team manager, educator, media promoter, and for two years as an expert for the Bioptron medical device. She founded the ZEPTEr MEDICAL General practice Department in 2016. She participated in two medical studies; she is the coauthor of the paper *Nano-Biophysical Approach in Medical Therapy by Hyperpolarized Light*, presented at the VI World Congress of Nano Science and Nanotechnology in Singapore in 2016.

**Dr. Aleksandar Nešković:** doctor of medicine, graduated from the Faculty of Medicine of the Belgrade University. From 2008 to 2014, he worked as an assistant and manager of a call center. He is employed at the Zepter International as a medical consultant and executive manager, currently at the ZEPTEr MEDICAL General practice Department. He participated in one medical study; he is the coauthor of the paper *Nano-Biophysical Approach in Medical Therapy by Hyperpolarized Light*, presented at the VI World Congress on Nano Science and Nanotechnology in Singapore in 2016.

**Dr. Milica Komnenić:** doctor of medicine, graduated from the Faculty of Medicine of the Belgrade University in 2005. She passed the state examination and completed post-graduate studies in the domain of health care policy and management. She worked at the primary health care center D.Z. „Novi Beograd“, at the clinical center UHMC „Bežanijska kosa“, „Hexalab“, and DeSheli as an expert consultant. Presently she is employed at the ZEPTEr MEDICAL General practice Department. At the 54th Congress of the Biomedical Science Students of Serbia, she presented a paper; she is the coauthor of the paper *Nano-Biophysical Approach in Medical Therapy by Hyperpolarized Light*, presented at the VI World Congress on Nano Science and Nanotechnology in Singapore in 2016.

**Dr. Đuja Lazić:** doctor of medicine, graduated from the Faculty of Medicine of the University Clinical Center in Tuzla in 1986. During 1986–1995, she worked as a physician-general practitioner at the primary health care center D.Z. „Srebrenik“ – in Tuzla and in Bjeljina. In 1998 – 2002, she attended specialist studies in clinical pharmacology at the Faculty of Medicine of the Belgrade University. She was employed, from 1995 to 2012, as the executive chairperson of pharmaceuticals distribution and as the responsible person for pharmacovigilance and introduction of HACCP and ISO standards. Since 2014, she is working at the Zepter International, as a medical consultant. She is the coauthor of the paper *Nano-Biophysical Approach in Medical Therapy by Hyperpolarized Light*, presented at the VI World Congress on Nano Science and Nanotechnology in Singapore in 2016.

**Dr. Aleksandra Ignjatović:** doctor of medicine, graduated in 2013 from the Faculty of Medicine of the Belgrade University with average mark 9.11. She worked as a demonstrator at the department of Histology and Embryology of the Faculty of Medicine during 2008–2012. She completed medical internship at the primary health care center D. Z. „Vračar“

and at the clinical center HMC „Zvezdara“ in 2013–2014. She is working at the Zepter International as a medical consultant and manager for business cooperation. Presently, she is with the ZEPTEr MEDICAL General practice Department. At the 54th Congress of Biomedical Science Students of Serbia, she presented a paper, and is the coauthor of the paper *Nano-Biophysical Approach in Medical Therapy by Hyperpolarized light*, presented at the VI World Congress on Nano Science and Nanotechnology in Singapore in 2016.

**Dr. Jelena Simić:** doctor of medicine, graduated from the Faculty of Medicine at the University of Priština -Kosovska Mitrovica in 2012. She completed medical internship at the primary health care center D.Z. „Kosovska Mitrovica“ and at the Health Center in Kosovska Mitrovica. She participated at the 50th and the 51th Congress of Biomedical Sciences Students of Serbia with papers in the field of psychiatry, as author, and as coauthor in the domain of otorhinolaryngology. From 2014 to 2016, she worked at the Zepter International as a medical consultant. Presently, she is employed at the ZEPTEr MEDICAL General practice Department. She is the coauthor of the paper *Nano-Biophysical Approach in Medical Therapy by Hyperpolarized light*, presented at the VI World Congress on Nano Science and Nanotechnology in Singapore in 2016.

**Dr. Daniela Mitrović:** doctor of medicine, graduated in 2005 from the Faculty of Medicine at the University of Belgrade. She passed the state examination and completed postgraduate studies in the field of health care policy and management. She worked at the primary health care center D.Z. „Novi Beograd“, clinical center UHMC „Bežanijska kosa“, Hexalab and DeSheli as an expert consultant. Presently, she is employed at the ZEPTEr MEDICAL General practice Department. At the 54th Congress of Biomedical Science Students of Serbia, she presented a paper, and is the coauthor of the paper *Nano-Biophysical Approach in Medical Therapy by Hyperpolarized light*, presented at the VI World Congress on Nano Science and Nanotechnology in Singapore in 2016.

**Dr. Miloš Mladenović:** doctor of medicine, graduated in 2012 from the Faculty of Medicine of the Belgrade University, and completed specialist academic studies in 2013. He volunteered at the Clinical Center of Serbia (KCS) and the Hospital Medical Center „Zvezdara“. He is presently employed at the ZEPTEr MEDICAL General practice Department on the application of linearly polarized and hyperpolarized light in skin disease treatment. He participated in four international conferences and is the coauthor of the paper *Nano-Biophysical Approach in Medical Therapy by Hyperpolarized light*, presented at the VI World Congress on Nano Science and Nanotechnology in Singapore in 2016.

**Dr. Zlatica Kecić:** doctor of medicine, graduated in 2013 from the Faculty of Medicine at the University of Belgrade. She worked at the clinical center „Dr. Dragiša Mišović“ and at the primary health care center D.Z. „Zvezdara“. During floods that hit Serbia in the spring of 2014, she volunteered as a physician and participated in the seminar „Fighting for Health“. She is the coauthor of the paper *Nano-Biophysical Approach in Medical Therapy by Hyperpolarized light*, presented at the VI World Congress on Nano Science and Nanotechnology in Singapore in 2016.

## Glossary

### Concepts, abbreviations and notation

**Action:** product of physical forces giving as a result a magnitude whose measure unit is Js. For example, Planck's constant has the character of action  $h = Ev$ ; any action based on force ( $F$ ), displacement ( $d$ ) and time ( $t$ ):  $A = F \times d \times t$ , or spin ( $A_s = s \times h/2\pi$ )

**Acupuncture:** English term for the healing method of the traditional Chinese medicine, regulating organism functions by applying pressure, needles, heat, or electromagnetism at acupuncture points.

**Acupuncture points:** a network of body loci formed during embryogenesis and represented on the body surface. These points are called *xue* in Chinese, which means *cave*, that is an aperture leading into body's interior up to the *Yin* and *Yang* channels, which are connected with the *wu ji*, emptiness (vacuum).

**Amniotic fluid:** fluid containing the embryo (fetus) during embryogenesis. It contains compounds taken by the fetus and its excretion products.

**Bloch sphere:** representation of electron quantum states. The quantum electron states  $|\uparrow\rangle|\downarrow\rangle$  and  $|0\rangle|1\rangle$  are represented by sphere poles, while their four superposed states are represented on the sphere's equator as:  $1/\sqrt{2}(|0\rangle + |1\rangle)$ ,  $1/\sqrt{2}(|0\rangle - |1\rangle)$ ,  $1/\sqrt{2}(|0\rangle + i|1\rangle)$ ,  $1/\sqrt{2}(|0\rangle - i|1\rangle)$ .

**Brewster's angle:** incident angle between diffuse light and matter according to which matter linearly polarizes light.

**C<sub>60</sub>** is a molecule the size of only one nanometer, composed of 60 carbon atoms which are ordered on a sphere surface in 12 pentagons (with diamagnetic properties) and 20 hexagons (with paramagnetic properties). It rotates ("twisting")  $1.8 \times 10^{10}$  times per second, generating in interaction with light an opto-magnetic Faraday-like effect, causes a rotation of the plane of polarization (hexagons) and Fibonacci sequential position of the plane of polarization (pentagons), generating hyperpolarized light.

**Cantor's triadic set:** is obtained when to an arbitrary series  $a_1, a_2, a_3, \dots, a_n$ , composed of 0 or 1, in the form of the set  $\{0,1\}_{1(N)}$ , a real number  $\sum_{n=1}^{\infty} (2a_n)3^{-n}$  is corresponded,



which is mapped onto the triadic set T. There is a uniform Cantor's triadic set and a random Cantor's triadic set (they are called triadic sets, but are actually dyadic-triadic sets). *Length* of the triadic set is 1, although its *measure* equals 0.

**Centriole:** microtubular structure composed of 27 microtubules distributed in triplets as enneads. A pair of centrioles is positioned so that they are mutually orthogonal and represent cell's organizational center. It is the main molecular machine of the mitotic spindle.

**Centrosome:** complex cell structure, besides a pair of centrioles, it includes connecting proteins.

**Cilium:** microtubular structure composed of 18 microtubules distributed in pairs as enneads. The basic driving mechanism of unicellular organisms' motion (such as paramecium, etc.) constituting part of many epithelial tissues of higher organisms.

**Collagen:** protein found in the extracellular space, the most prevalent protein in the human organism. It is composed of six amino acids, which form an  $\alpha$ -helix. Presently, 24 types of collagen are known. One of the vital collagen functions is in the reticular lamina of the basement membrane.

**Coupling:** connecting two or more elements or phenomena into a new unity having novel characteristics.

**De qi:** phenomenon experienced by the subject when the acupuncture needle reaches adequate depth (emptiness, vacuum). It is followed by a sensation of mild numbness, impregnating tissue by a subtle action.

**Extra-bioactive body points:** body loci formed during embryogenesis as singularities of the synergy between actions of noncovalent hydrogen bonds of microtubules within the cell, collagen in the extracellular matrix, and water in the organism. There are 397 extra-bioactive body points in man; they are connected via quantum entanglement through 12 basic, 6 extra and 2 central information quantum channels.

**Electron:** elementary particle, belongs to the lepton family, spin =  $\frac{1}{2}$ , mass  $9.109 \times 10^{-31}$  kg, electric charge  $1.602 \times 10^{-19}$  C, size  $2.817 \times 10^{-15}$  m (classical radius), De Broglie's wavelength  $\Lambda = 1.23$  nm (1000 times smaller than the photon's wavelength of the same energy 1 eV being  $\lambda = 1230$  nm).

**Electron tunneling:** quantum phenomenon- ability of an electron to penetrate a barrier and of the modified wave function to exert action.

**Elliptical polarization:** light polarization where there is a relative amplitude change in photons.

**Faraday effect** is a magneto-optical phenomenon which causes a rotation of the plane of polarization when light interacts with a magnetic field (paramagnetism of  $C_{60}$ ) in matter. This effect occurs in most optically transparent dielectric materials, including liquids, under the influence of magnetic fields.

**Fibonacci numbers:** number sequence having as base  $[0,0!]$  that generates numbers according to the rule that the addition of two adjacent numbers gives the next succeeding number:  $0+0!=1$ ,  $0!+1=2$ ,  $1+2=3$ ,  $2+3=5\dots$ , forming a sequence 1, 2, 3, 5, 8, 13, 21, 34, 55... The ratios between two successive numbers form the sequence  $\frac{1}{2}$ ,  $\frac{2}{3}$ ,  $\frac{3}{5}\dots$  converging to  $0.61803\dots = \phi$ , while the sequence  $\frac{2}{1}$ ,  $\frac{3}{2}$ ,  $\frac{5}{3}\dots$ , converges to  $1.61803\dots = \Phi$ , where  $\Phi - \phi = 1$  and  $1/\phi = \Phi$ . Since  $\phi = \frac{1}{2}(\sqrt{5}-1)$  and  $\Phi = \frac{1}{2}(\sqrt{5}+1)$ , one of their major characteristic is the icosahedral and dodecahedral symmetry. There are four Fibonacci numbers:  $\Phi$ ,  $\phi$ ,  $-\phi$ ,  $-\Phi$ , two are real values  $\Phi = \frac{1}{2}(\sqrt{5}+1)$ ,  $\phi = \frac{1}{2}(\sqrt{5}-1)$  while the other two numbers are complex  $-\Phi = \frac{1}{2}(i^2\sqrt{5} + 1)$ ,  $-\phi = \frac{1}{2}(i^2\sqrt{5}-1)$ .

**Fibonacci sphere:** sphere with poles  $|1\rangle$  and  $|\sqrt{5}\rangle$ , which by superposition give superposed states at the equator  $\frac{1}{2}(|\sqrt{5}\rangle + |1\rangle)$ ,  $\frac{1}{2}(|\sqrt{5}\rangle - |1\rangle)$ ,  $\frac{1}{2}(|i^2\sqrt{5}\rangle + |1\rangle)$ ,  $\frac{1}{2}(|i^2\sqrt{5}\rangle - |1\rangle)$ . The sphere surface is coded by complex Fibonacci numbers  $i^4\phi = 0.61803 + 0i^4$ , and  $i^4\Phi = 0.61803 + 1i^4$ , where  $0i^4 = (0 \oplus |0\rangle)$  and  $1i^4 = (1 \oplus |1\rangle)$  are classical-quantum codogenic elements of the Fibonacci sphere, and the value 0.61803 is the measure of interrelations between all codogenic sphere (CQC) elements.

**Fibonacci structure:** biomolecules or processes having a symmetry axis of the 5-th order or an icosahedral symmetry, i.e., dodecahedral symmetry.

**Flagellum:** microtubular structure composed of 18 microtubules, which are distributed in pairs as enneads, and 2 central microtubules. It is the basic driving system of organism's motion in unicellular organisms from the flagellate family, while in complex organisms it is incorporated in the tail of the male reproductive cell (spermatozoid).

**Fractal dimension:** non-integral dimension of the space or space-time.

**Full Moon phenomenon:** influence of the coupled reflected Sun's light off the Moon's surface and Moon's gravitation on persons expressing the biophysical Möbius effect.

**Geefton:** classical-quantum coupling (autocorrelation) of actions of gravitation, light, and electric charge in Fibonacci biological structures according to the law  $5D(-2_5)$  of the Fibonacci (CQC) sphere; spin  $[(-1)^{3/2} = (i^2)^{3/2} = (\mathbf{g}_{55})^{3/2}]$ .

**Geefton sphere:** a higher fractal structure of the Fibonacci sphere  $[\langle G^N \rangle, \langle G^S \rangle]$  of type  $(1/\sqrt{3})(\langle G^N \hat{n} \pm i^n \langle G^S \rangle)$ , where N- north pole, S-south pole,  $n = 1, 2, 3$  and 4.

**Gravitation:** attraction phenomenon of mass bodies, acts at a distance. It is proportional to the attracting masses, and inversely proportional to the square of their distance.

**Graviton:** carrier of the gravitation action, spin = 2, propagates with the velocity  $2.99 \times 10^8$  m/s.

**Gravitino:** carrier of the „dark matter“ and „dark energy“ action, spin = 3/2.

**Hausdorff's dimension:** measure of the local size of a number sequence (i.e., „space“), taking into account distance between each point (that is, „points“ in „space“). It can take integral and non-integral values. The concept of the Hausdorff's dimension was introduced in 1918 when mathematician Felix Hausdorff published a paper on the subject. *Theorem:* For each value of  $r > 0$  there is a fractal - Hausdorff's dimension  $r$  in the  $n$ -dimensional Euclidian space  $R^n$  ( $n \geq \lceil r \rceil$ ).

**Hyperpolarized light:** Fibonacci order of photon's electric field – the vertical linearly polarized light  $[-1,0,0]$  is changed sequentially into the horizontal linearly polarized light  $[1,0,0]$  on the Poincaré sphere according to the Fibonacci law  $[\Phi,1,\phi]$ .

**Larmor's frequency:** frequency defining quantum states of elementary particles such as electron ( $\omega_{\text{electron spin}} = 28.025$  GHz) and proton ( $\omega_{\text{proton spin}} = 42.5781$  MHz). The EPR (electron paramagnetic resonance) and NMR (nuclear magnetic resonance) devices were constructed based on these frequencies.

**Laser light:** monochromatic (of one wavelength), coherent (spatially and temporally in phase) light.

**Light:** phenomenon of electromagnetism - a set of photons, whose electromagnetic planes can be differently organized in space and time, dance of photons.

**Linearly polarized light:** organization of photons in the polarization plane according to photon energies. There is vertical  $[-1,0,0]$  and horizontal  $[1,0,0]$  linearly polarized light, according to the position of the electric field vector in space (vertical or horizontal).

**Moment of linear momentum:** vector product of the radius vector  $r$  and the linear momentum  $p$ :  $L = \vec{r} \times m\vec{v}$ . Also called orbital momentum, impulse momentum, angular momentum, impulse, torque.

**Orthogonal system:** a system of functions where the scalar product of even exponents of the system function equals  $\pm 1$ , and the scalar product of odd exponents of the system function equals  $\pm i$  (for example  $i = \sqrt{-1}$ ,  $i^2 = -1$ ,  $i^3 = -i$ ,  $i^4 = +1$ , etc.). The quantum system is part of this orthogonal system because  $QP - PQ = i\hbar/2\pi$ , where  $P$  represents the position of the entity in the coordinate system, and  $Q$  moment of the linear momentum of the entity in  $P$ .

**Perfect numbers:** number class whose factors added are equal to the number itself. The first four perfect numbers, known already by the ancient Greeks, are 6, 28, 496 and 8128. The sum of the reciprocal value of the perfect number and its reciprocal factors equals 2.

**Photon:** an elementary quantum particle of light, carrier of electromagnetic interaction, belongs to the boson family, spin = 1, propagation velocity in vacuum  $c = 2.99 \times 10^8$  m/s, various wavelengths ( $\lambda$ ) and frequencies ( $\nu$ ), observing  $c = \lambda\nu$ .

**Planck's constant:** universal physical constant, it has *action character*, it is equal to  $6.626 \times 10^{-34}$  Js.

**Poincaré sphere:** representation of polarized light types classification. On the poles of the sphere are the left-hand [0,0,-1] and the right-hand [0,0,1] circular polarizations, and on the equator the vertical [-1,0,0] and the horizontal [1,0,0] linear polarization, that is, linear polarization under the angles of  $+45^\circ$  [0,1,0] and  $-45^\circ$  [0,-1,0]. When the linear polarization of the photon is changed from vertical to horizontal according to the Fibonacci law, hyperpolarized light [ $\Phi, 1, \phi$ ] is obtained.

**Pseudospin:** space-time movement – rotation of the entity in which pseudospin coupling has taken place between the spins of photon, graviton and electron.

**Pseudospin coupling:** coupling of spins via their action in the medium, which is sensitive to their action.

**Quantum superposition:** the feature that a quantum system can be in two states at the same time.

**Synergy:** a new quality of the system after coupling of its constitutive elements.

**Spin:** fundamental quantum characteristic of bosons ( $spin = 1$ ), fermions (leptons and quarks,  $spin = 1/2$ ), Higgs ( $spin = 0$ ), graviton ( $spin = 2$ ), gravitino ( $spin = 3/2$ ); it has the action characteristic (Js), because it is a synergy with Dirac's constant ( $\hbar/2\pi$ ).

**Superposition:** process of pairing of electron's quantum bits (*qubit*)  $\frac{1}{2}|0\rangle$  and  $\frac{1}{2}|1\rangle$  into four superposed quantum states:  $\frac{1}{2}(|0\rangle + |1\rangle)$ ,  $\frac{1}{2}(|0\rangle - |1\rangle)$ ,  $\frac{1}{2}(|0\rangle + i|1\rangle)$ ,  $\frac{1}{2}(|0\rangle - i|1\rangle)$ , or of the geefton  $|1\rangle$  and  $|\sqrt{5}\rangle$  into  $\frac{1}{2}(|\sqrt{5}\rangle + |1\rangle)$ ,  $\frac{1}{2}(|\sqrt{5}\rangle - |1\rangle)$ ,  $\frac{1}{2}(i^2\sqrt{5}|1\rangle + |1\rangle)$ ,  $\frac{1}{2}(i^2\sqrt{5}|1\rangle - |1\rangle)$ .

**Water bridge:** phenomenon when water under the influence of the electric field forms a bridge between two dishes via a water jet that resists the gravitation action.

**Wave-particle dualism:** the principle that physical entities, like the photon and the electron, can behave as waves or as particles depending on the experiment chosen.

**Yero factorial:** ratio of right zero factorial (0!) and left zero factorial (!0) in notation  $\langle ! \rangle \equiv 1$  (Y is used because it is a symbol of human chromosome which possesses palindrome properties,  $\frac{1}{2}$  DNA sequence is enough to know the entire sequence).

## Abbreviations and Notation

- A – action  
 $A_q = h$  – quantum action  $10^{-34}$  Js  
 $A_{q/c}$  – quantum-classical action  $10^{-34} \leq A \leq 10^{-30}$  Js  
 $A_c$  – classical action  $A > 10^{-30}$  Js  
 AFM – Atomic Force Microscopy  
 ATP – adenosine triphosphate  
 CNS – central nervous system  
 $C_{60}$  – spheric molecule composed of 60 carbon atoms  
 $c$  – light velocity  
 $c_0$  – light velocity in vacuum  
 $C_0$  – unit sphere of dimension  $N = 0$   
 $C_n$  – unit sphere of the  $N$ -dimensional space  
 $D_H$  – Hausdorff's dimension  
 GTP – guanosine triphosphate  
 $e$  – base of the natural logarithm 2.7128  
 $\ddot{e}$  – geefton  
 $i^\perp$  – orthogonal system of type  $i^2 \perp i^4$  ( $_{-1} \perp 1$ )  
 $i^\perp E_3$  – subtle energy of dynamics of Earth's motion about the Sun  
 $i^\perp E_4$  – subtle energy of Sun's and Earth's motion within galaxy  
 $F$  – force  
 $F_{cas}$  – Casimir's force  
 $F_M$  – magnetic force  
 $F_E$  – electric force  
 $G$  – universal gravitational constant  $G = 6.674 \times 10^{-11}$  Nm<sup>2</sup>/kg<sup>2</sup>  
 $g$  – gravitation force at Earth's surface 9.81 m/s<sup>2</sup>  
 $\bar{g}$  – graviton  
 $g_{mnp}$  – gravitation action *micro, nano, pico*, value  $g = 9.81$  m/s<sup>2</sup>  
 $g_{110}^p$  – amplitude value of the constant gravitation action at Earth's surface of 110pg  
 $g_{55}$  – metric tensor component, value -1 in 5D  
 $\Delta G^0$  – Gibbs free energy  
 $i$  – imaginary unit, value :  $\sqrt{-1}$   
 $K$  – absolute zero -273.15 °C  
 MFM – Magnetic Force Microscopy  
 STM – Scanning Tunneling Microscope  
 TEWL – Trans-Epidermal-Water-Loss  
 $\nabla$  – nabla operator  
 $H$  – Hamiltonian  
 $H$  – enthalpy  
 $L$  – angular momentum  
 MT – microtubule

- $M(r)$  – mathematical expectation  
 $N$  – Dimension of space.  
 $n$  – Dimensionality of space (for a positive space structure the same as  $N$ , for a negative space-time structure different than  $N$  according to the Möbius effect)  
OAM – orbital angular momentum  
UVA – ultraviolet radiation of type A  
UVB – ultraviolet radiation of type B  
UVC – ultraviolet radiation of type C  
VIS – visible region of the electromagnetic spectrum  
NIR – near infrared radiation  
IR – infrared radiation  
 $h$  – Planck's constant  $6.626 \times 10^{-34}$  (Js)  
 $\phi$  – Fibonacci number 0.61803...  
 $i^4\phi$  – complex Fibonacci number  $0.61803 + 0i^4$   
 $\Phi$  – Fibonacci number 1.61803...  
 $i^4\Phi$  – complex Fibonacci number  $0.61803 + 1i^4$   
 $\psi$  – wave function  
 $\hbar$  – Dirac's constant ( $h/2\pi$ )  
 $\epsilon_0$  – electric permeability of vacuum  
 $\mu_0$  – magnetic permittivity of vacuum  
 $\epsilon_r$  – relative electric permeability of the medium  
 $\mu_r$  – relative magnetic permittivity  
 $0!$  – zero factorial, value equal 1  
 $\lambda$  – light wavelength  
 $\lambda_0$  – Kolmogorov's exponent  
 $\Lambda$  – De Broglie's wavelength  
 $r_*(r_{\pm})$  – hyperpolarized photon  $\langle r_{\perp}, r_{\parallel} \rangle$   
 $\langle ! \rangle$  – Yero fractional  $(0!/0) = \langle ! \rangle \equiv 1$

### SI prefixes\*

factor	prefix	symbol
$10^{24}$	yotta	Y
$10^{21}$	zetta	Z
$10^{18}$	exa	E
$10^{15}$	peta	P
$10^{12}$	tera	T
$10^9$	giga	G
$10^6$	mega	M
$10^3$	kilo	k
$10^2$	hecto	h
$10^1$	deca**	da

factor	prefix	symbol
$10^{-24}$	yocto	y
$10^{-21}$	zepto	z
$10^{-18}$	atto	a
$10^{-15}$	fermto	f
$10^{-12}$	pico	p
$10^{-9}$	nano	n
$10^{-6}$	micro	μ
$10^{-3}$	milli	m
$10^{-2}$	centi	c
$10^{-1}$	deci	d

\*The kilogram is the only SI unit with a prefix embedded in its name and symbol. For mass, the unit name „gram” and unit symbol „g” should be used with these prefixes, hence 10-6 kg can be written as 1 mg. Otherwise, any prefix can be applied to any SI unit.

\*\*Or „deka”.

**SI base units**

physical quantity	name	symbol
length	metre*	m
mass	kilogram	kg
time interval	second	s
electric current	ampere	A
thermodynamic temperature	kelvin	K
amount of substance	mole	mol
luminous intensity	candela	cd

\*Or „meter“.

**SI derived units**

physical quantity	name	symbol	equivalent units
catalytic activity	katal	kat	mols <sup>-1</sup>
electric capacitance	farad	F	CV <sup>-1</sup>
electric charge	coulomb	C	As
electric conductance	siemens	S	$\Omega^{-1}$
electric potential difference	volt	V	JC <sup>-1</sup>
electric resistance	ohm	$\Omega$	VA <sup>-1</sup>
energy, work, heat	joule	J	Nm
force	newton	N	m kg s <sup>-2</sup>
frequency	hertz	Hz	s <sup>-1</sup>
illuminance	lux	lx	cd sr m <sup>-2</sup>
inductance	henry	H	V A <sup>-1</sup> s
luminous flux	lumen	lm	cd sr
magnetic flux	weber	Wb	Vs
magnetic flux density	tesla	T	Vs m <sup>-2</sup>
plane angle	radian	rad	m m <sup>-1</sup>
power, radiant flux	watt	W	Js <sup>-1</sup>
pressure, stress	pascal	Pa	N m <sup>-2</sup>
radiation absorbed dose	gray	Gy	J kg <sup>-1</sup>
radiation dose equivalent*	sievert	Sv	[Jkg <sup>-1</sup> ]
radioactive activity	becquerel	Bq	s <sup>-1</sup>
solid angle	steradian	sr	m <sup>2</sup> m <sup>-2</sup>
temperature**	degree Celsius	C	K

\*To distinguish it from the gray, units of J kg<sup>-1</sup> should not be used for the sievert in practice.

\*\*The Celsius temperature. T<sub>c</sub>, is defined from the temperature in kelvin. T<sub>k</sub>, by T<sub>c</sub> = T<sub>k</sub> -273.15

## Recognized non-SI units

physical quantity	name	symbol	SI value
area	barn	b	$10^{-28} \text{m}^2$
energy	electron volt	eV	$\approx 1.602\,18 \times 10^{-19} \text{J}$
length	ångström	Å	$10^{-10} \text{m}$
	fermi*	fm	$10^{-5} \text{m}$
	micron**	$\mu\text{m}$	$10^{-6} \text{m}$
plane angle	degree		$(\pi/180) \text{rad}$
	arcminute	'	$(\pi/10\,800) \text{rad}$
	arcsecond	"	$(\pi/648\,000) \text{rad}$
pressure	bar	bar	$10^5 \text{N m}^{-2}$
time	minute	min	60s
	hour	h	3 600 s
	day	d	86 400 s
mass	unified atomic mass unit	u	$\sim 1.660\,54 \times 10^{-27} \text{kg}$
	tonne ***	t	$10^3 \text{kg}$
volume	litre ***	l, L	$10^{-3} \text{m}^3$

\* These are non-SI names for SI quantities.  
 \*\* Or "metric ton."  
 \*\*\* Or "liter". The symbol "l" should be avoided.

## General constants

speed of light in vacuum	c	2.997 924 58	$\times 10^8 \text{m s}^{-1}$
permeability of vacuum	$\mu_0$	$4\pi$	$\times 10^{-7} \text{H m}^{-1}$
		$= 12.566\,370\,614\dots$	$\times 10^{-7} \text{H m}^{-1}$
permittivity of vacuum	$\epsilon_0$	$1 / (\mu_0 c^2)$	$\text{Fm}^{-1}$
		$= 8.854\,187817\dots$	$\times 10^{-12} \text{Fm}^{-1}$
impedance of free space	$Z_0$	$\mu_0 c$	$\Omega$
		$= 376.730\,313\,461\dots$	$\Omega$
constant of gravitation	G	6.673(10)	$\times 10^{-11} \text{m}^3 \text{kg}^{-1} \text{s}^{-2}$
Planck constant	h	6.626 068 76(52)	$\times 10^{-34} \text{Js}$
		4.135 667 27(16)	$\times 10^{-15} \text{eV s}$
$h/(2\pi)$	$\hbar$	1.054 571 596(82)	$\times 10^{-34} \text{J s}$
in eV s		6.582 118 89(26)	$\times 10^{-16} \text{eV s}$
Planck mass, $(\hbar c/G)^{1/2}$	$m_{\text{pl}}$	2.176 7(16)	$\times 10^{-8} \text{kg}$
Planck length, $\hbar/(m_{\text{pl}} c) = (\hbar G/c^3)^{1/2}$	$l_{\text{pl}}$	1.6160(12)	$\times 10^{-35} \text{m}$
Planck time, $l_{\text{pl}}/c = (\hbar G/c^5)^{1/2}$	$t_{\text{pl}}$	5.390 6(40)	$\times 10^{-44} \text{s}$
elementary charge	e	1.602 176 462(63)	$\times 10^{-19} \text{C}$
magnetic flux quantum, $h/(2e)$	$\Phi_0$	2.067 833 636(81)	$\times 10^{-15} \text{Wb}$
Josephson frequency/voltage ratio	$2e/h$	4.83597898(19)	$\times 10^{14} \text{Hz V}^{-1}$
Bohr magneton, $e\hbar/(2m_p)$	$\mu_B$	9.27400899(37)	$\times 10^{-24} \text{JT}^{-1}$
		5.788 381 749(43)	$\times 10^{-5} \text{eV T}^{-1}$
$\mu_B/k$		0.671 713 1(12)	$\text{K T}^{-1}$
nuclear magneton, $e\hbar/(2m_p)$	$\mu_N$	5.050 783 17(20)	$\times 10^{-27} \text{JT}^{-1}$
		3.152451 238(24)	$\times 10^{-8} \text{eV T}^{-1}$
$\mu_N/\text{K}$		3.658 263 8(64)	$\times 10^{-4} \text{KT}^{-1}$
Zeeman splitting constant	$\mu_B/(\hbar c)$	46.686452 1(19)	$\text{m}^{-1} \text{T}^{-1}$



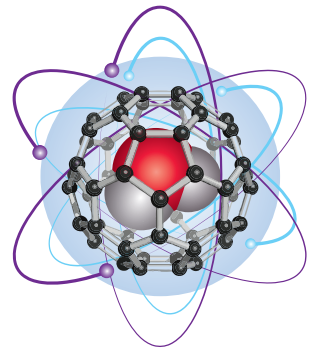
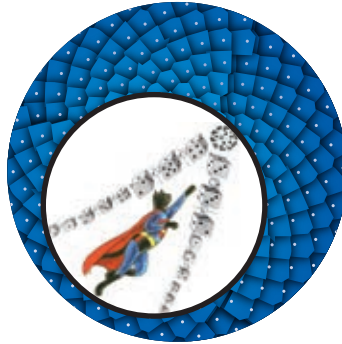
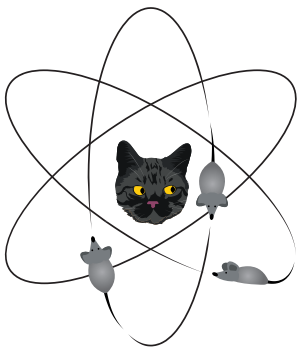
## Back side of tokins

---

Universe is not a system.,  
Universe is not a shape.  
Universe is a scenario.  
You are always in Universe.  
You can only get out of systems.

### Buckminster Fuller

Synrgetics, 1979.



**Schrödinger's cat** is a natural cat, she hunts 'real' mice, ie. physical laws of Nature. She looks at them, lurking, but can not catch them until they make that "error" and get too "close" to her.

**Fibonacci's cat** is a superstar cat that breaks through deterministic chaos (dice) and aims to reach for the Sky (the idea of life), which is of the same order as herself. But she has a limitation of inhabiting space and time, and she is a prisoner of the system.

**Gifton's cat** is a real hunter (the carbon atom and the  $C_{60}$  molecule at the same time, equal to the whole and the part), because she captured (trapped) a "mouse of life", ie. the water molecule, which is the information processing element of the base e.



zepter<sup>®</sup>  
BOOK WORLD

ISBN 978-86-7494-137-9

